Subsurface water reuse:
insights into the occurrence, fate, and transformation of organic micropollutants

Alessia Ore

2026

Propositions

1. The interplay between physicochemical properties of organic micropollutants and field microbiological and geochemical conditions determines the fate of organic micropollutants in nature-based solutions.
   (This thesis)

2. Despite the availability of advanced analytical tools, the persistence, mobility, and toxicity of transformation products remain overlooked in the development of new chemicals.
   (This thesis)

3. Overproduction, driven by mass consumerism, is the most mitigatable driver of global resource depletion.

4. Justifying weak environmental regulation of pharmaceuticals by their medical benefits neglects the broader ecological repercussions that ultimately affect human well-being.

5. Sufficient empathy, curiosity, and perseverance are essential to becoming vegan.

6. When time is intentionally reserved for self-care, overall productivity improves, despite the widespread assumption that extended working hours are more effective.

Propositions belonging to the thesis, entitled

Subsurface water reuse: insights into the occurrence, fate, and transformation of organic micropollutants

Alessia Ore
Wageningen, 26th June 2026

Subsurface water reuse: insights into the occurrence, fate, and transformation of organic micropollutants

Alessia Ore

Thesis Committee

Promotors

Dr N. B. Sutton
Associate professor in Environmental Technology
Wageningen University and Research

Prof. Dr A. P. van Wezel
Professor of Environmental Quality and Health
Utrecht University

Other members

Prof. Dr H. Smidt, Wageningen University and Research
Prof. Dr J. E. Drewes, Technical University of Munich, Germany
Dr F. Y. Lai, Swedish University of Agricultural Sciences, Uppsala, Sweden
Dr F. Béen, KWR Water Research Institute and Vrije Universiteit Amsterdam

This research was conducted under the auspices of the Graduate School for Socio-Economic and Natural Science of the Environment (SENSE)

Subsurface water reuse: insights into the occurrence, fate, and transformation of organic micropollutants

Alessia Ore

Thesis

submitted in fulfilment of the requirements for the degree of doctor

at Wageningen University

by the authority of the Rector Magnificus,

Prof. Dr C. Kroeze,

in the presence of the

Thesis Committee appointed by the Academic Board

to be defended in public

on Friday 26 June 2026

at 10:30 a.m. in the Omnia Auditorium.

Alessia Ore

Subsurface water reuse: insights into the occurrence, fate, and transformation of organic micropollutants.

276 pages.

PhD thesis, Wageningen University, Wageningen, the Netherlands (2026)

With references, with summaries in English and Italian

ISBN: 978-94-6534-363-1

DOI: 10.18174/681675

Table of Contents

Chapter 1 7

General introduction

Chapter 2 29

Presence of micropollutants and transformation products during subsurface irrigation with treated wastewater assessed by non-target screening analysis

Chapter 3 73

Removal, transport, and transformation of organic micropollutants in managed aquifer recharge: insights from target and non-target analyses

Chapter 4 115

Higher microbial diversity enhances the extent and rate of organic micropollutant biodegradation under aerobic and nitrate-reducing conditions

Chapter 5 159

Uncovering redox-specific biotransformation of organic micropollutants

Chapter 6 203

General discussion

References 225

Summary 251

Sommario 257

Acknowledgments 265

About the author | Publications 271

Chapter 1

General introduction

1.1 Urgent need for water reuse

Water scarcity is currently one of the most pressing global challenges, driven mainly by population growth and climate change. The global population, estimated at 8.2 billion people in 2024, grows by about 69 million people per year and could reach 10.2 billion people by the end of the century (United Nations, 2024a). Longer life expectancy and rising living standards have also increased water consumption worldwide.

In addition to population growth, increasing urbanization and high withdrawals for agriculture, industry, and energy production intensify pressure on freshwater resources (UN World Water Assessment Programme, 2015). Current global water withdrawal amounts to around 4600 km^3/year, of which the largest share (70%) is used in agriculture, 20% in industry, and 10% for domestic use (UN-Water, 2018). By 2050, water demand is expected to reach 5750 km^3/year, while only 4200 km^3/year can be sustainably supplied, resulting in a shortfall of 1550 km^3/year, i.e., 27% of the expected water demand (Figure 1.1) (UN-Water, 2018; Yuh et al., 2020). Overextraction of surface and groundwater threatens natural ecosystems, societal services, and human safety and well-being.

At the same time, climate change is intensifying water scarcity and variability in precipitation patterns, disrupting hydrological cycles and water quality worldwide. Extreme precipitation events and heatwaves will be more intense and longer, increasing flood and drought risks (UN World Water Assessment Programme, 2015). Even regions traditionally rich in water, such as the Netherlands, have already faced freshwater shortages in recent dry summers (Bartholomeus et al., 2023; Pronk et al., 2021). Worldwide, half the global population (4 billion people) already experiences water scarcity for at least one month per year, and one quarter live in water-stressed areas year-round (Khemka and Eberhard, 2025), a portion that will increase to around 2.95 billion people by 2050 (Figure 1.1) (UN-Water, 2018).

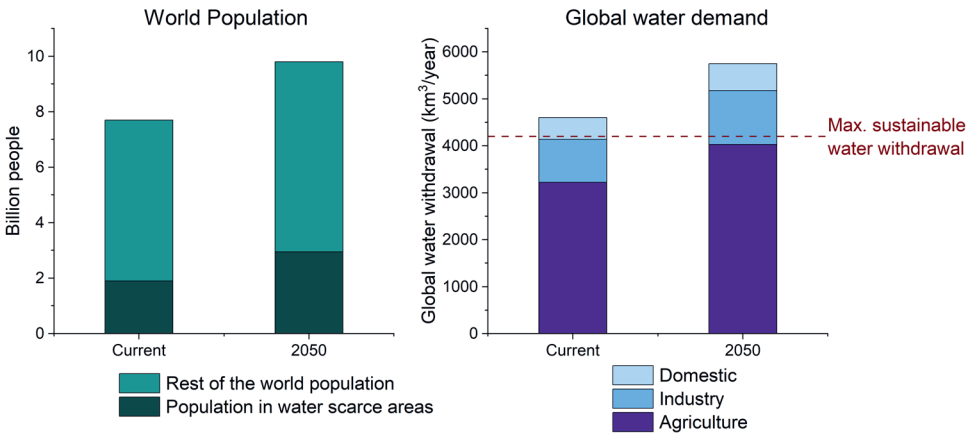

Figure 1.1. Increase in global population and global water demand, comparison of the current situation (2015-2024) with prospects for 2050 and maximum level of sustainable water withdrawal. (UN-Water, 2018; Yuh et al., 2020).

Groundwater is one of the major sources of freshwater, providing drinking water to at least half the global population and supplying more than 40% of irrigation water (UN World Water Assessment Programme, 2015). However, groundwater supplies are limited; already one-third of the largest groundwater systems are in distress or overexploited (UN-Water, 2018). The hydrological changes due to climate change and population growth also affect groundwater, which will be subjected to increased depletion in drought areas and will receive more polluted water in case of extreme precipitation, due to amplified recharge and mobilization of contaminants from the surface.

Adaptation to a growing population and climate-driven shortages in freshwater supply requires improved water management strategies. The Sustainable Development Goals (SDGs) reflect this need in SDG6, which aims at achieving a sustainable availability and management of water and sanitation for all (United Nations Department of Economic and Social Affairs, 2025). Water reuse has great potential to reduce the gap between demand and supply of freshwater. In particular, subsurface storage systems, being less vulnerable to evaporation and contamination, can support water reuse, enhance drought resilience, and improve water quality through natural soil passage. A major challenge to water reuse is achieving proper water quality, particularly the removal of organic micropollutants (OMPs), as investigated in this thesis.

1.2 Water reuse in the subsurface

Groundwater and subsurface water systems play a crucial role in the hydrological cycle and in water reuse. The subsurface consists of a water-unsaturated (vadose) zone and a water-saturated (phreatic) zone, separated by the groundwater table. This natural system offers sustainable solutions to alleviate the impacts of floods and droughts by providing storage space for water surplus, which can then be reused during water-scarce periods. In addition to water storage, subsurface systems can also improve water quality during soil passage.

Different techniques exist that intentionally enhance natural groundwater recharge for the purposes of water storage or treatment, collectively referred to as managed aquifer recharge (MAR) (Figure 1.2) (Dillon et al., 2009). All MAR technologies involve the intentional infiltration or injection of water into the subsurface, followed by recovery through pumps and wells for subsequent use (Dillon et al., 2009). These systems have been in use already for decades in many countries, particularly for drinking water production, as they can stabilize and improve surface water quality (Mumberg et al., 2024). Also, MAR technologies have been used for preventing saltwater intrusion, reducing evaporation losses of stored water, and sustaining groundwater-dependent ecosystems, thereby supporting biodiversity (Dillon et al., 2019, 2009; Maeng et al., 2011; Mumberg et al., 2024).

Examples of MAR techniques include aquifer storage and recovery (ASR), bank filtration, dune filtration, infiltration ponds, or soil aquifer treatment (SAT) (Figure 1.2). The choice of the technique is site-specific and depends on local hydrological characteristics, such as the type of aquifer, soil composition, presence of impermeable layers, surface land use, and the intended reuse purpose of the recovered water (Dillon et al., 2009). The main differences among MAR technologies concern the injection method and the type of water used.

The injection method largely depends on the type of aquifer. Confined aquifers, bounded at the top and bottom by impermeable layers, require wells to inject water directly into the aquifer. In contrast, unconfined aquifers do not have a confining layer at the top; the groundwater table represents their upper boundary and is free to fluctuate in response to water infiltrating through the surface and the vadose zone. In these systems, infiltration ponds, basins, or permeable soil layers are typically used for recharge (Dillon et al., 2009).

Different water sources can be used in MAR, including natural sources, like stormwater, rainwater, or groundwater transferred from other aquifers, as well as alternative water sources, such as treated wastewater and desalinated seawater. These alternative sources often contain elevated concentrations of nutrients, organic matter, metals, or OMPs (Maeng et al., 2011; Mumberg et al., 2024). Depending on the quality of the source water, pre-treatment before recharge and/or post-treatment after recovery may be needed to meet the standards for the production of industrial, irrigation, or drinking water (Dillon et al., 2009). Although MAR is generally effective at attenuating both organic and inorganic contaminants, it is not specifically designed for OMP removal, highlighting the need to better understand the fate of OMPs during subsurface passage.

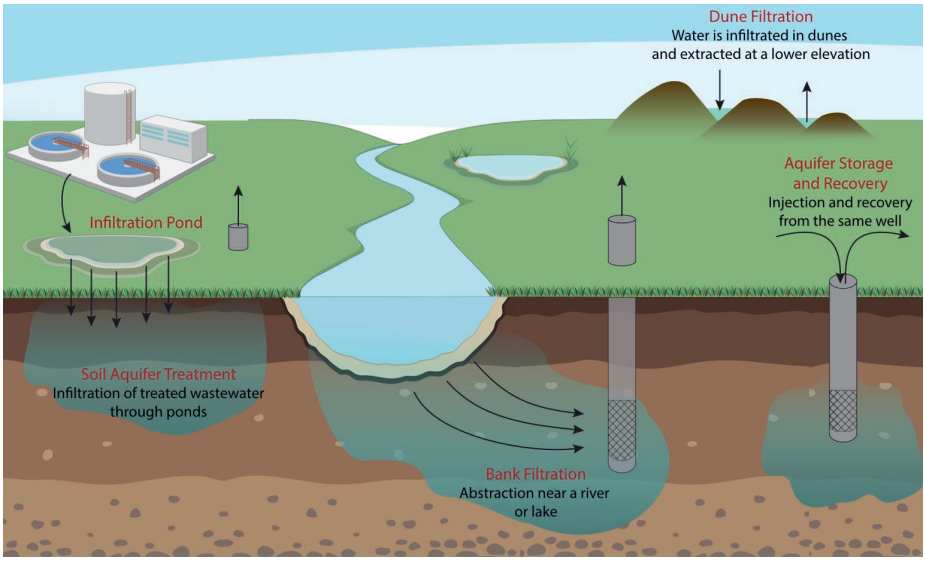

Figure 1.2. Schematic representation of different types of managed aquifer recharge. (https://BioRender.com)

1.3 Nature-based vs. engineered technologies for water treatment and reuse

Safe water reuse requires the removal of contaminants to achieve sufficient water quality for the intended water reuse purpose. Water treatment and reuse can be achieved through a wide range of technologies, from highly engineered systems to nature-based approaches (Khemka et al., 2023). Highly engineered systems include, for example, membrane filtration, reverse osmosis, activated carbon adsorption, and advanced chemical oxidation (Teodosiu et al., 2018). These technologies are generally fast and effective in removing salts (e.g., during desalination), pathogens (e.g., from wastewater), and, to some extent, OMPs (Luo et al., 2025). However, most engineered systems target a single physical-chemical property of the contaminants to be removed. Therefore, no single physical-chemical treatment technology can efficiently remove the broad spectrum of chemicals typically present in water. For example, membrane technologies separate solutes based on molecular size, while activated carbon depends on the sorption affinity of the contaminants (Shamshad and Rehman, 2025; Teodosiu et al., 2018). Moreover, highly engineered technologies have high energy demands and generate concentrated waste streams that require further treatment or regeneration (exhausted activated carbon). As a result, they involve high operational and maintenance costs (Luo et al., 2025). Also, technologies like advanced chemical oxidation can produce toxic byproducts if not optimized (Li and Mitch, 2018).

In contrast, nature-based technologies, like MAR or constructed wetlands, rely on natural biogeochemical processes to achieve low-energy and cost-effective water treatment. Biodegradation, sorption, and filtration occurring in soils and the subsurface can remove nutrients and OMPs without producing concentrated waste streams (Liu et al., 2024; Luo et al., 2025). Furthermore, these systems can provide multiple co-benefits, including groundwater recharge, carbon sequestration, biodiversity enhancement, and the creation of recreational areas (UN-Water, 2018). They can also improve water quality upstream of more engineered technologies, reducing energy and operational demand when further treatment is needed. However, nature-based technologies generally require larger areas and a longer time to achieve sufficient water treatment compared to more engineered systems (Liu et al., 2024). Their performance is also site-specific and depends on environmental factors like redox conditions, soil composition, microbial activity, and residence time (Aldas-Vargas et al., 2022; Branco et al., 2023; Meng et al., 2014). Understanding the mechanisms behind contaminant removal in nature-based systems, particularly the biodegradation and transformation of OMPs under different environmental conditions, is therefore crucial to optimizing their design and ensuring safe water reuse.

1.4 Key characteristics of OMPs in reused water

Water availability is not only limited by quantity but also by quality, which is increasingly threatened by pollution. Population growth, industrialization, and rising living standards contribute to the deterioration of water quality worldwide (UN World Water Assessment Programme, 2015). Among the contaminants of concern, the widespread occurrence of OMPs in the aquatic environment represents a global issue.

The term OMPs collectively refers to organic contaminants detected in the environment in the ng/L to low µg/L range, including pharmaceuticals, pesticides, industrial chemicals, and their transformation products (TPs) (Lapworth et al., 2012). These contaminants are continuously introduced into the environment, including subsurface water systems, through human activities, and are often not completely removed by water or wastewater treatment processes (Posselt et al., 2020). Some OMPs are currently included in European regulations (Section 1.5) and therefore frequently monitored, but many more are present in the environment, representing a black box for water reuse.

The OMP classification includes compounds with a wide range of chemical structures and physicochemical properties. Their environmental behavior and potential risks are primarily governed by three key characteristics: mobility, persistence, and toxicity. Depending on these characteristics, during water reuse, OMPs may pollute deep aquifers, accumulate in soil, or be present in the abstracted water, representing potential risks for environmental and human health.

1.4.1 Mobility

Mobility describes the potential of a substance to be transported and reach groundwater or locations far from its point of release (European Parliament and Council of the European Union, 2006a). The mobility of OMPs primarily depends on their polarity, which is governed by molecular structure. Polarity is given by an uneven distribution of electrons that generates dipoles or ionic charges, either permanent or pH-dependent (Reemtsma et al., 2016). Higher polarity generally enhances water solubility, but not necessarily mobility, since solid phases in the subsurface (e.g., soil, sediments) can also carry dipoles or ionic charges that attract polar OMPs. Organic soil constituents are typically negatively charged and therefore attract positively charged OMPs, but soil composition is very site-specific. As a result, OMP mobility in the subsurface strongly depends on sorption affinity.

Different coefficients describe OMP mobility, but none universally apply to all OMPs because neutral, permanently charged, and ionizable compounds behave differently. The octanol-water partition coefficient (K_{ow}) or solid-water partition coefficient (K_d) can be used for neutral compounds, often normalized to the organic carbon content of the soil or sediments (K_{oc}) (Reemtsma et al., 2016; Sigmund et al., 2022). Low K_{ow} or K_{oc} values indicate high

aquatic mobility. The threshold to consider an OMP as mobile is a log K_{oc} <3.0 (European Parliament and Council of the European Union, 2024). However, the K_{ow} and K_{oc} parameters are inadequate for charged or ionizable compounds, whose behaviour depends on pH, water hardness and soil or sediment composition (Sigmund et al., 2022). For such compounds, the distribution coefficient D_{ow} is a better proxy, as it accounts for the sum of all ionic species between octanol and in water at a given pH. Even though widely used due to the lack of a better descriptor widely accepted, D_{ow} is still an approximation because it does not consider interactions of hydrophobic parts of OMPs with octanol or soil (Sigmund et al., 2022). Nonetheless, D_{ow} is still a useful parameter to identify charged or ionizable OMPs as potentially mobile (Arp and Hale, 2022).

1.4.2 Persistence

According to the REACH (Registration, Evaluation, Authorisation and Restriction of Chemicals) regulation, a compound is considered persistent if its environmental half-life exceeds specific threshold values under standard test conditions, which must be demonstrated by the registrant (European Parliament and Council of the European Union, 2006a). The half-life determined in these standardized tests, i.e., the time required for a compound's concentration to decrease by 50%, reflects the degradation rate in the environment. For soils and sediments, compounds with a half-life greater than 120 days are classified as persistent (European Parliament and Council of the European Union, 2024).

The persistence of OMPs is closely linked to their environmental chemical risk, as slowly degraded OMPs may remain in the environment for extended periods and accumulate, increasing exposure potential and hampering the effective exposure management (McLachlan et al., 2017). Several standardized tests and guidelines have been developed to estimate OMP persistence, like the OECD 308 and 309 tests, which assess transformation in aquatic sediment systems under aerobic and anaerobic conditions and biodegradation in aerobic natural water, respectively (OECD, 2025, 2004). Although some of these tests were recently updated to reflect scientific advances, they remain simplifications of natural systems, as the obtained half-lives do not account for the high variability and complexity of environmental parameters. Degradation rates in soil depend on microbial activity, temperature, pH, nutrient availability, redox conditions, and the compound's bioavailability (Arp and Hale, 2022). Consequently, laboratory-derived half-lives are useful mainly for ranking intrinsic persistence under controlled conditions and for identifying non-persistent or potentially persistent OMPs (Arp and Hale, 2022; McLachlan et al., 2017).

Given the large number and structural diversity of OMPs, several computational approaches have been developed to estimate persistence when experimental data are lacking. For instance, the Biowin and OPEn structure–activity/property Relationship App (OPERA) are

Quantitative Structure–Activity Relationship (QSAR) models that predict biodegradability based on molecular descriptors, like hydrophobicity, molecular weight, and functional groups (Mansouri et al., 2018; US EPA, 2025). These models infer persistence by comparing the chemical structure of a compound with those of similar, experimentally tested substances, for which data are available in databases. QSAR tools are valuable screening methods for prioritizing substances and supporting regulatory assessment, but their predictions are valid only within specific applicability domains that define the chemical space covered by the training data (OECD, 2024).

1.4.3 Toxicity

Toxicity refers to the potential of a substance to cause adverse effects on living organisms, and it is one of the key properties defining the environmental and human health risk of OMPs (European Parliament and Council of the European Union, 2006a). Toxic effects depend on both exposure and intrinsic compound properties (Escher and Fenner, 2011). Many OMPs, including pharmaceuticals and pesticides, are biologically active by design, meaning they can interact with molecular targets in non-intended organisms even at low concentrations (Gutiérrez-Noya et al., 2021; Kümmerer, 2009). According to the REACH regulation, an OMP is considered toxic to aquatic organisms if the long-term no observed effect concentration (NOEC) is below 0.01 mg/L or if it is classified as carcinogenic, mutagenic, or toxic for reproduction (European Parliament and Council of the European Union, 2006a). Because experimental toxicity data are limited for the large number of OMPs, predictive models like QSARs and read-across approaches are often applied to estimate their toxic potential and for regulatory purposes (Cronin et al., 2025). Tools like the CERAPP and CoMPARA, which predict estrogenic and androgenic activity receptor activity (Mansouri et al., 2020, 2016), and MS2Tox, which estimates aquatic toxicity (Peets et al., 2022), allow the assessment of OMP toxicity when experimental data are unavailable.

1.5 European water policies

European regulations on OMPs in water are in continuous evolution. While specific regulatory thresholds for many OMPs are still lacking, recent revisions of European water legislation expanded the list of priority substances to include pesticides, pharmaceuticals, and industrial chemicals (Table 1.1). TPs are occasionally mentioned in regulations, although no specific limit values currently exist for individual TPs. Thus, despite the revisions, current water quality monitoring still focuses on a restricted set of OMPs, neglecting a large portion of OMPs (including TPs) that are detected in water but not regulated. Research is required to gain a better understanding of OMPs in water and, consequently, update regulations.

The Water Framework Directive (WFD, Directive 2000/60/EC) sets broad goals for achieving good chemical status of surface water and groundwater bodies (European Parliament and Council of the European Union, 2000). EU-wide thresholds are defined for nitrates and pesticides, while member states are responsible for setting thresholds for additional contaminants that could threaten water quality. According to the European Environmental Agency, 78% of the groundwater bodies and 30% of the surface waters were reported to be in good chemical status (European Environmental Agency, 2024). The WFD also includes a non-deterioration clause to prevent the degradation of water bodies currently in good status.

Two daughter directives, the Groundwater Directive (2006/118/EC) and the Environmental Quality Standards (EQS) Directive (2008/105/EC), were adopted under the WFD to define groundwater and surface water quality requirements (European Parliament and Council of the European Union, 2008, 2006b). The Drinking Water Directive (2020/2184) additionally complements the WFD by regulating water intended for human consumption (European Parliament and Council of the European Union, 2020a). In 2022, a proposal to revise the WFD, the EQS, and the Groundwater Directive was released, adding new substances of concern with well-documented harmful effects on the environment and human health, such as PFAS, a range of pesticides and pesticide-TPs, and some antibiotics (Table 1.1). The updated Drinking Water Directive (2020/2184) also introduced monitoring requirements and guideline values for selected OMPs with potential endocrine-disrupting effects (17-β-estradiol and nonylphenol) and a list of substances to be monitored (European Parliament and Council of the European Union, 2020a).

Regarding water reuse, Regulation (EU) 2020/741 establishes minimum quality requirements for the reuse of treated wastewater in agriculture, differentiated by crop type and irrigation method. However, these requirements currently do not address OMPs.

Overall, the European regulatory landscape for OMPs is dynamic and moving toward a more comprehensive control of OMPs. Nonetheless, the OMPs currently covered by existing policies represent only a fraction of the wide variety of contaminants in the aquatic environment, which may hinder safe water reuse and the responsible management of freshwater sources.

Table 1.1. Overview of OMPs included in the Drinking Water Directive, the EQS Directive, and the Proposal amending the WFD, the Groundwater Directive, and the EQS Directive. [a] Maximum allowed concentration depends on the availability of toxicity data.

OMP name	Max. concentration (µg/L)		
	Drinking Water Directive (EU) 2020/2184	EQS Directive (2008/105/EC)	Proposal amending WFD, Groundwater Directive, and EQS Directive (2022)
Industrial chemicals			
1,2-dichloroethane	3	10	-
Acrylamide	0.1	-	
Anthracene	-	-	0.1
Benzene	1	50	
Benzo(a)pyrene	0.01	-	0.27
Bisphenol-A	2.5	-	130
Brominated diphenylether	-	-	0.14
C10-C13 chloroalkanes	-	1.4	-
Di(2-ethylhexyl)-phtalate	-	1.3	-
Dichloromethane	-	20	-
Epichlorohydrin	0.1	-	-
Fluoranthene	-	-	0.12
Hexabromocyclododecane	-	-	0.5
Hexachlorobenzene	-	-	0.5
Hexachlorobutadiene	-	0.6	-
Naphtalene	-	-	130
Nonylphenol	0.3	-	2.1
Octylphenol	-	0.1	-
Pentachlorobenzene	-	0.01	-
Pentachlorophenol	-	1	-
Sum haloacetic acids	60	-	
Sum trichloroethylene and tetrachloroethylene	10	-	10
Tetrachloroethylene	-	10	-
Tributyltin compounds	-	0	-
Trichlorobenzenes	-	0.4	-
Trichloroethylene	-	10	-
Trichloromethane	-	2.5	-
Vinyl chloride	0.5	-	-
Natural toxin			
Microcystin-LR	1	-	-

Pesticides			
Acetamiprid	-	-	0.16
Aclonifen	-	-	0.12
Alachlor	-	0.7	-
Aldrin	0.03	-	-
Atrazine	-	-	2
Bifenox	-	-	0.04
Bifenthrin	-	-	0.01
Chlorfenvinphos	-	0.1	-
Chlorpyrifos	-	-	0.0026
Clothianidin	-	-	0.34
Cybutryne	-	-	0.02
Cypermethrin	-	-	0.001
DDT total	-	0.03	
Deltamethrin	-	-	0.00002
Dichlorvos	-	-	0.0007
Dieldrin	0.03	-	
Diuron	-	-	0.05
Endosulfan	-	0.01	
Esfenvalerate	-	-	0.01
Glyphosate	-	-	398.6
Heptachlor and heptachlor epoxide	0.03	-	0.0003
Hexachlorocyclohexane	-	0.04	
Imidacloprid	-	-	0.06
Isoproturon	-	1	
Nicosulfuron	-	-	0.23
Permethrin	-	-	0
Quinoxifen	-	-	2.7
Simazine	-	4	-
Sum aldrin, dieldrin, endrin, isodrin	-	0.01	-
Terbutryn	-	-	0.34
Thiachloprid	-	-	0.05
Thiamethoxam	-	-	0.77
Triclosan	-	-	0.02
Trifluralin	-	0.03	
Individual active substances in pesticides, including their relevant TPs	-	-	0.1

Individual non-relevant TPs	-	-	0.1/1/2.5/5[a]
Total active substances in pesticides, including their relevant TPs	-	-	0.5
Total non-relevant TPs	-	-	0.5/5/12.5[a]
Individual pesticides	0.1	-	-
Total pesticides	0.5	-	-
PFAS			
Sum of 24	-	-	0.004 (PFOA equivalents)
Sum PFAS	0.1	-	-
Total PFAS	0.5	-	-
Pharmaceuticals			
17 alpha-ethinylestradiol	-	-	0.00018
17-beta-estradiol	0.001	-	0.0002
Azithromycin	-	-	0.18
Carbamazepine	-	-	0.002
Clarithromycin	-	-	0.13
Diclofenac	-	-	250
Erythromicin	-	-	1
Estrone	-	-	0.0004
Ibuprofen	-	-	0.22
Sulfamethoxazole	-	-	0.01
Total pharmaceutical active substances	-	-	0.25

1.6 OMP fate in the subsurface

Once released into the environment, OMPs can reach the subsurface through different paths. Pesticides may leach from agricultural soils or infiltrate through intentional recharge of contaminated water (Drewes et al., 2003; Luo et al., 2019). Industrial compounds, pharmaceuticals, and personal care products and their TPs are frequently detected in wastewater treatment plant (WWTP) effluents, which can enter the subsurface after discharge into surface water (Golovko et al., 2021). The fate of OMPs once in the subsurface is still poorly understood. A combination of physical, chemical, and biological processes, together with the OMP-specific characteristics previously discussed, determines whether they are transported, retained, or transformed into TPs. However, the extent to which these processes interact and influence TP transport and formation needs further investigation.

1.6.1 Transport

Transport in the subsurface defines the spatial extent of OMP spreading and depends on both environmental factors, such as hydrology and soil structure, and OMP-specific properties like polarity, sorption affinity, and charge state (Section 1.4.1) (Schaper et al., 2019).

The movement and distribution of OMPs are hydrologically determined by advection (the movement of the OMPs with the bulk of groundwater) and dispersion, which indicates the OMP spreading and gradual reduction in concentration due to variations in the flow path and velocity (Tang and van der Zee, 2021). These processes are strongly influenced by the soil composition and hydraulic conditions.

Coarse-textured soils, such as sands, generally promote rapid movements due to higher hydraulic conductivity and limited interactions with OMPs, while fine-grained soils rich in clay and organic matter retard transport (Holzmann et al., 2021; Sigmund et al., 2022). Preferential flow paths caused by structural heterogeneities influence the flow velocity and contact with soil particles. Impermeable layers can slow vertical movement and promote lateral spreading, while cracks or water extraction wells increase the water flow through or towards them (Aldas-Vargas et al., 2022). Recharge dynamics or seasonal changes also influence transport. Intense precipitation or MAR events can accelerate vertical movement, while droughts can extend residence times in the unsaturated zone (Narain-Ford et al., 2022; Tang et al., 2023a).

Overall, the interplay between subsurface characteristics and OMP properties determines the transport of OMPs in the subsurface. Mobile compounds tend to migrate with groundwater and may reach deeper aquifers or the abstraction wells intact, while more hydrophobic compounds are prone to retention due to sorption, where they may undergo transformation. Understanding transport mechanisms is therefore essential to predict OMP fate and support the design of effective subsurface water reuse systems.

1.6.2 (Bio)degradation

Non-persistent OMPs can undergo abiotic or biological transformation in the subsurface, leading to TP formation. Most previous MAR research focused on the removal of specific OMPs to assess water quality improvements (Celiz et al., 2009), while TP formation in MAR has only recently gained attention due to the awareness that TPs may be more harmful than the corresponding PC (Fenner et al., 2021; Hermes et al., 2019; Mumberg et al., 2024; Zakhia et al., 2025). More research is therefore required to better understand OMP transformation and TP formation in MAR. Abiotic transformation includes processes such as hydrolysis and oxidation catalyzed by minerals like iron and manganese oxides present in groundwater systems (J. Wang et al., 2023). Biological transformation (i.e., biodegradation) is the major

environmental removal process for many OMPs, which consists of a chain of reactions that transform a parent compound (PC) into metabolites, or TPs (Fenner et al., 2013; Kern et al., 2011). Biodegradation can ultimately lead to mineralization, where OMPs are converted into inorganic compounds like water and CO_2. While TPs are often more mobile than their PC, their persistence and toxicity may either increase or decrease depending on the OMP and transformation pathway (Fenner et al., 2013; Stadler et al., 2012; Zahn et al., 2024). Mineralisation and biodegradation, however, require favourable conditions.

The primary factors influencing biodegradation in the subsurface include redox conditions, microbial community composition, and nutrient availability (Branco et al., 2023; Fenner et al., 2021). These are interdependent: redox conditions define the main electron acceptors available, which determine which microbial species thrive, and thus microbial community composition. Active microbial metabolism depends on the presence of suitable electron donors as well as essential nutrients. Additional factors, such as temperature, pH, and contaminant concentration, further influence biodegradation (Fenner et al., 2021; National Research Council, 1993).

Soil composition, redox conditions, and nutrient availability change with depth (Figure 1.3). According to the redox ladder, microorganisms sequentially use electron acceptors based on the energy yields of their reduction reactions. The greater energy yield is provided by oxygen, followed by nitrate, iron (III), sulfate, and finally CO_2. Aerobic conditions and biodegradable dissolved organic carbon (DOC) in the unsaturated zone generally favour biodegradation, whereas deeper groundwater environments are often substrate-limited and characterized by slower, anaerobic transformation (Drewes, 2009). Despite the prevalence of anaerobic conditions and redox layering in subsurface systems, anaerobic OMP biodegradation and TP formation remain insufficiently investigated. More research is therefore needed to better comprehend OMP transformation pathways and persistence under realistic subsurface conditions.

Key players in biodegradation are microbial species and their structure in microbial communities. OMP transformation can occur through metabolic degradation, where specific microorganisms use OMPs as growth substrates, or cometabolism, where OMPs are incidentally transformed during the metabolism of another substrate (Tran et al., 2013). Microbial diversity and abundance are depth-dependent (Figure 1.3). While abundance decreases with depth due to less availability of nutrients, diversity increases and has been associated with enhanced adaptation and higher metabolic process rates (Patsch et al., 2018), including biodegradation. This is likely due to greater richness (and thus greater chance of OMP degraders' presence), functional redundancy (i.e., presence of multiple species able to perform the same reaction), and complementary metabolic interactions

among species. These factors allow greater OMP biodegradation and further progress in biodegradation pathways, contributing to the attenuation of OMPs in the subsurface (Lindemann et al., 2016; Morris et al., 2013; Posselt et al., 2020; Stravs et al., 2019).

A better understanding of biodegradation and the factors influencing it is essential to gain insights into OMP fate in the environment and better assess their persistence. Consequently, accurate monitoring of both PCs and TPs is fundamental to evaluating the effectiveness of natural attenuation processes.

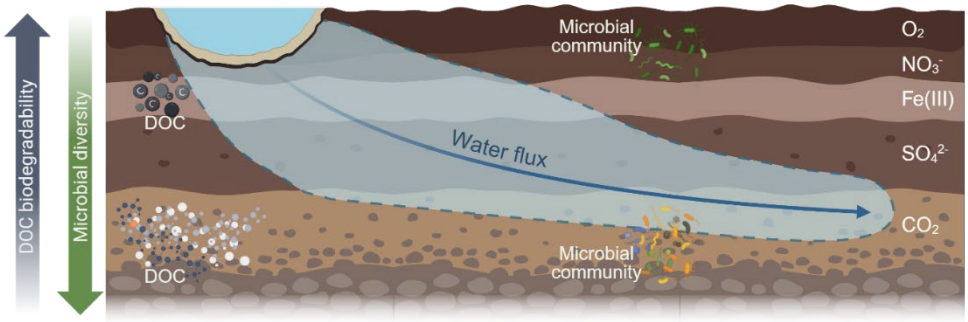

Figure 1.3. Schematic section of the subsurface. Dissolved organic carbon (DOC) biodegradability and nutrients availability are higher close to the surface, while microbial diversity increases with depth. On the left, the electron acceptors are reported according to the redox ladder. Created with the help of BioRender (https://BioRender.com)

1.7 OMP detection and assessment

To assess the occurrence of OMPs in reused waters and the efficiency of nature-based treatment systems, it is essential to characterize the composition of infiltrated, groundwater, and abstracted water. Monitoring OMPs typically relies on chromatographic separation coupled to mass spectrometry. The most common method is reversed-phase liquid chromatography coupled to mass spectrometry (RPLC-MS), which separates and identifies compounds based on their polarity and mass-to-charge ratio (m/z). Other chromatography techniques can extend the detectable chemical space to include more polar (hydrophilic interaction liquid chromatography - HILIC), charged (ion chromatography - IC), or volatile (gas chromatography - GC) compounds. High-resolution mass spectrometry (HRMS) has further advanced OMP detection by providing high mass accuracy and enabling the analysis of complex environmental mixtures of known and unknown OMPs, including TPs (Schymanski et al., 2014b).

Three main analytical approaches are currently applied to environmental samples: target analysis, suspect screening (SS), and non-target analysis (NTA) (Figure 1.4) (Krauss et al., 2010). Target analysis enables quantification and confident identification of compounds of interest, but is restricted to OMPs with available reference standards. Many of these reference standards are currently not available or unknown, given the large variety of OMPs

in the environment. In contrast, SS and NTA allow the detection of compounds without reference materials. SS relies on prior information, such as molecular formula or structure, to search for expected compounds, while NTA can be applied without prior knowledge, but demands extensive data processing and expert interpretation to identify unknowns.

Field investigations and laboratory studies provide complementary insights into the fate of OMPs in the environment. Laboratory studies enable the controlled investigation of processes and parameters influencing OMP removal, offering understanding at a fundamental level. However, these setups often oversimplify the complex and heterogeneous conditions of real subsurface systems. In contrast, field investigations realistically assess the occurrence and fate of OMPs under natural conditions, but are difficult to interpret due to the multitude of environmental factors that cannot be controlled.

Overall, advances in analytical techniques to measure OMPs in the field and laboratory have greatly expanded the chemical space that can be detected and our understanding of OMP fate. Despite this, challenges related to detection limits, matrix effects, and harmonization of data treatment remain (González-Gaya et al., 2021). Continued progress in analytical sensitivity and data harmonization will be key to improving the detection and comparability of OMP measurements across different studies.

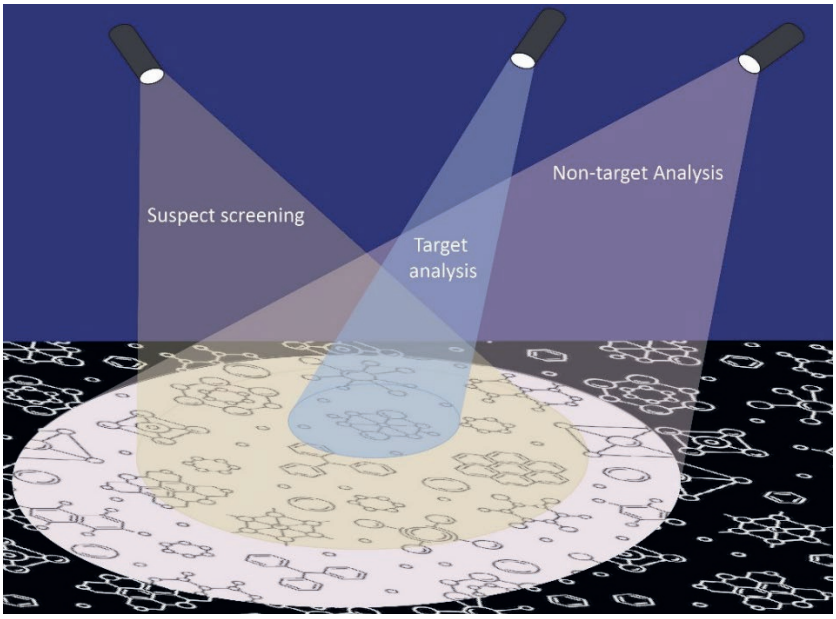

Figure 1.4. Graphical representation of the chemical space covered by target analysis, suspect screening, and non-target analysis. Adapted from Escher et al., 2020.

1.8 Knowledge gaps

Water reuse will be paramount in addressing future water scarcity, and the subsurface offers significant advantages for this purpose. However, as discussed, OMPs are ubiquitous in reused water, and may undergo (further) transformation into TPs in the subsurface. Several studies present TPs as potentially more threatening than their PCs for environmental and human health. Yet, many TPs remain unidentified, and their characteristics are largely unknown. Advancing TP identification in water reuse systems is therefore essential to better assess the risks associated with their presence in the environment. Despite growing research on OMPs in MAR and other nature-based systems, several knowledge gaps persist regarding their fate in the subsurface.

- *Which OMPs (and TPs) are present in reused water?*

A more comprehensive characterization of the chemical composition of reused water is needed. Recent analytical advances now allow the detection of previously unknown contaminants and TPs, offering a broader understanding of OMPs and TPs entering water reuse systems. This knowledge would improve risk assessment and guide the development of more effective and realistic regulations for water reuse, ensuring that they account for OMPs that are currently and actually present in reused water.

- *What is the effectiveness of soil passage for water reuse when TPs are also considered?*

While MAR systems and other nature-based technologies have been extensively studied for their removal of selected OMPs, they are rarely assessed comprehensively concerning TP formation and removal. Including TPs in the evaluation of treatment performance is essential to determine whether these systems truly improve water quality or if OMPs are transformed into potentially persistent or toxic products.

- *What is the fate of the OMPs (including TPs) in the subsurface?*

Once the OMPs enter the subsurface, their fate is still poorly understood. Field observations reveal complex interactions among hydrological, geochemical, and biological factors that influence their transport and transformation. Improving our understanding of these processes requires an integrated approach that combines field investigations with controlled laboratory studies. Such integration enables a realistic assessment of OMP occurrence under field conditions while disentangling the influence of key environmental factors on their transformation processes.

- *Which environmental factors determine OMP biodegradation and TP formation?*

Environmental conditions in the subsurface largely determine whether OMPs are transformed, retained, or persist. Redox conditions, microbial community composition, and diversity are among the key drivers of biodegradation and TP formation. Moreover, the

interplay between these environmental factors and intrinsic properties of OMPs, such as mobility and persistence, strongly influences their overall fate, dictating whether OMPs reach deeper aquifers or abstracted water intact, or are instead (further) transformed towards mineralization.

Integrating the knowledge obtained from field and laboratory studies will enhance our ability to predict the environmental fate of contaminants, continuously released into water bodies. With these predictions, better informed regulations can be developed that safeguard the environment while ensuring the safe and sustainable reuse of water resources.

1.9 Research objectives

In light of the knowledge gaps discussed in the previous section, this thesis aims to improve the understanding of OMP fate and TP formation processes in subsurface water systems. To achieve this, we combined target and non-target analyses in both field investigations and laboratory experiments to link real-world observations with a more fundamental understanding of the underlying processes. The integration of NTA across environmental and experimental settings aimed at a broader and more unbiased characterization of OMPs and their transformation dynamics in water reuse systems.

The research followed a progression from field scale to laboratory scale: starting with the characterization of OMPs and TPs in reused water and MAR systems under natural, uncontrolled conditions, and then focusing on the environmental parameters that govern OMP transformation under controlled settings.

Specifically, we aimed at:

- Characterizing the chemical composition of two types of reused water (surface water and WWTP effluent) in two distinct subsurface reuse systems (MAR and subsurface irrigation) to assess the occurrence of OMPs and TPs under real conditions.
- Evaluating the efficiency of the MAR system as a nature-based solution for improving water quality for drinking water production.
- Exploring OMP fate to determine transport in the field and (bio)transformation in both field and laboratory settings to better understand OMP fate and TP formation.
- Investigating, under controlled laboratory conditions, the effects of key environmental parameters, including redox conditions, microbial diversity, and inoculum origin, on OMP transformation processes.

This integrated approach provides a comprehensive framework to link field-scale observations with mechanistic insights, supporting the development of more effective and predictive strategies for water reuse.

1.10 Thesis outline

Below, we provide a short overview of the chapters in this thesis (Figure 1.5).

Chapter 2 focuses on a subsurface irrigation system where WWTP effluent is reused for below-ground irrigation of an agricultural field. Using NTA, we characterized the chemical composition of the reused WWTP effluent and assessed the occurrence and transport of OMPs in different directions relative to the infiltration pipes. Furthermore, we investigated transformation reactions and the occurrence of TPs in the subsurface.

Chapter 3 examines a MAR system in which surface water, impacted by OMPs from upstream WWTPs, is infiltrated via ponds and later abstracted for drinking water production. By comparing the chemical composition of infiltrated and abstracted water, we evaluated the efficiency of this system as a treatment step for potable water reuse. Samples collected from monitoring and abstraction wells along the infiltration pathway were analyzed using both target and non-target approaches to study their chemical composition, OMP transport, and the presence of TPs in the subsurface.

Chapter 4 investigates the influence of microbial diversity on OMP biodegradation and TP formation. Starting from a soil inoculum, we created microbial communities of decreasing diversity while maintaining similar structural composition. We monitored the biodegradation of 20 spiked OMPs and the formation of TPs over time under aerobic and nitrate-reducing conditions using target and suspect screening analyses. By comparing communities of different diversity, we evaluated the effects on biodegradation efficiency, rate, and completeness of the biodegradation pathway. In addition, we applied QSAR models to predict whether the detected TPs were potential dead-end products or toxic.

Chapter 5 explores the influence of redox conditions and inoculum origin on OMP biodegradation and TP formation. Nineteen spiked OMPs were incubated under four redox conditions: aerobic, nitrate-reducing, iron-reducing, and sulfate-reducing, using soil and ditch sediments as inocula. We identified OMPs that were consistently removed or persistent across the redox conditions tested, and examined redox-dependent biodegradation patterns. The persistence and toxicity of the TPs generated was further assessed through in-silico approaches and compared to that of the respective PCs.

Chapter 6 presents a general discussion on the main outcomes and implications of our research. We integrate the insights gained from field and laboratory studies to highlight our contribution to the understanding, monitoring, and treatment of OMPs and TPs in subsurface water reuse systems. Finally, we discuss opportunities for future research and improvements in tools and strategies that can support risk assessment and regulatory frameworks for sustainable water reuse.

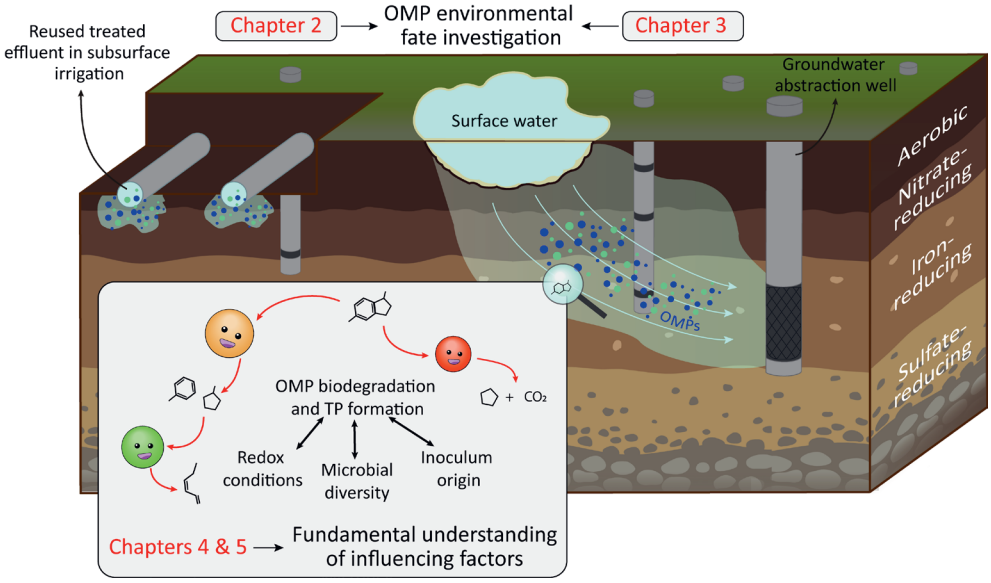

Figure 1.5. Schematic outline of this thesis. OMP = organic micropollutant; TP = transformation product. Parts of this figure were created with the help of BioRender (https://BioRender.com).

Chapter 2

Presence of micropollutants and transformation products during subsurface irrigation with treated wastewater assessed by non-target screening analysis

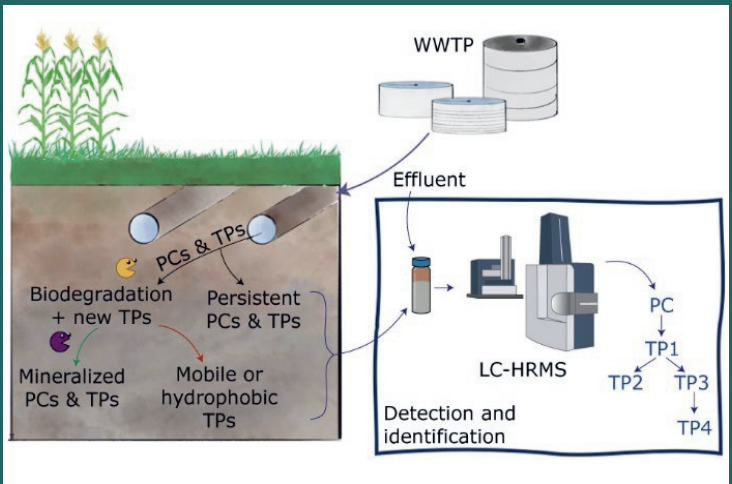

A modified version of this chapter has been published as:

Ore, A., Helmus, R., Narain-Ford, D.M., Bartholomeus, R., Sutton, N.B., van Wezel, A.P., **2025**. Presence of micropollutants and transformation products during subsurface irrigation with treated wastewater assessed by non-target screening analysis. **ACS EST Water**. https://doi.org/10.1021/acsestwater.4c00930

Abstract

While wastewater treatment plant (WWTP) effluent offers a potential alternative source for irrigation, the fate of organic micropollutants (OMPs), including transformation products (TPs), in effluent-irrigated fields remains largely unknown. Using non-target analysis (NTA), we investigated OMPs in WWTP effluent and their distribution throughout a full-scale subsurface irrigation (SSI) field where effluent was used for irrigation. Our results indicate that TPs accounted for approximately 80% of the detected effluent OMPs. Weather and SSI hydrology seem to influence OMP distribution and transformation. Wetter conditions promoted deeper leaching of OMPs in soil, and drier conditions favored their capillary rise and biotransformation, as shown by the detection of 37% more TPs in the rhizons during a dry year. On average 45 OMPs, at least 50% with a logD < 3, were detected at -2.3 m depth, highlighting their potential to reach groundwater and the importance of including TPs in further risk assessment.

This approach demonstrates how NTA and subsequent data analysis tools can support the identification of (unknown) OMPs and contribute to understanding OMP fate under field conditions, which is the first step in an exposure-driven environmental risk assessment. Overall, our study emphasizes the importance of carefully considering (unknown) OMPs for more responsible effluent reuse.

Keywords

Micropollutant transformation products; biodegradation; non-target analysis; subsurface irrigation; groundwater quality; mobile compounds; water reuse.

2.1 Introduction

Reuse of alternative water sources is a way to tackle freshwater scarcity, however, it is important to consider water quality to ensure safety. One alternative water source for agriculture is wastewater treatment plant (WWTP) effluent, which could be reused as irrigation water, given its predictable availability and monitorable quality (Helmecke et al., 2020). The intentional reuse of WWTP effluent can satisfy a portion of the freshwater demand for agriculture, accounting for 70% of the global freshwater withdrawal (United Nations, 2024b).

Reusing WWTP effluent poses potential risks to the environment and groundwater due to the presence of potentially hazardous contaminants. Conventional wastewater treatment processes are not fully effective at removing all organic micropollutants (OMPs), even with more advanced physical-chemical technologies (Escher and Fenner, 2011; Neef et al., 2022), due to the diverse OMP characteristics and the limitations of treatment conditions. A portion of OMPs often remains in the WWTP effluent (Helmecke et al., 2020; Loos et al., 2012; Petrie et al., 2015; Pistocchi et al., 2022), including pesticides, pharmaceuticals, PFAS, personal care products, and their transformation products (TPs) (Narain-Ford et al., 2021; Yuan et al., 2017). Notably, some TPs in the effluents may exceed the parent compounds (PCs) concentration and toxicity, highlighting the need for further investigation into their presence (Escher and Fenner, 2011; Stadler et al., 2012; Zahn et al., 2024).

The EU Regulation for Water Reuse (European Parliament and Council of the European Union, 2020b) encourages the use of treated wastewater in irrigation and addresses the minimum requirements for reuse. While OMPs, like pesticides and pharmaceuticals, are mentioned as additional requirements to manage human and environmental risks, no specific compounds or concentrations are referenced. European water guidelines (Council of the European Communities, 1991; Directorate-General for Environment, 2022a) and recent revisions (European Parliament, 2023; European Parliament et al., 2024) include some contaminants, but the lists are not representative of the variety of compounds in the effluent and overlook the majority of TPs (Revitt et al., 2021; Yuan et al., 2017). TPs are often sparingly included, as many remain unknown or are difficult to detect with the methods conventionally applied due to low concentrations and the lack of analytical standards (Brunner et al., 2019a; Fenner et al., 2021). Consequently, many OMPs go unnoticed in effluent discharge or reuse. Although it is not feasible to include all the relevant TPs and OMPs in water treatment regulations, more comprehensive water quality monitoring is required to better assess WWTP efficiency and the feasibility of effluent reuse in agriculture (Helmecke et al., 2020).

Subsurface irrigation (SSI) makes use of shallow underground pipe systems at depths of approximately 1 m below ground level, used for field drainage during wet periods. Flow can be reversed during dry periods, allowing infiltration of water, or in this case effluent (de Wit et al., 2022, 2024). Capillary action towards the plant roots and evapotranspiration by the plants result in the use of irrigated water within the field (de Wit et al., 2022). During SSI, effluent OMPs come in contact with soil and groundwater, where they may undergo biotic (i.e., biodegradation) or abiotic (e.g., hydrolysis) transformation, generating TPs or fully converting into inorganic substances (Fenner et al., 2021). Therefore, it is important to understand OMPs' fate following irrigation via SSI. Soil passage via SSI could act as additional treatment improving effluent quality via (bio)degradation (Narain-Ford et al., 2022; Tang et al., 2023a), but generally more mobile TPs are produced, potentially including persistent and toxic compounds (Fenner et al., 2013; Stadler et al., 2012; Zahn et al., 2024). Biodegradation plays a key role in OMP fate in natural systems, but its efficiency depends on several factors, like microbial community composition, organic carbon availability, redox conditions, and retention time (Fenner et al., 2021; Filter et al., 2021; Greskowiak et al., 2017). Moreover, some released OMPs may resist biodegradation and persist in the environment. Mobile and persistent contaminants, including TPs, could reach groundwater and compromise its quality (Drewes, 2009; Sinclair and Boxall, 2003).

To understand if effluent reuse with SSI is a viable option for water reuse, we investigated the OMPs in a WWTP effluent used in an SSI agricultural field, aiming to clarify its composition. Furthermore, we studied the presence of released OMPs and related TPs, coming from the effluent or formed in the field, in groundwater samples from the SSI field. In this study, raw NTA data were analyzed to detect OMPs in both WWTP effluent and groundwater samples. NTA allows tentative identification of unknown compounds, like TPs. Comprehensive TP-screening workflows with patRoon 2.3 (Helmus et al., 2022) were used to facilitate the data treatment, including automated TP screening. The work builds upon and complements previous research in the same agricultural field, in which OMPs were quantitatively studied using target analysis (Narain-Ford et al., 2022). This study addresses the knowledge gap on (unknown) contaminants in the effluent that could potentially pollute soil and groundwater. More information on the effluent composition and OMP fate in irrigated fields can support a more proper prioritization of compounds to be removed from effluents and the selection of suitable indicators to assess WWTP efficiency and effluent suitability for reuse.

2.2 Materials and methods

The analyzed NTA data come from an SSI field in Haaksbergen, the Netherlands, and the adjacent municipal WWTP (SI 2.1). The WWTP applies standard secondary treatment

technologies (suspended solids removal and biological treatment) to the water received from a combined sewer system. The total average residence time of water in the WWTP is approximately 20 hours during dry weather conditions and 3.5 hours during heavy rainfall. The WWTP effluent was reused from 2015 until 2022 during the growing season of feed crops via SSI, without residence in intermediate buffer basins. The SSI system consisted of parallel pipes located at -1.2 m depth and 6 m apart from each other (SI 2.1). The dataset included NTA data from two monitoring points in the SSI-irrigated field, each sampled at four depths in 2017 and 2019 when corn was grown on the field. The selection of the sampling location, depths, and years analyzed is based on the results of a chloride/bromide ratio test (Bartholomeus et al., 2017) to identify the locations receiving the WWTP effluent and the previous research by Narain-Ford et al. (Narain-Ford et al., 2022), who observed most removal of target OMPs between infiltration pipes. We chose to compare a location close to a pipe and one in between pipes to investigate TP presence as well as effluent OMP transformation and spreading in the field.

2.2.1 Study area and sample collection

The Haaksbergen SSI system and the sampling methods have been previously described by Narain-Ford et al. (Narain-Ford et al., 2022). The system has been monitored since 2015 to study its hydrology and follow effluent infiltration and OMPs' fate using targeted analyses (Narain-Ford et al., 2022; Tang et al., 2024b, 2023b). The effluent composition tends to be constant over time in terms of OMP presence, however, OMP concentration is affected by precipitation and temperature over year-round periods. Additionally, these earlier studies highlight the complexity of the hydrological fluxes in the system, which affect OMPs' fate.

The present research focuses on NTA data analysis from samples collected in 2017 and 2019. Considering the precipitation and reference evaporation data (KNMI, n.d.) from January 1st to the sampling date, the potential precipitation surplus was 3.4 mm in 2017, while 2019 was drier with a deficit of 23.3 mm. The 24-h composite WWTP effluent and water samples from two locations in the SSI field, taken at depths of -0.6 (i.e., rhizons, unsaturated zones above the level of infiltration), -1.3, -1.8, and -2.3 m (minifilters in the saturated zone), were selected for the NTA data treatment and interpretation. One replicate per effluent and field sample was available. The locations are hereafter referred to as *Close* and *Between,* referring to their position close-to an SSI infiltration pipe and in-between pipes, similar to Narain-Ford et al. (Narain-Ford et al., 2022) (SI 2.1).

The samples were collected in 250 mL HDPE bottles, stored at -20 °C immediately after reaching the laboratory on the sampling day, and thawed on the day of analysis. Effluent samples were collected on July 3rd, 2017, and July 11th, 2019, whereas the field samples were collected on July 3rd, 2017 (during subirrigation) and October 7th, 2019 (a few days after

the end of the subirrigation period). Rain episodes were registered during the three days preceding the effluent samplings: 23.5 mm in 2017 and 0.5 mm in 2019 (KNMI, n.d.). This selection of samples provided the most comparable NTA data between the two years and the position relative to infiltration pipes.

2.2.2 NTA samples preparation and data acquisition

The sample preparation for direct injection and the analysis in the LC-HRMS system, which produced the NTA data analyzed in this research, were performed by KWR Water Research Institute and are described in detail in SI 2.2. The LC-HRMS method has been used and validated in previous research (Béen et al., 2021; Brunner et al., 2019a). Briefly, a C18 column was used for liquid chromatography and an Orbitrap with an electrospray ionization source was used for mass spectrometry. In spring 2022, the samples were analyzed in positive and negative ionization modes along with blanks and performance standard (Table S2.2) samples containing target OMPs at known concentrations.

2.2.3 NTA data processing with patRoon

The NTA data from the selected samples were processed with patRoon 2.3.2, an open-source R-based workflow for non-target data analysis and automated TP screening (Helmus et al., 2022, 2021). HRMS blanks and performance standards were included in the patRoon dataset to ensure high-quality results. The workflow included several steps (Section 2.2.3.1) and simultaneously analyzed positive and negative ionization data. For some of the steps, default values were optimized based on the NTA equipment, following what was previously described (Helmus et al., 2021).

2.2.3.1 General description of the workflow

Two patRoon scripts (available in full in Supplementary scripts 2.1 and 2.2) were used to treat the raw data obtained from the LC-HRMS analysis of the effluent samples (Supplementary script 2.1) and the field samples (Supplementary script 2.2). A simplified version of the workflow (without TP screening) was used to analyze the NTA data of the performance standard samples, using the same parameters applied to the effluent and field samples (bottom of Supplementary script 2.1).

The workflows include the following steps and tools. Data transformation from *.raw* to *.mzML* (Martens et al., 2011) format was performed through ProteoWizard (Kessner et al., 2008), whereas the feature finding and sample grouping steps were done using OpenMS (Röst et al., 2016). The sample grouping step produces feature groups, consisting of features that are considered equivalent across multiple samples (Helmus et al., 2021). Subsequently, filtering steps (e.g., minimum intensity thresholds and blank removal) were applied to clean the data. A suspect screening step was included in the workflow to check for the presence

of the OMPs previously detected via target analysis over a 20-month period by Narain-Ford et al. (2022) in the Haaksbergen SSI field. These OMPs (46 pesticides, 29 pharmaceuticals, and 14 industrial chemicals listed in Table S2.3) were provided in a suspect list to the software and were considered as PCs for the subsequent TP screening step. Then, we performed a suspect screening looking for TPs of the full list of OMPs previously detected. In the TP-screening, BioTransformer (Djoumbou-Feunang et al., 2019) with the microbial degradation module enviPath (Wicker et al., 2016) was used to generate a list of TPs up to the second generation (Supplementary Excel -SE- 2 Table E1) that may originate from the PCs following biological transformation processes by environmental microbiota. After filtration for TPs of greater interest (see Supplementary scripts 2.1 and 2.2), this list was used to screen for predicted TPs in the samples. With the filters, we removed second-generation TPs with a mass ratio TP/PC lower than 60%. A componentization step was then included, and unwanted adducts and isotopes were manually removed from the dataset. The following annotation step used GenForm (Meringer et al., 2011) and MetFrag (Ruttkies et al., 2016) to assign a formula, a compound candidate, and an identification (ID) level to the peaks in the feature groups. The ID estimation in patRoon is based on Schymanski et al. (Schymanski et al., 2014a) with some modifications on the rules to assign the level, as reported in Table S2.4 and the patRoon handbook and manuals (Helmus, 2025, 2024). Briefly, in a suspect screening, Schymansky et al. assign the TP a starting ID level of 3, whereas in patRoon the starting level is 5. The level can improve in both cases with extra information retrieved from the analysis. Level 1 is only assigned if the suspect is confirmed by an analytical standard. All feature groups with assigned ID level 5 were removed from the dataset to improve the reliability of the results. Finally, PCs and TPs were linked to visualize compound transformation pathways in the final report. The feature groups were manually reviewed in patRoon to further clean the dataset by removing incorrectly integrated peaks before generating HTML reports.

Additional filters (Supplementary scripts 2.1 and 2.2) were applied to the feature groups to obtain a simplified dataset to generate figures and tables. The filters prioritized duplicate feature groups assigned to the same suspect and multiple suspects assigned to the same feature group. In these cases, only the feature group or suspect with the highest ID level was retained for plotting purposes. The MS(/MS) spectra fragments of the compounds in PC- and the performance standard lists were compared with those from MassBank (Horai et al., 2010) and PubChem (Kim et al., 2023). This last step ensured proper identification and allowed the assignment of ID level 1 to the suspect OMPs detected in both the performance standard and effluents and field samples (SE2 Tables E4, E5, and E6). A comparison of the TPs detected in the dataset with the TPs registered in the PubChem Transformations

database (Schymanski et al., 2024) (which includes transformation reactions from literature) was performed, the overlapping TP results are provided in SE2 Tables E2 and E3.

Experimental pH-dependent logK_{oc} values would have been ideal for assessing the mobility of ionizable compounds like the OMPs and TPs discussed in our study. Given the absence of this data for most TPs, logD was used to represent the hydrophobicity-driven portion of sorption (Arp and Hale, 2022; Reemtsma et al., 2016), which was the best approximation in our case. The charge was included to consider electrostatic interactions in soil, which is predominantly negatively charged. Charge and logD values at pH 7 (SE2 Table E7) were plotted against the distance between each sampling point and the infiltration pipe. The logD values of OMPs detected in the field were retrieved using the InChIKey from patRoon reports. Whenever possible, the InChIKey was converted to SMILES via the Chemical Identifier Resolver (National Cancer Institute, 2024), then used to predict the charge and logD of each contaminant with Chemicalize (ChemAxon, n.d.). For the location close to the pipe, the plotted distance corresponds to the vertical path between the pipe and the sampling point. For the location between pipes, the diagonal distance was used. The rhizons and the sampling points at -1.3 meters below ground level share the same distance from the pipe, resulting in overlap when plotted.

2.2.4 Data interpretation

Excel and R (Tidyverse packages) were used to treat the data obtained from the HTML reports. Additionally, the databases PPDB (Lewis et al., 2016), enviPath (Wicker et al., 2016), DrugBank (Law et al., 2014), EU Pesticides Database (European Commission, n.d.), EAWAG-BBD (biocatalysis/biodegradation database) (Gao et al., 2010), MassBank (Horai et al., 2010) and PubChem (Kim et al., 2023; Schymanski et al., 2024) were used to manually interpret the PCs and TPs detected and the transformation reaction involved.

The authors recognize some limitations in the present study. The TP prediction tool used in patRoon (Biotransformer) may have overlooked possible TPs, causing the TP-suspect list to be insufficiently inclusive. Alternatively, TPs may have been missed due to too high polarity causing early elution, low concentrations falling below detection limits, or peak intensities below the scripts' cut-off. TPs outside the chemical space handled by LC-HRMS would also be missed in our analysis. In designing the patRoon scripts, we aimed to balance the comprehensive screening of TPs with minimizing the introduction of uncertainties. The filters applied on the list used for TP screening (see previous section) helped prevent the erroneous assignment of small, nonspecific fragments to a specific PC, particularly when such fragments could originate from multiple PCs, but this could have resulted in overlooking of TPs formed later on in the transformation pathway. Target analysis would be needed for further confirmation of the TP results, but is often hampered by the lack of

knowledge on TP formation in the field (to which the study intends to contribute) and by the availability of analytical-grade TP standards.

Our dataset includes only one replicate per sampling point per year. Although we recognize that this is a small number of samples for a field study, the results are backed up by previous research in the same field and period and employing target analysis. Therefore, this study adds complementary information on TPs to the study of Narain-Ford et al. (Narain-Ford et al., 2022).

Our transformation reaction analysis is based on the predictions of BioTransformer (EAWAG-BBD Pathway Prediction System (Gao et al., 2010)) and the TPs' detectability and is different from canonical approaches studying OMP biodegradation pathways. To identify the types of reactions that produced the TPs detected in the dataset, we used the elemental changes in the PC-TPs components and the EAWAG-BBD (Gao et al., 2010) pathway prediction rules, both through patRoon and manual verification. In this research, with the term “OMPs” we refer to contaminants in general, which can be either PCs or TPs.

2.3 Results and Discussion

This study addresses the release of OMPs in WWTP effluent in an SSI-irrigated field through an NTA approach, aiming to shed more light on OMPs in the effluent and the field. In the first part of the Results and Discussion, the OMPs detected in the effluent are analyzed. In the second part, we focus on the OMPs detected in the SSI field, and in the third part, we investigate the transformation reactions behind the detected TPs.

2.3.1 Variability in the presence of parent compounds and transformation products in the WWTP effluent

A high proportion of the feature groups detected in the WWTP effluent samples was annotated as TPs, which are often overlooked in water quality monitoring programs. In 2017, feature groups corresponding to a total of 56 OMPs were detected, 43 of which were recognized as TPs; in 2019, 90 compounds, including 72 TPs, were found in the effluent (Figure 2.1, for more information on the OMPs, including ID level estimation, see SE2 Table E4). Eighteen of the 78 suspect TPs detected in the effluent dataset (including both years) are registered in the PubChem transformations database (Schymanski et al., 2024) (SE2 Table E2). Our results show that to fully assess effluent quality, monitoring should not only consider PCs but also a variety of TPs. We detected mostly pharmaceutical and pesticide TPs in the effluent samples of both 2017 and 2019, including pharmaceutical TPs that were not human metabolites and likely formed during wastewater treatment processes (SE2 Table E4). The PCs detected in the effluent samples are likely resistant, at least to a certain extent, to the treatment technologies applied. Examples, detected in our dataset and confirmed by

literature, are diclofenac (Alessandretti et al., 2021), furosemide (Golovko et al., 2021), 1H-benzotriazole (Loos et al., 2012), and acesulfame (Fu et al., 2020).

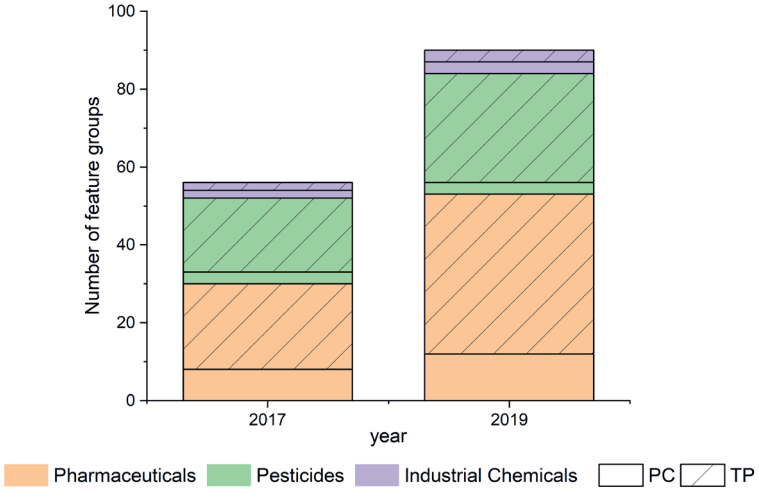

Figure 2.1. Feature groups corresponding to OMPs detected in the WWTP effluent in the normal precipitation (2017) and dry (2019) years, differentiated per contaminant type and in PCs and TPs.

For water reuse purposes, it is important to shed more light on TPs in the effluent. Most available studies in literature have focused on TPs from specific compounds and did not provide information on the wide range of TPs actually present in WWTP effluents. For instance, Letzel et al. (Letzel et al., 2015) studied the presence of sartans (blood pressure regulators) and their TPs in WWTP effluents, while Lei et al. (Lei et al., 2021) surveyed the benzodiazepines (anxiolytic drugs) and the TPs generated in 11 WWTPs. In our dataset, other blood pressure regulators (e.g. metoprolol) and mood-control (e.g. venlafaxine) drugs were detected, but no sartans or benzodiazepines specifically. While these studies provide insights into TP presence, they do not comprehensively assess effluent quality. In contrast, Beretsou et al. (Beretsou et al., 2022) conducted a more extensive study of OMPs in the influent and effluent of WWTPs, reporting 55 target compounds in the effluent, 15 of which were TPs, mainly deriving from pharmaceuticals. By analyzing the influent composition, they demonstrated that 8 of these TPs in the effluent were formed during the WWTP processes. Among these, tramadol-N-oxide, carbamazepine TPs, and venlafaxine TPs were also detected in our dataset. Although our study did not focus on the formation of TPs within WWTPs, Beretsou et al.'s findings (Beretsou et al., 2022)support our observation of newly formed pharmaceutical TPs in the WWTP effluent.

In our study, precipitation seemed to affect effluent quality in WWTPs, potentially diluting some OMPs to concentrations below the detection limits and/or reducing WWTP transformation efficiency due to shorter residence times (Neef et al., 2022). In 2017, 23.5

mm of rain was recorded over two days before sampling, compared to just 0.5 mm in 2019 (KNMI, n.d.). This likely contributed to the detection of 34 more feature groups (5 annotated as PCs and 29 as TPs) in 2019 than in 2017, with almost twice as many pharmaceutical TPs and one-third more pesticide TPs detected in 2019. For reuse purposes, it is advisable to perform effluent characterization with NTA during dry weather conditions (when more OMPs can be detected) as a realistic worst-case estimate of its impact on the receiving environment.

2.3.2 Presence of contaminants in the field

As a result of reuse in SSI systems, effluent contaminants enter soil and groundwater. In the subsurface, OMPs can undergo biological or abiotic transformations under different conditions compared to those in WWTPs, potentially resulting in the formation of different TPs. Thus, we performed a comprehensive non-target analysis of OMPs in the field irrigated with effluent via SSI. We present the OMPs detected in the SSI field, along with their mobility and the transformation reactions likely involved in TP formation, either in the field or the WWTP. More information on the compounds is present in SE, including the tentative chemical formula and structure of the OMPs, their estimated ID level, and the peak intensities per sample (SE2 Table E5).

2.3.2.1 OMPs in the field

Our results indicate that weather conditions and soil hydrology likely influence OMP distribution and TP formation in the SSI field. A total of 121 feature groups assigned to OMPs were detected in the field, with similar numbers in 2017 and 2019 (92 and 80, respectively – SE2 Table E5). In general, TPs represent the majority of OMPs at all depths in the whole dataset, but OMP distribution in the field varies based on the location. A higher number of OMPs (118 on average between the two years) and a greater proportion of PCs (24%) were detected close to the infiltration pipes, whereas in between pipes, fewer OMPs were detected (60 on average, with 18% of PCs), more or less evenly distributed over the sampled depth in both years (Figure 2.2). At the rhizons between pipes, only TPs were detected.

Close to the infiltration pipe, we observed different trends between the two years, which may be traced back to the weather effects on SSI hydrology. In 2017, more OMPs were detected between -1.3 and -1.8 m. The field samples of 2017 were taken after a heavy rainfall (KNMI, n.d.) that probably caused the leaching of OMPs to these depths. The hydrology of the system is complex (Tang et al., 2023a), but in more wet conditions, the lateral water fluxes to the stream and downward fluxes increase, whereas upward movement towards the rhizons decreases.

In 2019, most OMPs were detected in the rhizons. In this year, the groundwater table was considerably lower (on average 24 cm lower than in 2017) (de Wit et al., 2023) and might have favored the capillary rise of infiltrated water with OMPs (Tang et al., 2023a). A higher TP formation is also likely due to higher retention times and more aerobic conditions in the SSI system. In dryer conditions, besides an increased capillary rise, there is a slower movement of water laterally and downward. The capillary rise leads OMPs to more oxygenated zones where biodegradation is faster and more efficient (Filter et al., 2021), and slower water movement leads to higher retention times and thus possibly more biodegradation. Altogether, these water movements might explain the higher number of TPs observed in the rhizons in 2019.

Moreover, the results for 2019 can be related to the infiltration of more concentrated effluent during dry periods, which occurred more frequently in 2018 and 2019 (KNMI, n.d.), and higher OMP concentrations, which may lead to improved biotransformation and TP production (Fenner et al., 2021). This conclusion is supported by the previous study of Narain-Ford et al. (Narain-Ford et al., 2022), who observed higher background OMP concentrations in the field before the start of SSI in 2019 due to the very dry year of 2018, in which effluent was hardly diluted by rain during the infiltration period. This caused OMPs to reach high concentrations in the soil, which could not be completely washed out by precipitation in winter 2018-2019 and spring 2019.

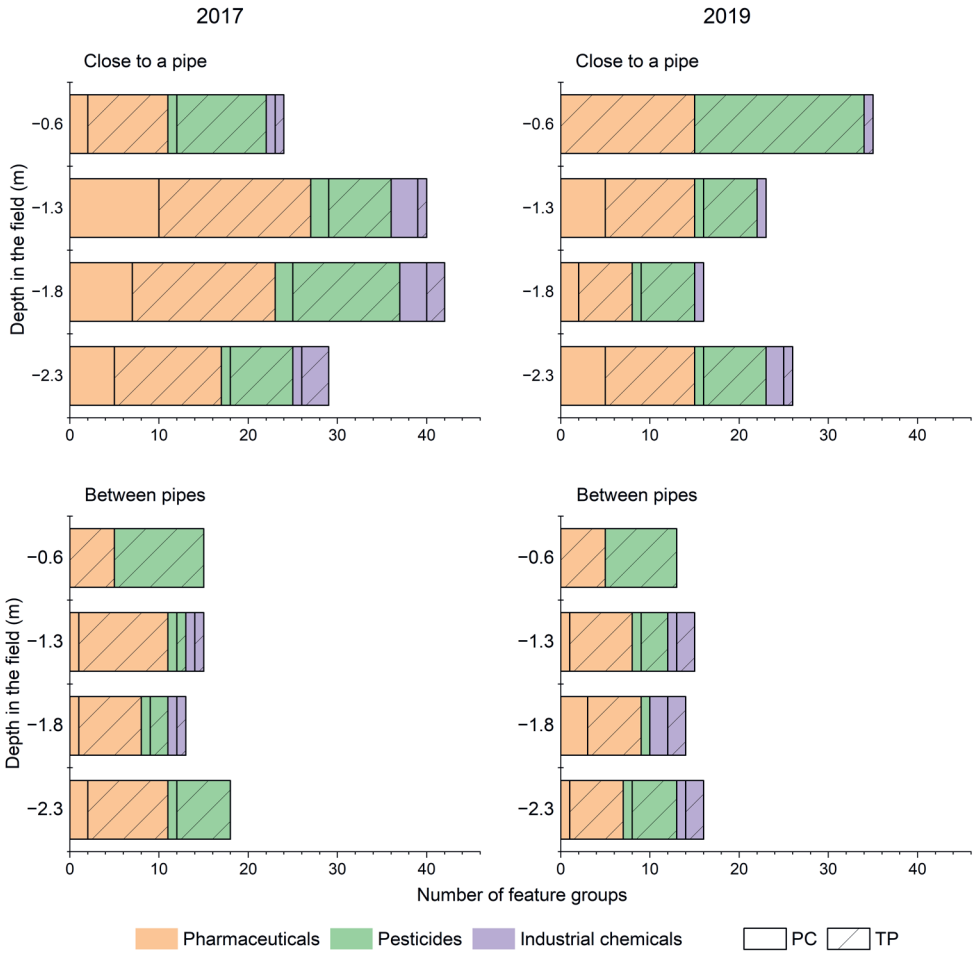

Figure 2.2. Distribution of OMPs in the SSI field in 2017 and 2019.

Overall, several OMPs (between 16 and 29) were also detected at -2.3 m in the field (Figure 2.2). As infiltration occurred at -1.2 m, the detection of OMPs at -2.3 m indicates their transport toward groundwater, probably due to their high mobility and/or persistence (Fenner et al., 2013). OMPs detected at the deepest sampling points include highly persistent and mobile PCs and related TPs, for example carbamazepine, venlafaxine, and venlafaxine-TPs, and highly persistent PCs and related TPs (1H-benzotriazole, DEET, and metolachlor-TPs), previously reported to resist removal processes (Golovko et al., 2021; Narain-Ford et al., 2022). The deeper groundwater in Haaksbergen is protected by an impermeable loamy clay layer below our sampling depths and by the high lateral flow toward the nearby surface water (de Wit et al., 2024). However, these geohydrological characteristics are specific to this site and might not occur in other SSI fields. Therefore,

reusing WWTP effluent through SSI requires careful consideration of persistent and mobile OMPs, including TPs, possibly present in the effluent or forming in the soil. Implementing additional measures to reduce the presence of OMPs in the WWTP influent (with responsible chemical use in households, commercial activities, and agriculture) and effluent (by upgrading WWTPs with advanced OMP treatment technologies) is needed to protect freshwater sources from OMP contamination (Helmecke et al., 2020; Mohr et al., 2020).

2.3.2.2 Mobility of OMPs in the field

The charge state and logD values at pH 7 were utilized to infer the mobility of OMPs in the field (SE2 Table E7). It has to be noted that these data could only be retrieved for a limited subset of the OMPs detected, namely 100% of the PCs and 30% of the TPs.

We investigated the correlation between OMPs' mobility indicators and OMPs' detection in the field in Figure 2.3. Most of the compounds detected with retrievable mobility indicators had a logD at pH 7 below 3, which indicates already moderate mobility (Arp and Hale, 2022). High logD values (>3) generally indicate low water mobility and a tendency for soil sorption. In SSI systems, OMPs with high sorption affinity remain close to the infiltration pipe and require attention, as they may accumulate in the field (Tang et al., 2024b). Typically, in temperate climates, the winter period between growing seasons allows for the restoration of an SSI field to low OMP background levels, aided by winter precipitation and drainage (Tang et al., 2024a). However, OMPs with high logD tend to sorb to soil particles, which can result in their retention in the field.

Narain-Ford et al. (Narain-Ford et al., 2022) observed an accumulation of highly persistent and low-mobility OMPs near SSI infiltration pipes. Similarly, in our dataset, the OMPs with higher logD were detected mostly close to the infiltration pipe (Figure 2.3). This was more evident in 2017 (Figure 2.3A), when a greater number of compounds with logD>1 were detected at distances less than 1 m from the infiltration pipe, compared to those at greater distances. Compounds like fipronil (logD = 4.49) and dimethenamid-p (logD = 2.92) were only detected close to the infiltration pipe in both years. Similarly to hydrophobic compounds, cationic OMPs stayed closer to the infiltration pipe, likely due to higher affinity for the negatively charged components of the soil matrix. This behavior is clear for PCs like sotalol – logD = -2.34 and tramadol – logD = 0.1, which, despite their low logD, were detected only in the well close to the infiltration pipe (Figure 2.3).

OMPs with lower logD values and higher mobility are of concern due to their potential to reach deeper groundwater aquifers. Very mobile compounds (logD<0), most of which TPs, were well distributed over the sampling points in the field. In 2019, very mobile TPs were predominant in the well between two pipes, some of which were not detected closer to the infiltration pipe, like triethyl-phosphate-TP2 (diethyl phosphate) and TP5 (ethyl dihydrogen

phosphate), with logD -1.93 and -3.05, respectively. Mobile compounds can travel considerable distances along with the water flow. Water movement in SSI is a combination of the fluxes of irrigation, drainage, natural groundwater flow, and capillary rise, causing water (and solutes) to move in different directions. Each of these fluxes is influenced by different conditions, among which are recent weather and SSI operations. This suggests that the OMP distribution in the field depends not only on mobility but also on other factors. For example, in dry periods, the capillary rise of water is higher than in wet conditions (Tang et al., 2023a). Recent effluent infiltration leads to more OMPs (of all mobility classes) being detected close to the pipes. Other factors are dispersion (Tang and van der Zee, 2021) and in-situ transformation processes (Brunner et al., 2019a), which might form new TPs with different mobility than the PC at any distance from the infiltration pipes.

Figure 2.3 clearly shows how TPs are more mobile than PCs, with PCs prevalent in the top part of the plots, and TPs with lower logD values. The identification and monitoring of more TPs and further evaluation of their persistence and possible toxicity are crucial for the safeguarding of deeper groundwater reservoirs, as their high mobility may allow them to travel considerable distances.

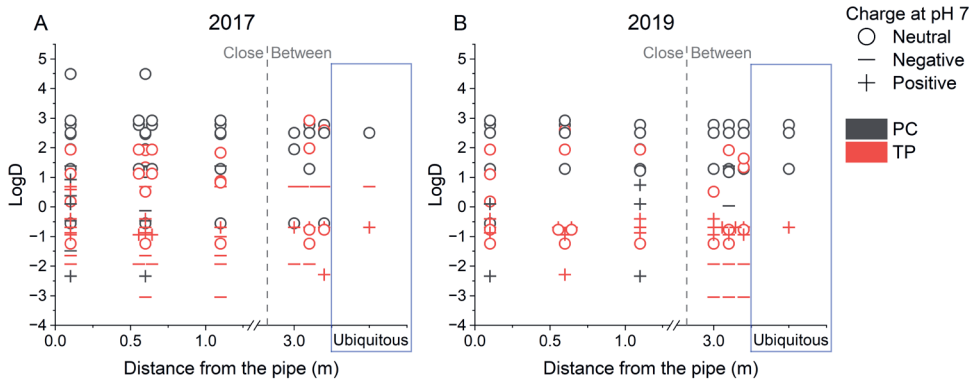

Figure 2.3. Mobility indicators (logD and charge, both at pH 7) of the PCs and TPs detected in the SSI field in 2017 (A) and 2019 (B) plotted against the distance between the infiltration pipe and the sampling point. The OMPs in the blue box were ubiquitous, i.e. detected at all sampled distances from the pipe.

2.3.3 Transformation of OMPs

Feature groups identified as TPs from many OMPs previously found in the SSI field were detected in our dataset (Table 2.2). Twenty-three out of the 101 TPs detected in the field dataset are registered in the PubChem transformation database (Schymanski et al., 2024) (for more information on the feature groups corresponding to these TPs, including their ID level estimation, see SE2 Table E3). The number of TPs detected per OMP class is similar in the two years, except for the pharmaceutical class, where a greater number of TPs was detected in 2017. Only a portion of TPs detected in the field were also found in effluent

samples, suggesting that some transformation may occur in the field. However, considering the limited number of effluent samples analyzed, the specific location of TP formation remains uncertain. Nonetheless, studies report OMP removal in the environment via different mechanisms, with biodegradation as the primary process, alongside sorption, abiotic transformation, and dilution (Achermann et al., 2020; Fenner et al., 2021; Filter et al., 2021; Hamann et al., 2016; Neef et al., 2022; Pujar et al., 2022). Therefore, it is reasonable to assume that OMPs released by the WWTP effluent undergo (further) transformation in the SSI field.

Table 2.2. List of OMPs for which TPs were detected in the field in 2017 and 2019.

Pharmaceuticals	**# TPs 2017**	**# TPs 2019**	**Pesticides**	**# TPs 2017**	**# TPs 2019**	**Industrial chemicals**	**# TPs 2017**	**# TPs 2019**
1-Hydroxyibuprofen	2	1	2,6-Dichlorobenzamide	1	2	HFPO-DA	0	1
2-(Methylamino)-pyridine	2	1	4,6-Dinitro-o-cresol	1	1	N-Phenyl urea	1	1
3-Hydroxy-carbamazepine	2	2	Ametryn	1	1	Triethyl phosphate	2	2
Atenolol	4	4	Atrazine	1	0			
Bezafibrate	2	1	Cyanazine	2	2			
Caffeine	1	1	DEET	2	1			
Climbazole	1	0	Desmetryne	1	1			
Clindamycin	4	3	Dimethametryn	1	1			
Clofibric acid	1	2	Diuron	1	1			
Diclofenac	1	0	Ethofumesate	0	4			
Dimethanamid-p	1	0	Fenuron	2	1			
Gemfibrozil	0	1	Linuron	1	1			
Ibuprofen	3	1	MCPB	1	1			
Lincomycin	1	1	MCPP	1	0			
Metoprolol	7	8	Metolachlor-s	8	8			
Paracetamol	1	0	Metribuzin	1	0			
Sotalol	3	3	Nicosulfuron	2	2			
Sulfamethazine	1	1	Prometon	0	1			
Tramadol	3	2	Propoxur	1	0			
Venlafaxine	3	1	Terbacil	1	0			
			Terbumeton	1	1			
			Triazophos	0	2			

Based on the predictions of the BioTransformer (Djoumbou-Feunang et al., 2019) interface in patRoon, we estimated which type of degradation reactions produced the TPs detected

in the dataset (Table 2.3). The transformation pathway prediction is limited to the PCs and TPs linked in the TP componentization step of the patRoon workflow and involves the use of the EAWAG-BBD Pathway Prediction System (Gao et al., 2010). Most of the TPs detected in our study were likely formed via demethylation or oxidation reactions. Oxidation is a very common reaction, often involved in OMP environmental transformation pathways (Fenner et al., 2013), especially under aerobic conditions. Demethylation can occur under both aerobic and anaerobic conditions, which might explain why we detected a higher number of demethylated TPs.

It is often reported in literature that aerobic reactions are more favourable for micropollutants biodegradation, but the specific reactions involved in degradation under field conditions are scarcely reported. Our results confirm the prevalence of aerobic biotransformation pathways in a real field setting and present other likely OMP transformation reactions that can occur once WWTP effluent is released in the SSI field.

Table 2.3. Number of transformation products per reaction type identified in the full study, in the effluent or in the field.

	# TPs detected in full study		**# TPs detected in effluent**		**# TPs detected in field**	
Transformation reaction	**2017**	**2019**	**2017**	**2019**	**2017**	**2019**
Cleavage	8	5	1	1	7	4
Decarboxylation	1	1	0	0	1	1
Dehalogenation	2	2	1	1	1	1
Demethylation	11	15	5	9	6	6
Hydrogenation	2	2	1	2	1	0
Hydrolysis	5	6	1	3	4	3
Hydroxyl group migration	2	2	0	0	2	2
Hydroxylation	2	2	1	2	1	0
Oxidation	8	8	3	4	5	4

It has to be noted that the TPs identified may subsequently have undergone further transformation in the field, and we are addressing only first- and second-generation TPs. Therefore, more transformation reactions than those reported here most likely occurred in the WWTP and the field. Nonetheless, our study assesses OMP transformation under real field conditions using TP predictions as included in the patRoon workflow. This approach offers a novel way to unravel in situ OMP transformation pathways and screen for TPs in water reuse scenarios. As TP monitoring in the environment is challenging but important to consider for water reuse purposes, the use of models and prediction tools can help prioritize and identify TPs that pose the greatest risks (Escher and Fenner, 2011; Stadler et al., 2012).

2.4 Conclusions

This study provides insights for water reuse by highlighting OMPs' presence in WWTP effluents and in the field when effluent is applied through SSI. Our results show that approximately 80% of the OMPs detected in the effluent are TPs (Figure 2.1, SE2 Table E4). A thorough understanding of TPs' presence in effluent and further fate in the environment is required to guide mitigation strategies, such as the responsible use of chemicals and the implementation of advanced OMP removal. Our comparison of effluent quality after heavy rainfall (2017) with dry weather (2019) underlines the importance of conducting NTA effluent characterization in dry conditions. This approach enables a more accurate assessment of effluent reuse feasibility by using a worst-case water quality scenario when OMPs (particularly from households) are not diluted by rainwater.

Our findings indicate that precipitation and soil hydrology likely influence OMP distribution and transformation in the SSI field. Wetter conditions in 2017 promoted downward leaching, while drier conditions in 2019 likely favored capillary rise and enhanced biotransformation due to longer retention times and more aerobic conditions (Figure 2.2). Our analysis of transformation reactions, using the prediction tools included in our patRoon workflows, confirmed the prevalence of aerobic processes in TP formation and identified other transformation reactions possibly occurring in the SSI field. Demethylation, a reaction possible under both aerobic and anaerobic conditions, was involved in the formation of most first and second-generation TPs detected in our study.

Mobility (here expressed by the logD) plays a relevant role in OMP distribution, as highly mobile OMPs can move along with the water in the complex SSI hydrological system and potentially reach any distance from the infiltration pipes. We mainly detected highly mobile TPs at the greatest distance from the infiltration pipe, highlighting the importance of considering TPs in OMP risk assessment. Cationic and relatively low-mobility OMPs (e.g., sotalol and tramadol), as expected, remained close to the infiltration pipes and might accumulate in the field (Narain-Ford et al., 2022).

Future studies building on our approach should consider some improvements for a more comprehensive assessment of OMPs in WWTP effluents and SSI fields. Increasing the number of samples would strengthen the understanding of OMP fate. Additionally, further evaluating effects and exposure, for instance with (eco)toxicity tests, and (semi-)quantification of relevant OMPs – prioritized for persistence, mobility, and potential toxicity – would improve the completeness of risk assessment for OMP release via SSI. More investigation on PFAS with dedicated NTA workflows is also advisable to address current concerns about their environmental presence.

Overall, our study highlighted the need for careful consideration of OMP presence and fate in SSI systems and similar applications to support decision-making on effluent reuse practices and promote a more conscious future water reuse.

Acknowledgments

This research was performed within the framework of the research program AquaConnect, funded by the Dutch Research Council (NWO, grant-ID P19-45) and public and private partners of the AquaConnect consortium and coordinated by Wageningen University and Research. Additionally, the sampling and sample analysis were performed with the funds from the "Re-USe of Treated effluent for agriculture (RUST)" with project number ALWGK.2016.016, funded by the Netherlands Organization for Scientific Research (NWO), KWR Water Research Institute, and KnowH2O. Dennis Vughs from KWR Water Research is acknowledged for providing the NTA data and technical information on the performance of the NTA protocol.

Supplementary Information

SI 2.1 Sampling location

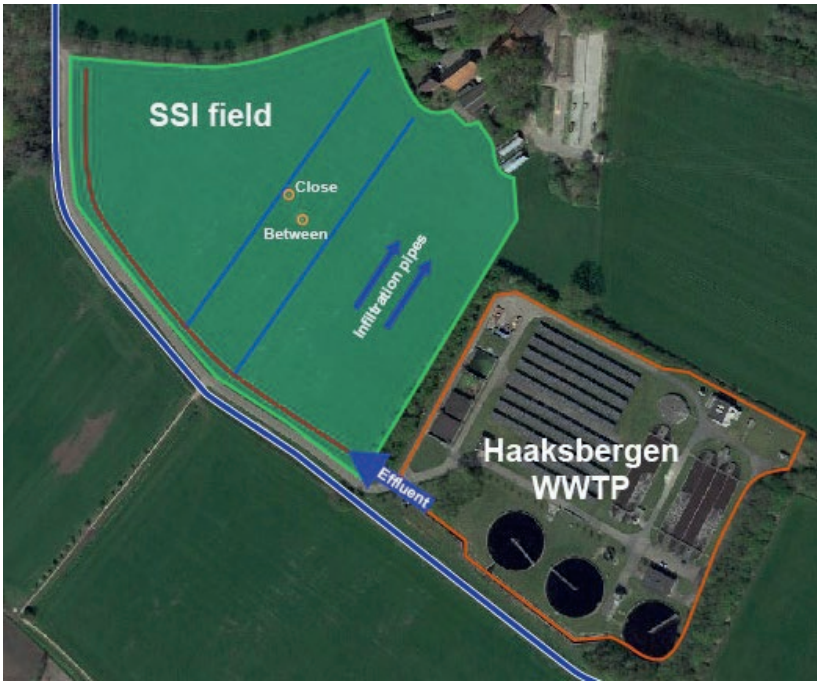

Figure S2.1. Subsurface irrigated (SSI) agricultural field adjacent to the Haaksbergen wastewater treatment plant (WWTP), the Netherlands. WWTP effluent is provided underground through parallel infiltration pipes (only two are schematically represented with blue lines). The red line represents the pipe connecting all infiltration/drainage pipes. The distance between pipes is not in scale compared to reality. "Close" and "Between" are the analyzed monitoring wells.

SI 2.2 Sample preparation and LC-HRMS analysis method

The samples were filtered using 0.20 µm Phenex filters (Phenomenex, Torrance, USA) and were spiked with an internal standard stock solution at a final concentration of 1 µg/L before analysis (Table S2.1). The LC-HRMS method has been used and validated in previous NTA studies (Béen et al., 2021; Brunner et al., 2019b). Chromatographic separation of the samples (1x) was performed using an XBridge BEH C18 XP column (150 × 2.1 mm I.D., particle size 2.5 µm, Waters, Etten-Leur, The Netherlands) in combination with a 2.0 × 2.1 mm I.D. Phenomenex SecurityGuard Ultra column (Phenomenex, Torrance, USA). The column temperature was maintained at 25 °C. Eluent A consisted of ultrapure water and 0.05% formic acid. Eluent B consisted of acetonitrile and 0.05% formic acid. The gradient started with 5% B and was held constant for 1 min. Next, the gradient increased from 5% B to 100% B in 24 minutes, and the level of B remained at 100% for 4 min. Then, the level of B was decreased to 5% in 0.5 min, and the column was equilibrated at 5% B for 4.5 min. The

flow rate was 0.25 mL/min, and 100 µL of the sample was injected into the LC column. Performance standard samples with spiked target micropollutants (Table S2.2) and blank samples containing internal standards in ultrapure water (Table S2.1) were run every 15−20 samples to check for contamination and carryover. A Tribrid Orbitrap Fusion mass spectrometer (Thermo- Fisher Scientific, Bremen, Germany) provided with an electrospray ionization source was interfaced with a Vanquish HPLC system (ThermoFisher Scientific). With every batch run, mass calibration was performed using a Pierce FlexMix calibration solution to obtain a mass error of <2 ppm. The vaporizer and capillary temperature were maintained both at 300 °C, respectively. The RF lens was set to 50%. Sheath, auxiliary, and sweep gases were set to arbitrary units of 40, 10, and 5, respectively. The source voltage was set to 3.0 kV in the positive mode and −2.5 kV in the negative mode. Full-scan high-resolution mass spectra were recorded from 80 to 1300 m/z, with a resolution of 120000 FWHM. The data-dependent acquisition was performed using a high-collision dissociation (HCD) with stepped collision energies of 20, 35, and 50% and an FT resolution of 15000 FWHM.

Table S2.1. Internal standard list with chemical formula, monoisotopic mass, MS ionization mode, and retention time (RT in the LC column) in minutes, respectively, following the columns from left to right.

Internal standard	Formula	M+H/M-H	MS ionization	RT (min)
Atrazine-d5	C8D5H9ClN5	221.13243	+	14.47
Atenolol-d7	C14D7H15N2O3	274.21426	+	3.79
Bezafibrate-D6	C19D6H14ClNO4	368.15302	+	15.9
Climbazole-d4	C15D4H13ClN2O2	297.13024	+	14.44
Diglyme-D14	C6D14O3	149.18945	+	5.41
Diuron-d6	C9D6H4Cl2N2O	239.06196	+	14.99
Fenuron-d5	C9D5H7N2O	170.13362	+	9.41
Linuron-d6	C9D6H4Cl2N2O2	255.05687	+	17.17
Metoprolol-d7	C15D7H18NO3	275.23466	+	9.48
Nicosulfuron 3-d6	C15D6H12N6O6S	417.14579	+	12.21
Prometryne-d7	C10D7H12N5S	249.18733	+	14.52
Propazine-d7	C9D7H9ClN5	237.16064	+	16.29
Sotalol-d7	C12D7H13N2O3S	280.17068	+	4.65
Sulfamethoxazole-13C6	C4[13]C6H11N3O3S	260.07952	+	10.77
Tramadol-13C,D3	C15[13]CD3H22NO2	268.21799	+	9.51
Trimethoprim-D9	C14D9H9N4O3	300.20166	+	7.79
Venlafaxine-d6	C17D6H21NO2	284.24912	+	11.06
4-Nitrophenol-2,3,5,6-d4	C6D4HNO3	142.04477	-	11.66
Bentazon-d7	C10D7H5N2O3S	246.09352	-	14.42

Fipronil-(pyrazole-13C3, cyano-13C)	C8[13]C4H4Cl2F6N4OS	438.94485	-	19.92
Fluroxypyr-d2	C7D2H3Cl2FN2O3	254.97140	-	12.84
Furosemide-d5	C12D5H6ClN2O5S	334.03183	-	13.38
Gemfibrozil-D6	C15D6H16O3	255.18728	-	20.09
Ibuprofen-d3	C13D3H15O2	208.14223	-	18.76
MCPA-D3	C9D3H6ClO3	202.03558	-	15.29
Methoxyfenozide-d3	C22D3H25N2O3	370.22155	-	18.36
Pentachlorophenol-13C6	[13]C6HCl5O	268.85986	-	20.73

Table S2.2. Name, SMILES, and retention time (RT) in the LC column in minutes of the target OMPs spiked in the performance standard samples.

Name	**SMILES**	**RT (min)**
1H-benzotriazole	C1=CC2=NNN=C2C=C1	7.96
2,4-Dichlorophenoxyacetic acid	C1=CC(=C(C=C1Cl)Cl)OCC(=O)O	15.26
2,6-Dichlorobenzamide/ BAM	C1=CC(=C(C(=C1)Cl)C(=O)N)Cl	8.18
2-Hydroxyquinoline	C1=CC=C2C(=C1)C=CC(=O)N2	9.16
3-Hydroxycarbamazepine	C1=CC=C2C(=C1)C=CC3=C(N2C(=O)N)C=C(C=C3)O	11.64
4,6-Dinitro-o-cresol	CC1=CC(=CC(=C1O)[N+](=O)[O-])[N+](=O)[O-]	15.91
4-Hydroxyquinoline	C1=CC=C2C(=C1)C(=O)C=CN2	5.98
Acesulfame	CC1=CC(=O)[N-]S(=O)(=O)O1.[K+]	3.19
Ametryn	CCNC1=NC(=NC(=N1)SC)NC(C)C	12.82
Antipyrine/Phenazone	CC1=CC(=O)N(N1C)C2=CC=CC=C2	8.64
Atenolol	CC(C)NCC(COC1=CC=C(C=C1)CC(=O)N)O	3.78
Azinophos-ethyl	CCOP(=S)(OCC)SCN1C(=O)C2=CC=CC=C2N=N1	19.19
Bentazon	CC(C)N1C(=O)C2=CC=CC=C2NS1(=O)=O	14.47
Bezafibrate	CC(C)(C(=O)O)OC1=CC=C(C=C1)CCNC(=O)C2=CC=C(C=C2)Cl	15.92
Caffeine	CN1C=NC2=C1C(=O)N(C(=O)N2C)C	6.83
Carbamazepine	C1=CC=C2C(=C1)C=CC3=CC=CC=C3N2C(=O)N	13.23
Climbazole	CC(C)(C)C(=O)C(N1C=CN=C1)OC2=CC=C(C=C2)Cl	14.3
Clindamycin	CCCC1CC(N(C1)C)C(=O)NC(C2C(C(C(C(O2)SC)O)O)O)C(C)Cl	10.62
Cyanazine	CCNC1=NC(=NC(=N1)Cl)NC(C)(C)C#N	12.98
DEET	CCN(CC)C(=O)C1=CC=CC(=C1)C	14.81
Desmetryne	CC(C)NC1=NC(=NC(=N1)NC)SC	11.1
Diclofenac	C1=CC=C(C(=C1)CC(=O)O)NC2=C(C=CC=C2Cl)Cl	18.31
Diglyme/ diethylene glycol dimethyl	COCCOCCOC	5.68
Dimefuron	CC(C)(C)C1=NN(C(=O)O1)C2=C(C=C(C=C2)NC(=O)N(C)C)Cl	16.08
Dimethanamid-p	CC1=CSC(=C1N(C(C)COC)C(=O)CCl)C	17.33

Diuron	CN(C)C(=O)NC1=CC(=C(C=C1)Cl)Cl	15.06
Ethofumesate	CCOC1C(C2=C(O1)C=CC(=C2)OS(=O)(=O)C)(C)C	18.46
Fenuron	CN(C)C(=O)NC1=CC=CC=C1	9.43
Fipronil	C1=C(C=C(C(=C1Cl)N2C(=C(C(=N2)C#N)S(=O)C(F)(F)F)N)Cl)C(F)(F)F	19.89
Fluroxypyr	C(C(=O)O)OC1=NC(=C(C(=C1Cl)N)Cl)F	12.84
Furosemide	C1=COC(=C1)CNC2=CC(=C(C=C2C(=O)O)S(=O)(=O)N)Cl	13.42
Gemfibrozil	CC1=CC(=C(C=C1)C)OCCCC(C)(C)C(=O)O	20.12
Ibuprofen	CC(C)CC1=CC=C(C=C1)C(C)C(=O)O	18.73
Lincomycin	CCCC1CC(N(C1)C)C(=O)NC(C2C(C(C(C(O2)SC)O)O)O)C(C)O	6.85
Linuron	CN(C(=O)NC1=CC(=C(C=C1)Cl)Cl)OC	17.22
MCPA	CC1=C(C=CC(=C1)Cl)OCC(=O)O	15.31
MCPP-p	CC1=C(C=CC(=C1)Cl)OC(C)C(=O)OCC2=C(C(=C(C(=C2F)F)F)F)F	16.49
Metamitron	CC1=NN=C(C(=O)N1N)C2=CC=CC=C2	
Methoxyfenozide	CC1=CC(=CC(=C1)C(=O)N(C(C)(C)C)NC(=O)C2=C(C(=CC=C2)OC)C)C	18.37
Metoprolol	CC(C)NCC(COC1=CC=C(C=C1)CCOC)O	9.4
N-Phenyl urea	C1=CC=C(C=C1)NC(=O)N	7.69
Pentachlorophenol	C1(=C(C(=C(C(=C1Cl)Cl)Cl)Cl)Cl)O	20.7
PFBA	C(=O)(C(C(C(F)(F)F)(F)F)(F)F)O	8.93
PFOA	C(=O)(C(C(C(C(C(C(C(F)(F)F)(F)F)(F)F)(F)F)(F)F)(F)F)(F)F)O	16.75
Prometon	CC(C)NC1=NC(=NC(=N1)OC)NC(C)C	11.55
Prometryne	CC(C)NC1=NC(=NC(=N1)SC)NC(C)C	14.52
Propazine	CC(C)NC1=NC(=NC(=N1)Cl)NC(C)C	16.36
Prosulfocarb	CCCN(CCC)C(=O)SCC1=CC=CC=C1	22.01
Saccharin	C1=CC=C2C(=C1)C(=O)NS2(=O)=O	5.31
Simetryne	CCNC1=NC(=NC(=N1)SC)NCC	11.1
Sotalol	CC(C)NCC(C1=CC=C(C=C1)NS(=O)(=O)C)O	4.57
Spiromesifen	CC1=CC(=C(C(=C1)C)C2=C(C3(CCCC3)OC2=O)OC(=O)CC(C)(C)C)C	
Sulfamethazine	CC1=CC(=NC(=N1)NS(=O)(=O)C2=CC=C(C=C2)N)C	8.37
Sulfamethoxazole	CC1=CC(=NO1)NS(=O)(=O)C2=CC=C(C=C2)N	10.73
Tebuthiuron	CC(C)(C)C1=NN=C(S1)N(C)C(=O)NC	
Terbumeton	CCNC1=NC(=NC(=N1)OC)NC(C)(C)C	11.78
Tramadol	CN(C)CC1CCCCC1(C2=CC(=CC=C2)OC)O	9.43
Triclosan	C1=CC(=C(C=C1Cl)O)OC2=C(C=C(C=C2)Cl)Cl	21.11
Triethyl phosphate	CCOP(=O)(OCC)OCC	10.94
Trimethoprim	COC1=CC(=CC(=C1OC)OC)CC2=CN=C(N=C2N)N	7.82
Venlafaxine	CN(C)CC(C1=CC=C(C=C1)OC)C2(CCCCC2)O	10.96

SI 2.3 Suspect list for parent compounds

Table S2.3. OMPs previously detected in the Haaksbergen field and used as parent compounds list, with type of chemical, SMILES, and retention times (RT) in the LC column in minutes. The RT was not available for OMPs not present in the performance standard list (Table S2.2).

Name	Type	SMILES	RT (min)
1H-benzotriazole	Industrial chemical	C1=CC2=NNN=C2C=C1	7.96
1-Hydroxyibuprofen	Pharmaceutical	CC(C)C(C1=CC=C(C=C1)C(C)C(=O)O)O	
2-(Methylamino)pyridine	Pharmaceutical	CNC1=CC=CC=N1	
2,4,5-Trichlorophenoxyacetic acid	Pesticide	C1=C(C(=CC(=C1Cl)Cl)Cl)OCC(=O)O	
2,4-Dichlorophenoxyacetic acid	Pesticide	C1=CC(=C(C=C1Cl)Cl)OCC(=O)O	15.26
2,6-Dichlorobenzamide	Pesticide	C1=CC(=C(C(=C1)Cl)C(=O)N)Cl	8.18
2-Hydroxyquinoline	Industrial chemical	C1=CC=C2C(=C1)C=CC(=O)N2	9.16
3-Hydroxycarbamazepine	Pharmaceutical	C1=CC=C2C(=C1)C=CC3=C(N2C(=O)N)C=C(C=C3)O	11.64
4,6-Dinitro-o-cresol	Pesticide	CC1=CC(=CC(=C1O)[N+](=O)[O-])[N+](=O)[O-]	15.91
4-Hydroxyquinoline	Industrial chemical	C1=CC=C2C(=C1)C(=O)C=CN2	5.98
6-hydroxyquinoline	Industrial chemical	C1=CC2=C(C=CC(=C2)O)N=C1	
Acesulfame K	Industrial chemical	CC1=CC(=O)[N-]S(=O)(=O)O1.[K+]	3.19
Paracetamol	Pharmaceutical	CC(=O)NC1=CC=C(C=C1)O	
Ametryn	Pesticide	CCNC1=NC(=NC(=N1)SC)NC(C)C	12.82
Antipyrine	Pharmaceutical	CC1=CC(=O)N(N1C)C2=CC=CC=C2	8.64
Atenolol	Pharmaceutical	CC(C)NCC(COC1=CC=C(C=C1)CC(=O)N)O	3.78
Atrazine	Pesticide	CCNC1=NC(=NC(=N1)Cl)NC(C)C	
Azinophos-ethyl	Pesticide	CCOP(=S)(OCC)SCN1C(=O)C2=CC=CC=C2N=N1	19.19
Bentazon	Pesticide	CC(C)N1C(=O)C2=CC=CC=C2NS1(=O)=O	14.47
Bezafibrate	Pharmaceutical	CC(C)(C(=O)O)OC1=CC=C(C=C1)CCNC(=O)C2=CC=C(C=C2)Cl	15.92
Caffeine	Pharmaceutical	CN1C=NC2=C1C(=O)N(C(=O)N2C)C	6.83
Carbamazepine	Pharmaceutical	C1=CC=C2C(=C1)C=CC3=CC=CC=C3N2C(=O)N	13.23
Chloroxuron	Pesticide	CN(C)C(=O)NC1=CC=C(C=C1)OC2=CC=C(C=C2)Cl	
Climbazole	Pharmaceutical	CC(C)(C)C(=O)C(N1C=CN=C1)OC2=CC=C(C=C2)Cl	14.3
Clindamycin	Pharmaceutical	CCCC1CC(N(C1)C)C(=O)NC(C2C(C(C(C(O2)SC)O)O)O)C(C)Cl	10.62
Clofibric acid	Pharmaceutical	CC(C)(C(=O)O)OC1=CC=C(C=C1)Cl	
Clomazone	Pesticide	CC1(CON(C1=O)CC2=CC=CC=C2Cl)C	
Cyanazine	Pesticide	CCNC1=NC(=NC(=N1)Cl)NC(C)(C)C#N	12.98
DEET	Pesticide	CCN(CC)C(=O)C1=CC=CC(=C1)C	14.81
Desmetryne	Pesticide	CC(C)NC1=NC(=NC(=N1)NC)SC	11.1
Diclofenac	Pharmaceutical	C1=CC=C(C(=C1)CC(=O)O)NC2=C(C=CC=C2Cl)Cl	18.31

Diglyme	Industrial chemical	COCCOCCOC	5.68
Dimefuron	Pesticide	CC(C)(C)C1=NN(C(=O)O1)C2=C(C=C(C=C2)NC(=O)N(C)C)Cl	16.08
Dimethametryn	Pesticide	CCNC1=NC(=NC(=N1)SC)NC(C)C(C)C	
Dimethanamid-p	Pharmaceutical	CC1=CSC(=C1N(C(C)COC)C(=O)CCl)C	17.33
Diuron	Pesticide	CN(C)C(=O)NC1=CC(=C(C=C1)Cl)Cl	15.06
Ethofumesate	Pesticide	CCOC1C(C2=C(O1)C=CC(=C2)OS(=O)(=O)C)(C)C	18.46
Fenuron	Pesticide	CN(C)C(=O)NC1=CC=CC=C1	9.43
Fipronil	Pesticide	C1=C(C=C(C(=C1Cl)N2C(=C(C(=N2)C#N)S(=O)C(F)(F)F)N)Cl)C(F)(F)F	19.89
Fluometuron	Pesticide	CN(C)C(=O)NC1=CC=CC(=C1)C(F)(F)F	
Fluoxastrobin (, trans-)	Pesticide	CO\N=C(\C1=NOCCO1)C1=C(OC2=C(F)C(OC3=C(Cl)C=CC=C3)=NC=N2)C=CC=C1	
Fluroxypyr	Pesticide	C(C(=O)O)OC1=NC(=C(C(=C1Cl)N)Cl)F	12.84
Furosemide	Pharmaceutical	C1=COC(=C1)CNC2=CC(=C(C=C2C(=O)O)S(=O)(=O)N)Cl	13.42
Gemfibrozil	Pharmaceutical	CC1=CC(=C(C=C1)C)OCCCC(C)(C)C(=O)O	20.12
HFPO-DA	Industrial chemical	C(=O)(C(C(F)(F)F)(OC(C(C(F)(F)F)(F)F)(F)F)(F)F)F)O	
Ibuprofen	Pharmaceutical	CC(C)CC1=CC=C(C=C1)C(C)C(=O)O	18.73
Imidacloprid	Pharmaceutical	C1CN(C(=N[N+](=O)[O-])N1)CC2=CN=C(C=C2)Cl	
Ioxynil	Pesticide	C1=C(C=C(C(=C1I)O)I)C#N	
Ketoprofen	Pharmaceutical	CC(C1=CC(=CC=C1)C(=O)C2=CC=CC=C2)C(=O)O	
Lincomycin	Pharmaceutical	CCCC1CC(N(C1)C)C(=O)NC(C2C(C(C(C(O2)SC)O)O)O)C(C)O	6.85
Linuron	Pesticide	CN(C(=O)NC1=CC(=C(C=C1)Cl)Cl)OC	17.22
MCPA	Pesticide	CC1=C(C=CC(=C1)Cl)OCC(=O)O	15.31
MCPB	Pesticide	CC1=C(C=CC(=C1)Cl)OCCCC(=O)O	
MCPP	Pesticide	CC1=C(C=CC(=C1)Cl)OC(C)C(=O)OCC2=C(C(=C(C(=C2F)F)F)F)F	16.49
Mesotrione	Pesticide	CS(=O)(=O)C1=CC(=C(C=C1)C(=O)C2C(=O)CCCC2=O)[N+](=O)[O-]	
Methabenzthiazuron	Pesticide	CNC(=O)N(C)C1=NC2=CC=CC=C2S1	
Methoxyfenozide	Pesticide	CC1=CC(=CC(=C1)C(=O)N(C(C)(C)C)NC(=O)C2=C(C(=CC=C2)OC)C)C	18.37
Metolachlor-s	Pesticide	CCC1=CC=CC(=C1N(C(C)COC)C(=O)CCl)C	
Metoprolol	Pharmaceutical	CC(C)NCC(COC1=CC=C(C=C1)CCOC)O	9.4
Metribuzin	Pesticide	CC(C)(C)C1=NN=C(N(C1=O)N)SC	
Naproxen	Pharmaceutical	CC(C1=CC2=C(C=C1)C=C(C=C2)OC)C(=O)O	
Neburon	Pesticide	CCCCN(C)C(=O)NC1=CC(=C(C=C1)Cl)Cl	

Nicosulfuron	Pesticide	CN(C)C(=O)C1=C(N=CC=C1)S(=O)(=O)NC(=O)NC2=NC(=CC(=N2)OC)OC	
N-Phenyl urea	Industrial chemical	C1=CC=C(C=C1)NC(=O)N	7.69
Pentachlorophenol	Pharmaceutical	C1(=C(C(=C(C(=C1Cl)Cl)Cl)Cl)Cl)O	20.7
PFBA	Industrial chemical	C(=O)(C(C(C(F)(F)F)(F)F)(F)F)O	8.93
PFOA	Industrial chemical	C(=O)(C(C(C(C(C(C(C(F)(F)F)(F)F)(F)F)(F)F)(F)F)(F)F)(F)F)O	16.75
Prometon	Pesticide	CC(C)NC1=NC(=NC(=N1)OC)NC(C)C	11.55
Prometryne	Pesticide	CC(C)NC1=NC(=NC(=N1)SC)NC(C)C	14.52
Propanil	Pesticide	CCC(=O)NC1=CC(=C(C=C1)Cl)Cl	
Propazine	Pesticide	CC(C)NC1=NC(=NC(=N1)Cl)NC(C)C	16.36
Propoxur	Pesticide	CC(C)OC1=CC=CC=C1OC(=O)NC	
Prosulfocarb	Pesticide	CCCN(CCC)C(=O)SCC1=CC=CC=C1	22.01
Pyridafol	Industrial chemical	C1=CC=C(C=C1)C2=NNC(=CC2=O)Cl	
Saccharin	Industrial chemical	C1=CC=C2C(=C1)C(=O)NS2(=O)=O	5.31
Simetryne	Pesticide	CCNC1=NC(=NC(=N1)SC)NCC	11.1
Sotalol	Pharmaceutical	CC(C)NCC(C1=CC=C(C=C1)NS(=O)(=O)C)O	4.57
Sulfamethazine	Pharmaceutical	CC1=CC(=NC(=N1)NS(=O)(=O)C2=CC=C(C=C2)N)C	8.37
Sulfamethoxazole	Pharmaceutical	CC1=CC(=NO1)NS(=O)(=O)C2=CC=C(C=C2)N	10.73
Teflubenzuron	Pesticide	C1=CC(=C(C(=C1)F)C(=O)NC(=O)NC2=CC(=C(C(=C2F)Cl)F)Cl)F	
Terbacil	Pesticide	CC1=C(C(=O)N(C(=O)N1)C(C)(C)C)Cl	
Terbumeton	Pesticide	CCNC1=NC(=NC(=N1)OC)NC(C)(C)C	11.78
Thiacloprid	Pesticide	C1CSC(=NC#N)N1CC2=CN=C(C=C2)Cl	
Tramadol	Pharmaceutical	CN(C)CC1CCCCC1(C2=CC(=CC=C2)OC)O	9.43
Triazophos	Pesticide	CCOP(=S)(OCC)OC1=NN(C=N1)C2=CC=CC=C2	
Triclosan	Industrial chemical	C1=CC(=C(C=C1Cl)O)OC2=C(C=C(C=C2)Cl)Cl	21.11
Triethyl phosphate	Industrial chemical	CCOP(=O)(OCC)OCC	10.94
Trimethoprim	Pharmaceutical	COC1=CC(=CC(=C1OC)OC)CC2=CN=C(N=C2N)N	7.82
Venlafaxine	Pharmaceutical	CN(C)CC(C1=CC=C(C=C1)OC)C2(CCCCC2)O	10.96

SI 2.4 patRoon identification level rules

Table S2.4. Rules for the assignation of the identification levels in patRoon. Level 3b was not applicable in this study, as the suspect lists did not contain fragment information. (Adapted from the handbook of patRoon (Helmus, 2025) updated on 24/04/2024).

Level	Description	Rules
1	Target match	Retention time deviates <12 seconds from the suspect list. In our research, level 1 was assigned to the parent compounds detected in both the performance standard and the samples with NTA.

2a	Good MS/MS library match	Suspect is top-ranked in the compound annotation results. The individualMoNAScore (MetFrag) is at least 0.9 and no other candidates were matched with the MS library.
3a	Fair library match	The individualMoNAScore is at least 0.4.
3b	Known MS/MS match	At least 3 (or all if the suspect list contains less) fragments from the suspect list must match.
3c	Good in-silico MS/MS match	The annotation MS/MS similarity (annSimComp column) is at least 0.7.
4a	Good formula MS/MS match	Suspect is top-ranked formula candidate, annotation MS/MS similarity (annSimForm column) is at least 0.7 and isotopic match (isoScore) of at least 0.5. The latter two scores are at least 0.2 higher than next best ranked candidate.
4b	Good formula isotopic pattern match	Suspect is top ranked formula candidate and isotopic match (isoScore) of at least 0.9 and at least 0.2 higher than next best ranked candidate.
5	Unknown	All else.

Supplementary scripts

Supplementary Script 2.1

```
library(patRoon)

# -------------------------
# initialization
# -------------------------

workPath <- "*file_directory*"
setwd(workPath)

# Load analysis table
anaInfoPos <- read.csv("analyses-pos.csv")
anaInfoNeg <- read.csv("analyses-neg.csv")

# -------------------------
# features
# -------------------------

# Find all features
# NOTE: see the reference manual for many more options
fListPos <- findFeatures(anaInfoPos, "openms", noiseThrInt = 4E3,
chromSNR = 5, chromFWHM = 3, minFWHM = 1, maxFWHM = 30, mzPPM = 5)

fListNeg <- findFeatures(anaInfoNeg, "openms", noiseThrInt = 4E3,
chromSNR = 5, chromFWHM = 3, minFWHM = 1, maxFWHM = 30, mzPPM = 5)

fList <- makeSet(fListPos, fListNeg, adducts = c("[M+H]+", "[M-H]-"))

# Group and align features between analyses
fGroups <- groupFeatures(fList, "openms", rtalign = TRUE)

# Basic rule based filtering
fGroups <- fGroupsF <- filter(fGroups, preAbsMinIntensity = 100,
absMinIntensity = 1E5, relMinReplicateAbundance = 1,
                  maxReplicateIntRSD=0.75, blankThreshold=5,
removeBlanks=TRUE, retentionRange = NULL, mzRange = NULL)

# -------------------------
# suspect screening for PCs
# -------------------------

# Load suspect list
suspList <- read.csv("*file_path*", stringsAsFactors = FALSE)
```

```
# NOTE: onlyHits is set to FALSE to ensure TPs can be found below
fGroups <- screenSuspects(fGroups, suspList, rtWindow = 6, mzWindow =
0.002, onlyHits = FALSE)

# To check which parents were found
write.csv(screenInfo(fGroups), "parents found in effluents.csv", quote =
TRUE, row.names = FALSE)

# -------------------------
# transformation products
# -------------------------

# Obtain TPs from list of OMPs previously detected in Haaksbergen
TPs <- TPsUF <- generateTPs("biotransformer", parents = suspList, type =
"env", generations = 2, calcSims = FALSE)

TPs <- filter(TPs, removeParentIsomers = TRUE, removeTPIsomers = FALSE,
removeDuplicates = FALSE)

TPs <- delete(TPs, j = function(tab, par)
{
    parNM <- parents(TPs)[match(par, name)]$neutralMass # parent neutral
mass
    # remove if high generation (>1) and mass is <60% of that of the
parent
    # generation one TPs are always kept and the rest only if their mass
is sufficiently high (>=60%)
    return(tab$generation > 1 & (tab$neutralMass / parNM) < 0.6)
})

TPslistCheck <- as.data.table(TPs)

# Screen TPs after filtration
suspListTPs <- convertToSuspects(TPs, includeParents = FALSE)
write.csv(suspListTPs, "SuspectListOfTPs.csv", quote = TRUE, row.names
=FALSE)

# Amend with TP screening
fGroups <- screenSuspects(fGroups, suspListTPs, rtWindow = 6, mzWindow =
0.002, onlyHits = TRUE, amend = TRUE)

# ---------------------------------
# Checking for adducts and isotopes
# ---------------------------------
```

```
# generate components from filtered fGroups
components <- generateComponents(fGroupsF, "cliquems", ppm = 7)

# Only keep results with adducts/isotope annotations
componentsF <- delete(components, j = function(ct, ...) is.na(ct$isonr)
& (is.na(ct$adduct_ion) | !ct$adduct_ion %in% c("[M+Na]+", "[M+K]+",
"[M+NH4]+", "[M-H2O]-", "[M+H]+", "[M-H]-")))

# Only keep components with at least one feature group also present in
the suspect screened data
componentsF <- delete(componentsF, j = function(ct, ...) !any(ct$group
%in% names(fGroups)))

# Remove components with only one feature group
componentsF <- filter(componentsF, size = c(2, 1E6))

# manually check/filter components
checkComponents(componentsF, fGroupsF, session = "components_check.yml")

componentsF <- filter(componentsF, checkComponentsSession =
"components_check.yml")

# To filter out unwanted adducts/isotopes:
# 1. Run checkComponents() with the newly filtered components and clean
all the results with wrong peak grouping
# 2. Note that down which fGroups were assigned with unwanted adducts,
i.e. anything that is not M+H or M-H
# 3. Delete these manually, eg fGroups <- delete(fGroups, j =
c("fGroupName1", "fGroupsName2"))
# 4 Do _not_ run selectIons()

# 1. none removed
# 2. "M198_R142_8713", "M204_R658_9624", "M213_R889_11250",
"M265_R138_21546", "M281_R139_24922", "M258_R795_19959",
"M274_R795_23360", "M259_R413_20211", "M278_R699_24247"
fGroups <- delete(fGroups, j = c("M198_R142_8713", "M204_R658_9624",
"M213_R889_11250", "M265_R138_21546", "M281_R139_24922",
"M258_R795_19959", "M274_R795_23360", "M259_R413_20211",
"M278_R699_24247"))

# -------------------------
# annotation
# -------------------------

# Retrieve MS peak lists
avgMSListParams <- getDefAvgPListParams(clusterMzWindow = 0.005)
```

```
mslists <- generateMSPeakLists(fGroups, "mzr", maxMSRtWindow=5,
       precursorMzWindow=0.5,
       avgFeatParams = avgMSListParams,
       avgFGroupParams = avgMSListParams)
# Rule based filtering of MS peak lists. You may want to tweak this. See
the manual for more information.
mslists <- filter(mslists, absMSIntThr = NULL, absMSMSIntThr = NULL,
relMSIntThr = NULL, relMSMSIntThr = 0.02,
                  topMSPeaks = NULL, topMSMSPeaks = 10)

# Calculate formula candidates
formulas <- generateFormulas(fGroups, mslists, "genform", relMzDev = 5,
elements = "CHNOPSClBr", oc = FALSE, calculateFeatures = TRUE,
featThresholdAnn =0.75, setThresholdAnn = 0)

convertToMFDB(TPs, "TP-database.csv", includeParents = TRUE)
# Calculate compound structure candidates
compounds <- generateCompounds(fGroups, mslists, "metfrag", dbRelMzDev =
5, fragRelMzDev = 5, fragAbsMzDev = 0.002,
                               database = "csv",
                               extraOpts = list(LocalDatabasePath = "TP-
database.csv"),  maxCandidatesToStop = 2500, setThresholdAnn= 0)

compounds <- addFormulaScoring(compounds, formulas, updateScore = TRUE)

# Annotate suspects
fGroups <- annotateSuspects(fGroups, formulas = formulas, compounds =
compounds, MSPeakLists = mslists, IDFile = "idlevelrules.yml")

#Remove ID level 5
fGroupsLowLev <- filter(fGroups, maxLevel = 4, negate = TRUE)
fGroupsLowLev <- filter(fGroupsLowLev, onlyHits = TRUE) # (need to do
this in two steps as we negate above)
# fGroupsLowLev now contains all suspects with L5
write.csv(screenInfo(fGroupsLowLev), "TPs_ID5.csv", quote = TRUE,
row.names = FALSE)

# to proceed with L4 or better:
fGroups <- filter(fGroups, maxLevel = 4, onlyHits = TRUE)

# -------------------------
# Parent and TP linkage
# -------------------------

# You probably want to prioritize the data before componentization.
Please see the handbook for more info.
```

```
componentsTP <- generateComponents(fGroups[, suspects = suspList$name],
"tp", fGroupsTPs = fGroups, TPs = TPs, MSPeakLists = mslists, formulas =
formulas, compounds = compounds, ignoreParents = TRUE)

# retDirMatch: If TRUE only keep TPs with an expected chromatographic
retention direction compared to the parent.
componentsTP <- filter(componentsTP, retDirMatch = TRUE, minSpecSim =
NULL, minSpecSimPrec = NULL, minSpecSimBoth = NULL, minFragMatches =
NULL, minNLMatches = NULL)

# Only keep linked feature groups
fGroups_linked <- fGroups[results = componentsTP]

checkFeatures(fGroups) #creates a checked-features.yml file
fGroups <- filter(fGroups, checkFeaturesSession = TRUE)

# FILTERS TO PLOT

# if the same suspect is assigned to multiple fGroups, select the one
with the best ID level
fGroupsToPlot_bestID <- filter(fGroups, selectHitsBy = "level", onlyHits
= TRUE)

# same, but highest average sample intensity
fGroupsToPlot_bestID_int <- filter(fGroupsToPlot_bestID, selectHitsBy =
"intensity", onlyHits = TRUE)

# if the same fGroup is assigned to multiple suspects, only keep the the
one with highest ID level
fGroupsToPlot <- filter(fGroupsToPlot_bestID_int, selectBestFGroups =
TRUE, onlyHits = TRUE)

# OVERLAP TPs WITH PUBCHEM DATABASE

# NOTE: keep generations the same as for biotransformer
TPsPC <- generateTPs("library", parents = suspList, generations = 2,
calcSims = FALSE)

screeningTabOv <- data.table::copy(screenInfo(fGroups))
screeningTabOv[, inPC := {
  parentName <- sub("-TP[[:digit:]]+$", "", name)
  InChIKey %in% TPsPC[[parentName]]$InChIKey
}, by = seq_len(nrow(screeningTabOv))]
screeningTabOv <- screeningTabOv[inPC == TRUE] # full overlap table
unique(screeningTabOv$name) # just the unique TP names (no duplicate
lines)
```

```
write.csv(screeningTabOv, "OverlappingPubChem-BioTransformer.csv", quote
= TRUE, row.names = FALSE)

table4fGroups <- as.data.table(fGroups, onlyHits=T)

# -------------------------
# reporting
# -------------------------

# Advanced report settings can be edited in the report.yml file.
report(fGroups, MSPeakLists = mslists, formulas = formulas, compounds =
       compounds, components = componentsTP,
      TPs = TPs, settingsFile = "report.yml", openReport = TRUE)

# To plot
report(fGroupsToPlot, MSPeakLists = mslists, formulas = formulas,
compounds =   compounds, components = componentsTP,
      TPs = TPs, settingsFile = "report_toPlot.yml", openReport = TRUE)


# ------------------------------------------------------------------------
# PERFORMANCE STANDARD
# ------------------------------------------------------------------------

# Load analysis table
anaInfoPos_PS <- read.csv("PerfSt_analyses-pos.csv")
anaInfoNeg_PS <- read.csv("PerfSt_analyses-neg.csv")

# -------------------------
# features in Perf St
# -------------------------
fListPos_PS <- findFeatures(anaInfoPos_PS, "openms", noiseThrInt = 4E3,
chromSNR = 5, chromFWHM = 3, minFWHM = 1,
                        maxFWHM = 30, mzPPM = 5)
fListNeg_PS <- findFeatures(anaInfoNeg_PS, "openms", noiseThrInt = 4E3,
chromSNR = 5, chromFWHM = 3, minFWHM = 1,
                        maxFWHM = 30, mzPPM = 5)

fList_PS <- makeSet(fListPos_PS, fListNeg_PS, adducts = c("[M+H]+", "[M-
H]-"))

# Group and align features between analyses
fGroups_PS <- groupFeatures(fList_PS, "openms", rtalign = TRUE)

# Basic rule based filtering
```

```
fGroups_PS <- fGroupsF_PS <- filter(fGroups_PS, preAbsMinIntensity =
100, absMinIntensity = 1E5, relMinReplicateAbundance = 1,
maxReplicateIntRSD = 0.75, blankThreshold = 5, removeBlanks = TRUE,
retentionRange = NULL, mzRange = NULL)

# ------------------------------------
# suspect screening for PCs in PerfSt
# ------------------------------------

# Load suspect list
suspList_PS <- read.csv("*file_path*.csv", stringsAsFactors = FALSE)

# NOTE: onlyHits is set to FALSE to ensure TPs can be found below
fGroups_PS <- screenSuspects(fGroups_PS, suspList_PS, rtWindow = 6,
mzWindow = 0.002, onlyHits = TRUE)

# To check which parents were found
write.csv(screenInfo(fGroups_PS), "Spiked and found in PerfSt.csv",
quote = TRUE, row.names = FALSE)

# --------------------------------
# COMPONENTISATION FOR PERF STAND
# --------------------------------

# generate components from filtered fGroups
components_PS <- generateComponents(fGroupsF_PS, "cliquems", ppm = 7)
# Only keep results with adducts/isotope annotations
componentsF_PS <- delete(components_PS, j = function(ct, ...)
is.na(ct$isonr) & (is.na(ct$adduct_ion) | !ct$adduct_ion %in%
c("[M+Na]+", "[M+K]+", "[M+NH4]+", "[M-H2O]-", "[M+H]+", "[M-H]-")))

# Only keep components with at least one feature group also present in
the suspect screened data
componentsF_PS <- delete(componentsF_PS, j = function(ct, ...)
!any(ct$group %in% names(fGroups_PS)))

# Remove components with only one feature group (useless)
componentsF_PS <- filter(componentsF_PS, size = c(2, 1E6))

# manually check/filter components
checkComponents(componentsF_PS, fGroupsF_PS, session =
"components_check_PS.yml")
componentsF_PS <- filter(componentsF_PS, checkComponentsSession =
"components_check_PS.yml")

#to filter out unwanted adducts/isotopes
```

```
fGroups_PS <- delete(fGroups_PS, j = c("M186_R568_1861",
"M210_R520_2325", "M213_R889_2410", "M250_R704_3437", "M254_R903_3542",
"M258_R795_3682", "M274_R700_4020", "M275_R646_4036", "M300_R505_4617",
"M360_R966_5824", "M383_R956_6202", "M390_R1103_6284"))

# -------------------------
# annotation
# -------------------------

# Retrieve MS peak lists
avgMSListParams <- getDefAvgPListParams(clusterMzWindow = 0.005)
mslists_PS <- generateMSPeakLists(fGroups_PS, "mzr", maxMSRtWindow = 5,
precursorMzWindow = 0.5, avgFeatParams = avgMSListParams,
avgFGroupParams = avgMSListParams)
# Rule based filtering of MS peak lists. You may want to tweak this. See
the manual for more information.
mslists_PS <- filter(mslists_PS, absMSIntThr = NULL, absMSMSIntThr =
NULL, relMSIntThr = NULL, relMSMSIntThr = 0.02, topMSPeaks = NULL,
topMSMSPeaks = 10)

# Calculate formula candidates
formulas_PS <- generateFormulas(fGroups_PS, mslists_PS, "genform",
relMzDev = 5, elements = "CHNOPSClBr", oc = FALSE, calculateFeatures
=TRUE, featThresholdAnn = 0.75, setThresholdAnn = 0)

# Calculate compound structure candidates
compounds_PS <- generateCompounds(fGroups_PS, mslists_PS, "metfrag",
dbRelMzDev = 5, fragRelMzDev = 5, fragAbsMzDev = 0.002, database =
"pubchemlite", maxCandidatesToStop = 2500, setThresholdAnn = 0)

compounds_PS <- addFormulaScoring(compounds_PS, formulas_PS, updateScore
= TRUE)

# Annotate suspects
fGroups_PS <- annotateSuspects(fGroups_PS, formulas = formulas_PS,
compounds = compounds_PS, MSPeakLists = mslists_PS, IDFile =
"idlevelrules.yml")

#Remove ID level 5
fGroupsLowLev_PS <- filter(fGroups_PS, maxLevel = 4, negate = TRUE)
fGroupsLowLev_PS <- filter(fGroupsLowLev_PS, onlyHits = TRUE) # (need to
do this in two steps as we negate above)
# fGroupsLowLev now contains all suspects with L5
write.csv(screenInfo(fGroupsLowLev_PS), "Compounds_perfSt_ID5.csv",
quote = TRUE, row.names = FALSE)
```

```
# to proceed with L4 or better:
fGroups_PS <- filter(fGroups_PS, maxLevel = 4, onlyHits = TRUE)

checkFeatures(fGroups_PS, session = "checked-features_PS.yml")
fGroups_PS <- filter(fGroups_PS, checkFeaturesSession = "checked-
features_PS.yml")

# -------------------------
# reporting Perf standard
# -------------------------

# Advanced report settings can be edited in the report.yml file.
report(fGroups_PS, MSPeakLists = mslists_PS, formulas = formulas_PS,
compounds = compounds_PS, settingsFile = "report_PS.yml", openReport =
TRUE)
```

Supplementary script 2.2

```
library(patRoon)

# -------------------------
# initialization
# -------------------------

workPath <- "*files_directory*"
setwd(workPath)

# Load analysis table
anaInfoPos <- read.csv("Field_analyses-pos.csv")
anaInfoNeg <- read.csv("Field_analyses-neg.csv")

# -------------------------
# features
# -------------------------

# Find all features
fListPos <- findFeatures(anaInfoPos, "openms", noiseThrInt = 4E3,
chromSNR = 5, chromFWHM = 3, minFWHM = 1, maxFWHM = 30, mzPPM = 5)

fListNeg <- findFeatures(anaInfoNeg, "openms", noiseThrInt = 4E3,
chromSNR = 5, chromFWHM = 3, minFWHM = 1, maxFWHM = 30, mzPPM = 5)

fList <- makeSet(fListPos, fListNeg, adducts = c("[M+H]+", "[M-H]-"))

# Group and align features between analyses
fGroups <- groupFeatures(fList, "openms", rtalign = TRUE)

# Basic rule based filtering
fGroups <- fGroupsF <- filter(fGroups, preAbsMinIntensity = 100,
absMinIntensity = 1E5, relMinReplicateAbundance = 1, maxReplicateIntRSD
= 0.75, blankThreshold = 5, removeBlanks = TRUE,
retentionRange = NULL, mzRange = NULL)

# -------------------------
# suspect screening for PCs
# -------------------------

# Load suspect list
suspList <- read.csv("*file_path*.csv", stringsAsFactors = FALSE)

# NOTE: onlyHits is set to FALSE to ensure TPs can be found below
```

```
fGroups <- screenSuspects(fGroups, suspList, rtWindow = 6, mzWindow =
0.002, onlyHits = FALSE)

# To check which parents were found
write.csv(screenInfo(fGroups), "parents found in field.csv", quote =
TRUE, row.names = FALSE)

# -------------------------
# transformation products
# -------------------------

# Obtain TPs from Dominique's list - we can modify here the generation
level
TPs <- generateTPs("biotransformer", parents = suspList, type = "env",
generations = 2, calcSims = FALSE)

# Filter TPs
TPs <- filter(TPs, removeParentIsomers = TRUE, removeTPIsomers = FALSE,
removeDuplicates = FALSE)

TPs <- delete(TPs, j = function(tab, par)
{
  parNM <- parents(TPs)[match(par, name)]$neutralMass # parent neutral
mass
  # remove if high generation (>1) and mass is <60% of that of the
parent
  # generation 1 TPs are always kept and the rest only if their mass is
sufficiently high (>=60%)
  return(tab$generation > 1 & (tab$neutralMass / parNM) < 0.6)
})

TPslistCheck <- as.data.table(TPs)

# Screen TPs
suspListTPs <- convertToSuspects(TPs, includeParents = FALSE)
write.csv(suspListTPs, "SuspectListOfTPs_FIELD.csv", quote = TRUE,
row.names = FALSE) # to share list of TPs suspects

# Amend with TP screening
fGroups <- screenSuspects(fGroups, suspListTPs, rtWindow = 6, mzWindow =
0.002, onlyHits = TRUE, amend = TRUE)

#--------------------------------------
# Checking for adducts and isotopes
#--------------------------------------
```

```
# generate components from filtered fGroups
components <- generateComponents(fGroupsF, "cliquems", ppm = 7)

# Only keep results with adducts/isotope annotations and remove exhotic
adducts
componentsF <- delete(components, j = function(ct, ...) is.na(ct$isonr)
& (is.na(ct$adduct_ion) | !ct$adduct_ion %in% c("[M+Na]+", "[M+K]+",
"[M+NH4]+", "[M-H2O]-", "[M+H]+", "[M-H]-")))

# Only keep components with at least one feature group also present in
the suspect screened data
componentsF <- delete(componentsF, j = function(ct, ...) !any(ct$group
%in% names(fGroups)))

# Remove components with only one feature group
componentsF <- filter(componentsF, size = c(2, 1E6))

# manually check/filter components
checkComponents(componentsF, fGroupsF, session = "components_check.yml")
componentsF <- filter(componentsF, checkComponentsSession =
"components_check.yml")

# to manually filter out unwanted adducts/isotopes
fGroups <- delete(fGroups, j = c("M193_R489_29110", "M212_R426_38526",
"M_239_R413_53204", "M222_R836_43707", "M230_R592_47902",
"M249_R719_58544", "M251_R212_59993", "M275_R844_75336",
"M264_R750_68453", "M293_R1065_87433", "M308_R338_97575",
"M341_R888_120145"))

# -------------------------
# annotation
# -------------------------

# Retrieve MS peak lists
avgMSListParams <- getDefAvgPListParams(clusterMzWindow = 0.005)
mslists <- generateMSPeakLists(fGroups, "mzr", maxMSRtWindow = 5,
precursorMzWindow = 0.5, avgFeatParams = avgMSListParams,
avgFGroupParams = avgMSListParams)

# Rule based filtering of MS peak lists.
mslists <- filter(mslists, absMSIntThr = NULL, absMSMSIntThr = NULL,
relMSIntThr = NULL, relMSMSIntThr = 0.02, topMSPeaks =NULL, topMSMSPeaks
= 10)

# Calculate formula candidates
```

```
formulas <- generateFormulas(fGroups, mslists, "genform", relMzDev = 5,
elements = "CHNOPSClBr", oc = FALSE, calculateFeatures = TRUE,
featThresholdAnn= 0.75, setThresholdAnn = 0)

convertToMFDB(TPs, "TP-database.csv", includeParents = TRUE)

# Calculate compound structure candidates
compounds <- generateCompounds(fGroups, mslists, "metfrag", dbRelMzDev =
5, fragRelMzDev = 5, fragAbsMzDev = 0.002, database = "csv", extraOpts =
list(LocalDatabasePath = "TP-database.csv"), maxCandidatesToStop = 2500,
setThresholdAnn = 0)

compounds <- addFormulaScoring(compounds, formulas, updateScore = TRUE)

# Annotate suspects
fGroups <- annotateSuspects(fGroups, formulas = formulas, compounds =
compounds, MSPeakLists = mslists, IDFile = "idlevelrules.yml")

#Remove ID level 5
fGroupsLowLev <- filter(fGroups, maxLevel = 4, negate = TRUE)
fGroupsLowLev <- filter(fGroupsLowLev, onlyHits = TRUE) # (need to do
this in two steps as we negate above)
# fGroupsLowLev now contains all suspects with L5
write.csv(screenInfo(fGroupsLowLev), "FieldTPs_ID5.csv", quote = TRUE,
row.names = FALSE)

# to proceed with L4 or better:
fGroups <- filter(fGroups, maxLevel = 4, onlyHits = TRUE)

# -------------------------
# Parent and TP linkage
# -------------------------

componentsTP <- generateComponents(fGroups[, suspects = suspList$name],
"tp", fGroupsTPs = fGroups, TPs = TPs, MSPeakLists = mslists,
formulas = formulas, compounds = compounds, ignoreParents = TRUE)

# retDirMatch: If TRUE only keep TPs with an expected chromatographic
retention direction compared to the parent.
componentsTP <- filter(componentsTP, retDirMatch = TRUE, minSpecSim =
NULL, minSpecSimPrec = NULL, minSpecSimBoth = NULL, minFragMatches =
NULL, minNLMatches = NULL)

# Only keep linked feature groups
fGroups_linked <- fGroups[results = componentsTP]
```

```
checkFeatures(fGroups) #creates a checked-features.yml file
fGroups <- filter(fGroups, checkFeaturesSession = TRUE)

# FILTERS TO PLOT

# if the same suspect is assigned to multiple fGroups, select the one
with the best ID level
fGroupsToPlot_bestID <- filter(fGroups, selectHitsBy = "level", onlyHits
= TRUE)

# same, but highest average sample intensity
fGroupsToPlot_bestID_int <- filter(fGroupsToPlot_bestID, selectHitsBy =
"intensity", onlyHits = TRUE)

# if the same fGroup is assigned to multiple suspects, only keep the the
one with highest ID level
fGroupsToPlot <- filter(fGroupsToPlot_bestID_int, selectBestFGroups =
TRUE, onlyHits = TRUE)

# OVERLAP TPs WITH PUBCHEM
# NOTE: keep generations the same as for biotransformer
TPsPC <- generateTPs("library", parents = suspList, generations = 2,
calcSims = FALSE)

screeningTabOv <- data.table::copy(screenInfo(fGroups))
screeningTabOv[, inPC := {
  parentName <- sub("-TP[[:digit:]]+$", "", name)
  InChIKey %in% TPsPC[[parentName]]$InChIKey
}, by = seq_len(nrow(screeningTabOv))]
screeningTabOv <- screeningTabOv[inPC == TRUE] # full overlap table
unique(screeningTabOv$name) # just the unique TP names (no duplicate
lines)

write.csv(screeningTabOv, "OverlappingPubChem-BioTransformer_FIELD.csv",
quote = TRUE, row.names = FALSE)

# -------------------------
# reporting
# -------------------------

# Advanced report settings can be edited in the report.yml file.
report(fGroups, MSPeakLists = mslists, formulas = formulas, compounds =
compounds, components = componentsTP, TPs = TPs, settingsFile =
"report.yml", openReport
```

Supplementary Excel 2

Supplementary Excel (SE) tables can be downloaded from:
https://doi.org/10.1021/acsestwater.4c00930

Chapter 3

Removal, transport, and transformation of organic micropollutants in managed aquifer recharge: insights from target and non-target analyses

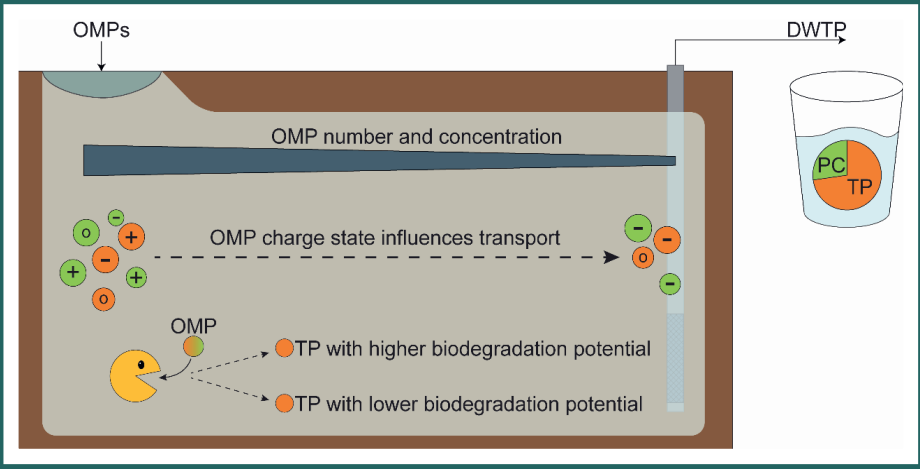

A modified version of this chapter has been published as:

Ore, A., Sigmund, G., Specker, J., Helmus, R., Aguilar-Alarcón, P., Schriks, M., van Wezel, A.P., Sutton, N.B., **2025**. Removal, transport, and transformation of organic micropollutants in managed aquifer recharge: Insights from target and non-target analyses. **Water Research**. https://doi.org/10.1016/j.watres.2025.124409

Abstract

Managed aquifer recharge (MAR) systems can reduce the stress on groundwater resources by intentionally infiltrating and abstracting (surface) water for drinking water production. Organic micropollutant (OMP) removal and transformation products (TPs) formation in MAR depend on several factors, including their sorption and biodegradation potential. Via target and non-target analyses, we monitored OMPs (parent compounds + TPs) from infiltrated water to abstracted groundwater and drinking water. Our results show that MAR improves water quality, with 61% of the 31 OMPs in the infiltrated water being removed by >90%. However, persistent contaminants, including artificial sweeteners and PFAS, were not removed and reached drinking water. The charge state of hydrophilic OMPs determined transport, which was driven by electrostatic interactions with soil: positively charged OMPs were retained near the infiltration point, while negatively charged OMPs travelled to the groundwater abstraction wells. Our results reveal important blind spots in the standard list of priority OMPs measured to assess drinking water quality. Specifically, non-target analysis revealed 50% more OMPs than those detected using target analysis, and uncovered many overlooked TPs. 46 TPs were detected in groundwater but were absent in infiltrated water, indicating possible OMP biodegradation in MAR. However, 28 possibly persistent TPs were also detected in the MAR system. Therefore, post-treatment technologies targeting persistent and mobile contaminants should be applied to complement MAR at the drinking water treatment plant. Our findings can contribute to optimizing MAR systems for improved OMP removal and highlight the need for a more comprehensive approach to water quality assessment for cleaner drinking water production.

Keywords

Micropollutant biodegradation; water reuse; drinking water quality; transformation products; non-target screening.

3.1 Introduction

In the Netherlands, freshwater scarcity due to intensive water use and droughts has increased the interest in water reuse technologies to safeguard groundwater resources. Managed aquifer recharge (MAR) is a nature-based technology employing intentional infiltration or injection of recycled water, including surface water and treated wastewater, into groundwater (Dillon et al., 2009). MAR has been in use for decades in many countries, mainly for drinking water production, as it ensures a stable water quantity for stressed groundwater systems (Dillon et al., 2019; Maeng et al., 2011; Mumberg et al., 2024). However, concerns about its effect on natural groundwater quality remain, due to the presence of organic micropollutants (OMPs), including polar and persistent compounds, in the infiltrated water (Drewes, 2009; Maeng et al., 2011). MAR systems are not specifically designed for OMP removal, causing OMPs to potentially accumulate, leach, or transform in the subsurface, thus possibly impacting drinking water sources.

Infiltration in MAR can be achieved via ponds that allow the water to percolate through soil, where chemical, physical, and biological processes alter water quality (Regnery et al., 2017). Once in the subsurface, the OMPs infiltrating with water are removed primarily via biodegradation, but they can also undergo sorption or other abiotic transformation processes (Narain-Ford et al., 2020). However, OMP transformation is often incomplete and leads to the formation of transformation products (TPs), which are generally more mobile and may be more persistent or toxic than the parent compounds (PCs) (Hübner et al., 2022; Oberleitner et al., 2021).

Knowledge of OMP fate, TP formation, and their transport in MAR systems is limited (Mumberg et al., 2024; Specker et al., 2025). TPs are often overlooked because they are challenging to detect and partly unknown. Nonetheless, there is increasing focus on their identification for a more comprehensive environmental chemical risk assessment, especially using high-resolution mass-spectrometry (HRMS) technologies, which allow broader OMP detection (Escher and Fenner, 2011; Ore et al., 2025a; Zahn et al., 2024). OMP fate and TP formation in the subsurface depend on several factors, including OMP physicochemical and intrinsic properties (e.g. charge state, mobility, persistence) and *in situ* environmental conditions, including hydrogeology, redox conditions, dissolved organic carbon availability, soil and microbial compositions (Maeng et al., 2011; Zhou et al., 2025). Additionally, Dutch MAR system conditions differ from other countries due to the generally high groundwater tables in the Netherlands. The unsaturated zone between the ground surface and the groundwater table is thin, resulting in more anaerobic conditions and allowing the artificially infiltrated water to mix with naturally infiltrating groundwater almost immediately. These factors must be considered to understand OMP fate and TP formation in MAR.

Although TPs are not specifically listed in current European water regulations, they are indirectly addressed. The Water Framework Directive (WFD) sets groundwater quality standards for pesticides and their relevant metabolites, and the proposed *Amendment to the WFD, the Groundwater Directive, and the Environmental Quality Standards Directive* extends these standards to include active pharmaceutical substances and relevant pharmaceutical TPs (Directorate-General for Environment, 2022b; European Parliament and Council of the European Union, 2006b, 2000). These regulations provide general criteria for assessing TP relevance, focusing on toxicity, persistence, and potential bioaccumulation, yet they often leave room for interpretation. Given the uncertain but increasing inclusion of TPs in regulation, studying them is important to assess their environmental presence, potential exposure, and relevance for regulatory inclusion.

Our study investigated the occurrence of OMPs (including PCs and TPs) in a Dutch MAR system with infiltration ponds, which is used to produce drinking water and to compensate for groundwater abstraction. Through liquid chromatography (LC)-HRMS-based target and non-target analyses of water samples collected along the water infiltration path, we aimed to: (1) assess the extent to which MAR can improve water quality for drinking water production, taking into account both target and non-target analyses of OMPs; and (2) infer the effect of OMP charge state, mobility and persistence on their fate and removal in MAR. We present novel insights into the occurrence and behavior of (unknown) OMPs in MAR systems, contributing to a more comprehensive exposure assessment and improved management of OMPs in the environment.

3.2 Materials and Methods

3.2.1 Description of the site

The samples were collected from a drinking water production area in the east of the Netherlands, managed by Vitens drinking water company. The soil in the area is mainly composed of sand and clay layers. The study area consists of multiple groundwater abstraction fields that supply drinking water to nearby municipalities. Our study focuses on the Olden-Eibergen abstraction field, where groundwater has been abstracted since 1935 through six wells at 19-30 m depth below ground level (phreatic abstraction).

The groundwater in the area is supplied by natural infiltration of rain and surface water and by artificial active infiltration via a MAR system since 1975. Water is diverted from the river Berkel to infiltration ponds, which account for approximately 20% of the abstracted water at Olden-Eibergen. River Berkel's water quality is affected by five wastewater treatment plants (WWTPs) in Germany and agricultural runoff along the waterway. The land use in the groundwater catchment and protection area is mainly forest and agricultural, with grassland

and arable farming that may contribute to pesticides or veterinary pharmaceuticals leaching.

The raw water from Olden-Eibergen is further treated in the nearby drinking water treatment plant, mainly by sand filtration and softening (details in SI 3.2.1). The water is mixed with water from other abstraction fields and production stations and stored in a subsurface reservoir before distribution.

Before this study, a bromide tracer test estimated that in Olden-Eibergen the infiltrated water travels through the subsurface for approximately one year before reaching the abstraction wells (Cirkel, 2017). Bromide breakthrough was followed from the injection point near the pond to the abstraction well (AW) with the highest infiltration contribution (AW1). Our study includes data from two tracer test monitoring wells (M1 and M2), AW1, and another abstraction well (AW2) within the infiltration area but not included in the tracer test (Figure 3.1).

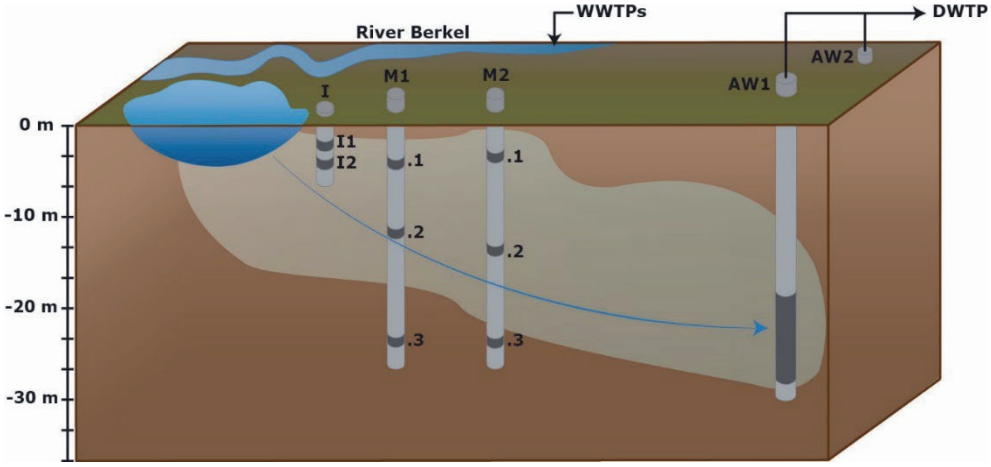

Figure 3.1. Schematic representation of the MAR system. Water from the river Berkel (receiving wastewater treatment plant -WWTP- effluents) is infiltrated via a pond. The monitoring wells (I, M1, and M2) are along the infiltration path to the abstraction well that attracts the most infiltrated water (AW1) from the pond. The abstracted water from AW1 and AW2 is pumped to the drinking water treatment plant (DWTP). The sampling points' depth refers to the scale on the left of the figure.

3.2.2 Sample collection

A sampling campaign at 11 sampling points was performed in June 2023 (Figure S3.1, Table S3.1), including groundwater from two depths of the monitoring well I (proxy for the infiltrated water composition), three depths for each of the monitoring wells M1 and M2 and abstracted water from two AWs (AW1 and AW2) within the infiltration area. A drinking water sample was taken at the production facility, composed of a mixture of abstracted groundwater from the Olden-Eibergen and other nearby abstraction fields (Table S3.2). These groundwater locations were selected based on their position along the water

infiltration path through the subsurface. The details of the water sampling procedure are reported in SI 3.2.2.

Macrochemistry data and OMP concentrations over 5 years (2015-2020) were shared by Vitens and used as supporting data for our in-depth analysis of a single time point (Supplementary Excel -SE- 3 Table E1).

3.2.3 Environmental data collection

During the sampling campaign, pH, electroconductivity, and temperature were measured *in situ*, and water samples were taken for chloride, nitrate, nitrite, manganese, iron, sulfate, bromide, carbonate, carbonic acid, methane, and dissolved organic carbon measurements. Vitens performed these analyses and provided the results (relevant measured parameters are reported in Table S3.3).

3.2.4 OMP analysis

The samples were analyzed with target (both by Vitens and at the University of Amsterdam - UvA) and non-target analyses (at UvA) to quantify and qualify OMPs, respectively. Vitens' target data were mainly used to discuss results, whereas UvA target data were used as a support for non-target data analysis only (e.g., OMP identification level assignment).

Vitens' target analysis used high-pressure liquid chromatography (HPLC) coupled with Triple Quad/Trap mass-spectrophotometry to quantify OMPs in samples via direct injection, using a target list of 371 compounds. SI 3.2.4 and Table S3.4 provide more information on Vitens' instrumentation and method.

Before UvA target and non-target analyses, samples were concentrated by solid phase extraction (SPE) with Oasis HLB (200 mg) from Waters™, following the method as previously described (Albergamo et al., 2018). Before SPE, the samples, procedural blanks (i.e., Milli-Q water), and controls (i.e., Milli-Q spiked with 98 target OMPs at 125 ng/L) (40 mL) were spiked with a mixture of 36 isotope-labeled internal standards at 50 ng/L. After cartridge loading, washing, elution with methanol, and evaporation under nitrogen to 0.1 mL, the extracts were diluted 1:5 in MilliQ water, resulting in a final labeled internal standard concentration of 4 µg/L and an enrichment factor of 80. The extracts were stored at -20 °C until analysis with target and non-target methods using a Bruker Daltonics system composed of ultra-high-performance liquid chromatography (using a Kinetex® UPLC Biphenyl column) coupled with trapped ion mobility spectrometry, quadrupole time of flight, and high-resolution tandem mass spectrometry (SI 3.2.4 and Tables S3.5 and S3.6 report more information on UvA target and non-target methods).

3.2.4.1 Non-target analysis (NTA) data treatment with patRoon

The non-target data treatment was performed through open-source software, including TIMSCONVERT 2.0.0 (Luu et al., 2022) for converting raw .tdf data to .mzML format, and patRoon 2.3.3 (Helmus, 2024) for screening TPs and predicting metabolic pathways. During conversion with TIMSCONVERT, the raw data was centroided and the trapped ion mobility arrays were excluded to allow compatibility with patRoon. The script is similar to our previous study (Ore et al., 2025a), but algorithm-specific parameters were optimized for the instrumentation and dataset (Supplementary Script 3.1). Specifically, OpenMS (Röst et al., 2016) feature finding and filtering parameters were optimized by adjusting *chromFWHM* (peak width at half the peak height), *chromSNR* (signal-to-noise ratio), and the absolute minimum peak intensity. After subtracting blanks (instrumental for the controls and SPE procedural for SPE samples), only peaks detected in all triplicate measurements were retained. A first suspect screening was performed to screen for 158 OMPs. The compounds detected in our samples with target analysis by Vitens, the spiked target OMPs in the SPE controls, and the spiked isotope-labeled internal standards were included in this suspect list. MzMine (Schmid et al., 2023) was used to inspect chromatograms for non-detected OMPs expected to be found in the samples based on target analysis results and spiked OMPs. Mostly, non-detection was due to peak intensity below the threshold applied in the script or presence of the same peak in the blanks (e.g., trifluoroacetic acid – TFA). A second suspect screening was then applied to screen for TPs up to the third generation that may have been formed from 410 OMPs, which included compounds regularly targeted by Vitens (n=276) and those spiked in the SPE control samples (n=134). The TP suspect list was generated via BioTransformer (Djoumbou-Feunang et al., 2019) with the environmental microbial degradation module (enviPath – (Wicker et al., 2016)), and included more than 15000 possible TPs (SE3 Table E2). In addition to the prioritization steps previously applied (Ore et al., 2025a), when multiple suspects with the same identification (ID) level were assigned to the same feature group, the priority was first given to PCs among the suspects (detected in the control samples or target analysis), then to the suspect with the highest compound candidate ranking. Feature groups assigned exclusively to TP candidates were removed if detected in control samples, as these should not contain biodegradation TPs, suggesting potential misannotation. Also, TPs formed later than the third stage of the transformation pathway were not addressed. Additionally, every OMP and potential TP thereof with a peak intensity lower than the applied threshold (min. intensity 7500) was not included in the dataset. Results from the UvA target analysis and the first suspect screening step were used to confirm target OMPs detection in NTA and manually assign ID level 1 when detected with both target and non-target analyses.

3.2.5 Data interpretation

The average OMP composition (i.e., type and concentration of OMPs) at sampling points I1 and I2 (Figure 1) was used as the reference for infiltrated water composition in the interpretation of target and non-target results. This accounts for the high variability in OMP concentration in surface and pond water. If the concentration at I1 or I2 was below the limit of quantification (LOQ, Table S3.4), half of the LOQ was assigned to the non-detected sample for averaging. Historical data on water composition in well I was used to support our observation and previous detection of OMPs (SE3, Table E1). Vitens' target data were used to calculate OMP removal efficiencies according to Equation 3.1, where $C_{i,inf.water}$ and $C_{i,AW}$ are the concentrations of the OMP (i) in the infiltrated water and the abstraction well, respectively.

Equation 3.1. Removal efficiency of an OMP (i).

$$RE_i = \frac{(C_{i,inf.water} - C_{i,AW})}{C_{i,inf.water}} \quad (3.1)$$

For per- and polyfluoroalkyl substances (PFAS), the relative potency factor (RPF) was used to convert their concentrations to perfluorooctanoic acid (PFOA) equivalents, allowing comparison with environmental regulations (Council of the European Union, 2025; Directorate-General for Environment, 2022a).

3.2.6 Mobility and persistence data collection

The log D_{ow} is the pH-dependent hydrophobicity proxy that takes OMP speciation into account and was used as a rough estimate of OMP mobility. The log D_{ow} parameter was calculated for each OMP detected via (Vitens) target analysis at pH 7 via ChemAxon using the SMILES of the OMPs detected in the samples (logD Predictor plugin (ChemAxon, n.d.)). ChemAxon was also used to predict the charge state of OMPs detected via target and non-target analyses at pH 7.

To estimate persistence in the MAR system of OMPs detected with target and non-target analysis, Biowin3 scores were obtained from the EPI Suite™ software (US EPA, 2025) using SMILES. Biowin3 estimates the probability of ultimate biodegradation for a given compound, i.e., the time it would take to undergo mineralization under aerobic conditions. In NTA results interpretation, the structure of the candidate with the highest priority (prioritized as explained in Section 3.2.4.1) was considered for Biowin3 calculations.

3.3 Results and Discussion

3.3.1 MAR improves water quality for most target OMPs except PFAS

The five WWTPs upstream in the River Berkel affected the quality of the water entering the MAR system, as shown by the detection of OMPs that can be traced back to WWTP origins

(Table 3.1). Particularly, the infiltrated water contained contaminants at relatively high concentrations, like the artificial sweetener sucralose (1.07 µg/L) and the X-ray contrast medium iopamidol (0.72 µg/L), observed also in previous monitoring campaigns (SE3 Table E1). TFA was also detected at relatively high concentrations (2.85 µg/L), but still well below the UBA (Umweltbundesamt-German Environmental Agency) proposed limit of 21 µg/L (UBA, 2020). TFA origin is not only related to WWTPs but also to atmospheric deposition or breakdown of fluorinated compounds (Freeling et al., 2020; Joerss et al., 2024), including pesticides that might have been applied to the fields along the waterway.

The target analysis results showed that soil passage in MAR improved the quality of the infiltrated water, providing a better starting point for drinking water production than surface water affected by WWTP effluents. Comparing infiltrated water with abstracted water (average of AW1 and AW2), the sum of PFAS concentration decreased from 2.91 to 1.52 µg/L during soil passage, and the total concentration of the other OMPs decreased from 4.38 µg/L to 1.67 µg/L. Excluding PFAS, the total OMP concentration was reduced by 62%, with 61% of the OMPs in the infiltrated water showing removal efficiencies higher than 90%, and 16 OMPs removed to concentrations below the LOQ in AW1. Our results are similar to a recent study on a similar water reuse technology, riverbank filtration (Muschket et al., 2024). While some OMPs were efficiently removed in the MAR system, others were not, and some even showed increased concentrations in the abstracted water compared to the infiltrated water. Examples are industrial products and pesticide-TPs, previously reported as persistent in the environment. Artificial sweeteners, like cyclamate, acesulfame, and sucralose, are often considered tracers of anthropogenic contamination (Lange et al., 2012). They showed an average removal of 35%, but acesulfame and cyclamate concentrations increased in AW1 compared to the infiltrated water. Metolachlor-TPs and dimethenamide-TPs were removed by only 35 to 49% in the water abstracted from AW1, and exceeded the Groundwater Framework Directive limit of 0.1 µg/L (European Parliament and Council of the European Union, 2006b). Their concentrations in AW2 were higher than in the infiltrated water, likely due to formation during soil passage (Krutz et al., 2004; Stamper and Tuovinen, 1998).

PFAS primarily persisted during MAR, with minimal removal observed. Some PFAS compounds showed reduced concentrations in AW1 compared to the infiltrated water, while others had higher concentrations (Table 3.2), possibly due to temporal variability in PFAS input. According to the hydrological regional model AMIGO (Arcadis et al., 2008; Cirkel, 2017), AW1 receives most of the infiltrated water, explaining the broader PFAS detected in this well. In contrast, many PFAS were not detected in AW2. The observed concentration decrease in AW1 and the absence of many PFAS in AW2 were most likely due to dilution with naturally infiltrating groundwater (further discussed in Section 3.3.4).

*Table 3.1. OMPs in the infiltrated water and their removal efficiency (RE) in the abstraction wells within the infiltration area and finished drinking water (mixed with other produced waters), target data. Color code: dark green = RE > 90%; light green 60% < RE < 90%; yellow 40% < RE < 60%; red RE < 40%. Italic font indicates parent compounds. Between parenthesis, the type of OMP is indicated (I = industrial component, P = pesticide, Ph = pharmaceutical). NA = Not measured. * Average concentration of two depths of monitoring well I (half the LOQ was used when one of the two depths was <LOQ).*

OMP name	Infiltrated water*	Abstraction well 1		Abstraction well 2		Finished drinking water	
	C (µg/L)	C (µg/L)	RE%	C (µg/L)	RE%	C (µg/L)	RE%
1,3-Diphenylguanidine (I)	0.017	<0.01	< LOQ	<0.01	< LOQ	<0.01	< LOQ
1H-benzotriazole (I)	NA	0.039		NA		NA	
4-methyl-1H-benzotriazole (I)	0.111	0.020	82%	<0.01	< LOQ	<0.01	< LOQ
5-methyl-1H-benzotriazole (I)	0.039	<0.01	< LOQ	<0.01	< LOQ	<0.01	< LOQ
Acesulfame (I)	0.112	0.140	-25%	0.040	64%	0.130	-16%
AMPA (P)	0.075	<0.02	< LOQ	<0.02	< LOQ	<0.02	< LOQ
BAM (P)	0.033	<0,01	< LOQ	0.017	48%	0.018	45%
Bentazon (P)	<0.01	0.014		0.021		0.019	
Carbamazepine (Ph)	0.049	<0.01	< LOQ	<0.01	< LOQ	<0.01	< LOQ
Cyclamate (I)	0.024	0.029	-23%	<0.02	< LOQ	<0.02	< LOQ
DEET (P)	0.009	<0,01	< LOQ	<0.01	< LOQ	<0.01	< LOQ
Diatrizoic acid (Ph)	0.240	<0.05	< LOQ	<0.05	< LOQ	<0.05	< LOQ
Dimethenamide-ESA (P)	0.350	0.190	46%	0.500	-43%	0.160	54%
Dimethenamide-OA (P)	0.150	0.079	47%	0.400	-167%	0.072	52%
Gabapentin (Ph)	0.266	0.135	49%	0.037	86%	0.049	82%
Iohexol (Ph)	0.093	<0.05	< LOQ	<0.05	< LOQ	<0.05	< LOQ
Iomeprol (Ph)	0.019	<0.01	< LOQ	<0.01	< LOQ	<0.01	< LOQ
Iopamidol (Ph)	**0.720**	0.180	75%	0.027	96%	0.130	82%
Irbesartan (Ph)	0.008	<0.01	< LOQ	<0.01	< LOQ	<0.01	< LOQ
Metformin (Ph)	0.008	<0.01	< LOQ	<0.01	< LOQ	<0.01	< LOQ
Metolachlor-ESA (P)	0.465	0.290	38%	0.210	55%	0.170	63%
Metholachlor-OA (P)	0.200	0.130	35%	0.260	-30%	0.120	40%
Phenazone (Ph)	0.008	<0.01	< LOQ	<0.01	< LOQ	<0.01	< LOQ
Primidone (Ph)	0.026	0.025	2%	<0.01	< LOQ	0.010	61%
Sucralose (I)	**1.075**	0.360	67%	0.076	93%	0.100	91%
Sulfamethoxazole (Ph)	0.010	<0.01	< LOQ	<0.01	< LOQ	<0.01	< LOQ
Sulfapyridine (Ph)	0.009	<0.01	< LOQ	<0.01	< LOQ	<0.01	< LOQ
Tetraglyme (I)	0.027	0.024	11%	<0.01	< LOQ	<0.01	< LOQ
Topramezone (P)	0.014	<0.01	< LOQ	<0.01	< LOQ	<0.01	< LOQ
Trans-10,11 dihydro-10,11-dihydroxy-carbamazepine *(Ph)*	0.217	0.086	60%	0.013	94%	0.031	86%
Valsartan (Ph)	0.015	<0.01	< LOQ	<0.01	< LOQ	<0.01	< LOQ
Total	**4.385**	**1.741**	**61%**	**1.601**	**63%**	**1.009**	**77%**

Table 3.2. PFAS detected in the infiltrated water and their removal efficiency (RE) based on actual concentrations in ng/L in the abstraction wells within the infiltration area and finished drinking water (mixed with other produced waters), target data. Color code: dark green = RE > 90%; light green 60% < RE < 90%; yellow 40% < RE < 60%; red RE < 40%. The RPF (Relative Potency Factor) is relative to PFOA (expressed in ng PFOA equivalents per liter) (Council of the European Union, 2025; Directorate-General for Environment, 2022b).

PFAS name	RPF	Infiltrated water		Abstraction well 1			Abstraction well 2			Finished drinking water		
		C [ng/L]	C*RPF [ng eq/L]	C [ng/L]	C*RPF [ng eq/L]	RE%	C [ng/L]	C*RPF [ng eq/L]	RE%	C [ng/L]	C*RPF [ng eq/L]	RE%
Heptafluorobutyric acid (HFBA)	NA	NA	-	11.00	-		NA	-		NA	-	
TFA	0.002	2885.00	5.77	1630.00	3.26	44%	1280.00	2.56	56%	662.00	1.32	77%
TFMS	NA	<0.01	-	77.00	-		20.00	-		13.00	-	
Perfluorobutanesulfonamide (FBSA)	NA	0.46	-	0.51	0.51	-11%	<0.3	<0.3	< LOQ	<0.3	<0.3	< LOQ
Perfluorobutanesulfonic acid (PFBS)	0.001	3.40	0.00	2.80	0.00	18%	2	0.00	41%	<2	<2	< LOQ
Perfluorobutanoic acid (PFBA)	0.05	4.85	0.24	4.40	0.22	9%	5.40	0.27	-11%	<2	<2	< LOQ
Perfluoroheptanoic acid (PFHpA)	0.505	2.65	1.34	1.40	0.71	47%	0.79	0.40	70%	0.45	0.23	83%
Perfluorohexanesulfonamide (FHxSA)	NA	<0.2	-	0.21	-		<0.2	-		<0.2	-	
Perfluorohexanesulfonic acid (PFHxS)	0.6	0.97	0.59	0.49	0.29	50%	<0.2	<0.2	< LOQ	<0.2	<0.2	< LOQ
Perfluorohexanoic acid (PFHxA)	0.01	3.60	0.04	2.4	0.02	33%	<1	<1	< LOQ	<1	<1	< LOQ
Perfluorononanoic acid (PFNA)	10	0.30	3.05	0.63	6.30	-107%	<0.5	<0.5	< LOQ	<0.5	<0.5	< LOQ
Perfluorooctanesulfonic acid (PFOS)	2	<0.2	<0.2	0.44	0.88		<0.2	<0.2		<0.2	<0.2	
Perfluorooctanoic acid (PFOA)	1	6.95	6.95	3.00	3.00	57%	1.90	1.90	73%	1.40	1.40	80%
Perfluorooctanoic acid (PFOA) branched	1	0.94	0.95	0.63	0.63	33%	0.68	0.68	28%	<0.5	<0.5	< LOQ
Perfluoropentanesulfonic acid (PFPeS)	0.3005	0.34	0.10	0.20	0.06	42%	<0.2	<0.2	< LOQ	<0.2	<0.2	< LOQ
Perfluoropentanoic acid (PFPeA)	0.03	3.45	0.10	2.40	0.07	30%	1.5	0.05	57%	<1	<1	< LOQ
Total		2912.93	**19.13**	1737.51	**15.95**	40%	1312.27	**5.86**	55%	676.85	2.95	77%

In the produced drinking water, the OMP concentrations were lower than in the abstracted water. The concentrations of PFAS and pharmaceuticals were within the proposed limit for

the new Water Framework and the Groundwater Directives (Directorate-General for Environment, 2022b). However, pesticide-TPs and the total pesticide concentration (0.56 µg/L) exceeded the limit set by the Drinking Water Framework Directive (European Parliament and Council of the European Union, 2020a). Previous studies have shown that the sand filtration technologies applied at the drinking water treatment plant of our study have low efficiencies in OMP removal (Tröger et al., 2020; Wang et al., 2022). Thus, the quality improvement observed from abstracted to produced water was most likely due to the mixing with abstracted water from wells less impacted by the MAR system (Table S3.2). In fact, AW1 and AW2 contributed only 2.7% and 3.1%, respectively, to the finished drinking water (Table S3.2). Despite their small contribution, the study of AW1 and AW2 was important for evaluating MAR performance, as they were the most impacted by the infiltration. Our results confirm that MAR is an effective preliminary step to drinking water treatment, but it may not be sufficient to comply with environmental regulations without further treatment or mixing with other water sources. Drinking water treatment plants relying solely on simple treatment steps (i.e., sand filtration) could benefit from the implementation of advanced technologies to remove persistent OMPs, like activated carbon filtration, reverse osmosis, or oxidation (Fischer et al., 2019; Piai et al., 2019; Sadia et al., 2024). These advanced treatments would still benefit from MAR as a pretreatment step that reduces the contaminant loads (Tröger et al., 2020).

Overall, MAR improves infiltrated surface water quality and is an important step in the drinking water treatment process. We observed different removal efficiencies for the OMPs detected in the infiltrated water, indicating that, next to dilution, also sorption and (bio)degradation explain the decreased OMP concentrations. These processes are affected by OMPs' intrinsic characteristics, including hydrophobicity and persistence, which we address in Sections 3.3.3 - 3.3.5.

3.3.2 NTA uncovers a wide range of TPs of potential concern

NTA detected a wider range of OMPs, particularly TPs, that were not included in the target analysis, making NTA a powerful tool for a comprehensive water quality assessment. Our results show that NTA detected 50% more OMPs than target analysis, mainly TPs, which are often overlooked in routine water quality monitoring (Figure 3.2, SE3 Table E3). Despite differences in analytical approaches, OMP detection trends in subsurface water samples align well between target and non-target results. In both cases, fewer OMPs were detected in abstracted water compared to infiltrated water, again confirming that water quality improves during soil passage.

Furthermore, NTA revealed a significantly higher number of OMPs in the finished drinking water than in the water from AW1 (n=+12), and AW2 (n=+11) (Figure 3.2). This trend was

not observed in the target analysis, where the OMP number in drinking water was lower than in the abstracted water. The additional OMPs detected via NTA in drinking water were mainly pharmaceutical TPs, including TPs from roxithromycin and azithromycin, with substantial confidence level (ID level 3, SE3 Table E3). This suggests that some TPs may originate from drinking water treatment processes, where the abstracted water was treated and mixed with water from other abstraction fields.

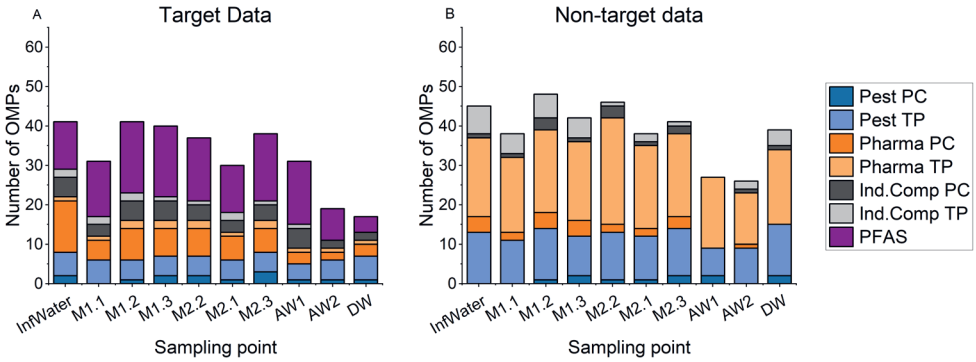

Figure 3.2. Comparison of the number of OMPs detected with target analysis and with non-target analysis per sampling point. PC = parent compounds; TP = transformation products; PFAS = per- and polyfluoroalkyl substances; InfWater = infiltrated water; M = monitoring well; AW = abstraction well; DW = drinking water.

Prediction tools and automated TP screening facilitate treatment of complex environmental data, but despite script parameter optimization for selectivity and sensitivity, the prioritization steps introduced constraints. TPs formed exclusively through abiotic reactions or pathways not covered by the used BioTransformer environmental microbial module were missing from the suspect list. Nonetheless, there is considerable overlap between biotic and abiotic TPs (Helmus et al., 2025), and our primary focus was on biodegradation. Additionally, while NTA detected more OMPs overall, some compounds identified in target analysis were missing in the NTA dataset, particularly some PCs and the entire PFAS category (Figure 3.2). Some PFAS were initially detected with NTA but later removed during prioritization due to low ID level (e.g., TFMS), low peak intensity, or detection in blank samples (e.g., TFA). Differences in sample pre-treatment (SPE) and analytical instrumentation between methods may also explain discrepancies in PFAS and PC detection.

Despite the limitations of using NTA, these findings highlight the added value of NTA for water quality assessment. The detection of additional TPs in reused, treated, and produced water helps bridge current gaps in monitoring and highlights the need to include TPs in routine assessments. Our results can support updates to water quality regulations to better reflect the diversity of OMPs in the environment. Overall, NTA complements target analysis by providing a more comprehensive view of water quality.

3.3.3 OMP charge state gives indications on transport in MAR

The charge state of OMPs influences their distribution between soil and water and therefore affects OMP transport in MAR. Other environmental factors, like pH, transformation processes, hydrology, soil composition, and organic matter content, also contribute to the transport of OMPs (Kodešová et al., 2015; Regnery et al., 2017; Schaffer et al., 2012).

When comparing the influence of OMP charge state and log D_{ow}, charge gave more insights into OMP transport in MAR. The soil-water partitioning coefficient normalized to the fraction of organic carbon in soil, K_{oc}, would have been a more suitable parameter than log D_{ow} to describe OMP mobility. All compounds (n=23) for which an experimental log K_{oc} could be retrieved showed values <3, which corresponds to the "mobile" criteria according to the PMT (persistent, mobile, toxic) classification set in the European CLP (classification, labelling, and packaging) guideline documents (European Parliament and Council of the European Union, 2024). The available experimental log K_{oc} values were well related to the observed OMP mobility, with the median log K_{oc} decreasing from 1.2 to 0.4 from the infiltration location to the abstraction wells, respectively (Figure S3.2). However, experimental K_{oc} values were missing for 60% of the OMPs in our study (Figure S3.3), making the available subset unrepresentative of the full range of OMPs detected in MAR. Thus, the more broadly available log D_{ow} (hydrophobicity proxy) was considered.

Hydrophobicity-based assessment of OMP mobility is widely used to explain OMP transport in the environment (Sigmund et al., 2022). However, log D_{ow} was insufficient to describe the OMP transport in MAR, in line with previous observations (Muschket et al., 2024; Sigmund et al., 2022). Although the results showed significant removal of OMPs with log $D_{ow} > 0$, from 21 OMPs in the infiltrated water to 14 in AW1 and 5 in AW2 (Figure 3.3), the log D_{ow} distribution along the traveled distance did not vary substantially (Figure S3.4). This is likely because OMPs with greater hydrophobicity and lower mobility might have been removed before the water reached the subsurface in the MAR system. For example, these OMPs might have been removed in the WWTP, surface water, or the pond bed.

In contrast, OMP charge state showed correlation with transport in MAR. Neutral and positively charged OMPs were detected mainly within 50 m from the infiltration point (Figure 3.3). The zwitterion and positively charged OMPs were detected in low numbers and, except for the zwitterion gabapentin (log D_{ow} -1.27), did not reach either of the abstraction wells, situated at 88 m (AW2) and 99 m (AW1) distance. Only half of the neutral OMPs travelled along the water flow and reached the abstraction wells. On the other hand, most of the negatively charged compounds reached AW1. This group included PFAS, known to be very mobile and persistent (Reemtsma et al., 2016), and OMPs with very low hydrophobicity,

such as acesulfame ($logD_{ow}$ -1.49), cyclamate ($logD_{ow}$ -1.77), and dimethenamide-TPs ($logD_{ow}$ -0.79 and -0.64).

A few neutral compounds with log D_{ow} > 0 were detected in the abstracted water. Their detection so far from the infiltration pond was not expected based on the observed trend, given the absence of negative charge and relatively high hydrophobicity. These neutral compounds included 1H-benzotriazole (log D_{ow} 1.26), which could have multiple sources, including atmospheric deposition (Zhao et al., 2024). Additionally, some TPs could have formed in the subsurface, like 4-methyl-1H-benzotriazole (log D_{ow} 1.77) and trans-10,11-dihydrodihydroxycarbamazepine (log D_{ow} 0.81).

The observed OMP behavior in MAR was likely due to electrostatic interactions, including ion exchange with soil and hydrophobic partitioning. Previous research showed that polar, hydrophylic OMPs can persist in MAR systems with long travel times and stable biogeochemical conditions (Albergamo et al., 2019). Moreover, in our study area, various clay and loam layers are present in the subsurface, though their distribution is uncertain and likely discontinuous (Cirkel, 2017). Given that clay content is positively correlated with soil cation exchange capacity and sorption of cationic compounds (Holzmann et al., 2021; Khaledian et al., 2017), and that aromatic compounds can form π-π bonds with the humic and more aromatic fractions of organic matter (Sigmund et al., 2022), the soil composition of the specific MAR system may explain why OMP charge significantly influenced transport. Since the OMPs detected in the subsurface had a low hydrophobicity and experimental K_{oc} values were largely missing, we could not relate transport behavior to this more robust parameter for soil sorption affinity. However, introducing OMP charge state substantially improved our capacity to better explain their transport in MAR. We believe that this has added value for MAR design in other locations, as the combined study of site-specific soil composition, hydrology, and physico-chemical characteristics of the OMPs in the infiltrated water could help predict MAR efficiency and design field systems.

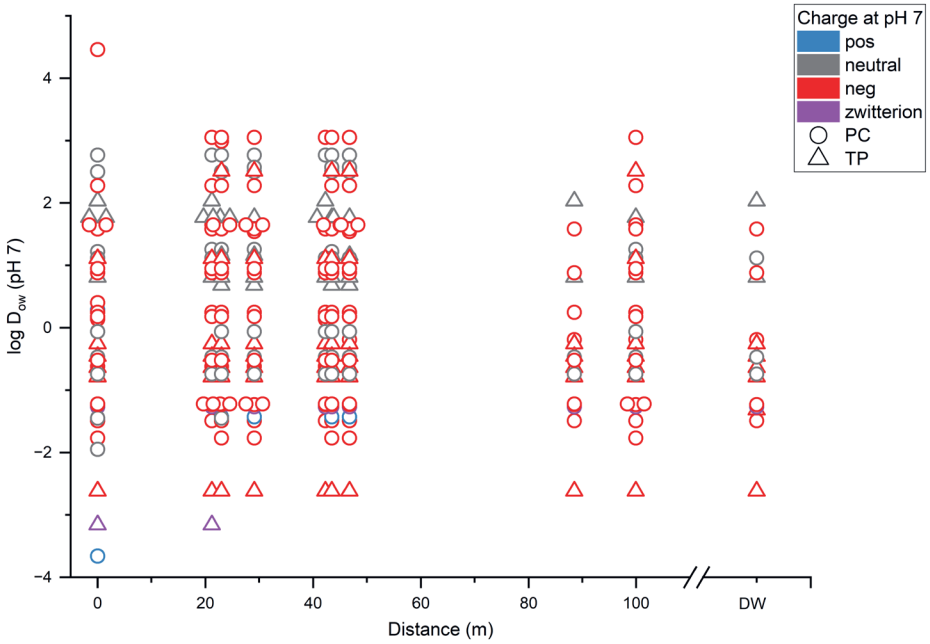

Distance (m)	0	21.22	23.02	29.10	42.32	43.48	46.79	99.9 (AW1)	88.49 (AW2)	DW
# positive	2	0	1	1	0	1	1	0	0	0
# neutral	13	9	13	12	9	12	11	7	4	5
# negative	23	20	24	24	19	21	23	22	13	11
# zwitterion	2	2	1	1	1	1	1	1	1	1
# $logD_{ow}$ >2	5	4	6	6	3	6	6	3	1	1
# 0 < $logD_{ow}$ < 2	16	12	15	15	12	14	14	11	4	4
# -2 < $logD_{ow}$ < 0	16	13	17	16	13	14	15	15	12	11
# $logD_{ow}$ < -2	3	2	1	1	1	1	1	1	1	1
TOT	**40**	**31**	**39**	**38**	**29**	**35**	**36**	**30**	**18**	**17**

Figure 3.3. The graph provides OMPs' log D_{ow} and charge state along the travelled distance from the water infiltration point. The symbol shape indicates if the OMP is a parent compound (PC) or transformation product (TP), and the color indicates the OMP charge state, where pos = positive, and neg = negative charge. The table below indicates the number of OMPs for each category of charge and hydrophobicity (log D_{ow}) along the travelled distance.

3.3.4 PFAS are persistent in MAR systems

PFAS are known to be very persistent chemicals, and this was reflected in our dataset, where concentrations remained largely stable over the travel time points (Figure 3.4). In total, 16 PFAS were detected above the LOQ in at least one sampling point along the travel time. Most PFAS detected have a chain length of four or more carbon atoms and, except heptafluorobutyric acid, were detected at ng/L concentrations. Contrarily, shorter chain PFAS, particularly the ultrashort chain TFA, had higher concentrations in the order of µg/L. This is likely because they can be generated from the breakdown of longer-chain PFAS or the (bio)degradation of other OMPs containing a TFA/TFMS moiety (Joerss et al., 2024). PFAS concentrations were generally higher in AW1 than AW2, reflecting the hydrology of the site. According to the AMIGO model, AW1 receives most of the infiltrated water, while AW2 is

more influenced by naturally occurring groundwater. This suggests that the PFAS detected in AW1 likely originate from water infiltration in MAR, while the lower concentrations in AW2 are likely due to dilution rather than degradation.

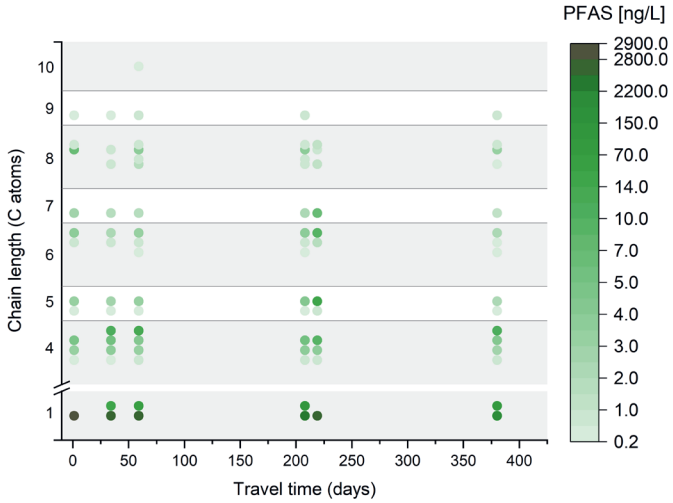

Figure 3.4. PFAS concentrations in the MAR system (in ng/L), categorized by carbon-chain length, with the number of carbon atoms (C atoms) on the y-axis (horizontal lines define the group boundaries), and the travel time in days on the x-axis.

TFA is extremely persistent and mobile, and is thus a chemical of high concern for potential accumulation in the water cycle (Arp et al., 2024). The TFA concentrations detected in our study were higher than the average concentration detected in groundwater in Germany (average 1.36 µg/L (Joerss et al., 2024)) or the Netherlands (average 408 ng/L in groundwater, 971 ng/L in surface water (Schepens et al., 2023)). Concentrations similar to ours were found in the Vechte River, which, like the Berkel, originates from the German region of Münsterland and is heavily affected by pesticide releases (Sturm et al., 2022).
TFA can be seen as a final TP from different sources: pharmaceuticals, pesticides, and volatile TFA-precursors (e.g., refrigerants) (Arp et al., 2024). Due to the volatile precursors and TFA characteristics, rain is one of the major sources of TFA in the environment, together with pesticides (Sturm et al., 2022). The widespread atmospheric deposition and the possible breakdown of TFA-precursors in soil and infiltrating water might explain the higher concentrations detected in our study. Given the observed concentrations in drinking water resources and the documented accumulation potential of TFA in the environment, our findings support the inclusion of TFA in regulatory frameworks.

3.3.5 TP detection indicates potential for OMP biodegradation in MAR

We used target and non-target analyses to assess TP formation in the MAR system. We assessed the Biowin3 scores and the charge state at pH 7 of the detected OMPs to evaluate

their potential biodegradation and mobility. A Biowin3 score below 3 implies mineralization under aerobic conditions would take months or longer, indicating OMP persistence, whereas the threshold of 2.5 distinguishes between “fast” (>2.5) and “slow” (<2.5) biodegradation (US EPA, 2025).

Our results suggest potential biodegradation within MAR, as TPs were detected along the subsurface travel path (Table S3.7). In our study, 86 feature groups annotated as candidate TPs were detected by NTA, 46 of which were not present in the infiltrated water. To generate the TP suspect list for screening the NTA data, BioTransformer (environmental microbial metabolism option) was used, which predicts biodegradation by environmental microorganisms (Djoumbou-Feunang et al., 2019). This approach, therefore, focused our analysis on TPs most likely formed via biodegradation in MAR. The predicted transformation pathway (Wicker et al., 2016), charge, and the structural information of the TPs are provided in Supplementary Excel Table E3. Most of the 46 TPs detected only in the subsurface were pharmaceutical TPs (n=25), followed by pesticide TPs (n=18) and industrial compound TPs (n=3), indicating that biodegradation and TP formation may occur during soil passage in the MAR system. Previous studies showed biodegradation in MAR (Alidina et al., 2014; Hübner et al., 2022; Maeng et al., 2011) but largely focused on PC removal, with limited insight into TP formation and persistence (Albergamo et al., 2019; Jou-Claus et al., 2024; Oberleitner et al., 2021). For example, X-ray contrast agents showed significant removal in MAR (Maeng et al., 2011), with iopamidol degradation positively correlated with nitrate concentrations (Hamann et al., 2016; Stuyfzand et al., 2007). Our findings align with these results and provide further insights on possible TP formation, as iopamidol-TP candidates were detected under nitrate-reducing conditions (Tables S3.3, S3.7, SE3 Table E3).

Biowin3 scores of the OMPs detected with target analysis were all below 3, suggesting low biodegradation potential (Figure S3.5). More biodegradable OMPs (Biowin3 >3) were likely removed before entering the MAR system, potentially during wastewater treatment or in surface water, where light and aerobic conditions promote OMP breakdown (Honti et al., 2023; Monteiro and Boxall, 2010). This could be expected as the target list for routine monitoring of the drinking water company likely focused on persistent compounds of potential concern.

We employed Biowin3, developed for aerobic conditions, despite the fact that our MAR system had mainly nitrate-, sulfate-, and iron-reducing conditions, as we found Biowin3 more suitable than Biowin7’s focus on methanogenic conditions (Figure S3.6) (US EPA, 2025). Some discrepancies between the Biowin3 predicted times for biodegradation and our observations remain. For instance, X-ray contrast agents (e.g., iohexol, iomeprol,

iopamidol) have Biowin3 scores around 2 (Table S3.7), yet candidate-TPs were detected within 34 days from infiltration (SE3 Table E3).

NTA revealed candidate TPs with varying biodegradation potential, as shown by the wider Biowin3 interquartile ranges in Figure 3.5, highlighting a greater variability in TP biodegradation potential compared to PCs. Twenty candidate TPs had Biowin3 scores above 3, like phenoxyacetic acid (2,4-dichlorophenoxyacetic acid-TP9), which may be further degraded in the environment. On the other hand, 28 TPs with Biowin3 <2.5 were also detected, including multiple metolachlor-TPs, indicating limited biodegradation potential and possible persistence in the subsurface. Overall, TPs had lower mean and median Biowin3 values than PCs in the subsurface (Figure 3.5).

In addition to the biodegradability potential assessment, we also predicted TP charge at pH 7, as electrostatic interactions were shown to be significant for OMP transport in MAR (Section 3.3.3). Of the 86 TPs, 43 were neutral, 25 negatively charged, 10 positively charged, and 8 zwitterionic. The predominance of neutral and anionic TPs suggests that many may be mobile in MAR, highlighting the need for further monitoring.

These results indicate the possible formation of mobile and persistent TPs during MAR, with potential implications for drinking water quality. While Biowin3 and charge help, toxicological studies would still be needed to complete TP risk assessment. Finally, the discrepancies between Biowin3 predictions and observed degradation suggest the need for models that account for MAR-relevant anaerobic conditions.

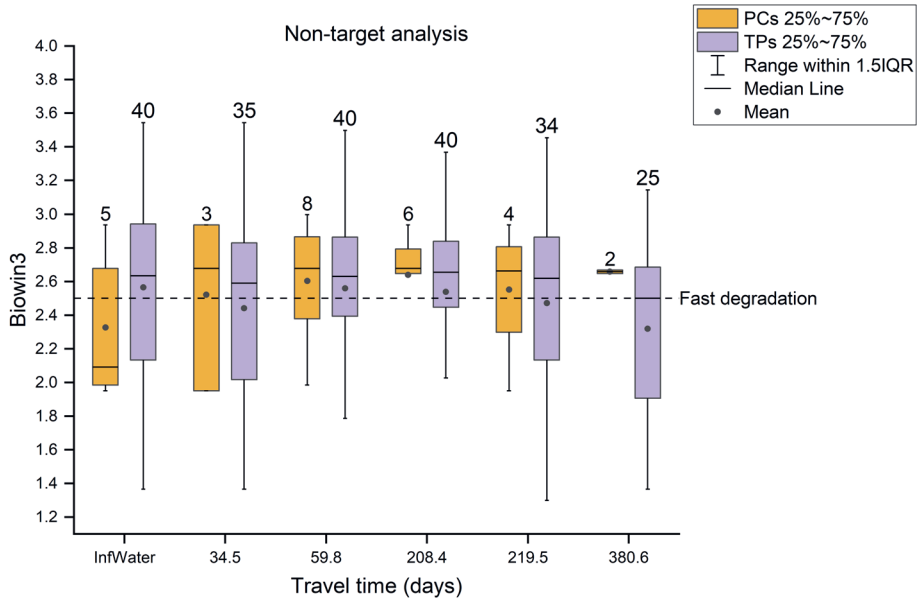

Figure 3.5. Trends in Biowin3 scores of the OMPs detected with NTA along the travel time points. PC = parent compound; TP = transformation product; IQR = interquartile range; threshold for fast degradation according to the

EPI Suite™ model: Biowin3 = 2.5. The number of PCs and TPs per travel time point is reported on top of each boxplot. The travel time (days) derives from a tracer test performed before this study and is not available for all the sampled points.

3.4 Conclusions

Our findings highlight MAR as a valuable barrier in drinking water treatment, with >90% removal efficiency for 61% of the target OMPs. NTA confirmed this trend and revealed TP presence and possible TP formation in the subsurface, suggesting ongoing biodegradation. However, some OMPs persisted and were detected in the drinking water, such as artificial sweeteners, TPs, and PFAS, including TFA. This suggests that MAR could be further optimized by engineering subsurface conditions (Hübner et al., 2022) and complemented by post-MAR technologies for persistent OMPs. NTA was valuable for characterizing the reused, abstracted, and finished water, and it can help draft a more effective target list for routine monitoring.

OMP removal in MAR depends on multiple factors, including intrinsic OMP characteristics and *in-situ* environmental conditions. In particular, our findings suggest a multidimensional interplay among the intrinsic OMP characteristics of charge state, hydrophobicity, and biodegradation potential. While highly hydrophobic (log D_{ow} >4) and easily biodegradable (Biowin3 >3) OMPs were likely removed in surface water before reaching the MAR system, charge state emerged as a key predictor of transport in MAR for more hydrophilic OMPs. Neutral and positively charged OMPs were mainly removed early in the infiltration pathway, likely due to electrostatic interactions with soil components, while anionic OMPs reached the abstraction wells. The detection of 46 TPs not present in the infiltrated water indicated potential biodegradation in MAR, but also raised concerns about the formation of possibly persistent and mobile TPs. Alongside biodegradable TPs, some persistent TPs, often overlooked in routine monitoring, may form in the subsurface and impact drinking water quality. Further research should address their toxicity and fate under varying redox conditions to improve predictive models and support regulatory inclusion of TPs.

Understanding the combined influence of hydrophobicity, charge state, and biodegradation potential could enhance our knowledge of OMP fate in MAR and inform future MAR system design for better OMP removal. While MAR clearly improves water quality, minimizing the use and production of persistent OMPs remains crucial. Our study emphasizes the need for more comprehensive water quality monitoring that integrates TPs, improved predictive tools, and regulatory adjustments to safeguard drinking water.

Acknowledgments

This research was performed within the framework of the research program AquaConnect, funded by the Dutch Research Council (NWO, grant-ID P19-45) and public and private partners of the AquaConnect consortium and coordinated by Wageningen University and Research. We thank Bert Overbeek from Vitens for his support during the sampling campaign.

Supplementary Information

SI 3.2 Materials and methods

SI 3.2.1 Description of the site

In the drinking water treatment plant, the raw water from Haarlo and Olden-Eibergen passes through rapid sand filters to remove iron and manganese and convert ammonia to nitrate. The water is later mixed with semifinished water from other pumping stations (Lochem, Noordijk), and softening is applied in pellet reactors using sodium hydroxide. Subsequently, the water is treated with double-layer rapid filtration (sand/anthracite) to remove carryover, e.g. small calcium-carbonate particles. Finally, the water is mixed with drinking water from the production station Hengelo 't Klooster and stored in a subsurface reservoir.

SI 3.2.2 Sample collection

The water sampling from wells in Figure S1 was performed by an operator who flushed each sampling point by discharging the volume of the well three times before collecting the sample. The silicon rubber tubings were replaced between sampling points to avoid cross-contamination. The samples were stored in bottles specific to each of the analyses performed by Vitens, i.e. macrochemistry and OMP target analysis. Samples for target and non-target analysis (NTA) to be performed at UvA (University of Amsterdam) were collected in 2 L methanol-pre-washed HDPE (high-density polyethylene) bottles and stored at -20 °C until sample preparation.

Figure S3.1. Map of the sampling locations included in the study. I = Infiltration point reference; M = Monitoring well; DWTP = Drinking Water Treatment Plant; AW = Abstraction Well.

Table S3.1. List of sampling points, depth (in meters below ground level) of the top and bottom of the sampling filter, distance from the monitoring well I (where artificial infiltration water was sampled), and travel time in days according to the tracer test by (Cirkel, 2017). The travel time was not available for all sampling points.

Sampling point	Depth filter top (m)	Depth filter bottom (m)	Distance from well I (m)	Travel time (days)
I1	-2.15	-3.15	-	≤1
I2	-4.05	-5.05	-	≤1
M1.1	-4.07	-5.07	21.22	34.5
M1.2	-12.08	-13.08	23.02	59.8
M1.3	-23.04	-24.04	29.10	-
M2.1	-3.05	-4.05	42.32	219.5
M2.2	-13.07	-14.07	43.48	208.4
M2.3	-23.06	-24.06	46.79	-
AW1	-20	-28.5	99.90	380.6
AW2	-21	-29	88.49	-
Finished DW	-	-	-	-

Table S3.2. Contributions of different groundwater abstraction sites to the drinking water produced on 8 June 2023 (sampling day), with specific contributions from abstraction wells in Olden Eibergen.

Abstraction Field	Abstraction well	m^3/day	%
Klooster		21675.07	55.7%
Noordijk		3423.15	8.8%
Olden Eibergen		5914.59	15.2%
	P01	1133.55	2.9%
	P02	1328.38	3.4%
	P03	1186.50	3.0%
	P04 (AW1)	1062.53	2.7%
	P05 (AW2)	1203.64	3.1%
	P06	0.00	0.0%
Haarlo		7935.36	20.4%

Table S3.3. Physico-chemical characteristics of water sampling points. As described in the text, the infiltrated water is an average of the monitoring wells I1 and I2. I = infiltration point; M = monitoring well; AW = abstraction well; DW = drinking water. The depth is indicated in meters below the ground surface. DOC = dissolved organic carbon; ECV = electroconductivity.

Name	Top depth (m)	Bottom depth (m)	travel time (d)	DOC (mg/L)	pH in situ	ECV (mS/m)	NO_3 (mg/L)	NO_2 (mg/L)	Fe (mg/L)	Mn (mg/L)	SO_4 (mg/L)	CH_4 (µg/L)
I1	-2.15	-3.15	1	8.2	7.1	59.8	<1,0	<0,01	<0,01	0.078	58	130
I2	-4.05	-5.05	1	8.1	7.4	54.8	<1,0	0.41	<0,01	0.033	65	9.1
M1.1	-4.07	-5.07	34.5	7.1	7.4	58.9	16.9	0.03	<0,01	<0,005	66	<5
M1.2	-12.08	-13.08	59.8	6.3	7.5	67.4	<1,0	0.02	1.46	0.295	110	140
M1.3	-23.04	-24.04	-	6.1	7.5	64.9	<1,0	<0,01	3.3	0.221	51	1000
M2.1	-3.05	-4.05	219.5	6.9	7.2	58	3.33	0.05	<0,01	<0,005	67	<5

M2.2	-13.07	-14.07	208.4	4.8	7.4	81.4	<1,0	<0,01	3.74	0.316	110	290
M2.3	-23.06	-24.06	-	5.3	7.4	0.662	<1,0	<0,01	4.32	0.244	49	340
AW1	-20	-28.5	380.6	5.9	7.3	68.6	<1,0	<0,01	6.38	0.305	64	96
AW2	-21	-29	-	6.8	7.1	68.4	<1,0	<0,01	11.1	0.355	65	31
DW	-	-	-	3.7	7.8	51	7.96	<0,01	<0,01	<0,005	70	<5

SI 3.2.4 OMP analysis

Vitens target method

For the target analysis performed at Vitens by HPLC-Triple Quad/Trap MS, Atlantis HILIC Silica and X-Select HSS T3 liquid chromatography columns and pre-columns from Waters were used for highly polar (method VL-W-OC27) and polar (method VL-W-OC37) compounds, respectively. Eluents for method VL-W-OC27 were (A) Milli-Q water with 0.1% formic acid, (B) acetonitrile, and (C) 10% acetonitrile/90% Milli-Q water. For method VL-W-OC37, eluents were (A) water with 10 mmol ammonium acetate, 0.1% formic acid, and 1% methanol, (B) methanol containing 10 mmol ammonium acetate, 0.1% formic acid, and 10% Milli-Q water, and (C) 10% acetonitrile/90% Milli-Q water. For TFA (trifluoroacetic acid) and TFMS (trifluoromethanesulphonic acid) the analytical column Shodex, RSpak JJ-50 2D, 150 mm x 2.0 mm, 5 µm, from Separations was used, and the eluents were (A) Milli-Q water with 50 mM ammonium acetate (pH 9), (B) methanol, and (C) 20% acetonitrile/ 80% Milli-Q water with 10 mM ammonium acetate and 0.1% formic acid. In total, Vitens target analysis screened for 371 OMPs, most of which were below the limit of quantification (LOQ). Table S3.4 reports the OMPs detected above the LOQ in at least one field sample and the corresponding LOQ for each compound.

Table S3.4. LOQ for compounds measured with Vitens target analysis. Note that for most PFAS the concentration unit is ng/L.

OMP	**LOQ [µg/L]**
1,3-diphenylguanidine	0.01
1H-benzotriazole	0.01
4-methyl-1H-benzotriazole	0.01
5-methyl-1H-benzotriazole	0.01
Acesulfame	0.01
Alachlor-ESA	0.02
Amantadine	0.01
Aminoantipyrine-4	0.02
AMPA	0.02
Atrazine-2hydroxy	0.02

BAM	0.01
Bentazon	0.01
Carbamazepine	0.01
Cyclamate	0.02
DEET	0.01
Diatrizoic acid	0.05
Dimethenamide-ESA	0.01
Dimethenamide-OA	0.01
Dimetridazole	0.02
Doxycycline	0.05
Gabapentin	0.01
Iohexol	0.05
Iomeprol	0.01
Iopamidol	0.01
Irbesartan	0.01
Isoproturon	0.01
Metformin	0.01
Metolachlor-ESA	0.01
Metolachlor-OA	0.01
Phenazone	0.01
Primidone	0.01
Sucralose	0.05
Sulfamethoxazole	0.01
Sulfapyridine	0.01
Tetraglyme	0.01
Topramezone	0.01
Trans-10,11 dihydro-10,11-dihydroxycarbamazepine	0.01
Valsartan	0.01
HFBA	0.1
TFA	0.1
TFMS	0.01
6:2 fluorotelomersulfonic acid (6:2 FTS) [ng/L]	0.5
Perfluoro-2-propoxypropanoic acid (HFPO-DA, GenX) [ng/L]	0.2
Perfluorobutanesulfonamide (FBSA) [ng/L]	0.3
Perfluorobutanesulfonic acid (PFBS) [ng/L]	2
Perfluorobutanoic acid (PFBA) [ng/L]	2
Perfluorodecanoic acid (PFDA) [ng/L]	0.3

Perfluoroheptanoic acid (PFHpA) [ng/L]	0.2
Perfluorohexanesulfonamide (FHxSA) [ng/L]	0.2
Perfluorohexanesulfonic acid (PFHxS) [ng/L]	0.2
Perfluorohexanoic acid (PFHxA) [ng/L]	1
Perfluorononanoic acid (PFNA) [ng/L]	0.2
Perfluorooctanesulfonic acid (PFOS) [ng/L]	0.2
Perfluorooctanoic acid (PFOA) [ng/L]	0.5
Perfluoropentanesulfonic acid (PFPeS) [ng/L]	0.2
Perfluoropentanoic acid (PFPeA) [ng/L]	1

UvA target method

The target analysis was performed using an ultra-high-performance liquid chromatography (UHPLC) system (Nexera 40 series, Shimadzu, Den Bosch, the Netherlands) equipped with a Kinetex® Biphenyl column (1.7 µm particle size, 100 Å pore size, 50 × 2.1 mm, Phenomenex, Utrecht, the Netherlands) maintained at 40 °C in the column oven, with the sample tray held at 10 °C. A 20 µL injection volume was used for each injection, both in positive and negative ionization. Chromatographic separation used a gradient at a constant flow rate of 0.4 mL/min: starting at 0 min with 100% Mobile Phase A, switching to 100% Mobile Phase B at 3.00 min, held until 4.80 min, and re-equilibrated to 100% A at 5.00 min. The mobile phases (Biosolve, Valkenswaard, the Netherlands) consisted of UPLC-grade water with 0.05% (≥99% purity) acetic acid (eluent A) and ULC/MS-CC/SFC grade methanol (eluent B).
The LC effluent was ionized with a negative and positive vacuum insulated probe heated electroSpray Ionization (VIP-HESI) source, and mass detection was carried out on a timsTOF Pro2 instrument employing trapped ion mobility spectrometry (TIMS, Bruker, Leiderdorp, the Netherlands). Mass and ion mobility instrumental calibration was performed by infusing directly 2mM sodium acetate (NaAc) and Agilent ESI-L low concentration mix (G1969-85000), separately, before sample analysis. In addition, 2mM NaAc/Tune mix (1:3) in a ULC/MS-CC/SFC grade water:methanol mixture (1:1, v:v, Biosolve – Valkenswaard, the Netherlands) was injected at the beginning of each sample run with a loop injection of 20 µL and used for internal calibration during data processing.
High resolution mass spectrometry (HR-MS) data were over a scan window of 20–1300 m/z and a mobility scan range from 0.1 to 1.5 v*s/cm² using 'TIMS stepping' mode. MS/MS data were recorded with broadband collision-induced dissociation (bbCID) mode using a collision energy set at 20.0 eV and 50.0 eV. More information on the TIMS setting can be found in Table S3.6. This method was developed by Specker et al. (in preparation).

The UHPLC-TIMS-QTOF-HR-MS data were analyzed using TASQ (Target Analysis for Screening and Quantitation) from Bruker (Version: 2023.1.5 10496). Extracted ion chromatograms (EICs) of respective analytes were generated with a mass tolerance of 3 mDa, and peaks were picked based on a retention time window not exceeding 0.5 min, and intensities < 1000 were excluded from the analysis. Reference collision cross-section (CCS) values were determined by averaging the mobility values of the three highest calibration points. All mobilograms were manually checked and reintegrated with a CCS tolerance set to a maximum of 2%, indicating a good mobility fit for identification.

Calibration curves were prepared in Milli-Q covering a range from 20 µg/L to 39 ng/L via serial dilution, with each level containing 4 µg/L of labelled internal standards. Linear calibration models were generated from at least seven calibration points, ensuring that residuals did not exceed 30% and reaching a coefficient of determination (R^2) of ≥ 0.99 to ensure good linearity.

Below, we report the recoveries of the SPE pre-treatment for the spiked OMPs (Table S3.5). While 98 OMPs were spiked in the control samples, the SPE recoveries could be calculated for 52 OMPs. This limitation is due to method restraints, such as missing internal standards and subsequent insufficient quality of the calibration line or matrix effects that may have suppressed some OMP signals.

Table S3.5. SPE recoveries calculated through target analysis of the spiked OMPs in the control samples.

OMP name	**Average recovery %**
10,11-Dihydro-10-hydroxycarbamazepine	65.22
2,4-Dichlorophenoxyacetic acid	90.43
2/8-Hydroxyquinoline	45.19
2-Hydroxyatrazine	93.28
3-Hydroxycarbamazepine	56.19
4/5-Methyl-1H-Benzotriazole	46.29
4-Hydroxydiclofenac	18.01
Antipyrine	95.71
Atenolol	131.44
Atrazin	49.73
Bezafibrate	119.57
Caffeine	27.73
Carbamazepine	127.19
Chloridazon	49.78
Citalopram	7.35
Clofibric acid	70.84
DEET	47.34

Diuoron	79.93
Fenuron	194.56
Fluconazole	48.90
Fluopyram	35.92
Furosemide	53.29
Gabapentin	17.75
Hydrochlorothiazide	108.77
Imidacloprid	44.90
Irbesartan	39.63
Isoproturon	108.63
Lamotrigine	42.32
Linuron	8.48
MCPA	122.08
Mecoprop	66.84
Metoprolol	105.63
N4-Acetylsulfamethoxazole	30.54
Neburon	5.56
O-Desmethylvenlafaxine	59.89
PFHpA	57.15
PFHxA	86.75
PFHxS	83.96
PFOA	90.28
Salicyclic acid	107.27
Sotalol	117.56
Sulfamethazine	52.77
Sulfamethoxazole	74.23
Terbuthylazine	32.26
Thiabendazole	18.81
Thiacloprid	108.11
Triclosan	5.29
Triethylphosphate	64.98
Trimethoprim	141.87
Tris(2-chloroethyl)phosphate	33.88
Tris(3-chloropropyl)phosphate	18.88
Venlafaxine	109.33

UvA non-target method and stability test

NTA was performed using the same UHPLC-TIMS-QTOF-HR-MS system used for UvA target analysis. A Kinetex® 100 mm long, 2.1 mm diameter, and 1.7 µm biphenyl 100 Å column was used for liquid chromatography in a UHPLC Nexera instrument, equipped with a binary LC-40AD XS gradient pumping system, SIL-40C XS autosampler, CTO-40A column oven, SPD-40 UV detector and SCL-40 controller (Shimadzu, Kyoto, Japan). For detection, we used a Bruker timsTOF Pro 2.0 system, a dual trapped ion mobility mass spectrometer (TIMS-MS) with Parallel Accumulation Serial Fragmentation (PASEF) and accurate and reproducible CCS determination, equipped with a VIP HESI source. More information on the settings is reported in Table S3.6. The mobile phases (purchased from Biosolve – Valkenswaard, the Netherlands) consisted of UPLC-grade water with 0.05% (≥99% purity) acetic acid (eluent A) and ULC/MS-CC/SFC grade methanol (eluent B). The column oven temperature was 40 °C, while the sample tray was at 10 °C. The phase gradient expressed with B percentage was 0% at the start, a gradual increase to 100% until minute 6, steady 100% concentration until minute 9.60, and back to 0% by minute 10. The stability time between injections was 2.5 minutes. The flow rate was 0.4 mL/min. Before starting an analysis batch and before each injection, the MS detector was internally calibrated with a 1:2 solution of sodium acetate (2 mM) and ESI-L low-concentration tuning mix. For each injection, 20 µL of sample were used, and each sample was measured in triplicate in positive and negative ionization. Blanks (Milli-Q) and a calibration line of target OMPs at known concentrations from 20.000 to 0.039 µg/L were measured at the beginning and end of each batch. Additionally, a blank and two points of the calibration line were measured every 16 samples.

To assess the reproducibility of the PASEF measurements, a batch of samples was measured in duplicates, twice with 13 days between measurements. The batch included a calibration line, SPE, and direct injection controls (i.e., control samples spiked with known OMPs that did not undergo SPE), and field samples collected in Eibergen. The RT (retention time) and m/z (mass over charge) variations were on average 0.02 min and 0.1 mDa, respectively, indicating good stability. Although NTA is not a quantitative analysis, and thus peak intensity is less relevant for data reproducibility, we calculated the peak intensity variation for the fourth calibration point (4 µg/L) and the lowest calibration point detected per OMP (most sensitive to intensity variation, with a peak intensity of at least 7500). We obtained a variation greater than 30% between measurements for 15% of the OMPs. Compound-specific variations were expected and the results were considered acceptable (Ng et al., 2020).

Table S3.6. Settings of target analysis (TA) and non-target analysis (NTA). Most settings overlap between the two methods, as the same instrument was used. Settings specific to each method are highlighted with different colors: yellow for TA and green for NTA.

Setting	Setting Parameter	Positive Mode	Negative Mode
MS	Scan Begin	20 m/z	20 m/z
	Scan End	1300 m/z	1300 m/z
Ion Source (VIP-HESI)	End Plate Offset	500 V	500 V
	Capillary	4500 V	4500 V
	Nebulizer	2.0 bar	2.0 bar
	Dry Gas	8.0 l/min	8.0 l/min
	Dry Temp	230 °C	230 °C
	Sheath Gas Temp	400 °C	400 °C
	Sheath Gas Flow	4.0 l/min	4.0 l/min
	Active Exhaust	Activated	Activated
Transfer	Deflection 1 Δ	60.0 V	- 60.0 V
	Funnel 1 RF (TA)	300.0 Vpp	300.0 Vpp
	Funnel 1 RF (NTA)	250.0 Vpp	250.0 Vpp
	isCID Energy	0.0 eV	0.0 eV
	Funnel 2 RF	250.0 Vpp	250.0 Vpp
	Multiple RF	150.0 Vpp	150.0 Vpp
Collision Cell	Collision Energy	10.0 eV	10.0 eV
	Collision RF	450.0 Vpp	450.0 Vpp
Quadrupole	Ion Energy	5.0 eV	5.0 eV
	Low Mass	70.00 m/z	70.00 m/z
Focus Pre TOF	Transfer Time	65.0 µS	65.0 µS
	Pre Pulse Storage	3.0 µS	3.0 µS
TIMS	1/K0 Start	0.1 v*s/cm²	0.1 v*s/cm²
	1/K0 End	1.5 v*s/cm²	1.5 v*s/cm²
	Ramp Time	100.0 ms	100.0 ms
	Accu. Time	100.0 ms	100.0 ms
	Duty Cycle (TA)	100.0 %	100.0 %
	Ramp Rate (TA)	9.08 Hz	9.08 Hz
	MS Averaging (TA)	1x	1x
TIMS – Offsets	Δt1 (Deflection Transfer -> Capillary Exit)	-20.0 V	20.0 V
	Δt2 (Deflection Transfer -> Deflection Discard)	-100.0 V	100.0 V
	Δt3 (Funnel 1 In -> Deflection Transfer)	50.0 V	-50.0 V
	Δt4 (Accumulation Trap -> Funnel 1 In)	50.0 V	-50.0 V
	Δt5 (Accumulation Exit -> Accumulation Transfer)	0.0 V	0.0 V
	Δt6 (Ramp Start -> Accumulation Exit)	30.0 V	-30.0 V
	Collision Cell In	140.0	-140.0
TIMS – Ion Charge Control	Target Intensity	7.50 M	7.50 M
TIMS – Advanced ParametersI	Set 1/K0 End for accumulation to	Deactivated	Deactivated
	Lock accumulation to mobility range	Activated	Activated
MS/MS (TA)	Scan Mode	bbCID	bbCID
	TIMS Stepping Profile	"bbCID pos. Small Molecules 100-800 m/z"	"bbCID neg. Small Molecules 100-800 m/z"
	Collision Energy 1	20.0 eV	20.0 eV

	Collision Energy 2	50.0 eV	50.0 eV
MS/MS (NTA)	Scan Mode	PASEF	PASEF
	TIMS Stepping Profile	TIMS stepping PASEF pos metabolomics 75-750 m/z	TIMS stepping PASEF neg metabolomics 75-750 m/z
	Collision Energy 1	20.00 eV	20.00 eV
	Collision Energy 2	50.00 eV	50.00 eV
	Collision Energy 3	50.00 eV	50.00 eV
	Number of MS/MS scans	2	2
	Target Intensity	4000	4000
	Intensity threshold	100	100
	Charge Range Min.	0	0
	Charge Range Max.	1	1
	Active Exclusion	On	On
	Release after	0.10 min	0.10 min
	PASEF Isolation Peak Select.	Average m/z	Average m/z
	Isolation Mass Start	20.00 m/z	20.00 m/z
	Isolation Mass End	1300.00 m/z	1300.00 m/z
	Isolation Width Start	2.00 m/z	2.00 m/z
	Isolation Width End	8.00 m/z	8.00 m/z

SI 3.3 Results and discussion

SI 3.3.3 OMP charge state gives indications on OMP transport in MAR

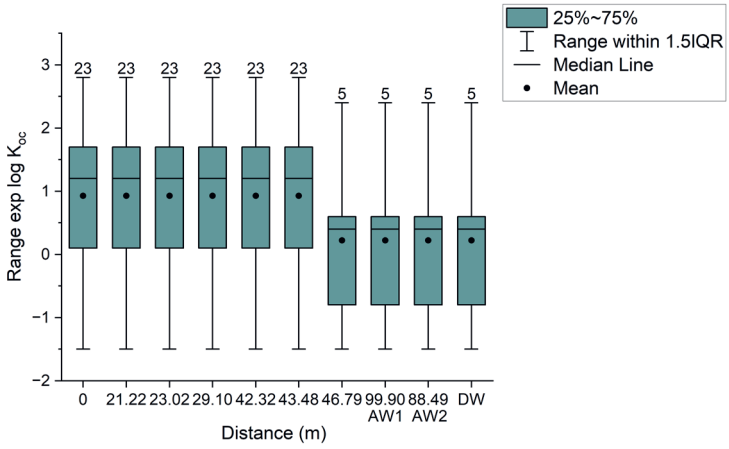

Figure S3.2. Range of log K_{oc} for the 23 OMPs for which a value was available. Experimental log K_{oc} data were retrieved from a previous extensive mobility assessment *(Arp and Hale, 2022)who compiled data from the eChemPortal (www.echemportal.org/echemportal) and the UFZ-LSER database (Ulrich et al., 2017).*

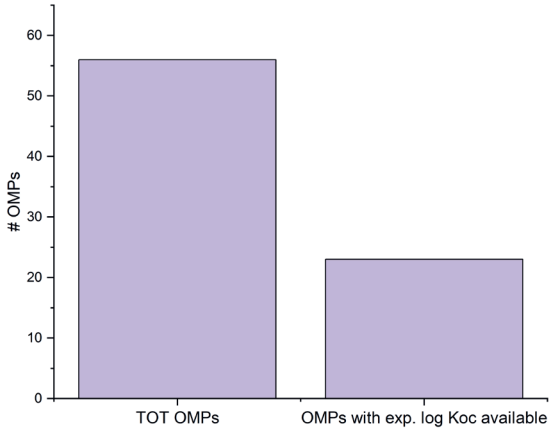

Figure S3.3. Comparison between OMPs detected with target analysis (left column) and subset for which the experimental log K_{oc} was available.

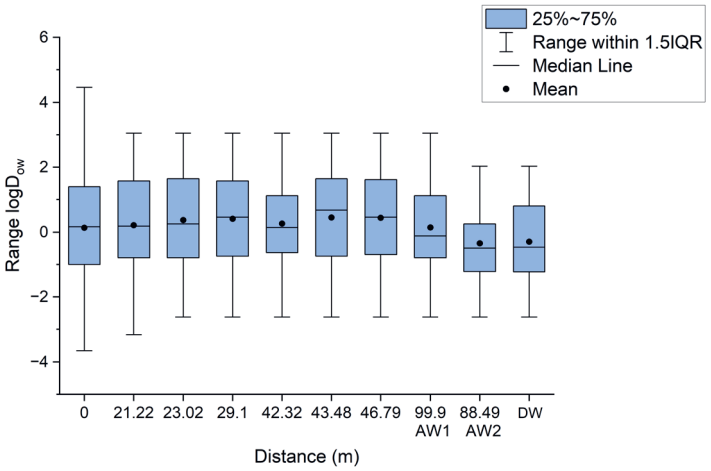

Figure S3.4. Distribution of OMP log D_{ow} in sampling points at growing distance from the water infiltration point.

SI 3.3.5 TP detection indicates potential for OMP biodegradation in MAR

Table S3.7. OMPs detected with target analysis with corresponding charge, Biowin3 score, number of feature groups detected via non-target analysis and annotated as potential TPs of the corresponding OMP, and concentration in µg/L in the travel time sampling points obtained through target analysis. If the concentration fell below the limit of quantification (LOQ), it was reported as "<LOQ," indicating the specific LOQ value.

				Concentration [µg/L]					
OMP	**Charge**	**Biowin3**	**TPs**	**Inf. Water**	**M1.1**	**M1.2**	**M2.2**	**M2.1**	**AW1**
1,3-diphenylguanidine	pos	2.62	0	0.02	<0.01	<0.01	<0.01	<0.01	<0.01
1H-benzotriazole	neutral	2.94	0	NA	0.60	0.23	NA	NA	0.04
4-methyl-1H-benzotriazole	neutral	2.83	0	0.11	0.16	0.16	0.15	0.07	0.02
5-methyl-1H-benzotriazole	neutral	2.83	0	0.04	0.03	0.01	<0.01	0.01	<0.01
Acesulfame	neg	2.84	1	0.11	0.10	0.22	0.23	0.06	0.14
Amantadine	pos	2.68	1	<0.01	<0.01	0.02	0.02	<0.01	<0.01
4-aminoantipyrine	neutral	2.64	1	<0.02	<0.02	0.04	0.03	<0.02	<0.02
AMPA	zwitterion	2.98	0	0.07	0.04	<0.02	<0.02	<0.02	<0.02
2-hydroxyatrazine	neutral	2.27	0	<0.02	<0.02	0.02	0.03	<0.02	<0.02
BAM	neutral	2.31	1	0.03	0.03	<0.01	<0.01	0.04	<0.01
Bentazon	neg	2.67	0	<0.01	<0.01	<0.01	<0.01	<0.01	0.01
Carbamazepine	neutral	2.68	0	0.05	0.05	0.05	0.03	0.052	<0.01
Cyclamate	neg	2.8	0	0.02	<0.02	0.04	0.04	<0.02	0.03
DEET	neutral	2.65	0	0.01	<0.01	0.02	0.02	<0.01	<0.01
Diatrizoic acid	neg	1.69	0	0.24	0.11	0.11	<0.05	0.25	<0.05
Dimethenamide-ESA	neg	2.47	1	0.35	0.42	0.28	0.28	0.37	0.19
Dimethenamide-OA	neg	2.19	0	0.15	0.17	0.12	0.07	0.15	0.08
Gabapentine	neutral	3.00	0	0.27	0.04	0.40	0.40	0.06	0.14
Iohexol	neutral	2.05	1	0.09	<0.05	<0.05	<0.05	<0.05	<0.05
Iomeprol	neutral	1.98	2	0.02	<0.01	0.02	<0.01	<0.01	<0.01
Iopamidol	neutral	1.98	2	0.72	0.15	0.98	0.13	0.77	0.18
Irbesartan	neg	2.28	1	0.01	<0.01	<0.01	<0.01	<0.01	<0.01
Isoproturon	neutral	2.67	0	<0.01	<0.01	<0.01	0.011	<0.01	<0.01
Metformin	pos	2.91	0	0.01	<0.01	<0.01	<0.01	<0.01	<0.01
Metolachlor-ESA	neg	2.45	8	0.46	0.40	0.46	0.44	0.41	0.29
Metolachlor-OA	neg	2.73	5	0.20	0.20	0.16	0.14	0.17	0.13
Phenazone	neutral	2.80	0	0.01	<0.01	<0.01	0.01	<0.01	<0.01
Primidone	neutral	2.42	0	0.03	0.02	0.04	0.05	0.02	0.03
Sucralose	neutral	2.36	0	1.07	0.70	0.70	0.19	1.10	0.36
Sulfamethoxazole	neg	2.43	0	0.01	<0.01	<0.01	<0.01	0.02	<0.01
Sulfapyridine	neg	2.30	0	0.01	<0.01	<0.01	<0.01	<0.01	<0.01

Tetraglyme	neutral	2.66	6	0.03	<0.01	0.03	0.04	0.02	0.02
Topramezone	neg	2.3	0	0.01	<0.01	<0.01	<0.01	0.01	<0.01
Trans-10.11 dihydro-10.11-dihydroxycarbamazepine	neutral	2.92	0	0.22	0.13	0.23	0.17	0.12	0.09
Valsartan	neg	2.84	2	0.01	<0.01	0.02	0.01	<0.01	<0.01

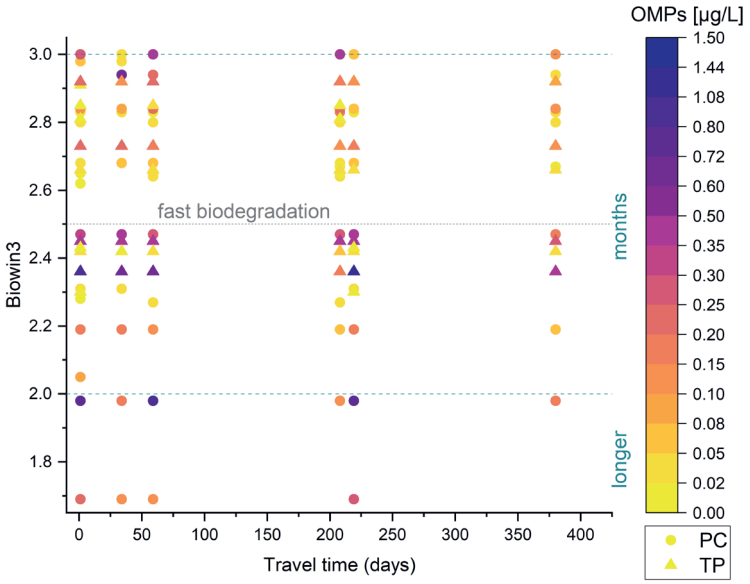

Figure S3.5. Biowin3 scores and concentration in µg/L along the travel time sampling points of the OMPs detected via target analysis in the MAR system. A Biowin3 value between 2 and 3 indicates a predicted biodegradation rate of months, while if Biowin3 is smaller than 2, the biodegradation is predicted to take longer than months. The 2.5 threshold delineates "slow" and "fast" biodegradation.

Considering the Biowin7 scores of the OMPs detected in our study, most of them show values <0.5, resulting in very slow biodegradation (US EPA, 2025). This is likely because methanogenic conditions are the least favorable for biodegradation, being at the very end of the redox energy-yielding scale (Rivett et al., 2008). In MAR, the redox conditions vary from aerobic, in the unsaturated zone, to nitrate and sulfate-/iron-reducing conditions, typical of the depths at which the groundwater is abstracted.

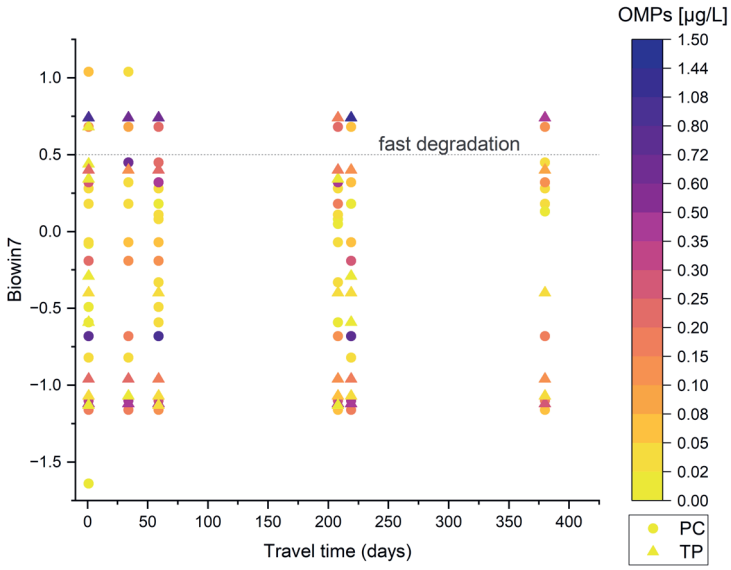

Figure S3.6. Biowin7 scores and OMP concentrations [µg/L] along the travel time points (target analysis data). The threshold value of 0.5 indicates fast degradation (Biowin7 > 0.5) under methanogenic conditions.

Supplementary script 3.1

```
library(patRoon)

# -------------------------
# initialization
# -------------------------
workPath <- "*File Path*"
setwd(workPath)
# Load analysis table
anaInfoPos <- read.csv("samples-pos.csv")
anaInfoNeg <- read.csv("samples-neg.csv")
# -------------------------
# features
# -------------------------
# Find all features
fListPos <- findFeatures(anaInfoPos, "openms", noiseThrInt = 1000,
chromSNR = 5, chromFWHM = 10, minFWHM = 1, maxFWHM = 20)

fListNeg <- findFeatures(anaInfoNeg, "openms", noiseThrInt = 1000,
chromSNR = 5, chromFWHM = 10, minFWHM = 1, maxFWHM = 20)

fGroups_pos <- groupFeatures(fListPos, "openms", rtalign = FALSE)
fGroups_neg <- groupFeatures(fListNeg, "openms", rtalign = FALSE)

fGroups_pos <- fGroupsF_pos <-  filter(fGroups_pos, preAbsMinIntensity =
100, absMinIntensity = 7500, relMinReplicateAbundance = 1,
maxReplicateIntRSD = 0.75, blankThreshold = 5, removeBlanks = TRUE,
retentionRange = NULL, mzRange = NULL)

fGroups_neg <- fGroupsF_neg <-  filter(fGroups_neg, preAbsMinIntensity =
100, absMinIntensity = 7500, relMinReplicateAbundance = 1,
maxReplicateIntRSD = 0.75, blankThreshold = 5, removeBlanks = TRUE,
retentionRange = NULL, mzRange = NULL)
#--------------------------------------
# Checking for adducts and isotopes
#--------------------------------------

# generate components from filtered fGroups
components_pos <- generateComponents(fGroupsF_pos, "cliquems",
ionization = "positive", ppm = 7)
components_neg <- generateComponents(fGroupsF_neg, "cliquems",
ionization = "negative", ppm = 7)

# Only keep results with adducts/isotope annotations and remove unwanted
adducts
```

```
componentsF_pos <- delete(components_pos, j = function(ct, ...)
is.na(ct$isonr) & (is.na(ct$adduct_ion) | !ct$adduct_ion %in%
c("[M+Na]+", "[M+K]+", "[M+NH4]+")))
print(componentsF_pos)

componentsF_neg <- delete(components_neg, j = function(ct, ...)
is.na(ct$isonr) & (is.na(ct$adduct_ion) | !ct$adduct_ion %in% c("[M-
H2O]-", "[M-H]-")))
print(componentsF_neg)

# Only keep components with at least one feature group also present in
the suspect screened data
componentsF_pos <- delete(componentsF_pos, j = function(ct, ...)
!any(ct$group %in% names(fGroups_pos)))
componentsF_neg <- delete(componentsF_neg, j = function(ct, ...)
!any(ct$group %in% names(fGroups_neg)))

# Remove components with only one feature group (useless)
componentsF_pos <- filter(componentsF_pos, size = c(2, 1E6))
componentsF_neg <- filter(componentsF_neg, size = c(2, 1E6))

# manually check/filter components
checkComponents(componentsF_pos, fGroupsF_pos, session =
"components_check_pos.yml")
componentsF_pos <- filter(componentsF_pos, checkComponentsSession =
"components_check_pos.yml")

checkComponents(componentsF_neg, fGroupsF_neg, session =
"components_check_neg.yml")
componentsF_neg <- filter(componentsF_neg, checkComponentsSession =
"components_check_neg.yml")

# to filter out unwanted adducts/isotopes
fGroups_pos <- selectIons(fGroups_pos, componentsF_pos, c("[M+H]+"))
fGroups_neg <- selectIons(fGroups_neg, componentsF_neg, c("[M-H]-"))

# Make sets and group features
fGroups <- makeSet(fGroups_pos, fGroups_neg, groupAlgo = "openms",
adducts = c("[M+H]+", "[M-H]-"))

# -------------------------
# suspect screening
# -------------------------

# Load suspect list
suspList <- read.csv("*Suspect list path", stringsAsFactors = FALSE)
```

```
# Set onlyHits to FALSE to retain features without suspects (eg for NTA)
fGroups <- screenSuspects(fGroups, suspList, rtWindow = 12, mzWindow =
0.005, onlyHits = FALSE)

# -------------------------
# transformation products
# -------------------------

# Load parent suspect list
suspListParents <- read.csv("*Suspect List for TPs*", stringsAsFactors=
FALSE)

# Obtain TPs
TPs <- TPs_UF <- generateTPs("biotransformer", parents =
suspListParents, type = "env", generations = 3, calcSims = FALSE)

TPs <- filter(TPs, removeParentIsomers = TRUE)

# to remove TPs that may be assigned wrongly (unspecific assignment)
TPs <- delete(TPs, j = function(tab, par)
{
  parNM <- parents(TPs)[match(par, name)]$neutralMass # parent neutral
mass
  # remove if high generation (>1) and mass is <60% of that of the
parent
  # generation 1 TPs are always kept and the rest only if their mass is
sufficiently high (>=60%)
  return(tab$generation > 1 & (tab$neutralMass / parNM) < 0.6)
})

# Screen TPs
suspListTPs <- convertToSuspects(TPs, includeParents = FALSE)
write.csv(suspListTPs, "SuspectListOfTPs.csv", quote = TRUE, row.names =
FALSE)

# Amend with TP screening
fGroups <- screenSuspects(fGroups, suspListTPs, rtWindow = 12, mzWindow
= 0.005, onlyHits = TRUE, amend = TRUE)

# -------------------------
# annotation
# -------------------------

# Retrieve MS peak lists
avgMSListParams <- getDefAvgPListParams(clusterMzWindow = 0.005)
```

```
mslists <- generateMSPeakLists(fGroups, "mzr", maxMSRtWindow = 5,
precursorMzWindow = 0.5, avgFeatParams = avgMSListParams,
avgFGroupParams = avgMSListParams)

# Rule based filtering of MS peak lists.
mslists <- filter(mslists, absMSIntThr = NULL, absMSMSIntThr = NULL,
relMSIntThr = NULL, relMSMSIntThr = 0.05, topMSPeaks = NULL,
topMSMSPeaks= 25)

# Calculate formula candidates
formulas <- generateFormulas(fGroups, mslists, "genform", relMzDev = 5,
elements = "CHNOPSClFI", oc = FALSE, calculateFeatures = FALSE,
featThresholdAnn = 0.75, setThresholdAnn = 0)

convertToMFDB(TPs, "TP-database.csv", includeParents = TRUE)

# Calculate compound structure candidates
compounds <- generateCompounds(fGroups, mslists, "metfrag", dbRelMzDev =
5, fragRelMzDev = 5, fragAbsMzDev = 0.002, database = "csv", extraOpts =
list(LocalDatabasePath = "TP-database.csv"), maxCandidatesToStop = 2500,
setThresholdAnn = 0)
compounds <- addFormulaScoring(compounds, formulas, updateScore = TRUE)

# Annotate suspects
fGroups <- annotateSuspects(fGroups, formulas = formulas, compounds =
compounds, MSPeakLists = mslists, IDFile = "idlevelrules.yml")

# -------------------------
# Filters to remove low ID
# -------------------------

fGroups_lowID <- filter(fGroups, maxLevel = 4, negate = TRUE)
fGroups_lowID <- filter(fGroups_lowID, onlyHits = TRUE)
# fGroups lowID should now contain all features with L5
write.csv(screenInfo(fGroups_lowID), "OMPs_lowID.csv", quote = TRUE,
row.names = FALSE)
lowID_table <- as.data.frame(fGroups_lowID, collapseSuspects = NULL)
write.csv(lowID_table, "DataFrame_lowID.csv", quote = TRUE, row.names =
FALSE)

# to proceed with L4 or better
fGroups <- filter(fGroups, maxLevel = 4, onlyHits = TRUE)

# -------------------------
# Parent and TP linkage
# -------------------------
```

```
componentsTP <- generateComponents(fGroups[, suspects = suspList$name],
"tp", fGroupsTPs = fGroups, TPs = TPs, MSPeakLists = mslists, formulas =
formulas, compounds = compounds)

componentsTP <- filter(componentsTP, retDirMatch = TRUE, minSpecSim =
NULL, minSpecSimPrec = NULL, minSpecSimBoth = NULL, minFragMatches =
NULL, minNLMatches = NULL)

checkFeatures(fGroups)
fGroups <- filter(fGroups, checkFeaturesSession = TRUE)

# -----------------------
# Filters for plotting:
# -----------------------

# if the same suspect is assigned to multiple fGroups, select the one
with the best ID level
fGroupsToPlot_bestID <- filter(fGroups, selectHitsBy = "level",
onlyHits=TRUE)
print(fGroupsToPlot_bestID)

# if the same fGroup is assigned to multiple suspects, this will only
keep the one with highest ID level
fGroupsToPlot <- filter(fGroupsToPlot_bestID, selectBestFGroups = TRUE,
onlyHits = TRUE)
print(fGroupsToPlot)
write.csv(screenInfo(fGroupsToPlot), "fGroupsToPlot.csv", quote = TRUE,
row.names = FALSE)

# -------------------------
# reporting
# -------------------------

report(fGroups, MSPeakLists = mslists, formulas = formulas, compounds =
compounds, components = componentsTP, TPs = TPs, settingsFile =
"report.yml", parallel =FALSE, openReport = TRUE)

checkFeatures(fGroupsToPlot_bestID, "fGroupsToPlot_bestID.yml")
fGroupsToPlot_bestID <- filter(fGroupsToPlot_bestID,
checkFeaturesSession = "fGroupsToPlot_bestID.yml")

report(fGroupsToPlot_bestID, MSPeakLists = mslists, formulas = formulas,
compounds = compounds, components = componentsTP, TPs = TPs,
settingsFile = "report_4Feb2025.yml", openReport = TRUE, parallel =
FALSE)
```

Supplementary Excel 3

Supplementary Excel (SE) tables can be downloaded from:
https://doi.org/10.1016/j.watres.2025.124409

Chapter 4

Higher microbial diversity enhances the extent and rate of organic micropollutant biodegradation under aerobic and nitrate-reducing conditions

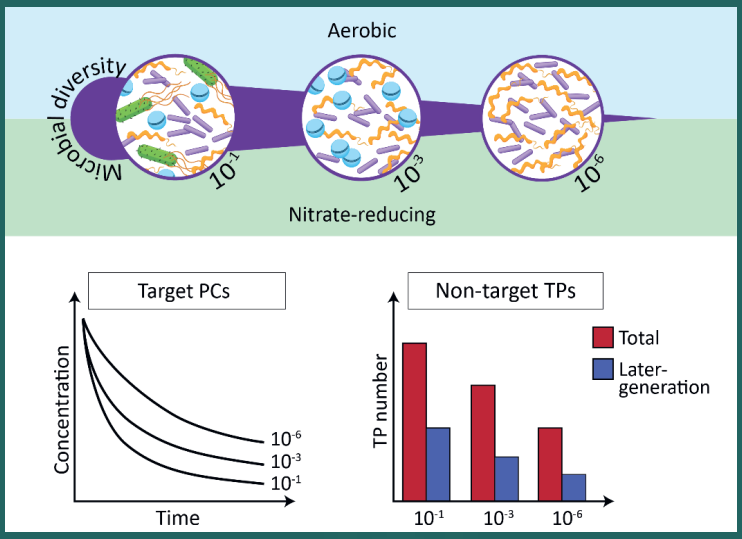

A modified version of this chapter has been published as:

Ore, A., Palm, E.H., van Wezel, A.P., Sutton, N.B., **2025**. Higher microbial diversity enhances the extent and rate of micropollutant biodegradation under aerobic and nitrate-reducing conditions. **Water Research**.
https://doi.org/10.1016/j.watres.2025.124921

Abstract

Organic micropollutant (OMP) biodegradation rates and pathways in environmental and engineered systems depend on several factors, including redox conditions and microbial diversity. We investigated the impact of these two variables on the degradation of 20 OMPs. Soil microbial communities with three diversity levels were generated via solid-phase dilution-to-extinction. After a regrowth period, communities were incubated with OMPs under aerobic and nitrate-reducing conditions. High and medium microbial diversity led to more OMPs being degraded, up to 15 and 8 under aerobic and nitrate-reducing conditions, respectively, compared to 11 and 4 under low diversity. Higher diversity also led to increased biodegradation rates and formation of a broader range of transformation products (TPs), including later-generation TPs. For TPs detected across multiple diversity levels and redox conditions, lag phases before initial detection were shorter in higher diversity and aerobic conditions. Biodegradation under nitrate-reducing conditions was slower and less efficient, yet the positive correlation with microbial diversity remained (mean $r_{aerobic} = 0.28$ and $r_{nitrate\text{-}reducing} = 0.26$, $p < 0.01$). Redox-specific TP production and taxonomic differences suggested distinct biodegradation pathways under different redox conditions. While some TPs persisted until the end of the incubation, none were predicted to be dead-end TPs according to BioTransformer. However, predictions with OPERA's CERAPP and CoMPARA modules revealed two TPs with potential endocrine-disrupting effects. Our study highlights that microbial diversity and redox conditions strongly influence OMP degradation rates and pathways, and thus TP formation. Moreover, our results suggest a threshold in microbial diversity below which functional capacity is affected. Diversity should therefore be considered in standardized tests evaluating OMP persistence in the environment.

Keywords

Microbial diversity; micropollutants biodegradation; transformation products; non-target screening; redox conditions.

4.1 Introduction

Biological transformation (i.e., biodegradation) is one of the main processes for environmental and engineered degradation of organic micropollutants (OMPs), consisting of a chain of reactions that transform a parent compound (PC) into transformation products (TPs) (Fenner et al., 2013; Kern et al., 2011). OMPs, if biodegradable, are thus broken down to increasingly less complex TPs and, under favourable conditions, can be fully mineralised into inorganic compounds. Several environmental factors influence biodegradation, including the availability of electron acceptors (redox conditions), nutrients, and carbon substrates. These factors also select for microbial community composition, diversity and activity, thus dictating which PCs are degraded and which TPs are formed (Branco et al., 2024, 2023; Fenner et al., 2021; Redeker et al., 2018).

Microbial diversity, i.e., the variety of different bacterial species present in a system, is central to OMP biodegradation. Previous studies showed that diversity is positively correlated with adaptation and metabolic rates, which can lead to improved biodegradation activity (Patsch et al., 2018). OMP biodegradation can be seen as a specialized function not common to all microorganisms in a population (Singh et al., 2014). Therefore, more diverse communities are more likely to include bacterial species capable of OMP biodegradation (Coll et al., 2020). Moreover, due to the often relatively low OMP concentrations in the environment, cometabolism is more common than metabolic OMP degradation (Fenner et al., 2021; National Research Council, 1993). In cometabolism, OMPs are transformed incidentally while microbes grow on a primary substrate that supplies the energy and carbon required for their growth and respiration (Tran et al., 2013). As a result, environmental biodegradation of OMPs typically leads to the formation of TPs rather than complete mineralization (Fenner et al., 2021). In more diverse bacterial communities, complementary metabolic interactions among species can promote further transformation of these TPs. For instance, one organism's TP may become a substrate for another, enabling degradation to proceed further along the pathway, a mechanism often referred to as metabolic cross-feeding or synergy (Lindemann et al., 2016; Morris et al., 2013). This results in the formation of later-generation TPs, i.e. TPs from steps further down the metabolic pathway (Posselt et al., 2020; Stravs et al., 2019).

Knowledge on how microbial diversity influences OMP biodegradation and TP formation is still limited, especially across different redox conditions (Fenner et al., 2021; Patsch et al., 2018). Aerobic conditions are the most studied, as they often result in the most favorable conditions for OMP biodegradation due to a greater energy yield to the microorganisms. However, redox conditions differ in environmental and engineered compartments (e.g., shallow and deep soil, aquifers, anaerobic wastewater treatment), leading to different

microbial community compositions and TP formation pathways (Fenner et al., 2013). Compared to PC biodegradation, TP formation under different redox conditions is still understudied. However, TPs might be more persistent, mobile, or potentially more toxic than PCs, and it is therefore important to deepen the knowledge on TP formation from biodegradation processes in both engineered and natural systems (Zahn et al., 2024).

The goal of this study was to test the association between microbial diversity, OMP degradation, and TP formation under two redox conditions (i.e., aerobic and nitrate-reducing) in batch experiments. We used a solid-state dilution to extinction approach to serially dilute a starting soil inoculum and thus create microbial communities with differing diversity. We aimed to investigate how microbial diversity and redox conditions affect (1) OMP biodegradation and (2) TP formation in our systems. Our results contribute to the understanding of interconnections among TP formation, redox conditions, and microbial diversity and provide useful input to improve regulatory frameworks and standardized tests (e.g., REACH, OECD) for preserving environmental quality.

4.2 Materials and methods

4.2.1 Dilution to extinction

A soil-based dilution-to-extinction approach was used, in which an initial soil microbial inoculum was stepwise diluted to remove the less abundant species (Philippot et al., 2013; Posselt et al., 2020) and create communities with different diversity. The soil was from a previously studied agricultural field (Narain-Ford et al., 2022; Ore et al., 2025a). Serial dilutions (w/w) from 10^{-1} (highest diversity) to 10^{-6} (lowest diversity) were prepared using sterilized soil from the same location, which was sieved (4 mm) and autoclaved three times at 121°C for 15 minutes to ensure the absence of biologically active microorganisms. Diluted communities were homogenized first by manual shaking, followed by 72 hours in a rotating device, and then stored at 20°C in the dark for up to 4 days before batch setup. The 10^{-6} community bottles were prepared first, followed by 10^{-3} after two days, and 10^{-1} batches after 4 days from the 10^{-6} preparation. This short time difference was not expected to significantly affect the microbial regrowth and performance.

4.2.2 Experimental set-up

Batch incubations were prepared in triplicate at three microbial diversity levels (10^{-1}, 10^{-3}, and 10^{-6}) and under two redox conditions: aerobic and nitrate-reducing. Autoclaved 250 mL serum bottles were filled with 30 g of diluted soil and 150 mL of liquid medium (Table S4.1). The nitrate-reducing medium, with the same composition as the aerobic conditions, was prepared with boiled water cooled with a N_2 stream. Bottles were sealed with polytetrafluoroethylene stoppers, shaken, and 6 mL slurry samples were collected for DNA

analysis (pre-incubation start). Headspace gas exchange (0.5 atm overpressure) was performed with pressurized air (aerobic conditions) or N_2 (nitrate-reducing conditions). The bottles were incubated in the dark, to avoid OMP photodegradation, at 20°C on a 120 rpm shaker. A regrowth period of 62-66 days before OMP spiking was included, reflecting the 4-day difference in starting times among the diversity levels, to allow microbial populations to reach similar biomass levels post-dilution. At the end of the regrowth period, slurry samples were collected again, and qPCR (quantitative polymerase-chain-reaction) results indicated comparable microbial biomass across the diversity levels, namely $8.9 \times 10^4 \pm 3.3 \times 10^4$ copies/mg under aerobic and $1.5 \times 10^5 \pm 9.3 \times 10^4$ copies/mg under nitrate-reducing conditions (Figure S4.1). Microbial diversity was studied using alpha diversity metrics to evaluate differences between the diluted communities (10^{-1}, 10^{-3}, and 10^{-6}) and temporal changes within each community. A solution of 20 OMPs in sterilized Milli-Q water (at 7.5 mg/L each, within the solubility range of all OMPs selected) was then spiked into the biotic bottles to a concentration of 25 µg/L for each OMP (Table 4.1). This concentration was chosen to enable detection of TPs generated from the spiked OMPs. The mixture contained pesticides, pharmaceuticals, and industrial chemicals with different biodegradability and low sorption to the soil used. The bottles were incubated under the same conditions as during regrowth for 112 days after the OMP spike. Since the qPCR results at the beginning and end of the incubation with OMP showed comparable microbial biomass across the diversity batches (with the same redox – Figure S4.1), observed differences in OMP biodegradation and TP formation can be attributed primarily to microbial diversity.

Biotic blanks (n=3, 10^{-1} soil dilution) without OMPs were included for each redox condition to assess the background levels of OMPs and TPs. Abiotic controls (n=3) with only sterilized soil, medium, and N_2 headspace were used to assess OMP sorption. After OMP spike, the abiotic controls were incubated under the same conditions as the biotic for 72 hours, sorption being a fast process (Lim et al., 2023; Sithamparanathan et al., 2021), and sampled at the beginning and end of this period before being stored at 4°C to further inhibit microbial activity.

Table 4.1. OMPs spiked in the biotic and abiotic batches.

2,4-Dichlorophenoxyacetic acid (2,4-D)	Diethyltoluamide (DEET)	Metformin (MTF)
2,6-dichlorobenzamide (BAM)	Diclofenac (DCF)	Metolachlor (MET)
Bentazon (BTZ)	Diglyme (DGY)	Metoprolol (MTP)
(1H)Benzotriazole (1H-BTR)	Dimetridazole (DMZ)	Paracetamol (PCM)
Caffeine (CAF)	Furosemide (FUR)	Sotalol (SOT)
Carbamazepine (CBZ)	Hydrochlorothiazide (HCZ)	Sulfamethoxazole (SMX)
Chloridazon (CLZ)	Mecoprop (MCPP)	

4.2.3 Chemical analyses

Gas samples from the headspace (2 mL) and liquid samples (2x2 mL) were taken from the biotic and blank batches at day 0, 7, 15, 28, 56, 70, 84, 98, and 112 after the OMP spike. Headspace analysis was performed to verify the preservation of aerobic (sufficient oxygen levels) or nitrate-reducing (absence of oxygen) conditions inside the bottles. Liquid samples were centrifuged at 15000 rcf for 10 minutes; 2 mL of supernatant was stored at -20°C in tubes with 2.5% acetonitrile (ACN), then thawed and centrifuged again before liquid chromatography-mass spectrometry (LC-MS) target OMP analysis (5% ACN in the final sample). The remaining 2 mL of supernatant was centrifuged again before use for nitrate analysis. These samples were stored at -20°C until OMP non-target analysis (NTA). Additionally, slurry samples (6 mL) for DNA extractions were taken at the start of the experiment, at the end of the regrowth period (just before OMP spiking – day 0), and at the end of the incubation (on day 116 after OMP spike). Slurry samples were stored at -80°C until DNA extraction. Details on the materials and methods used for headspace, nitrate, and DNA (extraction and quantification) analyses are provided in SI 4.2.3.

4.2.3.1 Microbial diversity analysis

DNA extracts were analyzed by Bioclear Earth B.V. using the default pipeline from USEARCH (Edgar, 2010), similarly to previous work (Yan et al., 2024). The samples were amplified with PCR using an Illumina® MiSeq™ System and prokaryotic primers (Pro341F and Pro805R) to target the variable regions V3 and V4 of the 16S ribosomal RNA gene of bacteria. Quality control was performed, and samples collected at the start of the regrowth period did not pass the quality check, therefore were excluded. Alpha diversity was quantified using two complementary metrics: the number of Amplicon Sequence Variants (ASVs) and the Shannon diversity index. ASV richness reflects the total number of distinct taxa detected in a community, providing a measure of taxonomic breadth. The Shannon index accounts for both richness and evenness, weighting taxa by relative abundances to capture community structure complexity. These two metrics together capture the extent and balance of microbial diversity across dilution levels and redox conditions.

4.2.3.2 OMP target analysis

Target OMPs analysis was performed with liquid chromatography (UHPLC ExionLC™ AD 30) coupled with mass spectrometry (SCIEX Triple Quad™ MS 5500, USA). The UHPLC column (Kinetex Core-Shell Polar C18 2.6 µm, 100 Å, 150x2.1 mm), connected to a Guard pre-column (Phenomenex™, USA), was operated at 35 °C with a flow of 0.3 mL/min. Eluent A (Milli-Q water with 0.1% v/v formic acid) and B (ACN with 0.1% v/v formic acid) composed the mobile phase. The chromatographic separation gradient started with 95% eluent A, which

decreased linearly to 20% from 0.5 to 3.5 minutes, then remained constant at 20% until 7.5 min. The initial conditions (95% A and 5% B) were repristinated with a linear gradient from 7.5 to 8.5 minutes. From 8.5 to 12.4 minutes, the composition was kept constant to stabilize the system before the next injection. The analyzed samples (25 µL) contained 5% ACN and included internal standards (mecoprop-d_6, furosemide-d_5, caffeine-d_9, sulfamethoxazole-d_4, benzotriazole-d_4, carbamazepine-d_{10}, diclofenac-d_4). The list of target compounds is the same as the spiked parent compounds (Table 4.1) with the addition of 4,5-methyl-benzotriazole and desphenyl-chloridazon, which were not spiked but included in the target list to assess their formation as TPs. A mixed solution of these compounds was used to build a calibration curve from 250 ng/L to 1000 ng/L (5% ACN in the final samples).

4.2.3.3 Non-target OMP analysis

NTA was performed with a Bruker Daltonics system composed of ultra-high-performance liquid chromatography (UHPLC) equipped with a Kinetex® UPLC column (100 mm long, 2.1 mm diameter, and 1.7 µm biphenyl 100 Å) and coupled with trapped ion mobility spectrometry, quadrupole time of flight, and high-resolution tandem mass spectrometry (HR-MS/MS) with Parallel Accumulation Serial Fragmentation (PASEF). The mobile phases (from Biosolve – the Netherlands) were UPLC-grade water with 0.05% acetic acid and UHPLC/MS grade methanol. The specifics of the method were previously described (Ore et al., 2025c). The samples were analyzed with direct injection after double centrifugation at 15000 rcf for 10 minutes.

4.2.4 Data treatment and interpretation

4.2.4.1 Removal efficiency and half-life

Removal efficiencies of OMPs were calculated with Equation 4.1.

Equation 4.1. Removal efficiency of an OMP (A), where $C_{A,\,start}$ and $C_{A,\,end}$ are the concentrations of the OMP at the beginning (day 0) and the end (day 112) of the incubation with OMPs, respectively.

$$RE_A = \frac{(C_{A,start} - C_{A,end})}{C_{A,start}} \quad (4.1)$$

To calculate half-lives, i.e., when the OMP concentration equals half the initial concentration, a first-order reaction was assumed for OMP biodegradation. Experimental data were used to extrapolate the slope (k) of the biodegradation reaction (Equation 4.2), which was used to calculate the half-life (Equation 4.3).

Equation 4.2. First-order reaction to extrapolate the slope k. [A] is the concentration of the OMP at a specific time point (t) or at the beginning of the incubation with OMPs (t0).

$$\ln[A]_t = -k_t + \ln[A]_{t0} \quad (4.2)$$

Equation 4.3. Half-life formula assuming first-order reaction, where DT_{50} is the time when the OMP concentration is half the initial concentration, and k is the slope of the biodegradation reaction.

$$DT_{50} = -\frac{\ln 0.5}{k} \quad (4.3)$$

4.2.4.2 Non-target data treatment

Open source software was used to convert and treat the NTA data. TIMSCONVERT 2.0.0 (Luu et al., 2022) was used to convert raw .tdf data to .mzML format, while patRoon 2.3.3 (Helmus, 2024) was used to treat NTA data and screen for TPs. To allow compatibility with patRoon, the raw data were centroided, and the trapped ion mobility arrays were excluded during conversion. The patRoon script (Supplementary Script 4.1) was adapted from a previous study (Ore et al., 2025c) to suit the experiment. Specifically, the minimum peak intensity was set to 5000, and peaks present in at least two of the replicates were retained. A suspect screening for the spiked OMPs was performed, including the fragments m/z (mass to charge ratio) obtained from target analysis, to support the annotation. In the TP screening step, BioTransformer 3.0 (Djoumbou-Feunang et al., 2019; Wishart et al., 2022) with the environmental microbial prediction module (Wicker et al., 2016) was used to generate a list of predicted TPs up to 7 generations and to screen our dataset. The list included more than 15700 candidate-TPs (Supplementary Excel -SE- 4, Table E1), but only TPs detected in our dataset with peak intensities higher than 5000 and identification level (ID) 4 or higher were retained after annotation. Additionally, TPs present in the blanks, likely formed during the OMP spike solution preparation or with wrong annotation (i.e., showing carbon-atom hypervalence), were not retained. These prioritization steps caused the removal of many TPs that may have been formed in low abundance or with low-quality data, but guarantee a higher confidence in the annotation and the assignment of TPs to specific PCs. Visual investigation of TP peak intensities was performed through the HTML report of patRoon and mzMine (Schmid et al., 2023), where the replicates' average peak intensity was used.

4.2.4.3 In-silico predictions with BioTransformer and OPERA

The TP persistence predictions were done using BioTransformer 3.0 (for consistency with the same model used in patRoon) and a beta version of BioTransformer 4.0 (Djoumbou-Feunang et al., 2019; Tian et al., 2025; Wishart et al., 2022). The two versions differ in the handling of atom valencies and in some updated reaction rules. The predictions were run for 10 reaction steps using the environmental microbial module. The data was then processed using Python to identify all unique TPs (defined here as compounds sharing the same InChIKey) as well as the unique reactions. Potential dead-end TPs were also identified, defined here as TPs for which no further BioTransformer reaction rules applied, and therefore no further TP was returned by the model. Any compounds with errors produced

by the model (e.g., memory issues or the compound being outside the model's applicability) were excluded.

Toxicity predictions for all TPs annotated with sufficient confidence (Section 4.2.4.2) and for the 20 spiked OMPs were carried out for estrogen and androgen receptor activity, using the CERAPP (Mansouri et al., 2016) and CoMPARA (Mansouri et al., 2020) modules of OPERA, respectively. The model applicability domain was set according to Mansouri et. al. (2018).

4.3 Results and discussion

4.3.1 Soil-based dilution-to-extinction creates populations with different microbial diversity

Microbial DNA sequencing showed that the dilution-to-extinction was successful, as the alpha diversity metrics and ANOVA results confirmed the creation of microbial communities with significantly different diversity levels (Figure 4.1, SI 4.2.4, Table S4.2). Specifically, under aerobic conditions, the observed and Shannon diversity showed very distinct microbial diversity levels for the 10^{-1}, 10^{-3}, and 10^{-6} dilutions, spanning from 2156 to 436 Amplicon Sequence Variants (ASVs), and from Shannon values of 6.01 to 3.09. The aerobic populations maintained a significantly different diversity during the incubation (Table S4.2). Under nitrate-reducing conditions, the diversity levels were lower compared to aerobic, spanning from 1180 to 339 ASVs and Shannon values from 5.06 to 3.06 for the 10^{-1} and 10^{-6} dilutions, respectively. Moreover, the 10^{-6} dilution increased in diversity during incubation under nitrate-reducing conditions to reach similar levels as the 10^{-3} (Figure 4.1, Tables S4.2, S4.3).

The dilution-to-extinction approach is typically applied in liquid phase, where a microbial inoculum is suspended in a solution, serially diluted to remove the less abundant species, and subsequently used to inoculate soil or other experimental systems (Philippot et al., 2013; Stadler et al., 2012; Tardy et al., 2014). To the best of our knowledge, only Posselt et al. (2020) previously reported a solid-based dilution-to-extinction approach, in which baked sand was used to dilute a river sediment inoculum, to study the influence of microbial diversity and hyphoreic exchange flows on OMP removal (Posselt et al., 2020). As opposed to previous studies, for dilution, we used sterilized soil from the same location as the active inoculum. Compared to liquid extraction of soil microorganisms before liquid-based dilution-to-extinction, directly diluting active soil with sterilized soil as performed here (solid-based approach) may better preserve the native microbial community composition by minimizing disturbance.

Shannon diversity values from our undiluted soil and previously reported soils (Jayaramaiah et al., 2022; Sun et al., 2019) ranged from 6 to 9.08 (Table S4.4), highlighting how soil microbial diversity can differ across locations. Such differences in natural soils are comparable to those we created through dilution (with Shannon values spanning from 3.06

to 6.01) and may influence biodegradability test outcomes, particularly for compounds requiring specific degrading enzymes or metabolic synergies. Therefore, local soil microbial diversity should be considered when interpreting or comparing biodegradation results. Soil microbial diversity was consistently higher than in activated sludge (Martínez-Quintela et al., 2023; Stadler et al., 2012) or aquifers (Aldas-Vargas et al., 2019), indicating a broader taxonomic richness.

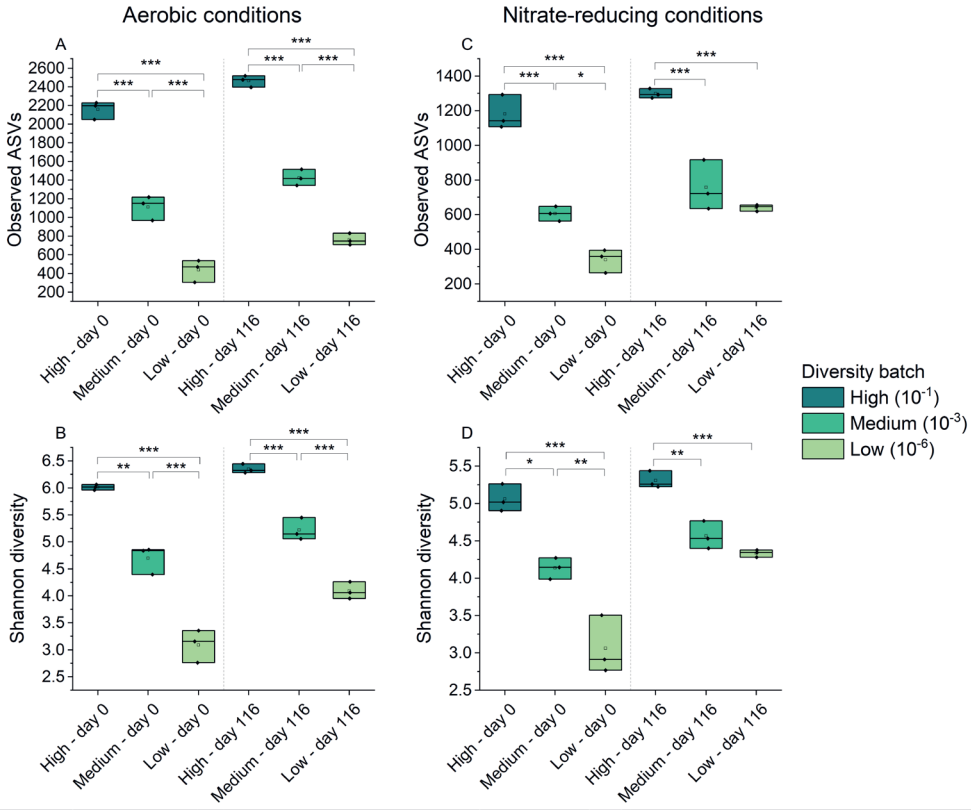

*Figure 4.1. Aerobic (left) and nitrate-reducing (right) alpha diversity results: observed number of ASVs (Amplicon Sequence Variants) in graphs A and C on the top row, and Shannon diversity in graphs B and D on the bottom row. Asterisks indicate significant differences: * p<0.05, ** p<0.01, *** p<0.001. The color shade differentiates the diversity batches in high diversity (10^{-1}, darker green), medium diversity (10^{-3}, medium green), and low diversity (10^{-6}, lighter green).*

Temporal analysis of microbial diversity within each condition revealed significant changes during incubation with OMPs, particularly under aerobic conditions and in low-diversity communities under both redox conditions (Table S4.3). Diversity increased over time, possibly due to the regrowth of species able to degrade or tolerate OMPs, as was previously observed (Posselt et al., 2020), or ongoing community shifts following dilution. This increase was more pronounced in less diverse communities (Table S4.3), probably due to lower functional redundancy and competition. In contrast, high-diversity communities remained

more stable, likely thanks to functional redundancy (de Souza et al., 2017; Girvan et al., 2005). Despite the increase over time, low-diversity communities did not reach the diversity levels of high-diversity conditions (Figure 4.1). The higher number of ASVs in the 10^{-1} population reflected a broader taxonomic composition, which likely supported functional redundancy and complementary metabolic capabilities, consistent with mechanisms such as co-metabolism and synergies that can support more efficient OMP biodegradation.

4.3.2 Microbial diversity influences the removal of spiked OMPs

OMP target analysis indicated a positive correlation between microbial diversity and both the number of spiked OMP degraded and their biodegradation rate. In more diverse communities (10^{-1} and 10^{-3} dilutions), more OMPs showed significant biodegradation, defined here as at least 30% higher removal than abiotic losses, under both aerobic and nitrate-reducing conditions compared to the low-diversity communities (10^{-6} dilution) (Tables 4.2 and S4.5). Under aerobic conditions, higher-diversity communities (10^{-1} and 10^{-3}) significantly degraded 15 of the 20 spiked OMPs, while the low-diversity community degraded only 11 OMPs. Moreover, compounds like sulfamethoxazole, chloridazon, and mecoprop showed high removal efficiencies in the high- and medium-diversity communities, but limited or no biodegradation in the low-diversity (Table S4.5). Biodegradation efficiencies were lower under nitrate-reducing conditions, with a maximum of 8 OMPs biodegraded. Still, the positive correlation with diversity remained evident, as only 4 OMPs, paracetamol, hydrochlorothiazide, metoprolol, and sotalol, achieved significant biodegradation in the 10^{-6} dilution (Tables 4.2, S4.5). Statistical analysis supported these trends (SI 4.2.4, Table S4.6). Pairwise t-test of removal efficiencies showed significant differences between the highest and lowest diversity levels under aerobic and nitrate-reducing conditions (p=4.1x10^{-6} and p=0.002, respectively), while difference between the highest and medium diversity was insignificant (p>0.05). The mean Pearson correlation coefficient (r) across individual OMPs and removal efficiency was 0.28 ± 0.43 (aerobic) and 0.26 ± 0.41 (nitrate-reducing), confirming the positive association between microbial diversity and biodegradation. Unlike Posselt et al. (2020), our experimental setup allowed us to differentiate OMP biodegradation from other removal mechanisms: abiotic removal (e.g., sorption, hydrolysis) was assessed through dedicated controls (Table S4.5), and photodegradation was excluded by incubating all bottles in the dark. This design and the qPCR results supported the confident attribution of observed differences in OMP degradation to microbial diversity, the only variable across systems under each redox condition.

Table 4.2. Number of parent compounds showing a removal efficiency (RE%) at least 30% higher than the abiotic removal by target OMP analysis; number of PCs for which TPs were detected with NTA.

Condition	#PC with RE%>30% (target)	#PC generating TPs (NTA)
AER 10^{-1}	14	7
AER 10^{-3}	15	6
AER 10^{-6}	11	3
NITR 10^{-1}	7	5
NITR 10^{-3}	8	4
NITR 10^{-6}	4	4

The DT_{50} analysis further confirmed that higher microbial diversity enhanced both the number of spiked OMPs degraded and their biodegradation rates, particularly under aerobic conditions. Lower diversity was associated with longer DT_{50}s, indicating slower degradation (Table 4.3, Figures S4.2, S4.3). For example, chloridazon and mecoprop had DT_{50}s of 35-40 and 68 days, respectively, under higher-diversity conditions, but their removal was negligible under low diversity. Furosemide and 2,4-D showed half-lives of 9-17 days under high and medium-diversity conditions, which extended to 69 and 40 days under low diversity.

Several 2,4-D-degrading genera were detected under all conditions, including *Variovorax*, *Bradyrhizobium*, *Novosphingobium*, *Sphingomonas*, *Cupriavidus*, *Burkholderia*, *Pseudomonas*, and *Rhodococcus* (Chen et al., 2024; Peng et al., 2025; Rutere et al., 2021; Y. Wang et al., 2023). Remarkably, their relative abundance was the highest in the 10^{-3} batches and the lowest in the 10^{-1} batches (SE4 Tables E2-E7). However, the shortest half-life was observed in the high-diversity community, suggesting that metabolic interactions among taxa (like metabolic synergies or cross-feeding), rather than degrader abundance alone, contributed to the efficient degradation of 2,4-D. Under nitrate-reducing conditions, fewer OMPs exhibited significant biodegradation (Table 4.3). Dimetridazole, metolachlor, and 2,4-D showed shorter half-lives under high and medium diversity, but negligible removal in low-diversity communities, confirming the correlation between OMP degradation rates and microbial diversity. Notably, a few compounds, including metoprolol, hydrochlorothiazide, and paracetamol, exhibited similar removal across all diversity and redox conditions (Tables 4.3 and S4.5). This is likely due to ubiquitous degradation mechanisms catalysed by broadly distributed enzymes or cometabolic pathways less dependent on community diversity (Coll et al., 2020; Stadler et al., 2018). These exceptions, however, did not alter the general trend that higher-diversity communities achieved better OMP biodegradation.

Overall, the low-diversity community exhibited significantly reduced biodegradation of the spiked OMPs and longer DT_{50}s, whereas the high and medium-diversity communities performed similarly. These results suggest that microbial diversity influences OMP biodegradation primarily under a certain diversity threshold. In our experiment, the diversity reduction between the 10^{-1} and 10^{-3} dilutions did not substantially alter OMP

biodegradation, while the 10^{-6} dilution fell below this threshold, resulting in reduced OMP biodegradation (Table S4.6). Moreover, under aerobic conditions, the 10^{-3} community showed higher respiration, indicating elevated microbial activity that could have further supported metabolic and cometabolic OMP degradation (Figure S4.4).

These findings support the hypothesis that microbial diversity (within the tested range) is a key driver for OMP biodegradation, influencing both the number of OMPs degraded and the rate of biodegradation. Higher diversity communities contained more taxa, increasing functional redundancy (i.e., multiple species potentially capable of degrading the same OMP) and likely promoting complementary metabolic interactions. Although our data do not directly demonstrate metabolic synergies, the observed trends are consistent with such mechanisms in more diverse microbial communities, as previously reported (Lindemann et al., 2016; Morris et al., 2013). Given the relatively high concentrations of spiked OMPs, both metabolic and cometabolic OMP biodegradation may have occurred. Metabolic degradation depends on the presence of specific microorganisms and enzymes, which may have been lacking in low-diversity communities. Metabolic synergies require the right combination of microbial species, which are more likely to occur in diverse communities.

*Table 4.3. Half-lives (DT_{50}) in days with standard deviation of each spiked OMP under aerobic and nitrate-reducing conditions. DT_{50} values were determined for OMPs showing >30% removal efficiency relative to abiotic losses. Some compounds (e.g., DEET and diglyme), therefore, exhibited long DT_{50} despite being considered generally recalcitrant. Cells with missing values (grey) indicate negligible biodegradation compared to the abiotic controls. Acronyms for OMPs are listed in Table 1. *Standard deviation not shown because only one replicate value was available.*

DT_{50} (days)	MTP	1H-BTR	CAF	CBZ	SMX	DEET	BAM	DMZ	SOT	DGY	MTF	MET	PCM	CLZ	DCF	FUR	MCPP	2,4-D	BTZ	HCZ
AER 10^{-1}	26.8 ± 2.2	42.9 ± 2.6	16.4 ± 5.4	110.3 ± 27.4	41.8 ± 8.6				34.3 ± 5.4			56.4 ± 6.2	2.4 ± 0.1	34.9 ± 4.6	19.9 ± 1.7	17.5 ± 1.2	67.9 ± 4.8	8.8 ± 0.1		54.1 ± 5.6
AER 10^{-3}	26.2 ± 1.5	31.8 ± 4.7	13.6 ± 0.4	108.9 ± 14.7		92.25*			26.0 ± 1.6	162.9 ± 101.8		76.4 ± 21.5	2.3 ± 0.8	40.2 ± 14.1	2.3 ± 0.2	16.9 ± 5.5	68.2 ± 33.8	12.5 ± 1.5		52.0 ± 10.0
AER 10^{-6}	25.7 ± 4.4	59.4 ± 23.4	13.8 ± 0.3	94.4 ± 9.1					51.5 ± 24.5			75.3 ± 14.4	1.6 ± 0.7		114.4 ± 36.9	69.4 ± 39.8		40.4 ± 14.2		56.6 ± 4.0
NITR 10^{-1}	25.1 ± 2.1							116.0 ± 8.2	28.1 ± 3.8			72.4 ± 5.3	2.3 ± 0.0					44.2 ± 2.5		52.8 ± 0.6
NITR 10^{-3}	25.8 ± 3.0		43.5 ± 29.4					71.7 ± 99.5	33.1 ± 3.4			64.2 ± 16.9	10.0 ± 7.6					44.6 ± 36.1		51.1 ± 4.5
NITR 10^{-6}	28.6 ± 2.9								46.0 ± 7.4				2.2 ± 2.0							57.8 ± 12.7

4.3.3 Diversity affects the rate of TP formation

Higher microbial diversity resulted in higher spiked OMP degradation rates (Section 4.3.2), enhancing the formation and further transformation of TPs. Under aerobic conditions, the high-diversity community produced the highest number of TPs, with 9 TPs detected using NTA from 7 different PCs (Figure 4.2, Table 4.2). This trend persisted clearly in the medium and low-diversity communities, with 7 and 5 TPs detected, respectively. The exclusive detection of certain TPs at higher diversity, like metolachlor-TP119 and hydrochlorothiazide-TP825, and absence in low-diversity communities suggests the availability of more biodegradation pathways at higher diversity (Table 4.4). Similar trends were observed under nitrate-reducing conditions, where 5 TPs were detected under high and medium diversity, compared to 4 under low diversity (Figure 4.2). Under nitrate-reducing conditions, especially at lower diversity, we detected TPs of PCs with negligible removal, suggesting minimal biotransformation even when overall degradation was within 30% of abiotic removal. This high threshold for defining spiked OMP biodegradation was selected to rigorously distinguish biological from abiotic processes, whereas NTA merely detects TP presence regardless of the PC degradation efficiency. Details on TP SMILES, ID levels, and the BioTransformer-predicted reaction rules are reported in SE4 Table E8.

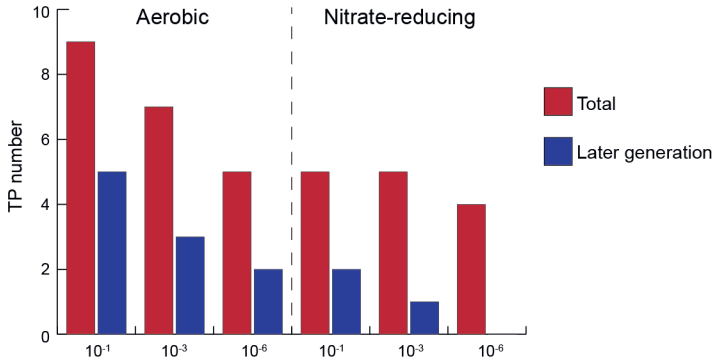

Figure 4.2. Number of TPs detected (total vs. TPs of generation ≥ 4) across high (10^{-1}), medium (10^{-3}), and low (10^{-6}) diversity and redox conditions.

In addition to higher numbers of TPs, the rate of TP formation and further degradation increased with higher diversity. For TPs detected across multiple diversity levels, e.g., metoprolol-TP20 and metolachlor-TP161, formation occurred earlier in higher diversity communities under both redox conditions (Table 4.4). Under aerobic conditions, metoprolol-TP20 (i.e., metoprolol acid) was detected by day 7 in the high-diversity community, compared to day 28 and 56 in medium and low-diversity communities, respectively. The TP's peak intensity increased and then decreased in high and medium-

diversity communities, whereas in the low-diversity community it continued rising throughout the incubation period (SE4 Table E9). This suggests metoprolol acid degraded further under higher diversity conditions, even though no later TPs could be confidently assigned. The same pattern was observed for 2,4-D-TP1 (2,4-dinitrophenol), which was completely transformed within 28 days in high-diversity communities, by day 56 under medium-diversity conditions, and was not fully removed under low-diversity conditions, although the peak intensity showed a constant decrease during incubation (Table 4.4, SE4 Table E9). Previous research also found persistence of some TPs during incubation under low diversity (Posselt et al., 2020). Metoprolol acid and metolachlor-TP161 were also detected under nitrate-reducing conditions, but only in higher diversity and after longer incubation compared to aerobic conditions. Similar to the lowest diversity aerobic conditions, metoprolol acid showed only an increasing peak intensity under nitrate-reducing conditions.

Table 4.4. TPs detected under aerobic and nitrate-reducing conditions, per diversity level (higher = 10^{-1}, lowest = 10^{-6}) during incubation. The TP generation is reported in the first column; the TP identification level (ID), as well as the removal efficiency (RE%) and half-life in days (DT50) of the corresponding parent compounds (PCs) are on the right. Standard deviations for RE% and DT50s are reported in Tables 4.3 and S4.5. Each TP includes the corresponding PC acronym (Table 4.1) in the first part of the name. Colored-TPs are unique to the corresponding diversity level.

AER 10^{-1}									
	0 d	**7 d**	**28 d**	**56 d**	**84 d**	**112 d**	**ID TP**	**RE% PC**	**DT_{50} PC (d)**
Gen 1	PCM-TP2						**3a**	**>99**	**2.4**
	2,4-D-TP1	2,4-D-TP1					**2a**	**>99**	**8.8**
				FUR-TP4	FUR-TP4	FUR-TP4	**3c**	**>98**	**17.5**
Gen 2		MTP-TP20	MTP-TP20	MTP-TP20	MTP-TP20	MTP-TP20	**3a**	**>97**	**26.8**
Gen 4					MET-TP119		**3c**	**81.9**	**56.4**
			MET-TP161	MET-TP161	MET-TP161	MET-TP161	**3c**	**81.9**	**56.4**
Gen 5		MET-TP235	MET-TP235	MET-TP235	MET-TP235	MET-TP235	**3c**	**81.9**	**56.4**
Gen 6			CLZ-TP65	CLZ-TP65	CLZ-TP65	CLZ-TP65	**1**	**88.5**	**34.9**
Gen 7			HCZ-TP825	HCZ-TP825	HCZ-TP825	HCZ-TP825	**3c**	**76**	**54.1**
AER 10^{-3}									
	0 d	**7 d**	**28 d**	**56 d**	**84 d**	**112 d**	**ID TP**	**RE% PC**	**DT_{50} PC (d)**
Gen 1	PCM-TP2						**3a**	**>96**	**2.3**
	2,4-D-TP1	2,4-D-TP1	2,4-D-TP1				**2a**	**>99**	**12.5**
				FUR-TP4	FUR-TP4	FUR-TP4	**3c**	**>98**	**16.9**
Gen 2			MTP-TP20	MTP-TP20	MTP-TP20	MTP-TP20	**3a**	**>98**	**26.2**
Gen 4			MET-TP161	MET-TP161	MET-TP161	MET-TP161	**3c**	**75.8**	**76.4**
Gen 5		MET-TP235	MET-TP235	MET-TP235	MET-TP235	MET-TP235	**3c**	**75.8**	**76.4**

Gen 6					CHZ-TP65	CHZ-TP65	**1**	**77.5**	**40.2**
AER 10^{-6}									
	0 d	**7 d**	**28 d**	**56 d**	**84 d**	**112 d**	**ID TP**	**RE% PC**	**DT_{50} PC (d)**
Gen 1	2,4-D-TP1	2,4-D-TP1	2,4-D-TP1	2,4-D-TP1	2,4-D-TP1	2,4-D-TP1	**2a**	**72.7**	**40.4**
				MTP-TP1			**3c**	**>97**	**25.7**
Gen 2				MTP-TP20	MTP-TP20	MTP-TP20	**3a**	**>97**	**25.7**
Gen 4					MET-TP161	MET-TP161	**3c**	**72.6**	**75.3**
Gen 5		MET-TP235	MET-TP235	MET-TP235	MET-TP235	MET-TP235	**3c**	**72.6**	**75.3**
NITR 10^{-1}									
	0 d	**7 d**	**28 d**	**56 d**	**84 d**	**112 d**	**ID TP**	**RE% PC**	**DT_{50} PC (d)**
Gen 1	PCM-TP2						**4b**	**>99**	**2.3**
	2,4-D-TP1	2,4-D-TP1	2,4-D-TP1	2,4-D-TP1	2,4-D-TP1	2,4-D-TP1	**2a**	**83.2**	**44.2**
Gen 2					MTP-TP20	MTP-TP20	**3a**	**>99**	**25.1**
Gen 4				MET-TP161	MET-TP161	MET-TP161	**3c**	**78.2**	**72.4**
Gen 6			FUR-TP1717	FUR-TP1717	FUR-TP1717	FUR-TP1717	**3c**	**<30**	-
NITR 10^{-3}									
	0 d	**7 d**	**28 d**	**56 d**	**84 d**	**112 d**	**ID TP**	**RE% PC**	**DT_{50} PC (d)**
Gen 1	PCM-TP2						**4b**	**>99**	**10.0**
	2,4-D-TP1	2,4-D-TP1	2,4-D-TP1	2,4-D-TP1	2,4-D-TP1	2,4-D-TP1	**2a**	**84.1**	**44.6**
					MET-TP1	MET-TP1	**3c**	**81.6**	**64.2**
Gen 3			SOT-TP53				**3c**	**97.4**	**33.1**
Gen 4						MET-TP161	**3c**	**81.6**	**64.2**
NITR 10^{-6}									
	0 d	**7 d**	**28 d**	**56 d**	**84 d**	**112 d**	**ID TP**	**RE% PC**	**DT_{50} PC (d)**
Gen 1	2,4-D-TP1	2,4-D-TP1	2,4-D-TP1	2,4-D-TP1	2,4-D-TP1	2,4-D-TP1	**2a**	**8.1**	-
Gen 2			MCPP-TP6	MCPP-TP6	MCPP-TP6	MCPP-TP6	**3c**	**<30**	-
Gen 3			SOT-TP53	SOT-TP53			**3c**	**94.2**	**46.0**
			FUR-TP86	FUR-TP86			**3c**	**<30**	-

Under aerobic conditions, chloridazon was biodegraded; however, the formation of the main TP chloridazon-TP65 (chloridazon-desphenyl) was diversity-dependent. Chloridazon-desphenyl was detected on day 14 in high-diversity communities, on day 56 under medium diversity, while it was not detected under the lowest diversity (Table 4.4). This observation was confirmed by target analysis, showing the gradual TP formation along with the PC degradation (Figure 4.3). The concentration of chloridazon-desphenyl in 10^{-1} and 10^{-3} consistently increased during incubation, suggesting its potential accumulation and

persistence in our system, as has been found previously (Zakhia et al., 2025)(SE4 Table E9). The absence of chloridazon-desphenyl in the low-diversity community may be linked to the lower abundance of *Chloroflexi*, a phylum previously associated with chloridazon biodegradation (Aldas-Vargas et al., 2022). In our study, many *Chloroflexi* genera present under high diversity were initially missing in medium and low-diversity communities. By the end of the incubation, the number of *Chloroflexi* genera in medium-diversity (17) approached that of the high-diversity community (18), but remained lower in the low-diversity community (12), likely limiting chloridazon biodegradation (SE4 Tables E2, E3, E4). Higher diversity also promoted further progression along degradation pathways, as more later-generation TPs (generation ≥4) were detected (Figure 4.2, Table 4.4). Five later-generation TPs were detected under higher diversity, compared to 3 and 2 in medium and low-diversity communities, respectively. This trend held under nitrate-reducing conditions, where later-generation TPs were detected only in the highest and medium-diversity communities (Figure 4.2).

Overall, higher diversity communities were faster in forming and further degrading TPs, likely due to greater functional redundancy and variety of possible degradation pathways. These results highlight how systems in which microbial diversity is the only variable can function differently, achieving different biodegradation results. This and previous studies (Coll et al., 2020; Davenport et al., 2022; Jayaramaiah et al., 2022; Posselt et al., 2020; Poursat et al., 2019) support the importance of considering microbial diversity in biodegradability tests, like the OECD 308 and 309, which will guide the regulatory status for contaminants in the environment, for example by including diversity metrics (e.g., ASV richness, Shannon index) to characterize the inoculum.

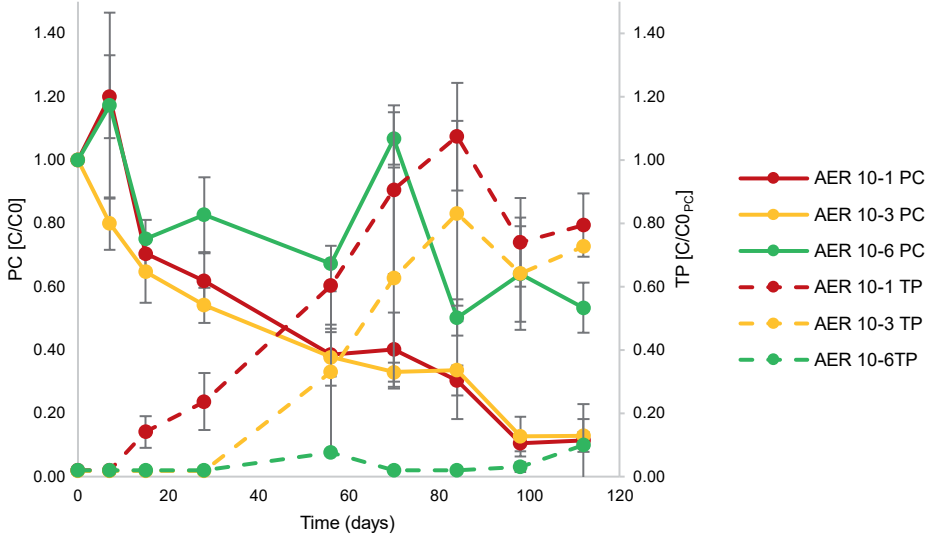

Figure 4.3. Concentrations (mol/L) over time of chloridazon (PC) and its TP (chloridazon-desphenyl = CLZ-TP65) normalized against chloridazon initial concentration, under aerobic conditions across high (10^{-1}), medium (10^{-3}), and low (10^{-6}) diversity.

Comparison of target and non-target analyses revealed that not all spiked OMPs with observed removal and short DT_{50}s had detectable TPs (Tables 4.3, 4.4, and S4.5). We expected the detection of 4-methylbenzotriazole or 5-methylbenzotriazole, as benzotriazole biodegradation was high under aerobic conditions (Table 3), and these TPs were previously detected (Posselt et al., 2020). However, target analysis confirmed its absence above the limit of quantification in our samples.

Although some TPs showed increasing peak intensity until the end of the incubation, BioTransformer predictions indicated that none were likely dead-end TPs (SE4 Tables E8, E9). Still, as BioTranformer does not consider environmental conditions, not all predicted reactions may have occurred under the specific conditions and timeframe of our experiment. The OPERA toxicity predictions (CERAPP and CoMPARA) suggested that some TPs may be potentially hazardous (Mansouri et al., 2018, 2016). In particular, 2,4-D-TP1 was predicted to exhibit potential estrogenic activity, and furosemide-TP1717 showed possible androgen receptor binding, unlike its PC (SE4 Tables E8, E10). While furosemide has been shown to exhibit weak estrogenic activity at high concentrations in vitro (Fent et al., 2006; Isidori et al., 2009), no androgenic effects have been reported. This highlights the importance of assessing TPs separately from their PCs in risk evaluations, as they may pose distinct environmental or health risks.

4.3.4 Redox conditions affect OMP degradation and TP formation

Overall, more spiked OMPs showed limited or no biodegradation (i.e., <30% removal compared to abiotic losses) or degraded more slowly under nitrate-reducing conditions than aerobic conditions. Microbial communities under aerobic conditions degraded up to 15 OMPs significantly, whereas a maximum of 8 were biodegraded under nitrate-reducing conditions (Table 4.2). Compounds like benzotriazole, caffeine, diclofenac, and furosemide exhibited >50% average biodegradation across the three diversity levels in aerobic conditions, but showed no significant biodegradation under nitrate-reducing conditions (Table S4.5).

For spiked OMPs biodegraded under both redox conditions, degradation was slower under nitrate-reducing conditions, as reflected by longer half-lives (Table 4.3). For example, 2,4-D half-lives were 9, 12, and 40 days across the three diversity levels under aerobic conditions, while it was approximately 44 days under nitrate-reducing conditions at higher diversity, and negligible under low diversity (10^{-6}). Similar patterns were observed for metoprolol and sotalol.

In contrast, paracetamol showed rapid degradation under both redox conditions, consistent with previous studies. Löffer et al. (2005) reported a half-life of 3.1 days for paracetamol in an aerobic sediment-water system, with TPs detected in water and non-extractable solid residues shortly after spiking (Löffler et al., 2005). The formation of p-aminophenol (paracetamol-TP2), detected in our study under both redox conditions, has also been reported in a fully aerated membrane bioreactor exhibiting denitrification inside the granules (Rios-Miguel et al., 2022). The conversion was attributable to *Pseudomonas spp.*, detected in our samples under both conditions, which were able to use paracetamol as a sole carbon, nitrogen, and energy source (Rios-Miguel et al., 2022; Zhang et al., 2013).

Redox conditions also influenced the transformation pathways of specific compounds. Some TPs, particularly from dehalogenation reactions such as 2-hydroxymetolachlor (metolachlor-TP1) and o-cresol (mecoprop-TP6), were detected only under nitrate-reducing conditions (Table 4.4). In other cases, different TPs from the same PC were detected under different redox conditions. For furosemide, TP4 formed aerobically, while TP1717 and TP86 formed under nitrate-reducing conditions. Similarly, metolachlor formed TP235 under aerobic conditions and TP1 under nitrate-reducing conditions (Table 4.4).

These differences in spiked OMP biodegradation and TP formation and further transformation are likely linked to differences in microbial community composition and metabolic energy yields. Nitrate-reducing communities showed lower ASV richness and Shannon diversity than aerobic ones (Figure 4.1). Furthermore, taxonomic analysis revealed 51 genera unique to aerobic conditions and 10 exclusive to nitrate-reducing conditions, highlighting the impact of redox conditions on community composition (SE4 Table E11). Several microbial families, including families known to contain OMP degraders (e.g., *Defluviicoccaceae, Rhodospirillaceae, Steroidobacteraceae*) (Peng et al., 2025), were absent under nitrate-reducing conditions. Of these, *Steroidobacteraceae* (strictly aerobic) were present only in 10^{-1} and 10^{-3} batches and showed increased abundance over time (SE4 Tables E2-E4). In contrast, nitrate-reducing conditions selected for some strictly anaerobic genera like *Anaerolinea* and *Azospirillum,* which have been associated with pesticide and hydrocarbon biodegradation (Bao et al., 2024; Cruz-Hernández et al., 2022) (SE4 Tables E5-E7). The overall higher biodegradation efficiency under aerobic conditions is also likely linked to the greater energy yield of aerobic respiration, which supports faster microbial growth and activity than nitrate reduction.

Our results indicate that redox conditions shape the microbial community, thus influencing both the rate and pathway of OMP biodegradation, and that some OMPs are recalcitrant under nitrate-reducing conditions. As redox conditions vary in engineered systems and shift with increasing soil depth, understanding redox-specific degradation and TP formation is

important for predicting OMP removal efficiency and the potential formation of novel, redox-specific TPs.

4.4 Conclusions

Our study demonstrates that microbial diversity, below a certain threshold, influences the extent and rate of OMP biodegradation. Communities with higher microbial diversity (10^{-1} and 10^{-3}) likely retained more degraders and achieved greater biodegradation efficiency. In contrast, low-diversity communities (10^{-6}) exhibited reduced biodegradation, probably due to the absence of specific degraders and reduced potential for complementary metabolic interactions among taxa. Although direct evidence for metabolic synergies was not obtained, the enhanced degradation in high-diversity communities aligns with previously reported cooperative mechanisms in complex microbial communities (Lindemann et al., 2016; Morris et al., 2013). Functional redundancy and metabolic interactions facilitated faster and more complete degradation, as shown by detecting intermediate and later-generation TPs. Delayed TP appearance in low-diversity populations indicated slower degradation processes. Overall, none of the 15 TPs detected were predicted to be dead-end, though two showed potential endocrine-disrupting effects.

The positive association between microbial diversity, OMP biodegradation, and TP formation was observed under aerobic and nitrate-reducing conditions. However, overall biodegradation was higher under aerobic conditions, likely reflecting both greater energy yields from aerobic respiration and broader microbial diversity. Redox-specific microbial taxa and TPs indicated distinct transformation pathways under different redox conditions. While our study included a range of pharmaceuticals, pesticides, and industrial chemicals, generalizing the observed relationship to other OMPs might require further confirmation.

Although we focused on bacterial diversity, fungi may also contribute to OMP biodegradation. Thus, future studies should include fungal diversity to provide a more comprehensive understanding of microbial contributions to OMP degradation. Moreover, assessing a broader range of redox conditions and further investigating the toxicological relevance of the TPs through ecotoxicity tests is recommended. Better understanding of the interplay between microbial diversity and redox conditions can support the design of more effective engineered and nature-based systems for OMP removal.

Overall, our findings underscore the critical role of microbial diversity in OMP fate. Many environmental stressors, including climate change, droughts, and intensive land management, reduce microbial diversity (Guerra et al., 2021; Knight et al., 2024). Our results suggest that biodiversity losses may lower microbial diversity below a critical threshold that hinders OMP biodegradation. These results highlight the importance of considering

microbial diversity in standardized tests for OMP persistence, like the OECD-308 and OECD-309 tests, and environmental and agricultural policies.

Acknowledgments

This research was performed within the framework of the research program AquaConnect, funded by the Dutch Research Council (NWO, grant-ID P19-45) and public and private partners of the AquaConnect consortium and coordinated by Wageningen University and Research. Emma H. Palm acknowledges funding from the European Union's Horizon 2020 research and innovation programme under grant agreement No 101036756, for project ZeroPM: Zero pollution of persistent, mobile substances.

We thank Livio Carlucci, Beatriz Alvarado Perry, Pieter Gremmen, and Lucian Wester for their support with the analyses at Wageningen University. Additionally, we thank Rick Helmus and Patricia Aguilar-Alarcón (University of Amsterdam) for their help with the non-target screening measurements and non-target data handling with patRoon, and Emma Schymanski (University of Luxembourg) for the inputs on the BioTransformer and OPERA predictions.

Supplementary Information

SI 4.2 Materials and methods

SI 4.2.1 Experimental set-up

Table S4.1. Liquid medium composition at the start of the incubation. Nutrients and trace element solutions were prepared according to (Lindeboom, 2014).

	C_{bottle}
Macronutrients	**mg/L**
$NaNO_3$	342
$MgSO_4$. 7 H_2O	54
$CaCl_2$. 2 H_2O	48
Micronutrients *	**mg/L**
$FeCl_2$. 4 H_2O	1.200
$MnCl_2$.4H2O	0.300
$CoCl_2$.6H2O	1.200
$ZnCl_2$	0.030
$CuCl_2$. 2H_2O	0.018
$(NH_4)_6Mo_7O_{24}$. 4H_2O	0.054
H_3BO_3	0.031
Na_2SeO_3 . 5 H_2O	0.060
$NiCl_2$. 6 H_2O	0.030
EDTA	0.600
Na-Resazurin	0.300
	mL/L
HCl 36%	0.216
Buffer (Sørensen, 2Na:1K - pH 7)	**g/L**
Na_2HPO_4	1.09
KH_2PO_4	0.53
Vitamins	**mg/L**
Biotin (vitamin H)	0.005
p-aminobenzoate (Na-salt)	0.013
Pantothenate (Na OR Ca-salt)	0.013
Folic acid (dihydrate)	0.005
Lipoic acid (thioctic acid)	0.013
Pyridoxine (vitamin B6)	0.025
Nicotinamide	0.013
Thiamine HCl (vitamin B1)	0.025
Riboflavin (vitamin B2)	0.013
Cyanocobalamine (vitamin B12)	2.50E-03

SI 4.2.3 Chemical and DNA analyses

Headspace analysis

Gas samples were analyzed to assess microbial respiration (O_2 consumption and CO_2 production) in the aerobic bottles and to verify the absence of O_2 in the nitrate-reducing batch bottles. Gas exchange with overpressure (approx. 1.5 bar) was applied anytime the pressure in the bottles reached similar values to the ambient pressure to avoid external air intrusion through the stoppers. For bottles under nitrate-reducing conditions, gas exchange was performed with 100% N_2 gas. For bottles under aerobic conditions, pressurized air was used and additional gas exchange was applied every time the oxygen concentration in the aerobic bottles was below 10% to ensure aerobic conditions were mainteined throughout the incubation. Gas chromatography (Shimadzu GC-2010) with H_2 as carrier gas (0.5 bar) was used, with a parallel combination of PoraBOND Q (50 m x 0.53 mm; 10 µm; Agilent™, USA) and CP-Molsieve 5Å (25 m x 0.53 mm; 50 µm; Agilent™, USA) columns. The temperature of 120°C was set for the injection, 65°C for the oven, and 150°C for the detector. The ideal gas law was used to convert the results in percentages to mol.

Nitrate analysis

Liquid samples were analyzed for nitrate concentration with ion chromatography (Dionex ICS6000 with autosampler AS-AP). The system comprised a guard column (AS17-C 2mm), an analytical column for anion analysis (Dionex IonPac AS17-C 2mm IC), a dynamically regenerated suppressor (Dionex ADRS 600 2 mm) and a conductivity detector.

DNA extraction

The DNeasy® PowerSoil Pro® Kit (Qiagen, Hilden, Germany) was used to extract the DNA from the pellet obtained after centrifugation of the slurry samples (6 mL) at 15000 rcf for 10 minutes. The manufacturer's protocol was followed, and 50 µL of the final eluent was used in two steps (25+25 µL) to optimize the elution of DNA from the membrane. The extracts were immediately quantified with a Qubit fluorometer (Quant-iT™ dsDNA High-Sensitivity Assay Kit, Invitrogen). The samples were stored at -20 °C until use for qPCR and Next Generation Sequencing (NGS).

DNA quantification

The DNA extracts were used for qPCR to assess the microbial biomass in the batches at three timepoints: the start of the regrowth period (62-66 days before the OMP spike), the day of the OMP spike (day 0), and at the end of the incubation (on day 116). SYBR Green Master Mix (Bio-Rad™) was used as a fluorescence dye, and the primers forward (341F) and reverse (534R) were used to quantify total bacteria targeting the 16S rRNA gene. A calibration line based on *E. coli* standard was built. The qPCR assays were performed in triplicate for each

DNA extract (2 µL in a total reaction volume of 10 µL). Blanks and no-template controls were included in the plate for quality checks. The amplification was done using a CFX Opus 96 Real-Time PCR system, with temperatures of denaturation of 95°C, annealing and extension of 65°C, and of melting curve from 65 to 95°C with a gradual increment of 0.5 °C per read. The results were expressed in copy numbers/g of sediment.

SI 4.2.4 Data treatment and interpretation

Statistical analyses

To evaluate the effect of the dilution-to-extinction on community alpha diversity (observed and Shannon), one-way analysis of variance (ANOVA) was performed at the beginning and end of the biotic incubation with OMPs, for both aerobic and nitrate-reducing conditions. When significant effects were found, post-hoc comparisons between diversity levels were conducted using Tukey's Honest Significant Difference (HSD) test. Moreover, to assess changes in alpha diversity between the beginning and end of the incubation, unpaired two-sample t-tests were used within each diversity level and condition. Significance was determined at $p < 0.05$.

Pairwise comparisons of removal efficiencies and half-lives between microbial diversity levels were conducted using paired *t*-tests. The tests were applied separately for each redox condition using data from individual replicate bottles to increase statistical robustness. To further assess the relationship between microbial diversity and biodegradation, Pearson correlation coefficients (r) were calculated between diversity level and either removal efficiency or half-life across all OMPs. The coefficient of determination ($R^2 = r^2$) was also reported to quantify the strength of these relationships.

All statistical analyses were performed in R (version 4.4.1) using base functions (aov(), TukeyHSD(), and t.test()), with additional support from the car and multcomp packages for ANOVA diagnostics and from the tidyverse, dplyr, tidyr, and purrr for data manipulation and pairwise analyses (Fox and Weisberg, 2019; Hothorn et al., 2008; R Core Team, 2024). Normality of residuals from ANOVA and t-test models was assessed visually using Q-Q plots and histograms. No substantial deviations from normality were observed.

SI 4.3 Results and discussion

SI 4.3.1 Soil-based dilution-to-extinction creates populations with different microbial diversity

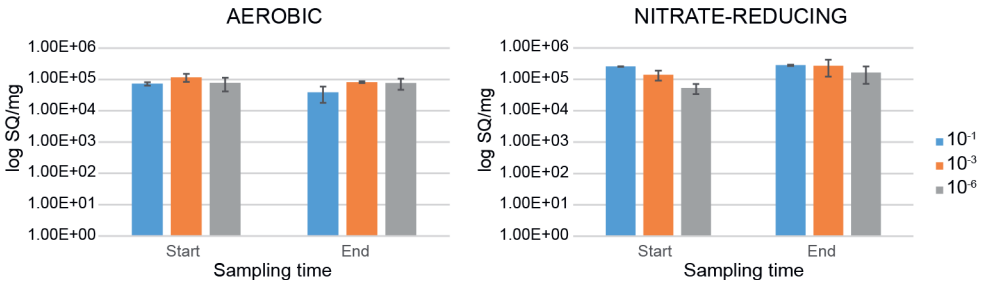

Figure S4.1. qPCR results in log of the copy numbers (SQ) per mg of slurry for batch triplicates. The results are shown at the start (day 0) and the end (day 116) of the incubation with micropollutants under aerobic and nitrate-reducing conditions, and at diversity level 10^{-1} (higher diversity), 10^{-3}, and 10^{-6} (lower diversity).

Table S4.2. Statistical analysis with ANOVA - pairwise comparison from TurkeyHSD to compare the batch diversity levels (10^{-1}, 10^{-3}, 10^{-6}) at each timepoint and condition. The difference is considered significant if $p<0.05$.

Redox condition	Day	Comparison	ASV Difference	ASV p-value	ASV Significant	Shannon Difference	Shannon p-value	Shannon Significant
Aerobic	Day 0	**Low-High**	-1720.33	3.90E-06	Yes	-2.92	1.11E-05	Yes
Aerobic	Day 0	**Medium-High**	-1045.67	7.82E-05	Yes	-1.32	1.07E-03	Yes
Aerobic	Day 0	**Medium-Low**	674.67	9.08E-04	Yes	1.61	3.61E-04	Yes
Aerobic	Day 116	**Low-High**	-1704.00	4.35E-07	Yes	-2.26	5.04E-06	Yes
Aerobic	Day 116	**Medium-High**	-1040.00	4.61E-06	Yes	-1.13	2.96E-04	Yes
Aerobic	Day 116	**Medium-Low**	664.00	6.90E-05	Yes	1.13	3.05E-04	Yes
Nitrate-reducing	Day 0	**Low-High**	-840.67	1.93E-05	Yes	-2.00	2.08E-04	Yes
Nitrate-reducing	Day 0	**Medium-High**	-574.00	1.7E-047	Yes	-0.93	0.012	Yes
Nitrate-reducing	Day 0	**Medium-Low**	266.67	0.010	Yes	1.07	5.75E-03	Yes
Nitrate-reducing	Day 116	**Low-High**	-658.00	2.04E-04	Yes	-0.97	2.39E-04	Yes
Nitrate-reducing	Day 116	**Medium-High**	-540.67	6.08E-04	Yes	-0.74	1.08E-03	Yes
Nitrate-reducing	Day 116	**Medium-Low**	117.33	0.289	No	0.23	0.152	No

Table S4.3. Statistical analysis: t-test to compare day 0 vs day 116 within each diversity level and redox condition. The difference is considered significant if p<0.05.

Redox condition	Diversity condition	Mean Day 0	Mean Day 116	Mean absolute difference	p value	Significant
Aerobic	Observed diversity - High	2156.00	2464.00	308.00	0.010	Yes
Aerobic	Observed diversity - Medium	1110.33	1424.00	313.67	0.025	Yes
Aerobic	Observed diversity - Low	435.67	760.00	324.33	0.014	Yes
Aerobic	Shannon Diversity - High	6.01	6.35	0.34	0.004	Yes
Aerobic	Shannon Diversity - Medium	4.70	5.22	0.52	0.053	No
Aerobic	Shannon Diversity - Low	3.09	4.09	1.00	0.007	Yes
Nitrate reducing	Observed diversity - High	1180.00	1298.33	118.33	0.115	No
Nitrate reducing	Observed diversity - Medium	606.00	757.67	151.67	0.157	No
Nitrate reducing	Observed diversity - Low	339.33	640.33	301	0.002	Yes
Nitrate reducing	Shannon Diversity - High	5.06	5.31	0.24	0.125	No
Nitrate reducing	Shannon Diversity - Medium	4.13	4.57	0.43	0.034	Yes
Nitrate reducing	Shannon Diversity - Low	3.06	4.33	1.27	0.005	Yes

Table S4.4. Comparison of alpha diversity indices (average values) across different systems/environmental compartments. Shannon values for undiluted soil were calculated dividing the difference between higher and lower diversity values by the number of dilution steps, and adding the obtained value to the highest diversity Shannon score.

Compartment	Dilution	Observed	Shannon	Calculated Shannon undiluted	Reference
Soil	Dilutions 10^{-1}, 10^{-3}, 10^{-6}	2156, 1110, 436 (ASV)	6.01, 4.70, 3.09	6.60	This study, aerobic (day 0)
Soil	Dilutions 10^{-1}, 10^{-3}, 10^{-6}	1180, 606, 339 (ASV)	5.06, 4.13, 3.06	5.46	This study, nitrate reducing (day 0)
Soil	Undiluted, unamended	2689 (OTU)	9.08	(already undiluted)	(Sun et al., 2019) Table
Soil	Undiluted low vs high diversity soils	1800-2500 (OTU)	6-7	(already undiluted)	(Jayaramaiah et al., 2022) Figure
Soil	Undiluted, grassland	691 (OTU)	-	(already undiluted)	(Crampon et al., 2018) Table
River sediment	Dilutions 10^{-1}, 10^{-3}, 10^{-6}	2500, 500, 500 (OTU)	5, 2.5, 2.5	5.50	(Posselt et al., 2020) Figure (day 0)
Activated sludge	Dilutions 10^{-2}, 10^{-4}, 10^{-7}	311, 123, 51 (OTU)	2.67, 2.02, 1.37	2.93	(Stadler et al., 2012) Table
Activated sludge	Undiluted	1524 (OTU)	2.25	(already undiluted)	(Martínez-Quintela et al., 2023) Table, denitrifying conditions
Aquifer	Undiluted	235 (ASV)	-	(already undiluted)	(Aldas-Vargas et al., 2019) text

SI 4.3.2 Microbial diversity influences removal of spiked OMPs

Table S4.5. Removal efficiency% (RE%) and standard deviations (St. Dev.) per each spiked OMP under abiotic, aerobic (AER), and nitrate-reducing (NITR) conditions. When the concentration at the end of the experiment was below the analytical limit of quantification (LOQ), its value was replaced with the LOQ (i.e., 0.25 µg/L).

RE %	MTP	1H-BTR	CAF	CBZ	SMX	DEET	BAM	DMZ	SOT	DGY	MTF	MET	PCM	CLZ	DCF	FUR	MCPP	2,4-D	BTZ	HCZ
ABIOTIC	65.82	36.48	39.57	24.58	42.69	10.52	18.72	18.66	50.16	9.49	51.59	35.62	34.89	39.75	21.67	11.49	11.14	10.06	7.07	30.96
ABIOTIC St. Dev.	7.44	8.11	9.30	15.16	6.13	14.88	7.77	10.25	11.07	13.43	8.73	14.27	8.80	1.05	5.32	16.25	15.76	14.23	10.00	17.49
AER 10^{-1}	>96.92	88.13	>98.68	62.86	92.44	29.93	24.20	39.49	96.27	37.25	71.16	81.88	>98.80	88.54	>98.80	>98.28	72.63	>98.81	-0.75	75.96
AER 10^{-1} St. Dev.	0.87	2.35	0.21	7.63	2.64	21.32	14.54	12.11	2.18	22.68	3.89	2.92	0.24	2.46	0.22	0.31	0.37	0.01	2.14	3.12
AER 10^{-3}	>97.65	94.06	>98.90	57.84	72.30	51.95	21.71	32.04	>97.95	49.74	73.27	75.78	>95.82	77.53	>98.92	>98.37	76.87	>99.03	2.65	82.18
AER 10^{-3} St. Dev.	0.26	2.10	0.18	10.73	32.39	32.30	21.94	16.10	0.29	25.01	0.65	8.58	2.55	16.94	0.29	0.25	14.23	0.10	27.39	2.58
AER 10^{-6}	>97.07	79.34	>98.77	61.87	65.26	24.63	25.51	40.27	89.15	20.94	75.78	72.63	>94.48	46.72	62.46	74.99	27.67	72.75	-1.20	79.70
AER 10^{-6} St. Dev.	1.05	13.87	0.17	9.66	30.76	12.67	12.63	13.06	11.67	17.58	4.40	7.79	6.68	7.96	7.95	18.56	18.64	22.51	3.06	3.83
NITR 10^{-1}	>98.76	58.46	69.16	54.46	N/A	8.38	26.21	60.00	>98.57	8.97	66.70	78.21	>98.97	50.01	18.54	-7.01	0.24	83.22	4.21	83.91
NITR 10^{-1} St. Dev.	0.00	0.66	2.05	1.30	N/A	4.46	1.28	3.34	0.00	3.57	2.93	1.11	0.00	5.09	1.50	3.59	3.14	0.81	1.58	0.83
NITR 10^{-3}	>98.76	57.18	86.92	53.76	N/A	6.32	24.66	82.41	97.42	6.95	65.18	81.65	>98.97	51.22	14.69	-10.67	-0.88	84.09	10.18	86.00
NITR 10^{-3} St. Dev.	0.00	5.97	14.77	7.19	N/A	11.20	9.35	28.54	1.00	9.72	6.60	7.47	0.00	8.15	10.81	11.04	13.93	16.70	14.36	1.21
NITR 10^{-6}	>98.76	65.96	64.32	50.77	N/A	4.95	26.33	42.85	94.19	0.30	64.31	64.55	>98.97	51.58	16.74	-20.00	-1.47	8.10	6.00	85.38
NITR 10^{-6} St. Dev.	0.00	9.52	3.60	1.00	N/A	4.15	3.48	1.62	0.74	7.94	0.48	2.06	0.00	3.20	5.96	6.29	3.94	2.37	3.15	0.64

Table S4.6. Results of the pairwise comparison of the removal efficiency (RE) and half-life (DT_{50}) per single bottle between microbial diversity levels and of the Pearson correlation coefficient (r) and coefficient determination R^2 between diversity and RE or DT_{50} under aerobic (AER) and nitrate-reducing conditions (NITR). The number of OMPs that could be included in the comparison, or which had enough data to compute r, is reported for each test (n OMPs).

Pairwise t-test								
Redox	**comparison**	**Observed difference RE**	**p value RE**	**n OMPs RE**	**Observed difference DT50**	**p valueDT50**	**n OMPs DT50**	
AER	-3 vs -1	0.708	0.764	54	-16.646	0.279	40	
AER	-6 vs -1	-12.267	4.06E-06	59	55.455	0.002	43	
AER	-6 vs -3	-12.720	0.001	54	68.144	0.005	37	
NITR	-3 vs -1	1.847	0.260	58	-17.040	0.059	25	
NITR	-6 vs -1	-7.061	0.002	60	158.544	0.113	26	
NITR	-6 vs -3	-9.165	0.002	58	87.249	0.082	27	
Pearson correlation coefficient per OMP								
Redox	**mean r RE**	**mean R^2 RE**	**St. Dev. r RE**	**n OMPs RE**	**mean r DT50**	**mean R^2 DT50**	**St. Dev. r DT50**	**n OMPs DT50**
AER	0.278	0.077	0.432	20	-0.304	0.092	0.549	16
NITR	0.256	0.066	0.409	18	-0.415	0.172	0.295	10

Biodegradation curves- aerobic conditions

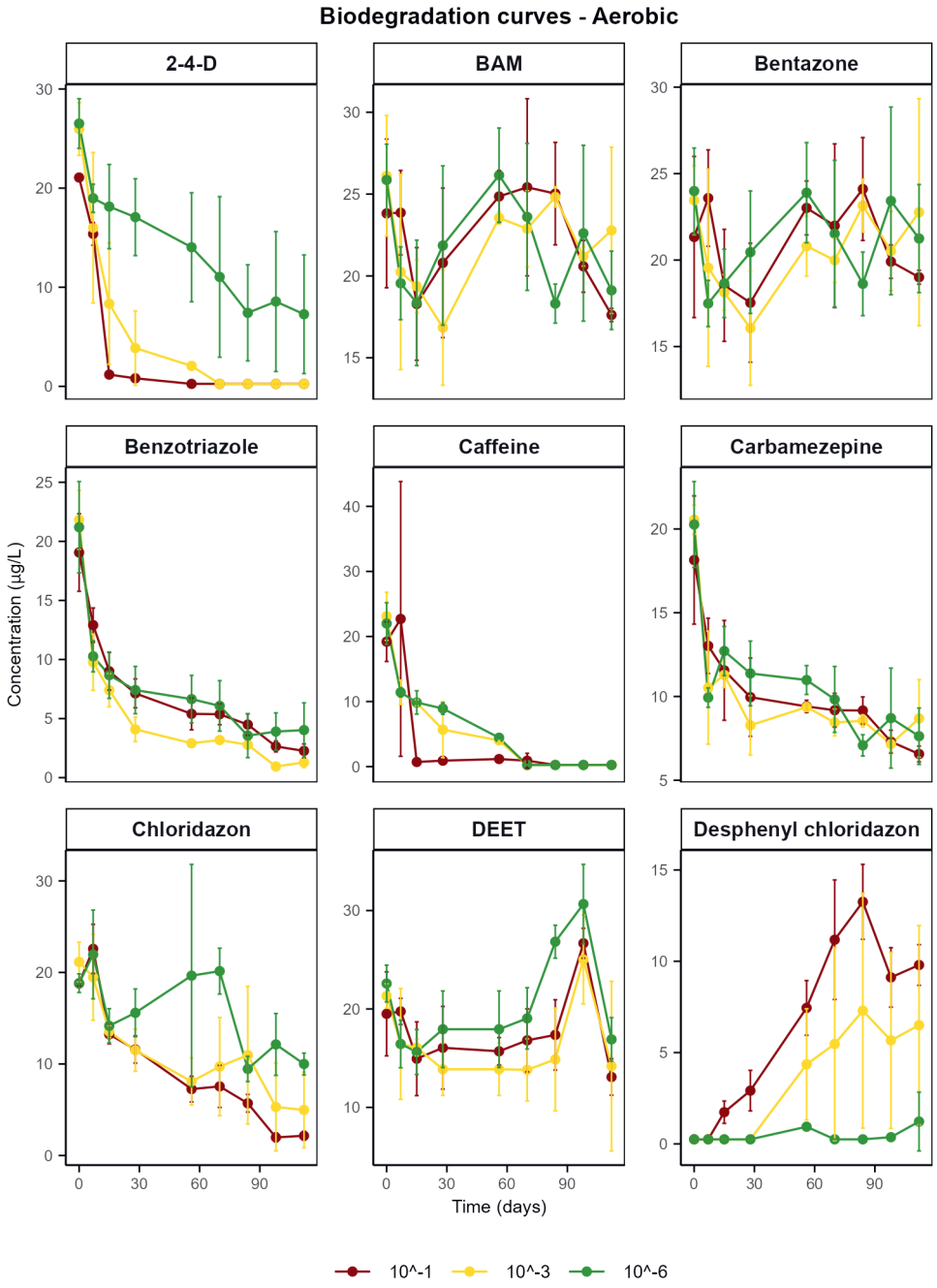

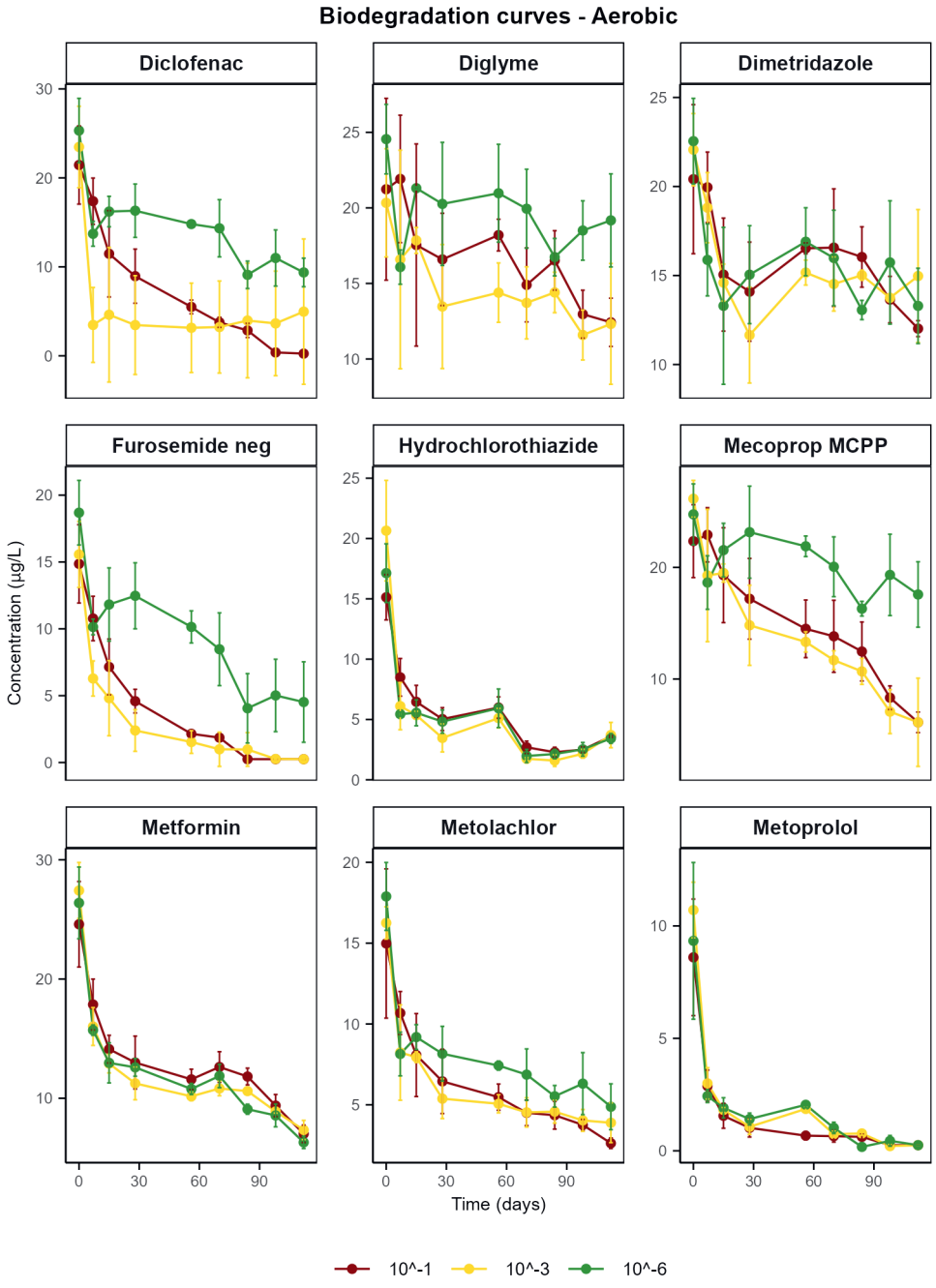
Biodegradation curves - Aerobic
Diclofenac
Diglyme
Dimetridazole
Furosemide neg
Hydrochlorothiazide
Mecoprop MCPP
Metformin
Metolachlor
Metoprolol
Concentration (µg/L)
Time (days)
10^-1
10^-3
10^-6

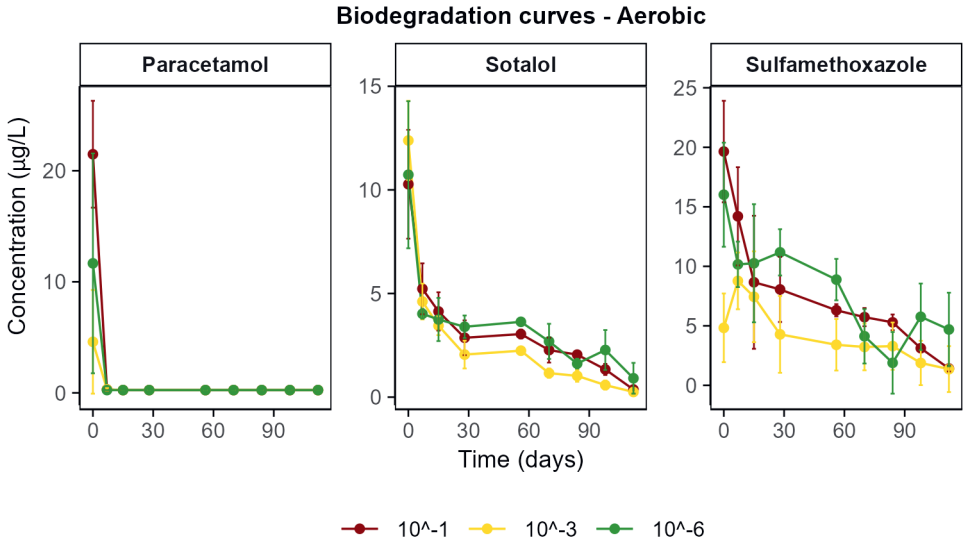

Figure S4.2. Compilation of biodegradation curves for each target OMP under aerobic conditions over the incubation period.

Biodegradation curves – nitrate-reducing conditions

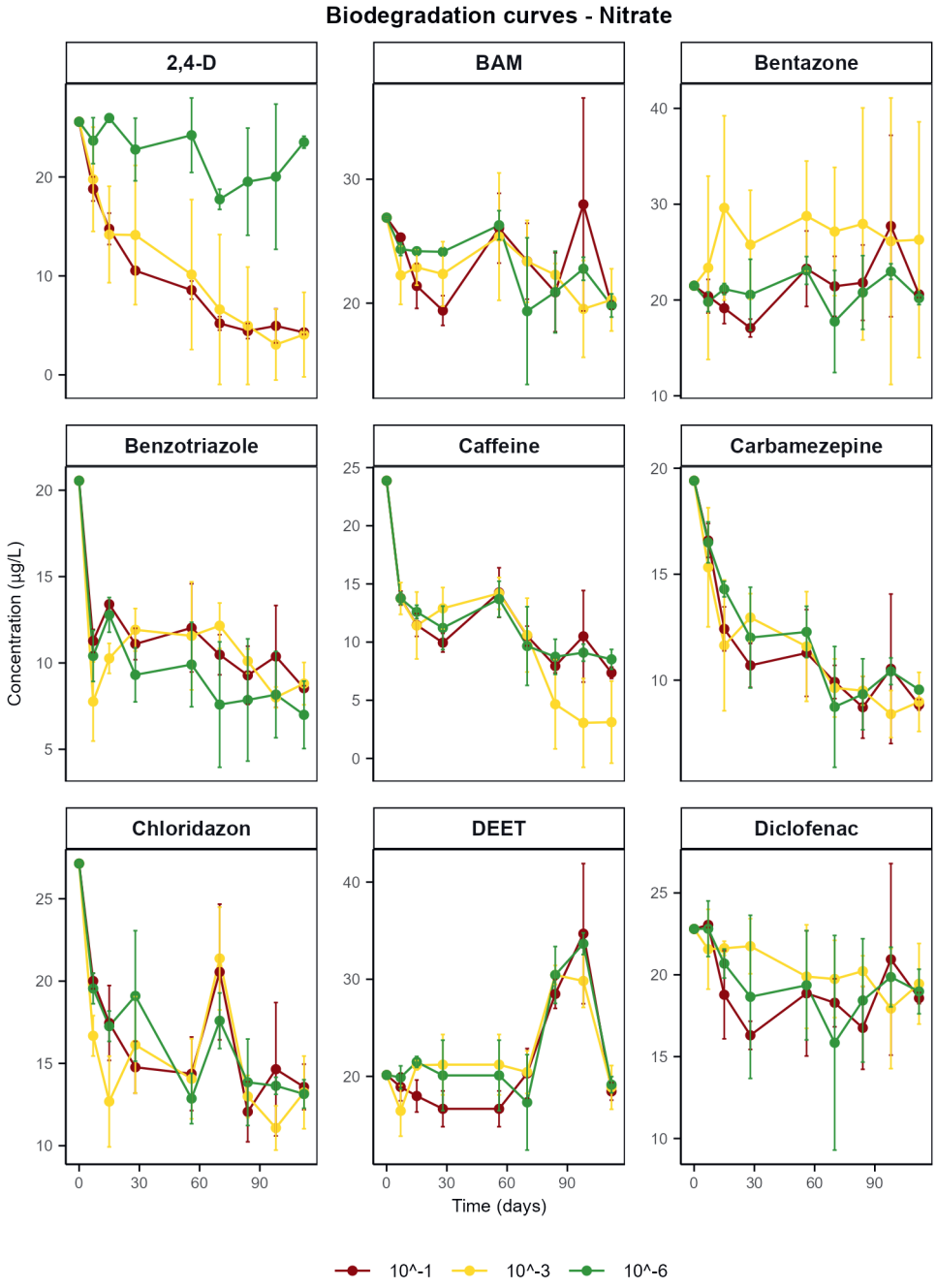

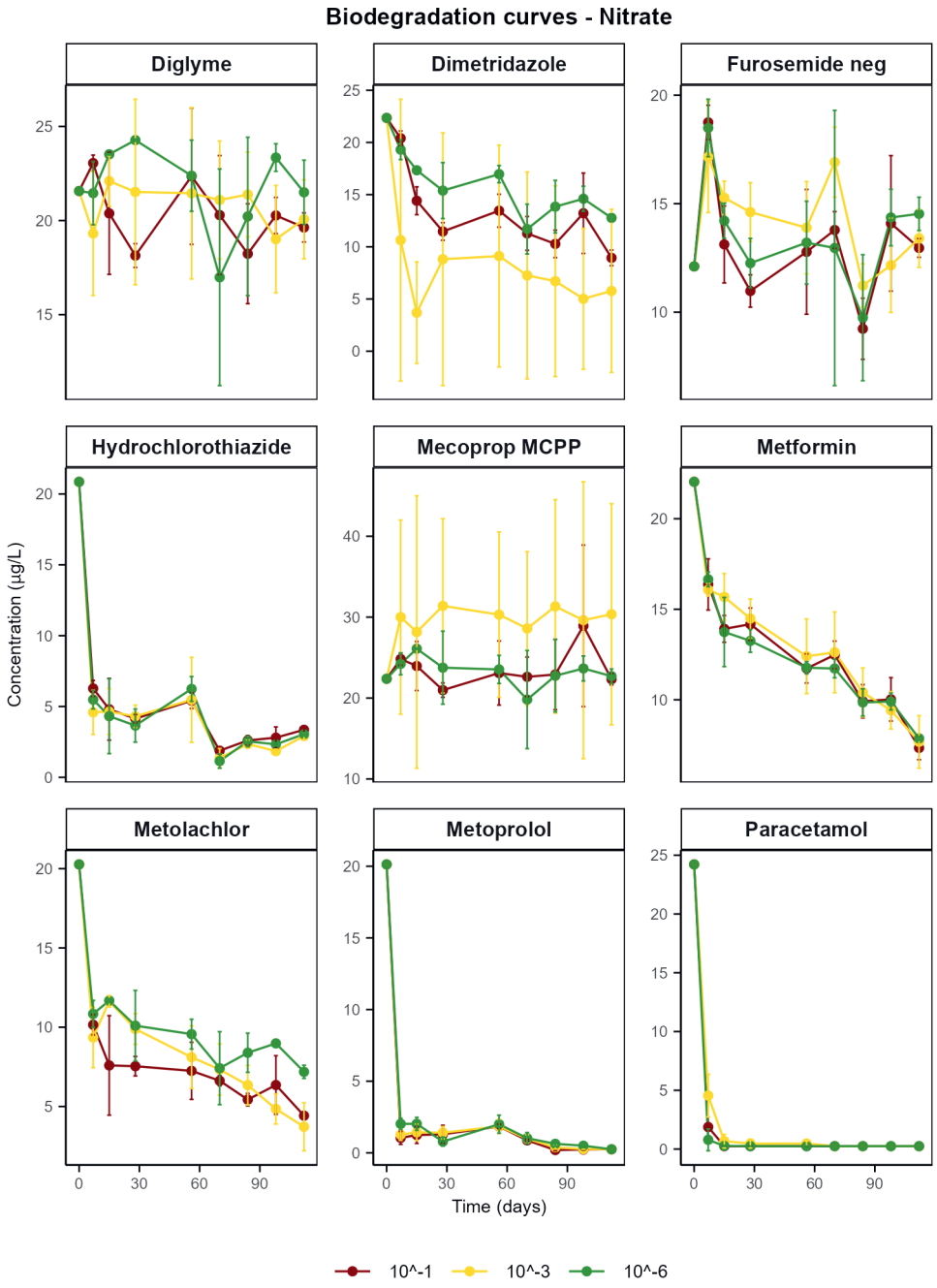
Biodegradation curves - Nitrate
Diglyme
Dimetridazole
Furosemide neg
Hydrochlorothiazide
Mecoprop MCPP
Metformin
Metolachlor
Metoprolol
Paracetamol
Concentration (µg/L)
Time (days)
10^-1
10^-3
10^-6

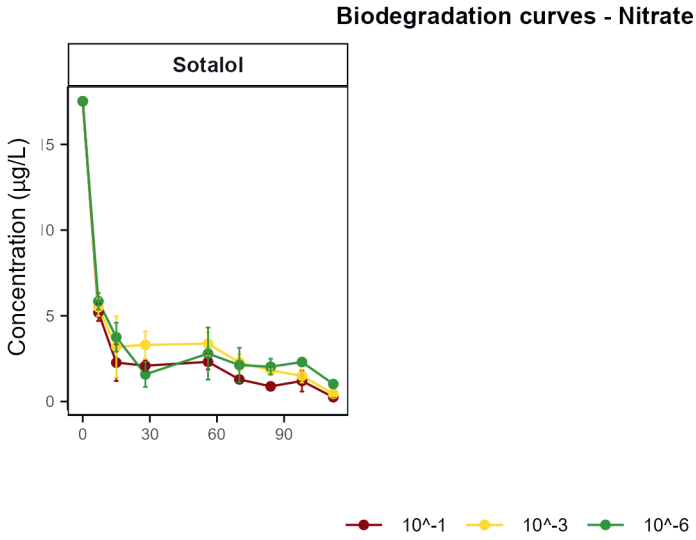

Figure S4.3. Compilation of biodegradation curves for each target OMP under nitrate-reducing conditions over the incubation period.

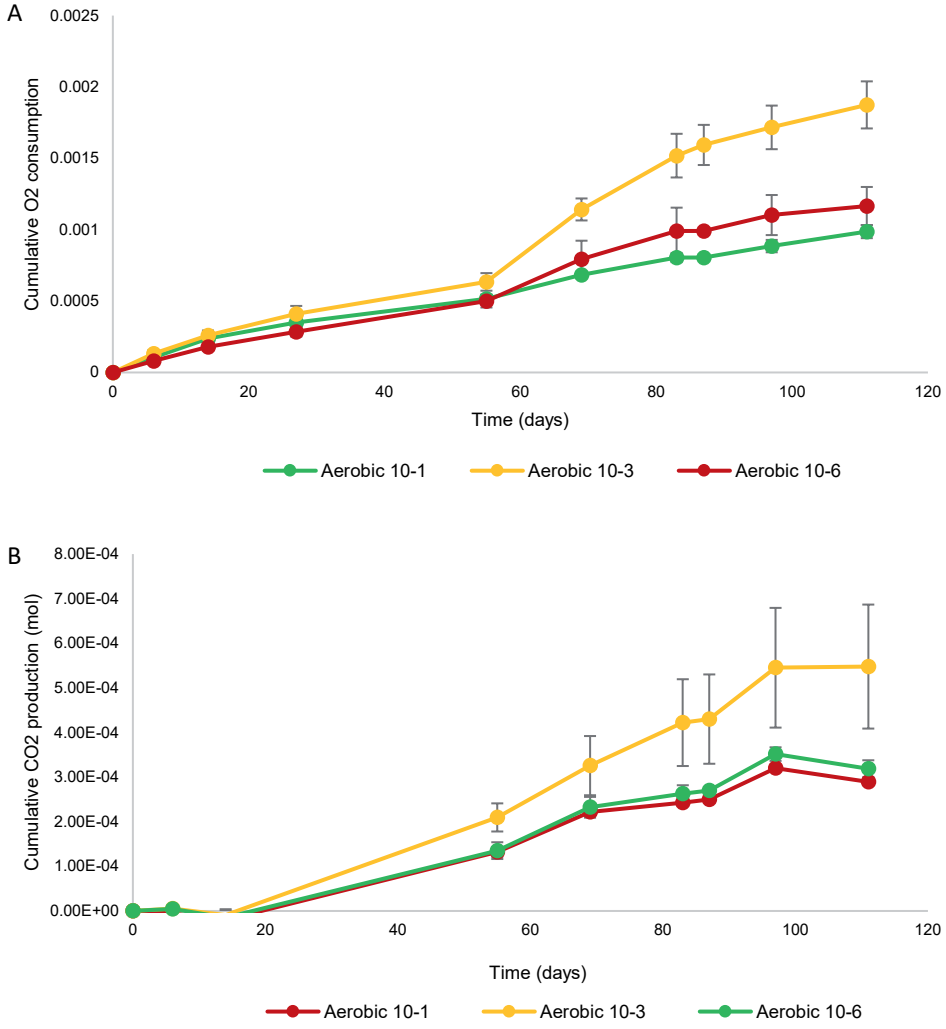

Figure S4.4. Proxy for microbial activity data across the diversity batch sets: A – Cumulative oxygen consumption under aerobic conditions; B – Cumulative CO_2 production across the diversity batch sets under aerobic conditions.

Supplementary script 4.1

```
library(patRoon)

# -------------------------
# initialization
# -------------------------

workPath <- "workpath directory."
setwd(workPath)

# Load analysis table
anaInfoPos <- read.csv("File with samples in positive ionization.csv")
anaInfoNeg <- read.csv("File with samples in negative ionization.csv")

# -------------------------
# features
# -------------------------

fListPos <- findFeatures(anaInfoPos, "openms", noiseThrInt = 1000,
chromSNR = 5, chromFWHM = 10, minFWHM = 1, maxFWHM = 20)

fListNeg <- findFeatures(anaInfoNeg, "openms", noiseThrInt = 1000,
chromSNR = 5, chromFWHM = 10, minFWHM = 1, maxFWHM = 20)

fGroups_pos <- groupFeatures(fListPos, "openms", maxGroupRT = 20,
rtalign = FALSE)
fGroups_neg <- groupFeatures(fListNeg, "openms", maxGroupRT = 20,
rtalign = FALSE)

# Basic rule based filtering
fGroups_pos <- fGroupsF_pos <- filter(fGroups_pos, preAbsMinIntensity =
100, absMinIntensity = 5000, relMinReplicateAbundance = 0.6,
maxReplicateIntRSD = 0.9, blankThreshold = 5, removeBlanks = TRUE,
retentionRange = NULL, mzRange = NULL)

fGroups_neg <- fGroupsF_neg <- filter(fGroups_neg, preAbsMinIntensity =
100, absMinIntensity = 5000, relMinReplicateAbundance = 0.6,
maxReplicateIntRSD = 0.9, blankThreshold = 5, removeBlanks = TRUE,
retentionRange = NULL, mzRange = NULL)

#--------------------------------------
# Checking for adducts and isotopes
#--------------------------------------
```

```
# generate components from filtered fGroups
components_pos <- generateComponents(fGroupsF_pos, "cliquems",
ionization = "positive", ppm = 7)
components_neg <- generateComponents(fGroupsF_neg, "cliquems",
ionization = "negative", ppm = 7)

# Only keep results with adducts/isotope annotations and remove unwanted
adducts
componentsF_pos <- delete(components_pos, j = function(ct, ...)
is.na(ct$isonr) & (is.na(ct$adduct_ion) | !ct$adduct_ion %in%
c("[M+Na]+", "[M+K]+", "[M+NH4]+")))
print(componentsF_pos)

componentsF_neg <- delete(components_neg, j = function(ct, ...)
is.na(ct$isonr) & (is.na(ct$adduct_ion) | !ct$adduct_ion %in% c("[M-
H2O]-", "[M-H]-")))
print(componentsF_neg)

# Only keep components with at least one feature group also present in
the suspect screened data
componentsF_pos <- delete(componentsF_pos, j = function(ct, ...)
!any(ct$group %in% names(fGroups_pos)))
componentsF_neg <- delete(componentsF_neg, j = function(ct, ...)
!any(ct$group %in% names(fGroups_neg)))

# Remove components with only one feature group (useless)
componentsF_pos <- filter(componentsF_pos, size = c(2, 1E6))
componentsF_neg <- filter(componentsF_neg, size = c(2, 1E6))

# manually check/filter components
checkComponents(componentsF_pos, fGroupsF_pos, session =
"components_check_pos.yml")
componentsF_pos <- filter(componentsF_pos, checkComponentsSession =
"components_check_pos.yml")

checkComponents(componentsF_neg, fGroupsF_neg, session =
"components_check_neg.yml")
componentsF_neg <- filter(componentsF_neg, checkComponentsSession =
"components_check_neg.yml")

# to filter out unwanted adducts/isotopes
fGroups_pos <- selectIons(fGroups_pos, componentsF_pos, c("[M+H]+"))
fGroups_neg <- selectIons(fGroups_neg, componentsF_neg, c("[M-H]-"))

# Make sets and group features
```

```
fGroups <- makeSet(fGroups_pos, fGroups_neg, groupAlgo = "openms",
adducts = c("[M+H]+", "[M-H]-"))

# -------------------------
# suspect screening
# -------------------------

# SEPARATE SUSP LIST WITH FRAGMENTS
suspListPos <- read.csv("Suspect list for PCs_positive.csv",
                        stringsAsFactors = FALSE)
suspListNeg <- read.csv("Suspect list for TPs_negative.csv",
                        stringsAsFactors = FALSE)

# Set onlyHits to FALSE to retain features without suspects
fGroups <- screenSuspects(fGroups, list(suspListPos, suspListNeg),
rtWindow = 12, mzWindow = 0.005, onlyHits = FALSE)

write.csv(screenInfo(fGroups), "SuspectsFound.csv", quote = TRUE,
row.names = FALSE)

# -------------------------
# transformation products
# -------------------------

# Load parent suspect list
suspListParents <- read.csv("Suspect list for PCs.csv", stringsAsFactors
= FALSE)

# Obtain TPs
TPs <- TPs_UF <- generateTPs("biotransformer", parents =
suspListParents, type = "env", generations = 7, calcSims = FALSE)

TPs <- filter(TPs, removeParentIsomers = TRUE)

# to remove TPs that may be assigned wrongly (unspecific assignment)
TPs <- delete(TPs, j = function(tab, par)
{
  parNM <- parents(TPs)[match(par, name)]$neutralMass # parent neutral
mass
  # remove if high generation (>1) and mass is <60% of that of the
parent
  # generation 1 TPs are always kept and the rest only if their mass is
sufficiently high (>=40%)
  return(tab$generation > 1 & (tab$neutralMass / parNM) < 0.4)
})
print(TPs)
```

```
# Screen TPs
suspListTPs <- convertToSuspects(TPs, includeParents = FALSE)
write.csv(suspListTPs, "SuspectListOfTPs.csv", quote = TRUE, row.names =
FALSE)

# Amend with TP screening
fGroups <- screenSuspects(fGroups, suspListTPs, rtWindow = 12, mzWindow
= 0.005, onlyHits = TRUE, amend = TRUE)

# -------------------------
# annotation
# -------------------------

# Retrieve MS peak lists
avgMSListParams <- getDefAvgPListParams(clusterMzWindow = 0.005)
mslists <- generateMSPeakLists(fGroups, "mzr", maxMSRtWindow = 5,
precursorMzWindow = 0.5, avgFeatParams = avgMSListParams,
avgFGroupParams = avgMSListParams)

# Rule based filtering of MS peak lists.
mslists <- filter(mslists, absMSIntThr = NULL, absMSMSIntThr = NULL,
relMSIntThr = NULL, relMSMSIntThr = 0.05, topMSPeaks = NULL,
topMSMSPeaks = 25)

# Calculate formula candidates
formulas <- generateFormulas(fGroups, mslists, "genform", relMzDev = 5,
elements = "CHNOPSClFI", oc = FALSE, calculateFeatures = TRUE,
featThresholdAnn = 0.75, setThresholdAnn = 0)

convertToMFDB(TPs, "TP-database.csv", includeParents = TRUE)

# Calculate compound structure candidates
compounds <- generateCompounds(fGroups, mslists, "metfrag", dbRelMzDev =
5, fragRelMzDev = 5, fragAbsMzDev = 0.002, database = "csv", extraOpts =
list(LocalDatabasePath = "TP-database.csv"), maxCandidatesToStop = 2500,
setThresholdAnn = 0)
compounds <- addFormulaScoring(compounds, formulas, updateScore = TRUE)

# Annotate suspects
fGroups <- annotateSuspects(fGroups, formulas = formulas, compounds =
compounds, MSPeakLists = mslists, IDFile = "idlevelrules.yml")

# -------------------------
# Filters to remove low ID
# -------------------------
```

```
fGroups_lowID <- filter(fGroups, maxLevel = 4, negate = TRUE)
fGroups_lowID <- filter(fGroups_lowID, onlyHits = TRUE)
# fGroups lowID should now contain all features with L5
write.csv(screenInfo(fGroups_lowID), "OMPs_lowID.csv", quote = TRUE,
row.names = FALSE)

# to visualize low ID fGroups enable the following --------------------
# lowID_table <- as.data.frame(fGroups_lowID, collapseSuspects = NULL)
# write.csv(lowID_table, "DataFrame_lowID.csv", quote = TRUE, row.names
= FALSE)

# to proceed with L4 or better
fGroups <- filter(fGroups, maxLevel = 4, onlyHits = TRUE)
print(fGroups)

# -------------------------
# Parent and TP linkage
# -------------------------

componentsTP <- generateComponents(fGroups[, suspects = suspList$name],
"tp", fGroupsTPs = fGroups, TPs = TPs, MSPeakLists = mslists, formulas =
formulas, compounds = compounds)

componentsTP <- filter(componentsTP, retDirMatch = TRUE, minSpecSim =
NULL, minSpecSimPrec = NULL, minSpecSimBoth = NULL, minFragMatches =
NULL, minNLMatches = NULL)

checkFeatures(fGroups)
fGroups <- filter(fGroups, checkFeaturesSession = TRUE)

# ------------------------
# Filters for plotting
# ------------------------

# if the same suspect is assigned to multiple fGroups, select the one
with the best ID level
fGroupsToPlot_bestID <- filter(fGroups, selectHitsBy = "level", onlyHits
= TRUE)
print(fGroupsToPlot_bestID)

# -------------------------
# reporting
# -------------------------

options(future.globals.maxSize = 2e9)
```

```
# Advanced report settings can be edited in the report.yml file.
report(fGroups, MSPeakLists = mslists, formulas = formulas, compounds =
compounds, components = componentsTP, TPs = TPs, settingsFile =
"report.yml", openReport = TRUE)

# Adjust based on the wanted filters for plotting
checkFeatures(fGroupsToPlot_bestID, "fGroupsToPlot_bestID.yml")
fGroupsToPlot_bestID <- filter(fGroupsToPlot_bestID,
checkFeaturesSession = "fGroupsToPlot_bestID.yml")

report(fGroupsToPlot_bestID, MSPeakLists = mslists, formulas = formulas,
compounds = compounds, components = componentsTP, TPs = TPs,
settingsFile = "report_bestID.yml", openReport = TRUE, parallel = FALSE)
```

Supplementary Excel 4

Supplementary Excel (SE) tables can be downloaded from:
https://doi.org/10.1016/j.watres.2025.124921

Chapter 5

Uncovering redox-specific biotransformation of organic micropollutants

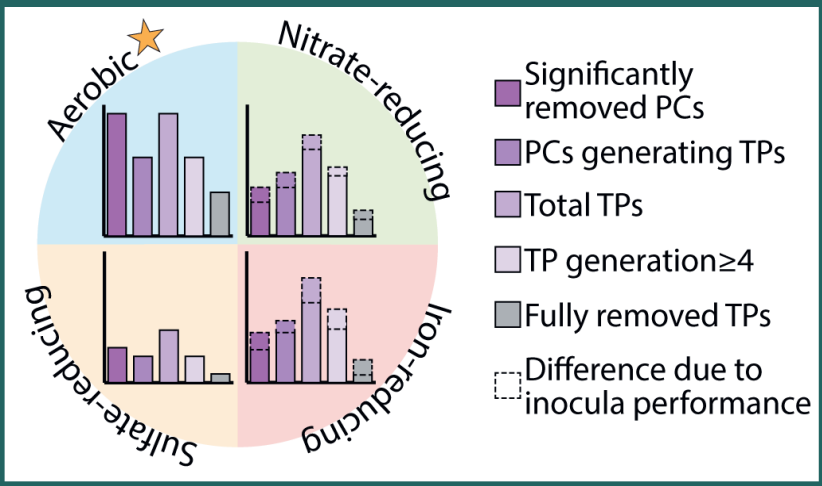

A modified version of this chapter has been published as:

Ore, A., Helmus, R., van Wezel, A.P., Sutton, N.B., **2026**. Uncovering redox-specific biotransformation of organic micropollutants. **Journal of Hazardous Materials** https://doi.org/10.1016/j.jhazmat.2026.141775

Abstract

Redox conditions are key environmental factors influencing organic micropollutants (OMPs) biodegradation in both nature-based and engineered treatment systems. Yet, OMP biodegradation and transformation product (TP) formation under different redox conditions are not fully understood, particularly using natural inocula. Here, we tested two natural inocula, from soil and ditch sediment, for biodegradation of 19 OMPs under four redox conditions: aerobic, nitrate-reducing, iron-reducing, and sulfate-reducing. Target and non-target analyses results confirmed aerobic conditions as the most favourable, resulting in the removal of up to 14 OMPs and producing up to 14 TPs, while sulfate-reducing conditions were the least effective, with 7 OMPs biodegraded and 8 TPs produced, consistent with the redox ladder. Under nitrate- and iron-reducing conditions, OMP biodegradation and TP formation were also influenced by the inoculum source. While some OMPs were well-removed (e.g., paracetamol and hydrochlorothiazide) or persistent (e.g., diglyme and bentazon) under all tested conditions, the fate of most OMPs was redox-dependent in both rate and progress along the degradation pathway. Redox-specific TPs revealed different biodegradation pathways, likely steered by the influence of redox conditions on microbial community composition and activity, or inocula pre-exposure to specific redox conditions. Using prediction tools (Biowin, MS2Tox, and MS2Quant), we further evaluated the relative biodegradability and toxicity of TPs compared to their parent compounds (PCs), and estimated the PC-TPs bioconversion efficiency. Our results provide a more comprehensive view of OMP fate and TP formation across redox conditions. These insights can support the optimization of OMP removal strategies in engineered and natural redox-shifting systems.

Keywords

Micropollutants biodegradation, redox conditions, transformation products, non-target screening, natural inocula.

5.1 Introduction

Organic micropollutants (OMPs) are currently detected in all portions of the water cycle, from rivers and groundwater to drinking water, reflecting their widespread anthropogenic use and incomplete removal in treatment systems (Lapworth et al., 2012; Ore et al., 2025c; White et al., 2019). Engineered biological systems (e.g., activated sludge in wastewater treatment plants, aerobic granular sludge) and nature-based technologies (e.g., constructed wetlands, managed aquifer recharge) contribute to their removal from water streams (Golovko et al., 2021; Hübner et al., 2022; Li et al., 2014). Several of these systems present varying redox conditions, which influence OMP removal efficiency. For instance, redox conditions change with depth during infiltration in managed aquifer recharge, while activated sludge present redox gradients across different layers (Narain-Ford et al., 2022; Rivett et al., 2008; Winkler et al., 2013).

Redox conditions strongly influence OMP biodegradation (Branco et al., 2023; Filter et al., 2021; Luo et al., 2019). The electron acceptors available under each redox condition (e.g., O_2, NO_3^-, Fe(III), SO_4^{2-}) provide different energy yields for microbial metabolism, thereby influencing microbial functional activity (Meckenstock et al., 2015). Moreover, microorganisms are often specialized to particular redox conditions: strictly aerobic bacteria cannot survive in anoxic environments, while anaerobes thrive under nitrate-, iron-, or sulfate-reducing conditions. Consequently, redox conditions shape microbial communities composition and the enzymatic functions they can perform (Fenner et al., 2021, 2013); oxidative enzymes dominate under aerobic conditions, whereas reductive enzymes like dehalogenases are more active under iron- or sulfate-reducing conditions (Achermann et al., 2020; Jugder et al., 2016). This, in turn, affects which OMPs can be biodegraded, at what rate, and via which transformation pathways, likely forming redox condition-specific transformation products (TPs). For instance, iopromide biodegradation was shown to proceed mainly through oxidative reactions under aerobic conditions, leading to the formation of a persistent TP (Schulz et al., 2008). In contrast, under anaerobic conditions, this TP was further degraded and different TPs were formed (Redeker et al., 2018). These studies highlight how redox conditions shape the pathways and outcomes of OMP biodegradation.

Biodegradation under aerobic conditions is generally faster and more efficient than under anaerobic conditions; still, some OMPs persist under aerobic environments and are more sensitive to biodegradation under anoxic conditions (Lapworth et al., 2012). Nonetheless, the interplay between redox conditions and biodegradation is not fully understood. Research more frequently focuses on aerobic systems, while anaerobic conditions are less investigated, and often the electron acceptor is not specified (Burke et al., 2017; Ghattas et

al., 2017). While previous research observed different reactions and TP formation in different environments (Brunner et al., 2019a; He et al., 2018; Kern et al., 2011), TPs have rarely been linked to specific redox conditions. Moreover, most studies applied activated sludge inocula, overlooking natural microbial communities that may respond differently due to their higher diversity, functional redundancy, and pre-exposure to fluctuating redox conditions (Ore et al., 2025b; Seth et al., 2024).

To address these gaps, we tested two natural inocula, soil and ditch sediments, across four redox conditions: aerobic, nitrate-reducing, iron-reducing, and sulfate-reducing. We aimed at (1) quantifying the degradation of 19 different OMPs across these redox conditions, (2) identifying TP formation and assessing their further degradation using target and non-target analyses, and (3) evaluating how the inoculum origin influences OMP biodegradation patterns. By systematically testing natural inocula across redox conditions, our study provides new insights into OMP fate and transformation in redox-stratified systems, supporting predictive understanding of OMP fate and the optimization of both engineered and nature-based treatment systems.

5.2 Materials and Methods

5.2.1 Experimental set-up

Batch bottles were prepared in triplicate to study four different redox conditions: aerobic, nitrate-reducing, iron-reducing, and sulfate-reducing conditions. Each redox condition was tested using two inocula with pre-exposure to OMPs, referred to hereafter as "soil" and "ditch". The soil inoculum was taken from a Dutch agricultural field with wastewater treatment plant effluent subirrigation, where the soil sample was taken over 2 m depth, below the groundwater table (Narain-Ford et al., 2022; Ore et al., 2025a). The ditch inoculum was sampled from beneath the water surface in a ditch near the Bennekom wastewater treatment plant, which receives effluent. The batch bottle incubations were performed in 250 mL serum bottles filled with 30 g of inoculum, 150 mL of medium, and headspace gas. Medium and headspace gas (Table S5.1) were specific for each redox condition, as previously reported by Ore et al. for aerobic and nitrate-reducing conditions media and Branco et al. for iron- and sulfate-reducing conditions media (Branco et al., 2023; Ore et al., 2025b). Additionally, as the dissolved organic carbon (DOC) concentrations of the inocula were low (3.7 mg/L for soil and 2.7 mg/L for ditch), extra DOC was added to support biodegradation; DOC was extracted in Milli-Q water from sterilized soil and added to the bottles to reach a final concentration of 10 mg/L. The experiments were acclimated for 20 (aerobic and nitrate-reducing conditions) to 34 (iron and sulfate-reducing conditions) days before the OMP spike. OMPs were added by spiking 0.5 mL of a Milli-Q water-based mixture of 19 OMPs (Table 5.1, 7.5 mg/L) into the incubation bottles to reach a final concentration

of 25 µg/L each. Such concentration was selected to increase the likelihood that intermediate TPs reached detectable concentrations during incubation. The mixture contained pesticides, pharmaceuticals, and industrial chemicals with different biodegradability.

Table 5.1. OMPs spiked in the biotic and abiotic batches.

2,4-Dichlorophenoxyacetic acid (2,4-D)	Diethyltoluamide (DEET)	Metolachlor (MET)
2,6-dichlorobenzamide (BAM)	Diclofenac (DCF)	Metoprolol (MTP)
Bentazon (BTZ)	Diglyme (DGY)	Paracetamol (PCM)
(1H)Benzotriazole (1H-BTR)	Furosemide (FUR)	Sotalol (SOT)
Caffeine (CAF)	Hydrochlorothiazide (HCZ)	Sulfamethoxazole (SMX)
Carbamazepine (CBZ)	Mecoprop (MCPP)	
Chloridazon (CLZ)	Metformin (MTF)	

The bottles were incubated at 20 °C, shaken at 120 rpm, and kept in the dark to avoid photodegradation. The incubation with OMPs lasted 76 days for aerobic and nitrate-reducing conditions, and 62 days for iron- and sulfate-reducing conditions. Abiotic controls were prepared in triplicate for both inocula (autoclaved three times at 121 °C for 15 minutes) and incubated for 72 h to assess OMP removal due to sorption or other abiotic processes. A 72 h period was chosen as it is generally sufficient to reach sorption equilibrium for a wide range of chemicals. To correct for the abiotic losses, the concentrations at the end of the abiotic incubation were used as the starting concentration to assess biodegradation removal efficiency (RE, Equation 5.1) and rate (expressed as half-life DT_{50}, Equation 5.2), assuming first-order reaction kinetics. In this work, biodegradation was defined as significant when RE corrected for abiotic losses was >30% and the half-life <120 days.

Equation 5.1. Removal efficiency of an OMP (A), where $C_{A,\,start}$ and $C_{A,\,end}$ are the concentrations of the OMP at the beginning (i.e. concentration at the end of the abiotic experiment) and the end (day 76 for aerobic and nitrate-reducing conditions, day 62 for iron- and sulfate-reducing conditions) of the incubation with OMPs, respectively.

$$RE_A = \frac{(C_{A,start} - C_{A,end})}{C_{A,start}} \quad (5.1)$$

Equation 5.2. Half-life formula assuming first-order reaction, where DT_{50} is the time when the OMP concentration is half the spiked concentration(corrected for abiotic losses, and k is the slope of the first-order biodegradation reaction.

$$DT_{50} = -\frac{\ln 0.5}{k} \quad (5.2)$$

5.2.2 Chemical analyses

Gas (2 mL) and liquid samples (4 mL) were collected from the incubation bottles using sterile syringes. Sampling was performed on day 0, 6, 13, 20, 34, 48, 62, and 76 for aerobic and nitrate-reducing conditions, and on day 0, 9, 20, 41, and 62 for iron- and sulfate-reducing

conditions. Gas samples were used to assess the headspace composition throughout the incubation via gas chromatography (GC – SI 5.2.2). GC data were used to estimate respiration (oxygen consumption and CO_2 production) under aerobic conditions and verify that anoxic conditions were preserved under nitrate, iron, and sulfate-reducing conditions. Liquid samples were used for nitrate and sulfate measurements through ion chromatography (SI 5.2.2), and for target and non-target OMP analyses.

5.2.2.1 OMP target and non-target analyses

The liquid samples were centrifuged at 15000 rcf and the supernatant was divided into two aliquots, one added with 2.5% acetonitrile and used for OMP measurement with target analysis, and the second used for OMP non-target analysis and ion chromatography. If not used on the same day, samples were stored at -20 °C until analysis.

Methodological details for OMP target and non-target analyses were previously reported by Ore et al. (Ore et al., 2025c, 2025b). Briefly, target analysis used an ultra-high performance liquid chromatography (UHPLC ExionLC™ AD 30) coupled with mass spectrometry (MS - SCIEX Triple Quad™ MS 5500, USA) system, which included a Kinetex Core-Shell Polar C18 (2.6 µm, 100 Å, 150x2.1 mm) UHPLC column. The eluents were Milli-Q water with 0.1% v/v formic acid and acetonitrile with 0.1% v/v formic acid. The 25 µL of injected samples contained a final 5% of acetonitrile and labelled internal standards to correct for instrumental recoveries.

Non-target analysis (NTA) of OMPs was performed using a Bruker Daltonics system on a subset of samples (day 0, 6, 20, 34, 62, and 76) for aerobic and nitrate-reducing conditions, and on all timepoint samples for iron- and sulfate-reducing conditions. The system included UHPLC equipped with a biphenyl Kinetex® UHPLC column (100 mm long, 2.1 mm diameter, and 1.7 µm 100 Å), trapped ion mobility spectrometry, quadrupole time of flight (qTOF), and high-resolution tandem mass spectrometry (HRMS/MS) using a vacuum insulated probe heated electrospray ionization ion source, operating in positive and negative mode, and using PASEF (Parallel Accumulation Serial Fragmentation) for MS^2 acquisition. The mobile phases (from Biosolve – the Netherlands) were UHPLC-grade water with 0.05% acetic acid and ULC/MS grade methanol.

5.2.3 Non-target data treatment and interpretation

Non-target data obtained from UHPLC-qTOF-HRMS/MS were first *m/z* recalibrated using Data Analysis to a ppm error below 0.8, then converted from .tdf to .mzML format using TIMSCONVERT 2.0.0 (Luu et al., 2022). During conversion, the raw data were centroided and the trapped ion mobility arrays were excluded to allow compatibility with patRoon 2.3.3 (November 2023 version). The latter is a software that runs on R (version 4.5.0) and RStudio

(version 2025.05.1-513) and allows the suspect screening of complex environmental non-target data. The patRoon script (Supplementary Script 5.1) included 5 main blocks: feature finding and grouping, PC screening, TP screening, annotation, and reporting, similarly to what was applied in previous studies (Ore et al., 2025b). Some parameters were further optimized compared to previous script versions: the minimum peak intensity threshold was lowered to 3000, the retention range was set to exclude the first elution minutes to remove peaks from the calibrant solution, and the TP screening included both TPs predicted by BioTransformer 3.0 (Djoumbou-Feunang et al., 2019; Wishart et al., 2022) with the environmental microbial module (Wicker et al., 2016) and TPs reported in PubChem (Kim et al., 2025), up to the 7th generation of transformation. Overall, the TP screening list included 16068 candidate TPs (Supplementary Excel -SE- 5, Table E1). Feature groups detected in the instrumental blanks or only in the abiotic samples were removed during data investigation. Additionally, all TPs with poor peak quality, an assigned identification level (ID) below 4, incorrect annotation (e.g., structural hypervalence), or that were detected in all samples with peak intensity higher in the abiotic than in the biotic samples, were not retained. This selection allowed the prioritization of TPs with higher confidence and more likely formed through biodegradation than abiotic reactions, but may have implied the removal of TPs formed in low abundance and with low-quality HRMS/MS data. Manual examination and correction of the peak integration was performed using the report generated via patRoon and the software mzMine 4.7.27 (Schmid et al., 2023). The average peak intensity of the triplicate samples was used to assess peak intensity trends during incubation under each redox condition and for both inocula, using the intensity normalized to the maximum intensity of each set.

5.2.3.1 Toxicity predictions and TP semi-quantification

Toxicity predictions for fish expressed as LC_{50} were obtained for the PCs and TPs detected via non-target analysis through MS2Tox (Peets et al., 2022), while semi-quantification of the TPs was performed using MS2Quant (Sepman et al., 2023). Both methods (MS2Tox and MS2Quant) were applied within the patRoon script using the suspect SMILES structures as the last steps of the non-target data workflow.

For toxicity assessment, a comparison of the predicted LC_{50}s for PCs and TPs was performed. Moreover, to assess the formation of TPs that represent a bigger risk to the environment than their PC, the biodegradability of PCs and TPs was considered. Similar to previous studies (Ore et al., 2025c), biodegradability was expressed by Biowin3 scores (Biowin version 4.10 from EPI Suite™), which predict the time required for an OMP to undergo full mineralization under aerobic conditions (US EPA, 2025). Biowin3 was shown to be the most suitable Biowin model to apply for environmental degradation (Ore et al., 2025c). LC_{50}s and

Biowin3 scores of TPs relative to corresponding PCs were simultaneously used to assess the formation of TPs with increased or decreased toxicity and biodegradability.

TP semi-quantification was performed using a calibrant list to translate compounds' ionization efficiencies into response factors, as previously done (Helmus et al., 2025). The calibrant set contained a total of 85 compounds detected in both positive and negative modes, and covering a wide range of ionization efficiencies. A calibration curve with 16 concentrations (0.016 to 16 µg/L) was used to predict response factors for annotated compounds in the experimental samples. The predicted response factors were then used to estimate TP concentrations in the samples under the different redox and inocula conditions. These predictions are associated with known uncertainties of 5-6 fold (Sepman et al., 2023). The predictions were therefore primarily used to estimate the bioconversion efficiency, expressed as the molar ratio between predicted TP concentrations formed and the concentration of the corresponding PC removed (target OMP data) over time. Predicted molar TP concentrations were converted to equivalent PC moles to account for differences in molecular weight between PC and TP, and a 1:1 stoichiometric conversion was assumed.

5.3 Results and discussion

5.3.1 Redox conditions determine OMP biodegradation rates

The biodegradation of 19 different OMPs was tested in batch experiments under aerobic, nitrate-reducing, iron-reducing, and sulfate-reducing conditions (Figures S5.1, S5.2). An OMP was defined as persistent if its half-life exceeded 120 days, following the European CLP (Classification, Labelling, and Packaging) regulation (European Parliament and Council of the European Union, 2024). Target LC-MS analysis revealed that some compounds, like paracetamol and hydrochlorothiazide, were readily biodegraded across all redox conditions and by both inocula, whereas others, including carbamazepine, 2,6-dichlorobenzamide, diglyme, and bentazone, were consistently persistent (Tables 5.2, S5.2). Presence of OMPs rapidly degradable under any redox condition may serve as an indicator of recent anthropogenic contamination (Sidhu et al., 2013; White et al., 2019). Despite high biodegradability, even low concentrations of these OMPs may have toxic effects on aquatic organisms, and their TPs might also be hazardous, as reported for paracetamol (Gutiérrez-Noya et al., 2021; Liu et al., 2019; Nunes et al., 2014). In contrast, the presence of compounds that persist across redox conditions represents a long-term environmental concern because, depending on their mobility and sorption affinity, they might pollute drinking water sources or accumulate in soil (Lapworth et al., 2015, 2012; Loos et al., 2010). For biodegradable compounds, further understanding TP formation or mineralization is key to assessing their environmental fate and risk, whereas for persistent OMPs, removal strategies should be optimized to prevent environmental release.

Table 5.2. Average biodegradation half-lives (DT_{50}s, days) with standard deviation of the 19 spiked OMPs per triplicate bottles under four redox conditions (aerobic, nitrate-reducing, iron-reducing, sulfate-reducing) and two inocula (soil and ditch). The DT_{50} value is missing for OMPs with removal efficiency not significant, i.e., below 30%. The last column on the right indicates the number of non-persistent PCs (i.e., with a DT_{50}<120 days).

Average DT_{50} (d)	MTP	1H-BTR	CAF	CBZ	SMX	DEET	BAM	SOT	DGY	MTF	MET	PCM	CLZ	DCF	FUR	MCPP	2,4-D	BTZ	HCZ	#PC DT_{50} <120
Aerobic soil	25.17 ± 3.64	65.07 ± 22.78	13.26 ± 1.32	143.09 ± 52.02	59.95 ± 10.95	142.75 ± 144.73	-	51.16 ± 10.09	258.08 ± 138.53	47.33 ± 4.51	80.58 ± 20.37	10.60 ± 0.07	9.20 ± 0.08	17.66 ± 2.41	10.83 ± 0.33	90.64 ± 20.58	7.53 ± 0.08	421.87 ± 388.05	43.58 ± 7.58	14
Nitrate-red. soil	42.45 ± 5.54	133.97 ± 21.83	-	233.92 ± 85.27	172.30 ± 89.48	-	-	6931.4 ± 0.1	856.90 ± 129.64	79.66 ± 8.77	156.55 ± 45.93	9.23 ± 0.23	-	671.71 ± 155.90	109.88 ± 30.49	307.90 ± 115.36	77.31 ± 14.07	512.85 ± 433.12	39.80 ± 5.51	6
Iron-red. soil	42.60 ± 4.27	-	-	-	17.76 ± 7.08	-	-	-	-	-	39.48 ± 3.31	28.15 ± 1.43	-	-	-	-	-	-	35.42 ± 4.07	5
Sulfate-red. soil	23.10 ± 1.76	-	-	132.22 ± 56.29	90.42 ± 30.80	-	-	107.52 ± 12.07	168.91 ± 90.51	6931.5 ± 0.1	23.51 ± 0.87	19.03 ± 0.60	-	-	100.07 ± 139.53	-	-	-	40.23 ± 3.53	7
Aerobic ditch	8.27 ± 0.18	59.73 ± 36.00	26.18 ± 5.93	349.40 ± 176.45	33.70 ± 38.62	8.96 ± 0.08	-	39.71 ± 2.51	1293.6 ± 706.04	14.44 ± 0.17	187.62 ± 28.39	10.70 ± 0.06	7.70 ± 0.28	26.15 ± 1.19	11.44 ± 1.08	14.78 ± 1.29	7.29 ± 0.07	-	38.33 ± 3.39	14
Nitrate-red. ditch	276.42 ± 159.85	-	40.52 ± 6.85	-	4653.6 ± 3528.8	-	-	6931.4 ± 0.1	3442.4 ± 3197.9	15.33 ± 0.19	2931.2 ± 3522.1	9.13 ± 0.08	-	-	42.42 ± 1.30	-	592.39 ± 243.57	-	40.78 ± 0.82	5
Iron-red. ditch	24.20 ± 4.08	182.69 ± 111.01	-	142.16 ± 76.33	8.21 ± 0.20	191.00 ± 126.84	-	91.14 ± 51.30	157.19 ± 108.62	69.74 ± 105.18	69.90 ± 19.88	38.35 ± 11.48	183.21 ± 111.71	-	-	209.50 ± 195.04	-	-	29.78 ± 5.57	7
Sulfate-red. ditch	50.92 ± 36.11	-	-	-	93.36 ± 108.56	-	-	-	-	54.93 ± 59.69	37.83 ± 36.63	29.99 ± 1.46	-	-	80.62 ± 88.31	-	-	-	37.04 ± 1.14	7

For most OMPs tested, biodegradation was redox-dependent (Tables 5.2, S5.2). Six OMPs (benzotriazole, sotalol, chloridazon, dichlofenac, furosemide, and 2,4-D) showed faster and more efficient biodegradation under aerobic conditions with both inocula, with half-lives ranging from 7 to 65 days. This was expected, given the higher energy yield to the microorganisms from aerobic respiration, and consistent with previous studies (Branco et al., 2023; Burke et al., 2017). Nonetheless, some OMPs persisted under aerobic but biodegraded under anaerobic conditions. For example, metolachlor was rapidly biodegraded under iron- and sulfate-reducing conditions (half-lives between 24 and 70 days), and sulfamethoxazole showed the shortest half-lives, 8 days in ditch and 18 days in soil, under iron-reducing conditions (Table 5.2). These OMPs are likely more sensitive to reduction than oxidation reactions, which require specific enzymes or conditions. For instance, studies showed that dehalogenase enzymes are commonly harboured by iron- and sulfate-reducing microorganisms (Jugder et al., 2016; Stiegler et al., 2023). In our study, metolachlor was still biodegraded to some extent under aerobic and nitrate-reducing conditions (>30%), but the long half-lives indicated slower conversion compared to deep anaerobic conditions. These findings align with previous studies (Branco et al., 2023; Martins et al., 2024; Stiegler et al., 2023).

Overall, aerobic conditions supported the highest number of degraded OMPs (14) with both inocula. However, biodegradation under other redox conditions did not follow the expected order of the redox ladder. Although nitrate is the second most favourable electron acceptor after oxygen, only 6 and 5 OMPs (in soil and ditch inocula, respectively) were significantly biodegraded under nitrate-reducing conditions (Table 5.2). These results are much lower compared to aerobic conditions (14 OMPs) and more comparable to deeper anaerobic conditions (5 to 7 OMPs). Low OMP biodegradation efficiencies under nitrate-reducing conditions have been previously reported (Branco et al., 2023). A possible explanation could be the presence of sulfamethoxazole in our spiked mixture, which was previously reported to inhibit the denitrification and alter the microbial community composition from concentrations as low as 1.27 µg/L (Underwood et al., 2011). This highlights that OMP biodegradation under different anaerobic conditions depends on more factors than only the energy yields, and is strongly compound- and community-specific.

5.3.2 TP formation is redox condition-dependent

The formation of TPs was observed across all tested redox conditions (Figure 5.1). With the soil inoculum, up to 14 TPs were detected under aerobic and iron-reducing conditions, followed by nitrate-reducing (12 TPs) and sulfate-reducing (8 TPs). With ditch sediments, the highest number of TPs was detected under nitrate-reducing conditions (16 TPs), followed by aerobic (14 TPs), iron-reducing (10 TPs), and sulfate-reducing conditions (7 TPs). Thus, TP

formation trends did not always align with PC biodegradation (Section 5.3.1), highlighting the value of coupling target and non-target approaches to better understand OMP fate. In soil, only 5 PCs showed significant biodegradation under iron-reducing conditions with target analysis (Table 5.2), yet up to 14 TPs originating from 8 different PCs were detected (Figure 5.1). Analytical differences and data treatment may explain this discrepancy; non-target analysis detected a broader range of OMPs, including TPs generated from limited PC degradation, while in target analysis we applied a threshold (RE>30%) to define significant biodegradation that lowered sensitivity. Moreover, under anaerobic conditions, microbial activity is generally reduced, resulting in slower PC removal and likely also slower TP degradation. In contrast, under aerobic conditions, higher microbial activity may support both rapid PC and TP biodegradation, resulting in TPs being consumed between sampling points or preventing TP build-up to detectable levels. This may explain why similar numbers of TPs were detected under aerobic and anaerobic conditions.

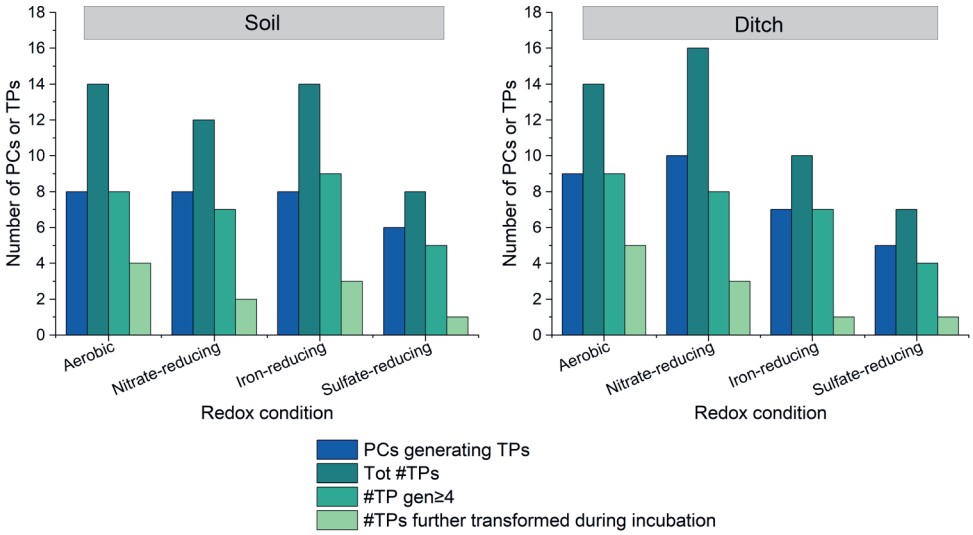

Figure 5.1. Overview of the NTA results, including the number of PCs generating TPs, the total number of TPs, TPs of generation 4 or higher, and TPs that were further transformed during incubation time, per inoculum.

In fact, redox conditions strongly influenced TP formation dynamics. In several cases, the TP formed from a given PC depended on redox conditions. For example, chloridazon yielded different redox-specific TPs under aerobic and nitrate-reducing conditions (Figure 5.2). Under aerobic conditions, chloridazon was transformed into chloridazon-desphenyl (TP58), which persisted throughout the incubation, whereas chloridazon-TP102 was formed only under nitrate-reducing conditions and was further degraded (Tables 5.3 and 5.4). The TPs reflect the reactions that likely occurred under different redox conditions: while chloridazon-desphenyl arose from N-dealkylation by oxygenase enzymes, chloridazon-TP102 involved

reductive steps such as dehalogenation. Notably, chloridazon-TP102 was predicted to be less toxic than chloridazon-desphenyl.

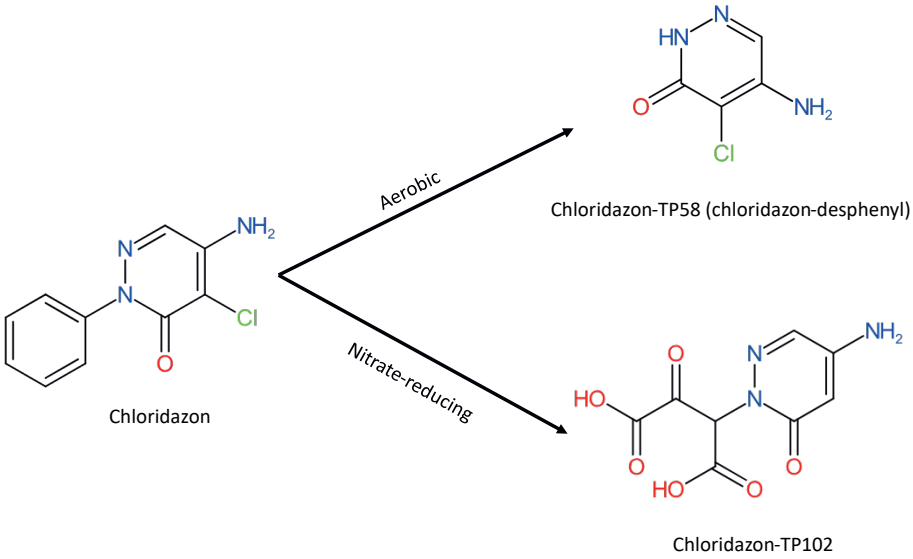

Figure 5.2. Different degradation pathways of chloridazon under aerobic and nitrate-reducing conditions.

Some TPs were uniquely detected under specific redox conditions across both inocula (Tables 5.3 and 5.4); 2 TPs, chloridazon-desphenyl and metolachlor-TP1167, were uniquely detected under aerobic conditions in both soil and ditch. In soil, one TP was unique to nitrate-reducing conditions and one to iron-reducing conditions, whereas in ditch sediments, 3 TPs were unique to nitrate-reducing and 3 to iron-reducing conditions. No TP was exclusively detected under sulfate-reducing conditions. The exclusive detection of these TPs may indicate either formation through redox-specific reactions (as in Figure 5.2) or reduced degradation rates that allowed them to reach detectable levels. Other TPs were not unique to a single redox condition, but commonly detected in either deep anaerobic or aerobic/nitrate-reducing conditions, indicating that similar reactions might happen thanks to anaerobes or facultative anaerobic bacteria. For example, caffeine-TP9 and metoprolol-TP78 (metoprolol acid) were detected only under aerobic and nitrate-reducing conditions, while metolachlor-TP189 or dichlobenil-TP7 only under iron- and sulfate-reducing conditions (Tables 5.3 and 5.4). Similar results for caffeine and metoprolol TPs have also been observed in previous studies (Ore et al., 2025b; Rutere et al., 2021; Summers et al., 2015; Yu et al., 2008). SE5 Tables E2 and E3 report extra information on the TPs detected in soil and ditch, respectively, including chemical structure identifiers, predicted transformation reactions that led to their formation, and common names.

Table 5.3. Overview of the TPs detected during the incubation with soil inoculum under four different redox conditions. Color shades indicate TPs unique to one (single color) or two (shading colors) redox conditions, while TPs with no color were common to three or four redox conditions. (The table continues on the next page)

TP generation	ID level	Aerobic						Iron				
		0 d	6 d	20 d	34 d	62 d	76 d	0 d	9 d	20 d	41 d	62 d
Gen 1	2a	2,4-D-TP1	2,4-D-TP1	2,4-D-TP1	2,4-D-TP1			2,4-D-TP1	2,4-D-TP1	2,4-D-TP1	2,4-D-TP1	2,4-D-TP1
	3c	MET-TP10	MET-TP10	MET-TP10	MET-TP10			MET-TP10				
Gen 2	2a		DEET-TP466	DEET-TP466	DEET-TP466	DEET-TP466	DEET-TP466		DEET-TP466	DEET-TP466	DEET-TP466	DEET-TP466
	3c					FUR-TP822	FUR-TP822		FUR-TP822	FUR-TP822	FUR-TP822	FUR-TP822
	3a		MTP-TP78	MTP-TP78	MTP-TP78	MTP-TP78						
Gen 3	2a		BAM-TP4	BAM-TP4	BAM-TP4	BAM-TP4	BAM-TP4		BAM-TP4	BAM-TP4	BAM-TP4	BAM-TP4
Gen 4	3a					CLZ-TP58	CLZ-TP58					
	3c	MET-TP74	MET-TP74	MET-TP74	MET-TP74	MET-TP74	MET-TP74	MET-TP74	MET-TP74	MET-TP74	MET-TP74	MET-TP74
	3c	HCZ-TP805	HCZ-TP805					HCZ-TP805				
	3c				MET-TP1167	MET-TP1167	MET-TP1167					
Gen 5	3c			MET-TP57	MET-TP57	MET-TP57	MET-TP57			MET-TP57	MET-TP57	MET-TP57
	3c							MET-TP189	MET-TP189	MET-TP189	MET-TP189	MET-TP189
Gen 7	4b	FUR-TP1339	FUR-TP1339	FUR-TP1339	FUR-TP1339	FUR-TP1339	FUR-TP1339					
	3c											
PubChem	3c							DCB-TP7	DCB-TP7	DCB-TP7	DCB-TP7	DCB-TP7
Only	3c								DEET-TP1344	DEET-TP1344	DEET-TP1344	DEET-TP1344
	2a								PCM-TP134	PCM-TP134	PCM-TP134	
	2a		HCZ-TP1190	HCZ-TP1190	HCZ-TP1190	HCZ-TP1190	HCZ-TP1190	HCZ-TP1190	HCZ-TP1190	HCZ-TP1190	HCZ-TP1190	HCZ-TP1190
	2a			HCZ-TP1189	HCZ-TP1189	HCZ-TP1189	HCZ-TP1189		HCZ-TP1189	HCZ-TP1189	HCZ-TP1189	HCZ-TP1189

Table 5.3 (continuation). Overview of the TPs detected during the incubation with soil inoculum under four different redox conditions. Color shades indicate TPs unique to one (single color) or two (shading colors) redox conditions, while TPs with no color were common to three or four redox conditions.

TP generation	ID level	Nitrate						Sulfate				
		0 d	6 d	20 d	34 d	62 d	76 d	0 d	9 d	20 d	41 d	62 d
Gen 1	2a	2,4-D-TP1	2,4-D-TP1	2,4-D-TP1	2,4-D-TP1	2,4-D-TP1	2,4-D-TP1	2,4-D-TP1	2,4-D-TP1	2,4-D-TP1	2,4-D-TP1	2,4-D-TP1
	3c	MET-TP10	MET-TP10	MET-TP10	MET-TP10	MET-TP10	MET-TP10	MET-TP10	MET-TP10	MET-TP10	MET-TP10	
Gen 2	2a	DEET-TP466	DEET-TP466	DEET-TP466	DEET-TP466	DEET-TP466	DEET-TP466					
	3c											
	3a		MTP-TP78	MTP-TP78	MTP-TP78	MTP-TP78	MTP-TP78					
Gen 3	2a		BAM-TP4	BAM-TP4	BAM-TP4	BAM-TP4	BAM-TP4		BAM-TP4	BAM-TP4	BAM-TP4	BAM-TP4
Gen 4	3a											
	3c	MET-TP74	MET-TP74	MET-TP74	MET-TP74	MET-TP74	MET-TP74					
	3c	HCZ-TP805	HCZ-TP805	HCZ-TP805	HCZ-TP805	HCZ-TP805	HCZ-TP805					
	3c											
Gen 5	3c		MET-TP57	MET-TP57	MET-TP57	MET-TP57	MET-TP57					
	3c							MET-TP189	MET-TP189	MET-TP189	MET-TP189	MET-TP189
Gen 7	4b	FUR-TP1339	FUR-TP1339	FUR-TP1339	FUR-TP1339							
	3c	CLZ-TP102	CLZ-TP102									
PubChem	3c									DCB-TP7	DCB-TP7	DCB-TP7
Only	3c								DEET-TP1344	DEET-TP1344	DEET-TP1344	DEET-TP1344
	2a											
	2a				HCZ-TP1190	HCZ-TP1190	HCZ-TP1190	HCZ-TP1190	HCZ-TP1190	HCZ-TP1190	HCZ-TP1190	HCZ-TP1190
	2a					HCZ-TP1189	HCZ-TP1189	HCZ-TP1189	HCZ-TP1189	HCZ-TP1189	HCZ-TP1189	HCZ-TP1189

Table 5.4. Overview of the TPs detected during the incubation with ditch inoculum under four different redox conditions. Color shades indicate TPs unique to one (single color) or two (shading colors) redox conditions, while TPs with no color were common to three or four redox conditions.(The table continues on the next page)

TP generation	ID level	Aerobic						Iron				
		0 d	6 d	20 d	34 d	62 d	76 d	0 d	9 d	20 d	41 d	62 d
Gen 1	2a	2,4-D-TP1	2,4-D-TP1	2,4-D-TP1				2,4-D-TP1	2,4-D-TP1	2,4-D-TP1	2,4-D-TP1	2,4-D-TP1
Gen 2	2a		DEET-TP466	DEET-TP466	DEET-TP466	DEET-TP466	DEET-TP466			DEET-TP466	DEET-TP466	DEET-TP466
	3a		MTP-TP78	MTP-TP78								
Gen 3	2a							BAM-TP4	BAM-TP4	BAM-TP4	BAM-TP4	BAM-TP4
	3c											
	3c			SOT-TP636								
	3c		MET-TP1072	MET-TP1072	MET-TP1072	MET-TP1072	MET-TP1072					
	3c											
Gen 4	3a				CLZ-TP58	CLZ-TP58	CLZ-TP58					
	3c	MET-TP74	MET-TP74	MET-TP74	MET-TP74	MET-TP74	MET-TP74	MET-TP74	MET-TP74	MET-TP74	MET-TP74	MET-TP74
	3c	HCZ-TP805	HCZ-TP805	HCZ-TP805	HCZ-TP805			HCZ-TP805				
	3c			MET-TP1167	MET-TP1167	MET-TP1167	MET-TP1167					
Gen 5	3c	MET-TP274	MET-TP274	MET-TP274	MET-TP274	MET-TP274	MET-TP274					
Gen 7	4b				FUR-TP1339	FUR-TP1339	FUR-TP1339					
	3c											
PubChem	3c									DCB-TP2	DCB-TP2	DCB-TP2
Only	3c							DCB-TP7	DCB-TP7	DCB-TP7	DCB-TP7	DCB-TP7
	3a	CAF-TP9	CAF-TP9									
	2a							CBZ-TP3696	CBZ-TP3696	CBZ-TP3696	CBZ-TP3696	CBZ-TP3696
	2a		HCZ-TP1190	HCZ-TP1190	HCZ-TP1190	HCZ-TP1190	HCZ-TP1190	HCZ-TP1190	HCZ-TP1190	HCZ-TP1190	HCZ-TP1190	HCZ-TP1190
	2a		HCZ-TP1189	HCZ-TP1189	HCZ-TP1189	HCZ-TP1189	HCZ-TP1189		HCZ-TP1189	HCZ-TP1189	HCZ-TP1189	HCZ-TP1189

Table 5.4 (continuation). Overview of the TPs detected during the incubation with ditch inoculum under four different redox conditions. Color shades indicate TPs unique to one (single color) or two (shading colors) redox conditions, while TPs with no color were common to three or four redox conditions.

TP generation	ID level	Nitrate						Sulfate				
		0 d	6 d	20 d	34 d	62 d	76 d	0 d	9 d	20 d	41 d	62 d
Gen 1	2a	2,4-D-TP1	2,4-D-TP1	2,4-D-TP1	2,4-D-TP1	2,4-D-TP1	2,4-D-TP1	2,4-D-TP1	2,4-D-TP1	2,4-D-TP1	2,4-D-TP1	2,4-D-TP1
Gen 2	2a		DEET-TP466	DEET-TP466	DEET-TP466	DEET-TP466	DEET-TP466		DEET-TP466	DEET-TP466	DEET-TP466	DEET-TP466
	3a		MTP-TP78	MTP-TP78	MTP-TP78	MTP-TP78	MTP-TP78					
Gen 3	2a	BAM-TP4	BAM-TP4	BAM-TP4	BAM-TP4	BAM-TP4		BAM-TP4				
	3c			SOT-TP1825	SOT-TP1825	SOT-TP1825						
	3c					SOT-TP636	SOT-TP636					
	3c					MET-TP1072	MET-TP1072					
	3c	FUR-TP2337	FUR-TP2337	FUR-TP2337								
Gen 4	3a											
	3c	MET-TP74	MET-TP74	MET-TP74	MET-TP74	MET-TP74	MET-TP74					
	3c	HCZ-TP805	HCZ-TP805	HCZ-TP805	HCZ-TP805	HCZ-TP805	HCZ-TP805	HCZ-TP805	HCZ-TP805	HCZ-TP805	HCZ-TP805	HCZ-TP805
	3c											
Gen 5	3c			MET-TP274	MET-TP274	MET-TP274	MET-TP274					
Gen 7	4b			FUR-TP1339	FUR-TP1339	FUR-TP1339	FUR-TP1339			FUR-TP1339	FUR-TP1339	FUR-TP1339
	3c	CLZ-TP102	CLZ-TP102	CLZ-TP102								
PubChem	3c											
Only	3c											
	3a			CAF-TP9	CAF-TP9	CAF-TP9	CAF-TP9					
	2a											
	2a					HCZ-TP1190	HCZ-TP1190	HCZ-TP1190	HCZ-TP1190	HCZ-TP1190	HCZ-TP1190	HCZ-TP1190
	2a			HCZ-TP1189	HCZ-TP1189	HCZ-TP1189	HCZ-TP1189		HCZ-TP1189	HCZ-TP1189	HCZ-TP1189	HCZ-TP1189

5.3.3 TP fate: persistence vs. further degradation

NTA results revealed how far OMP biodegradation progressed along transformation pathways under different redox conditions. This was reflected in the number of later-generation TPs (generation ≥4) and the number of TPs that were further transformed during incubation (i.e., disappeared before the end of the experiment) (Figure 5.1). Sulfate-reducing conditions were consistently the least effective, producing the lowest number of later-generation TPs and the fewest further transformations. This outcome likely reflects the low energy yielded from sulfate reduction compared to aerobic respiration or even iron reduction.

The TP peak intensity profiles further highlighted redox-dependent dynamics in TP formation and biodegradation (SE5 Table E4). In general, under aerobic conditions, more TPs showed decreasing or increasing-decreasing intensity trends, indicating further degradation, whereas such patterns were less common under anaerobic conditions (SE5 Table E4). Depending on redox conditions, in some cases, TPs were formed later and persisted until the end of the incubation, whereas in others they were further degraded and disappeared from detection (Tables 5.3 and 5.4). For example, metoprolol-TP78, sotalol-TP636, and caffeine-TP9 were detected under aerobic and nitrate-reducing conditions with ditch inoculum, but their fate changed based on redox conditions. Under aerobic conditions, these TPs were formed and further transformed to below detection levels before the end of the incubation (Table 5.4). Under nitrate-reducing conditions, instead, they showed increasing peak intensity trends throughout the incubation, suggesting limited further transformation (SE5 Table E4). Such bottlenecks likely contributed to the lower PC removal efficiency observed under nitrate-reducing conditions compared to aerobic conditions (Table S5.2). A different pattern was observed for 2,4-D-TP1: although present in abiotic controls, the higher starting peaks in biotic incubations and the degradation trends indicated microbial contribution in formation and degradation at different rates across redox conditions. 2,4-D-TP1 was completely degraded under aerobic conditions within 62 days in soil and 34 days in ditch (Tables 5.3 and 5.4), and also showed decreasing peak intensity under nitrate and iron-reducing conditions, indicating partial degradation at a slower rate. In contrast, under sulfate-reducing conditions, 2,4-D-TP1 peak intensity did not decline throughout the incubation (SE5 Table E4).

Although some TPs persisted until the end of the experiment, biodegradation generally produced less toxic and more biodegradable TPs (Figure 5.3, SE5 Table E5). The assessment with Biowin3 and MS2Tox indicated that most of the TPs detected in our study showed increased biodegradability and decreased toxicity compared to their PC, respectively, indicating that biodegradation may support OMP removal. Still, biotransformation did not

always lead to detoxification. Four TPs were predicted to be more toxic but also more biodegradable than their PC, suggesting that although they can be further degraded, they may still pose a risk if they accumulate before further removal. Of greater concern are TPs that are both more toxic and less biodegradable, as they may persist and accumulate to possibly toxic concentrations. In this study, 3 such TPs were (tentatively) identified, including caffeine-TP9, 2,4-D-TP1, and paracetamol-TP134. All three, however, did show further degradation during incubation, highlighting that the toxicity and persistence are relative to the PC and not absolute. None of the TPs were predicted to be both less biodegradable and less toxic. Knowledge on TP formed under different redox conditions may help optimize removal processes and prioritize OMP removal before discharge into the environment.

Semi-quantitative analysis indicated that not all TPs involved in PC biodegradation were detected. While in a previous work we could observe an almost complete transformation of chloridazon to chloridazon-desphenyl (Ore et al., 2025b), in this study, chloridazon-desphenyl accounted for only 37% (soil) and 29% (ditch) of chloridazon biodegradation under aerobic conditions (SE5 Table E6), despite the PC being removed >99%. Similarly, 4 (soil) and 5 (ditch) metolachlor TPs were detected, but explained only up to 44% (soil) and 22% (ditch) of the PC removed under aerobic conditions, and even smaller fractions under iron and sulfate-reducing conditions, where PC removal was higher. These gaps suggest that not all transformation steps were captured, and several TPs were missing from the predictions of our workflow. Mass thresholds during data treatment likely filtered out small molecules, and TPs more specific to anaerobic conditions were probably missed by BioTransformer and PubChem predictions, which use a combination of rules and machine learning trained on different conditions from those tested here. Thus, while the detected TPs capture key redox-dependent dynamics, the full extent of transformation was likely underestimated.

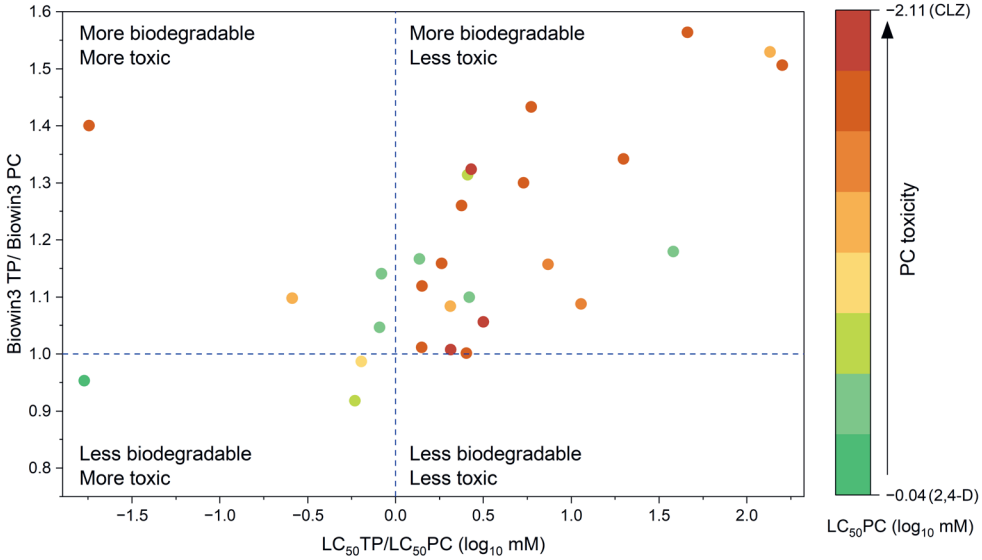

Figure 5.3. Biodegradability (expressed by Biowin3) and toxicity (LC50) of the TPs detected in soil and ditch with respect to their corresponding PC. The four quadrants indicate if the produced TP is more or less toxic and more or less biodegradable than the PC.

5.3.4 Effect of inoculum on OMP biodegradation and TP formation

Although the redox conditions played a more significant role in determining OMP fate, the origin of the inoculum also influenced biodegradation performance and TP formation. Differences in the efficiency and rate of PC biodegradation were observed between the used soil and ditch inocula (Table 5.2, S5.2). For example, under nitrate-reducing conditions, soil showed measurable removal (>30%) for 15 PCs, 6 of which had DT_{50} <120 days, compared to 11 and 5 PCs, respectively, in ditch. Also, some PCs were persistent only in one inoculum under nitrate-reducing conditions: metoprolol and 2,4-D persisted in ditch but not in soil, while caffeine was not removed in soil but was biodegraded in ditch. Differences were also observed in degradation rates, such as the faster biodegradation of metformin in ditch under nitrate-reducing conditions and the generally faster OMP biodegradation of the ditch inoculum under iron-reducing conditions (Table 5.2).

Moreover, the used soil and ditch inocula produced partly overlapping but also distinct sets of TPs, with 6 inoculum-specific TPs detected in soil and 8 in ditch (Tables 5.3 and 5.4). Even when the same TPs were formed, their dynamics differed between inocula, pointing to inoculum-specific capacities for further transformation.

These observations suggest that the used soil and ditch inoculum had distinct metabolic potentials, likely reflecting differences in microbial composition, functional redundancy, and pre-exposure history (Kennes-Veiga et al., 2022; Rios-Miguel et al., 2023). The ditch inoculum, collected below the water level in a shallow ditch, was likely exposed to

fluctuating aerobic-anaerobic conditions, favoring adaptation and enrichment of facultative anaerobes. This may have contributed to the formation of the 16 TPs under nitrate-reducing conditions (Figure 5.1). In contrast, the soil inoculum, sampled below the groundwater level, may have been adapted to iron-reduction metabolism, consistent with the detection of 14 TPs under iron-reducing conditions (Figure 5.1). Previous studies showed that pre-exposure to specific redox conditions can influence the microbial community composition and thus the presence of dedicated enzymes (e.g., reductases or dehalogenases) involved in OMP transformation pathways (Branco et al., 2023; Pett-Ridge and Firestone, 2005). Therefore, while redox conditions have a stronger influence on OMP fate, the origin and microbial composition of the inoculum also play a role in biodegradation and should be considered in experimental designs and standardized tests.

5.4 Conclusions

Our results demonstrate that OMP biodegradation and TP formation are predominantly influenced by redox conditions, and to a lesser extent by inoculum origin. Aerobic conditions were confirmed as the most favourable for biodegradation, while sulfate-reducing conditions consistently showed the lowest OMP biodegradation and number of detected TPs. Intermediate redox conditions (nitrate- and iron-reducing) showed more variable outcomes, where the origin of the inoculum and the pre-exposure to specific conditions likely influenced both PC and TP fate. These inoculum-specific effects suggest that microbial community composition and previous adaptation may influence OMP biodegradation and TP formation. Such influence could be further investigated through 16S rRNA sequencing or metagenomics (Achermann et al., 2020; Ghattas et al., 2017; Johnson et al., 2015; Rutere, 2020).

Different redox conditions also determined which TPs were detected and their fate. While some TPs were detected across multiple conditions, their formation and transformation were redox-dependent. Under aerobic conditions, several TPs formed and were completely removed, whereas the same compounds persisted throughout the incubation under anaerobic conditions. The comparison of target analysis on PC biodegradation with NTA results on TP formation and further degradation demonstrated that these methods capture different aspects of OMP fate. Target analysis showed the efficient removal of many PCs, while NTA revealed the formation of TPs, some of which could not be further degraded. Together, these techniques can provide a broader view of OMP biodegradation. Our results also highlighted that biodegradation generally produces more biodegradable and less toxic TPs. Nonetheless, biotransformation did not always correspond to detoxification, underscoring the importance of prioritizing TPs with predicted higher toxicity or persistence for ecotoxicity tests.

The semi-quantification analysis further revealed that only part of the biotransformation steps were captured in our study, likely due to limitations in the prediction tools, especially under anaerobic conditions. Improved databases that inform predictive models are needed, which would benefit from further identification of redox-specific TPs and reactions. Finally, since environmental systems rarely show stagnant redox zones, future studies should explore OMP fate across sequential redox environments, for example through column experiments (Falås et al., 2016). Such approaches would help clarify whether TPs that persist under one condition can be further degraded under another, improving our predictive understanding of OMP fate under both natural and engineered systems.

Acknowledgments

This research was performed within the framework of the research program AquaConnect, funded by the Dutch Research Council (NWO, grant-ID P19-45) and public and private partners of the AquaConnect consortium and coordinated by Wageningen University and Research. We thank Livio Carlucci, Beatriz Alvarado Perry, and Lucian Wester for their support with the analyses at Wageningen University, and Patricia Aguilar-Alarcón (University of Amsterdam) for her help with the non-target screening measurements.

Supplementary Information

SI 5.2 Materials and methods

Table S5.1. Headspace gas composition for the four redox conditions.

	Aerobic	Nitrate-reducing	Iron-reducing	Sulfate-reducing
Headspace gas	N_2 (80%) / O_2 (20%)	N_2 (100%)	N_2 (80%) / CO_2 (20%)	N_2 (80%) / CO_2 (20%)

SI 5.2.2 Chemical analyses

Gas chromatography

Headspace analysis was performed using a Shimadzu GC-2010 instrument with a parallel combination of PoraBOND Q (50 m x 0.53 mm; 10 µm; Agilent™, USA) and CP-Molsieve 5Å (25 m x 0.53 mm; 50 µm; Agilent™, USA) columns. H_2 was used as carrier gas (0.5 bar). The temperature for the injection was set to 120°C, 65°C for the oven, and 150°C for the detector. The ideal gas law was used to convert the results in percentages to mol.

Ion chromatography

Nitrate and sulfate concentrations in the biotic bottles were followed during incubation with ion chromatography (Dionex ICS6000 with autosampler AS-AP). The liquid samples were centrifuged twice at 150000 rcf for 10 minutes before the supernatant was used for analysis. The system used an analytical column (Dionex IonPac AS17-C 2mm IC) with a guard column (AS17-C 2mm), a Dionex ADRS 600 2 mm dynamically regenerated suppressor, and a conductivity detector.

SI 5.3 Results and discussion

SI 5.3.1 OMP biodegradation under different redox conditions

Table S5.2. Average removal efficiency of the 19 spiked OMPs per triplicate bottles under four redox conditions and with two inocula. Green color indicates a removal efficiency higher than 70%, pink indicates removal below 30%.

Average RE%	MTP	1H-BTR	CAF	CBZ	SMX	DEET	BAM	SOT	DGY	MTF	MET	PCM	CLZ	DCF	FUR	MCPP	2,4-D	BTZ	HCTZ
Aerobic soil	92.53 ± 1.44	57.60 ± 11.13	98.00 ± 0.00	47.78 ± 5.81	70.33 ± 3.07	61.46 ± 33.50	25.71 ± 8.57	77.37 ± 2.20	39.01 ± 6.67	74.63 ± 1.72	56.13 ± 3.73	99.88 ± 0.00	99.65 ± 0.00	95.03 ± 1.48	99.15 ± 0.00	56.44 ± 5.62	99.72 ± 0.00	37.90 ± 7.56	77.29 ± 2.64
Nitrate-reducing soil	84.33 ± 0.68	40.31 ± 4.75	0.26 ± 16.78	40.54 ± 4.81	94.92 ± 0.84	29.17 ± 4.56	25.65 ± 5.36	69.92 ± 2.35	34.47 ± 1.29	51.46 ± 5.42	48.79 ± 6.03	99.88 ± 0.00	29.41 ± 5.01	31.59 ± 6.60	70.58 ± 11.80	30.67 ± 9.09	57.06 ± 6.78	30.14 ± 4.83	74.75 ± 3.71
Iron-reducing soil	60.67 ± 1.08	12.17 ± 10.27	16.13 ± 13.35	12.09 ± 7.12	90.77 ± 7.82	15.39 ± 1.69	14.00 ± 5.45	15.43 ± 1.88	19.77 ± 2.50	-38.61 ± 4.30	62.04 ± 2.91	77.15 ± 1.89	11.64 ± 2.79	-4.69 ± 10.46	-9.70 ± 18.50	18.12 ± 5.02	14.41 ± 5.67	11.24 ± 2.74	71.58 ± 2.04
Sulfate-reducing soil	84.29 ± 2.07	13.36 ± 16.04	-171.94 ± 35.12	33.36 ± 8.18	36.24 ± 5.23	28.28 ± 16.29	18.38 ± 10.96	30.64 ± 7.32	35.40 ± 13.70	-10.28 ± 6.83	84.74 ± 2.19	92.19 ± 0.86	14.54 ± 14.43	7.58 ± 17.16	88.30 ± 9.44	20.76 ± 9.73	23.63 ± 10.19	24.29 ± 10.09	67.07 ± 3.57
Aerobic ditch	99.59 ± 0.00	69.66 ± 21.32	96.96 ± 0.00	41.33 ± 0.79	86.45 ± 19.22	99.63 ± 0.00	14.87 ± 8.56	78.69 ± 3.66	42.48 ± 1.57	94.02 ± 0.03	45.18 ± 9.86	99.89 ± 0.00	99.72 ± 0.00	88.98 ± 4.64	99.22 ± 0.00	96.57 ± 1.07	99.73 ± 0.00	29.95 ± 10.78	80.47 ± 2.20
Nitrate-reducing ditch	52.92 ± 8.90	11.21 ± 7.40	35.83 ± 15.15	20.11 ± 13.46	53.36 ± 69.93	25.58 ± 9.37	14.11 ± 8.10	44.29 ± 11.6	42.15 ± 10.25	96.79 ± 0.06	34.27 ± 9.36	99.88 ± 0.00	21.58 ± 10.42	13.21 ± 25.37	79.44 ± 12.40	21.86 ± 11.70	32.18 ± 3.93	19.18 ± 13.63	76.75 ± 1.77
Iron-reducing ditch	90.07 ± 3.04	33.02 ± 22.73	27.45 ± 33.90	36.62 ± 18.07	99.26 ± 0.00	30.96 ± 19.46	25.32 ± 17.65	54.30 ± 17.80	33.22 ± 25.30	99.46 ± 44.33	50.16 ± 12.79	66.35 ± 13.49	31.99 ± 22.54	17.06 ± 29.48	-2.47 ± 38.59	35.88 ± 27.58	29.36 ± 28.01	25.68 ± 23.97	78.32 ± 6.67
Sulfate-reducing ditch	67.79 ± 26.15	-10.59 ± 28.10	-442.57 ± 183.65	20.42 ± 0.48	48.03 ± 59.73	21.66 ± 1.58	10.99 ± 2.75	25.09 ± 8.97	24.33 ± 1.00	32.76 ± 42.77	73.82 ± 33.93	81.46 ± 0.47	15.08 ± 5.34	0.27 ± 1.35	95.96 ± 4.61	15.30 ± 7.71	17.58 ± 5.02	17.51 ± 3.37	69.48 ± 0.26

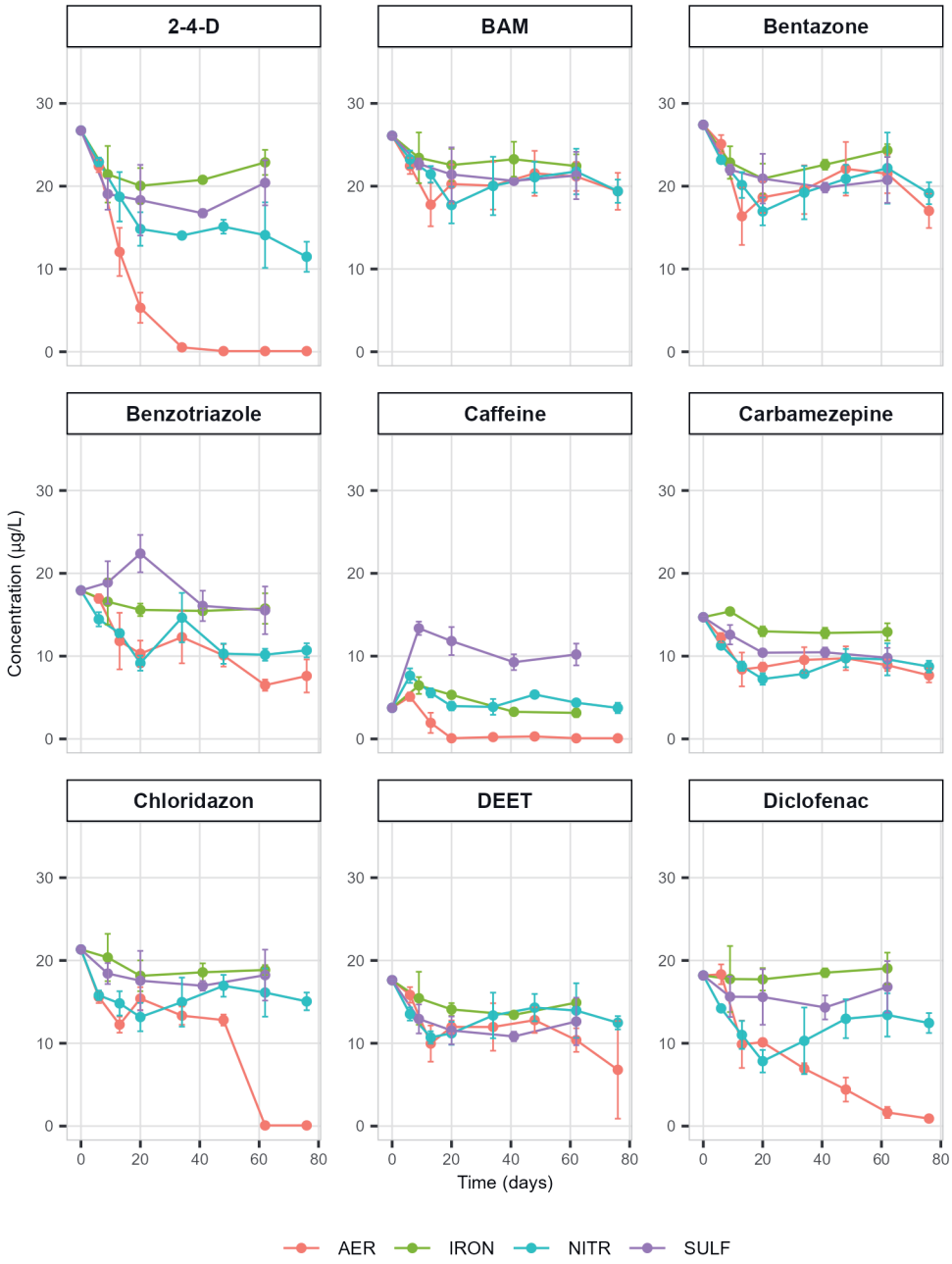

Figure S5.1. Biodegradation curves with soil inoculum under four redox conditions.

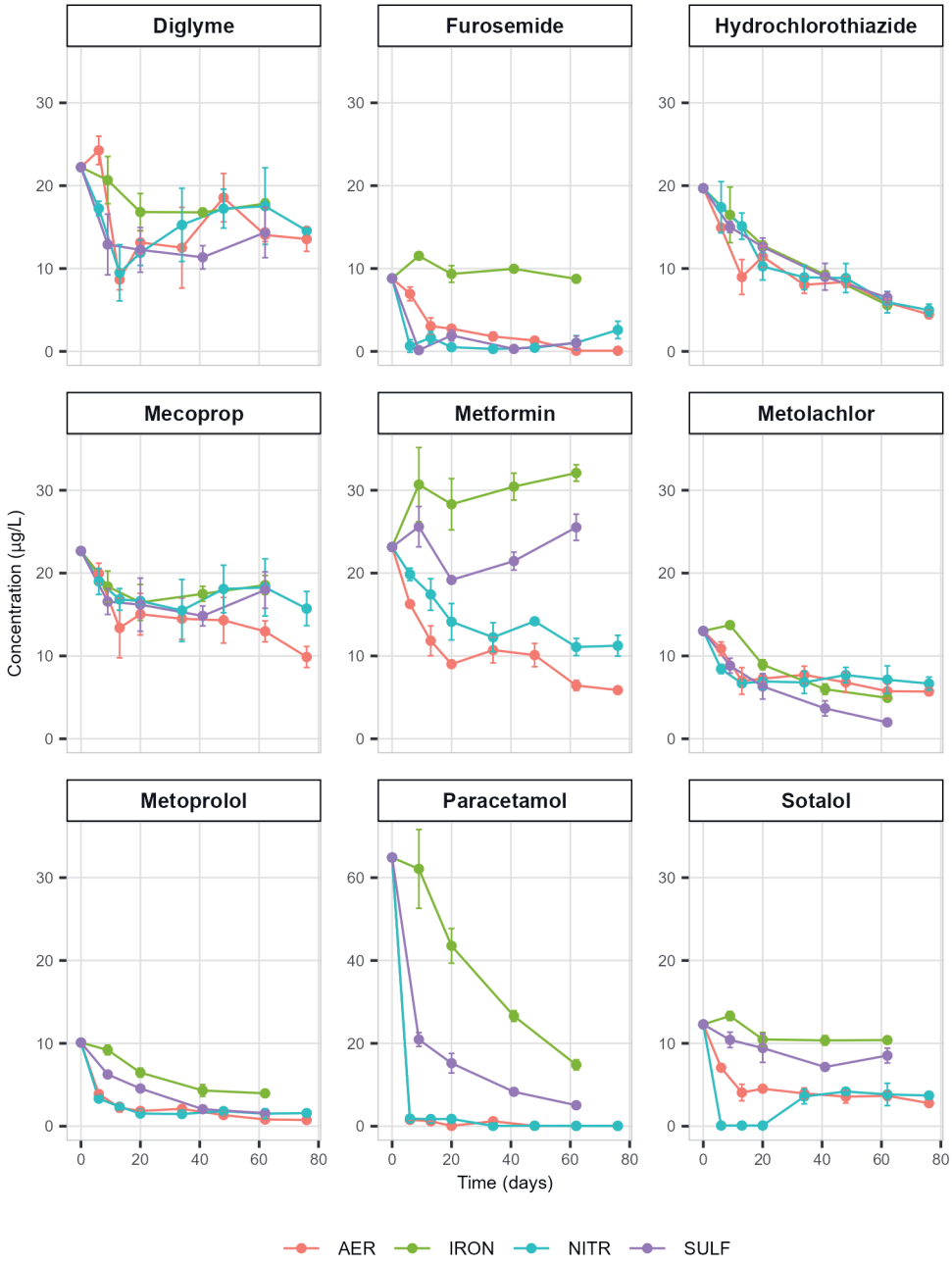

Figure S5.1 continuation. Biodegradation curves with soil inoculum under four redox conditions.

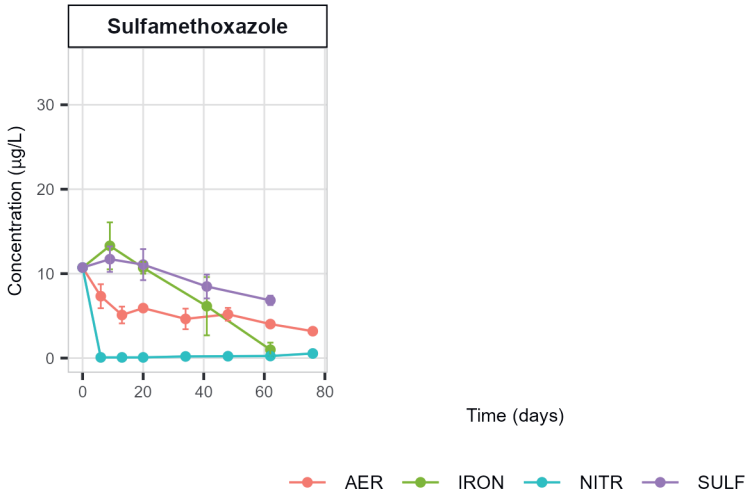

Figure S5.1 continuation. Biodegradation curves with soil inoculum under four redox conditions.

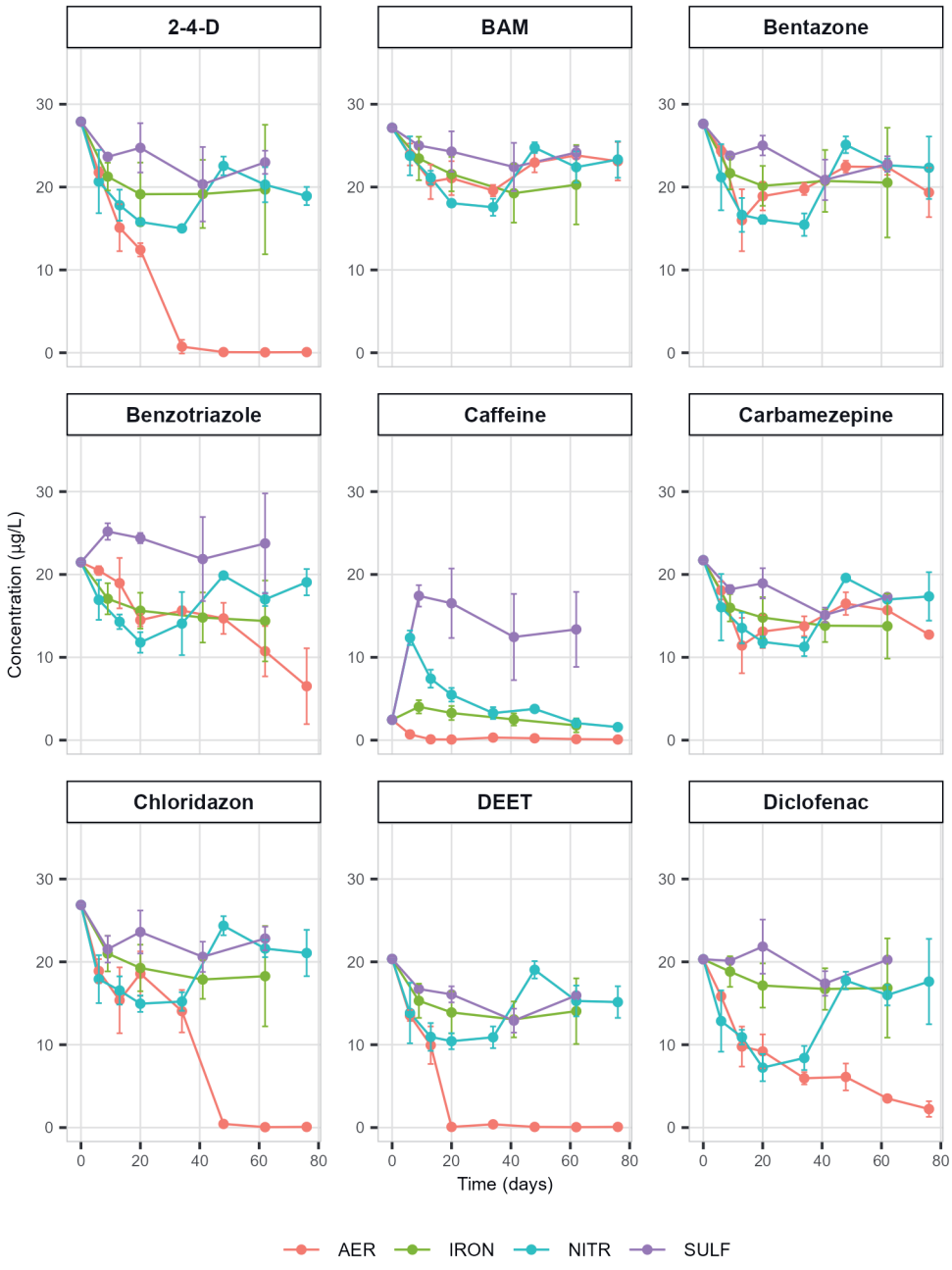

Figure S5.2. Biodegradation curves with ditch inoculum under four redox conditions.

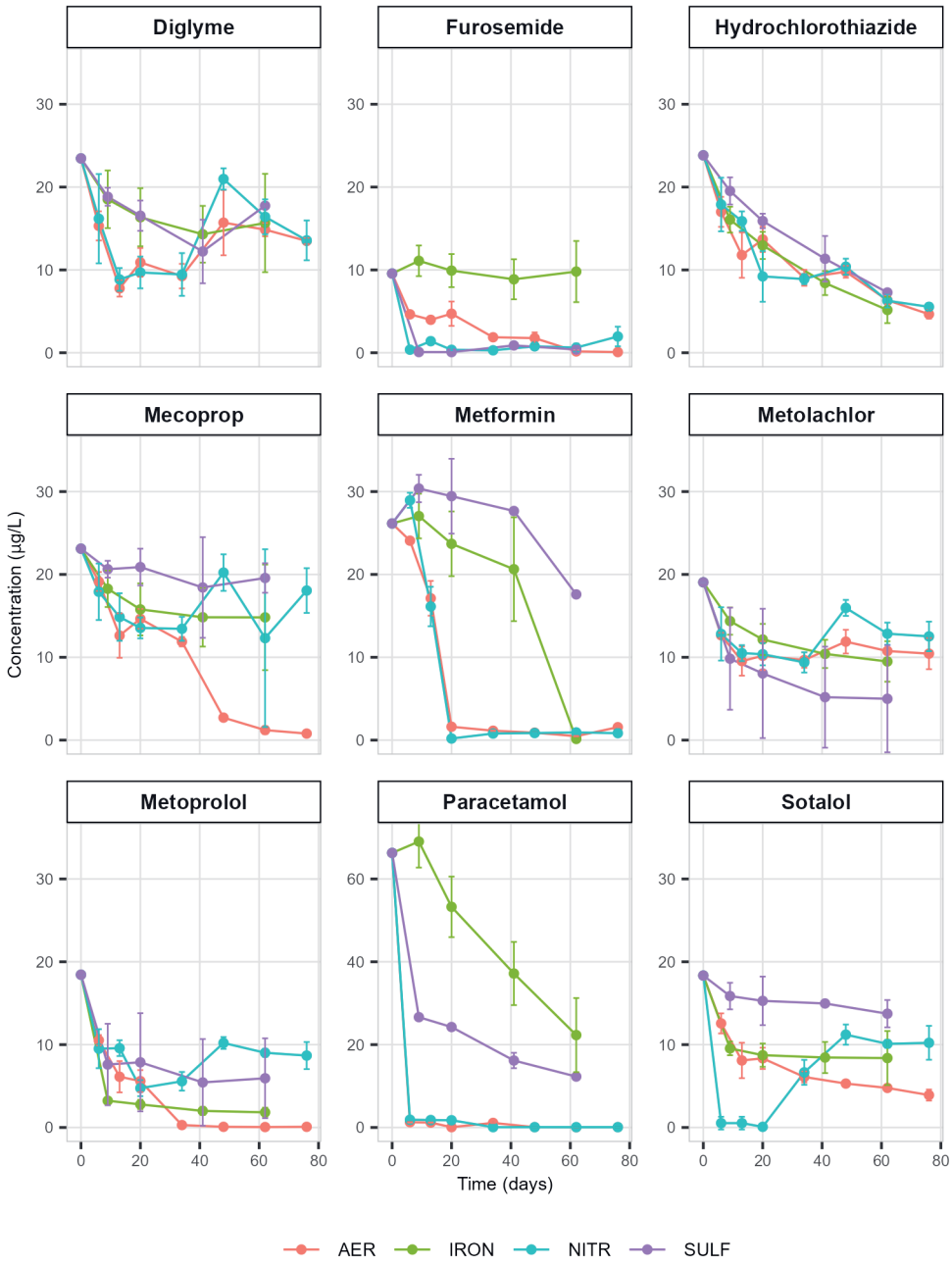

Figure S5.2 continuation. Biodegradation curves with ditch inoculum under four redox conditions.

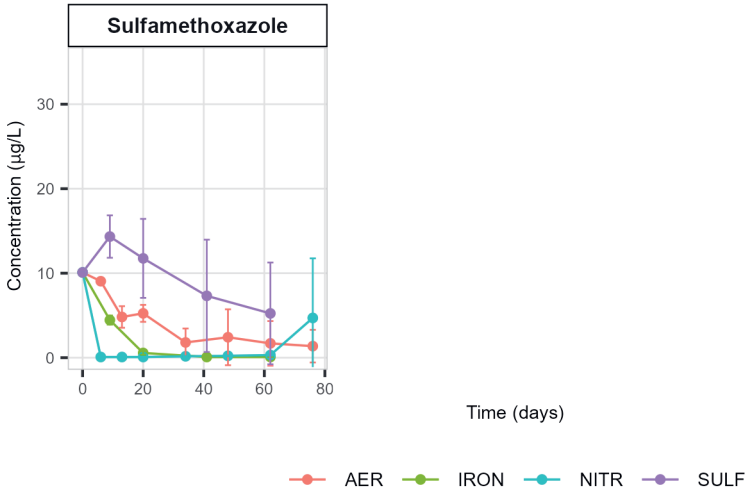

Figure S5.2 continuation. Biodegradation curves with ditch inoculum under four redox conditions.

Supplementary script 5.1

```
library(patRoon)

# -------------------------
# initialization
# -------------------------

workPath <- "*workpath diretory*"
setwd(workPath)

# Load analysis table
anaInfoPos <- read.csv("*sampleList*-pos.csv")
anaInfoNeg <- read.csv("*sampleList*-neg.csv")

# -------------------------
# features
# -------------------------

# Find all features
fListPos <- findFeatures(anaInfoPos, "openms", noiseThrInt = 1000,
chromSNR = 5, chromFWHM = 10, minFWHM = 1, maxFWHM = 20)

fListNeg <- findFeatures(anaInfoNeg, "openms", noiseThrInt = 1000,
chromSNR = 5, chromFWHM = 10, minFWHM = 1, maxFWHM = 20)

# Grouping features
fGroups_pos <- groupFeatures(fListPos, "openms", maxGroupRT = 24,
rtalign = FALSE)
fGroups_neg <- groupFeatures(fListNeg, "openms", maxGroupRT = 24,
rtalign = FALSE)

# Basic rule based filtering
fGroups_pos <- fGroupsF_pos <- filter(fGroups_pos, preAbsMinIntensity =
100, absMinIntensity = 3000, relMinReplicateAbundance = 0.6,
maxReplicateIntRSD = 0.8, blankThreshold = 5, removeBlanks = TRUE,
retentionRange = c(60, Inf), mzRange = NULL)

fGroups_neg <- fGroupsF_neg <- filter(fGroups_neg, preAbsMinIntensity =
100, absMinIntensity = 3000, relMinReplicateAbundance = 0.6,
maxReplicateIntRSD = 0.8, blankThreshold = 5, removeBlanks = TRUE,
retentionRange = c(60, Inf), mzRange = NULL)

#--------------------------------------
# Checking for adducts and isotopes
#--------------------------------------
```

```
# generate components from filtered fGroups
components_pos <- generateComponents(fGroupsF_pos, "cliquems",
ionization = "positive", ppm = 7)
components_neg <- generateComponents(fGroupsF_neg, "cliquems",
ionization = "negative", ppm = 7)

# Only keep results with adducts/isotope annotations and remove unwanted
adducts
componentsF_pos <- delete(components_pos, j = function(ct, ...)
is.na(ct$isonr) & (is.na(ct$adduct_ion) | !ct$adduct_ion %in%
c("[M+Na]+", "[M+K]+", "[M+NH4]+")))
print(componentsF_pos)

componentsF_neg <- delete(components_neg, j = function(ct, ...)
is.na(ct$isonr) & (is.na(ct$adduct_ion) | !ct$adduct_ion %in% c("[M-
H2O]-", "[M-H]-")))
print(componentsF_neg)


# Only keep components with at least one feature group also present in
the suspect screened data.
componentsF_pos <- delete(componentsF_pos, j = function(ct, ...)
!any(ct$group %in% names(fGroups_pos)))
componentsF_neg <- delete(componentsF_neg, j = function(ct, ...)
!any(ct$group %in% names(fGroups_neg)))

# Remove components with only one feature group (useless)
# 1-sized components cannot be used for annotation
componentsF_pos <- filter(componentsF_pos, size = c(2, 1E6))
componentsF_neg <- filter(componentsF_neg, size = c(2, 1E6))

# manually check/filter components
checkComponents(componentsF_pos, fGroupsF_pos, session =
"components_check_pos.yml")
componentsF_pos <- filter(componentsF_pos, checkComponentsSession =
"components_check_pos.yml")

checkComponents(componentsF_neg, fGroupsF_neg, session =
"components_check_neg.yml")
componentsF_neg <- filter(componentsF_neg, checkComponentsSession =
"components_check_neg.yml")

# to filter out unwanted adducts/isotopes
fGroups_pos <- selectIons(fGroups_pos, componentsF_pos, c("[M+H]+"))
fGroups_neg <- selectIons(fGroups_neg, componentsF_neg, c("[M-H]-"))
```

```
# Make sets and group features
fGroups <- makeSet(fGroups_pos, fGroups_neg, groupAlgo = "openms",
adducts = c("[M+H]+", "[M-H]-"))

# -------------------------
# suspect screening PCs
# -------------------------

# Load suspect lists with fragments to improve annotation, one per each
ionization method
suspListPos <- read.csv("*file directory*SpikedPCs_suspList_pos.csv",
                        stringsAsFactors = FALSE)
suspListNeg <- read.csv("*file directory*SpikedPCs_suspList_neg.csv",
                        stringsAsFactors = FALSE)

# Set onlyHits to FALSE to retain features without suspects (eg for full
NTA)
fGroups <- screenSuspects(fGroups, list(suspListPos, suspListNeg),
rtWindow = 12, mzWindow = 0.005, onlyHits = FALSE)

write.csv(screenInfo(fGroups), "Spiked&found.csv", quote = TRUE,
row.names = FALSE)
View(as.data.table(screenInfo(fGroups)))

# -------------------------
# transformation products
# -------------------------

# Load suspList of parent compounds without fragments
suspListParents <- read.csv("*file directory*suspList_forTPs).csv",
stringsAsFactors = FALSE)

# BioTransformer TP generation
TPs_BT <- TPs_BT_UF <- generateTPs("biotransformer", parents =
suspListParents, type = "env", generations = 7, calcSims = FALSE)
print(TPs_BT)

# Pubchem TP generation
TPs_PC <- TPs_PC_UF <- generateTPs("library", parents = suspListParents,
generations = 7)
print(TPs_PC)

# To combine and merge data from various algorithms to generate a
consensus
# note that biodegradation trees are lost by running the consensus
```

```
TPsCons <- consensus(TPs_BT, TPs_PC, labels = c("BT", "PC"))
print(TPsCons)

TPsCons <- filter(TPsCons, removeParentIsomers = TRUE)

# to remove TPs that may be assigned wrongly (unspecific assignment)
because the molecules are small
TPsCons <- delete(TPsCons, j = function(tab, par)
{
  parNM <- parents(TPsCons)[match(par, name)]$neutralMass # parent
neutral mass
  # remove if high generation (>1) and mass is <40% of that of the
parent
  # generation 1 TPs are always kept and the rest only if their mass is
sufficiently high (>=40%)
  return(tab$generation > 1 & (tab$neutralMass / parNM) < 0.4)
})
print(TPsCons)

# Screen TPs
suspListTPs <- convertToSuspects(TPsCons, includeParents = FALSE)
write.csv(suspListTPs, "SuspectListOfTPs.csv", quote = TRUE, row.names =
FALSE)

# Amend with TP screening
fGroups <- screenSuspects(fGroups, suspListTPs, rtWindow = 12, mzWindow
= 0.005, onlyHits = TRUE, amend = TRUE)

# -------------------------
# annotation
# -------------------------

# Retrieve MS peak lists
avgMSListParams <- getDefAvgPListParams(clusterMzWindow = 0.005)
mslists <- generateMSPeakLists(fGroups, "mzr", maxMSRtWindow = 5,
precursorMzWindow = 0.5, avgFeatParams = avgMSListParams,
avgFGroupParams = avgMSListParams)

# Rule based filtering of MS peak lists
mslists <- filter(mslists, absMSIntThr = NULL, absMSMSIntThr = NULL,
relMSIntThr = NULL, relMSMSIntThr = 0.05, topMSPeaks = NULL,
topMSMSPeaks = 25)

# Calculate formula candidates
```

```
formulas <- generateFormulas(fGroups, mslists, "genform", relMzDev = 5,
elements = "CHNOPSClFIBr", oc = FALSE, calculateFeatures = TRUE,
featThresholdAnn = 0.75, setThresholdAnn = 0)

convertToMFDB(TPsCons, "TP-database.csv", includeParents = TRUE)

# Calculate compound structure candidates
compounds <- generateCompounds(fGroups, mslists, "metfrag", dbRelMzDev =
5, fragRelMzDev = 5, fragAbsMzDev = 0.002, database = "csv", extraOpts =
list(LocalDatabasePath = "TP-database.csv"), maxCandidatesToStop = 2500,
setThresholdAnn = 0)
compounds <- addFormulaScoring(compounds, formulas, updateScore = TRUE)

# Annotate suspects
fGroups <- annotateSuspects(fGroups, formulas = formulas, compounds =
compounds, MSPeakLists = mslists, IDFile = "idlevelrules.yml")

# -------------------------
# Filters to remove low ID
# -------------------------

fGroups_lowID <- filter(fGroups, maxLevel = 4, negate = TRUE)
fGroups_lowID <- filter(fGroups_lowID, onlyHits = TRUE)
# fGroups lowID should now contain all features with L5
write.csv(screenInfo(fGroups_lowID), "OMPs_lowID.csv", quote = TRUE,
row.names = FALSE)

# if visualization of low ID fGroups is needed, enable the following ---
------
# lowID_table <- as.data.frame(fGroups_lowID, collapseSuspects = NULL)
# write.csv(lowID_table, "DataFrame_lowID.csv", quote = TRUE, row.names
= FALSE)

# to proceed with L4 or better
fGroups <- filter(fGroups, maxLevel = 4, onlyHits = TRUE)
print(fGroups)

# -------------------------
# Parent and TP linkage
# -------------------------

componentsTP <- generateComponents(fGroups[, suspects =
suspListParents$name], "tp", fGroupsTPs = fGroups, TPs = TPsCons,
MSPeakLists = mslists, formulas = formulas, compounds = compounds)
```

```
componentsTP <- filter(componentsTP, retDirMatch = TRUE, minSpecSim =
NULL, minSpecSimPrec = NULL, minSpecSimBoth = NULL, minFragMatches =
NULL, minNLMatches = NULL)

checkFeatures(fGroups)
fGroups_clean <- filter(fGroups, checkFeaturesSession = TRUE)

# Only keep linked feature groups
fGroups_linked <- fGroups_clean[results = componentsTP]

# ------------------------
# Filters for plotting
# ------------------------
# if the same suspect is assigned to multiple fGroups, select the one
with the best ID level

fGroupsToPlot_bestID_clean <- filter(fGroups_clean, selectHitsBy =
"level", onlyHits = TRUE)
print(fGroupsToPlot_bestID_clean)

# -------------------------
# reporting
# -------------------------

options(future.globals.maxSize = 2e9)

# COMPLETE REPORT (uncleaned fGroups)
report(fGroups, MSPeakLists = mslists, formulas = formulas, compounds =
compounds, components = componentsTP, TPs = TPsCons, settingsFile =
"report.yml", openReport = TRUE)

# Report based on the filters for plotting and cleaned fGroups (double-
checked)
checkFeatures(fGroupsToPlot_bestID_clean,
"fGroupsToPlot_bestID_clean.yml")
fGroupsToPlot_bestID_clean <- filter(fGroupsToPlot_bestID_clean,
checkFeaturesSession = "fGroupsToPlot_bestID_clean.yml")

report(fGroupsToPlot_bestID_clean, MSPeakLists = mslists, formulas =
formulas, compounds = compounds, components = componentsTP, TPs =
TPsCons, settingsFile = "report_bestID.yml", openReport = TRUE, parallel
= FALSE)

# To produce useful csv
bestID_dataframe_clean <- as.data.frame(fGroupsToPlot_bestID_clean,
collapseSuspects = NULL) # contains useful info, including SMILES
```

```
write.csv(bestID_dataframe_clean,
"DataFrame_fGroupsToPlotBestID_clean.csv", quote = TRUE, row.names =
FALSE)

# to see TP generation and transformation rules(use the SMILES or
InChIKey instead of the name to find the corresponding TPs in TPs_BT or
TPs_PC)
View(as.data.table(TPs_BT))
View(as.data.table(TPs_PC))

# to get the molecular weight from the SMILES
library(dplyr)
bestID_dataframe_clean_MW <- bestID_dataframe_clean %>%
  mutate(MW = patRoon:::babelConvert(susp_SMILES, "smi", "MW", mustWork
= TRUE))

write.csv(bestID_dataframe_clean_MW, "MW_bestID_dataFrame.csv", quote =
TRUE, row.names = FALSE)

# ------------------------------------------------------------------------
# PREDICTING TOXICITY AND CONCENTRATIONS
# ------------------------------------------------------------------------

# Toxicity ----------------------------------------------------------------

# MS2Tox is a machine learning tool for predicting ecotoxicity of
unidentified chemicals in water by nontarget LC/HRMS (tested with
toxicity on fish)
# based on high-resolution, accurate MS2 spectra

# tox in log mM
fGroups_tox_logmM <- predictTox(fGroupsToPlot_bestID_clean, concUnit =
"log mM")
fGroups_tox_logmM <- calculateTox(fGroups_tox_logmM)
toxicities(fGroups_tox_logmM)
Tox_results_logmM <- as.data.table(fGroups_tox_logmM)[!is.na(LC50),
c("group", "LC50", "LC50_types")]
write.csv(as.data.table(toxicities(fGroups_tox_logmM)),
"ToxicityPredictionsResults_logmM.csv", quote = TRUE, row.names = FALSE)

# Concentrations prediction -----------------------------------------------
# Uses MS2Quant, a machine learning model that enables prediction of
concentration from fragmentation (MS2) spectra of detected, but
unidentified chemicals
# It is a regression model that uses ionization efficiency
```

```
# ionization efficiency values are predicted from structural
fingerprints that can be computed from the SMILES notation of the
identified chemicals

anaInfoPos_calibr <- read.csv("*file directory*calibr-pos.csv",
stringsAsFactors = FALSE)
anaInfoNeg_calibr <- read.csv("*file directory*calibr-neg.csv",
stringsAsFactors = FALSE)

# Find all features
fListPos_calibr <- findFeatures(anaInfoPos_calibr, "openms", noiseThrInt
= 1000, chromSNR = 5, chromFWHM = 10, minFWHM = 1, maxFWHM = 20)

fListNeg_calibr <- findFeatures(anaInfoNeg_calibr, "openms", noiseThrInt
= 1000, chromSNR = 5, chromFWHM = 10, minFWHM = 1, maxFWHM = 20)

# Grouping features
fGroups_pos_calibr <- groupFeatures(fListPos_calibr, "openms",
maxGroupRT = 24, rtalign = FALSE)
fGroups_neg_calibr <- groupFeatures(fListNeg_calibr, "openms",
maxGroupRT = 24, rtalign = FALSE)

# Basic rule based filtering
fGroups_pos_calibr <- fGroupsF_pos_calibr <- filter(fGroups_pos_calibr,
preAbsMinIntensity = 100, absMinIntensity = 3000,
relMinReplicateAbundance = 0.6, maxReplicateIntRSD = 0.9, blankThreshold
= 5, removeBlanks = TRUE, retentionRange = c(60, Inf), mzRange = NULL)

fGroups_neg_calibr <- fGroupsF_neg_calibr <- filter(fGroups_neg_calibr,
preAbsMinIntensity = 100, absMinIntensity = 3000,
relMinReplicateAbundance = 0.6, maxReplicateIntRSD = 0.9, blankThreshold
= 5, removeBlanks = TRUE, retentionRange = c(60, Inf), mzRange = NULL)

# Make sets and group features
# fGroups_calibr <- makeSet(fGroups_pos_calibr, fGroups_neg_calibr,
groupAlgo = "openms", adducts = c("[M+H]+", "[M-H]-"))

# Screen for compounds in calibration ---------------------------------

CalibList_pos <- read.csv("*file directory*SuspListCalibr-pos.csv",
stringsAsFactors = FALSE)
CalibList_neg <- read.csv("*file directory*SuspListCalibr-neg.csv",
stringsAsFactors = FALSE)

# screen separately for + and -
```

```
fGroups_calibr_pos <- screenSuspects(fGroups_pos_calibr, CalibList_pos,
rtWindow = 12, mzWindow = 0.005, adduct = "[M+H]+", onlyHits = TRUE)

fGroups_calibr_neg <- screenSuspects(fGroups_neg_calibr, CalibList_neg,
rtWindow = 12, mzWindow = 0.005, adduct = "[M-H]-", onlyHits = TRUE)

write.csv(screenInfo(fGroups_calibr_pos), "Calibrantsfound_pos.csv",
quote = TRUE, row.names = FALSE)
write.csv(screenInfo(fGroups_calibr_neg), "Calibrantsfound_neg.csv",
quote = TRUE, row.names = FALSE)
View(as.data.table(screenInfo(fGroups_calibr_pos)))
View(as.data.table(screenInfo(fGroups_calibr_neg)))

concs_pos <- read.csv("*file directory*CalibrantsConcs_pos.csv",
stringsAsFactors = FALSE)
concs_neg <- read.csv("*file directory*CalibrantsConcs_neg.csv",
stringsAsFactors = FALSE)

# POS CALIBRANTS ------------------------------------------------------
calibrants_pos <- getQuantCalibFromScreening(fGroups_calibr_pos,
concs_pos, areas = FALSE)

# Optimization - reiterative
calibrants_pos <- calibrants_pos[intensity > 0] # removes calibrants
with no peak intensity

upperConcs_pos <- c(
    Antipyrine = 4.000,
    Bezafibrate = 12.800,
    Chloridazon = 4.000,
    Gabapentin = 4.000,
    Isoproturon = 12.800,
    Lamotrigine = 12.800,
    "N4-Acetylsulfamethoxazole" = 4.000,
    "O-Desmethylvenlafaxine" = 4.000,
    Pyridafol = 12.800,
    Setraline = 12.800,
    Sulfamethazine = 12.800,
    Sumatriptan = 4.000,
    Terbutryn = 8.000,
    Tramadol = 8.000,
    "Venlafaxine HCl" = 12.800
)
lowerConcs_pos <- c(
  Antipyrine = 0.031,
  Chloridazon = 0.1,
```

```
  "O-Desmethylvenlafaxine" = 0.250
)

calibrants_pos <- calibrants_pos[
  is.na(upperConcs_pos[name]) | conc <= upperConcs_pos[name] &
    (is.na(lowerConcs_pos[name]) | conc >= lowerConcs_pos[name])
]

calibrants_pos[, c("RSQ", "residual") := {
  model <- summary(lm(intensity ~ conc, weights = 1/conc))
  slope <- model$coefficients[2]; intercept <- model$coefficients[1]
  list(
    model$r.squared,
    (intensity - (slope * conc + intercept)) / intensity * 100
  )
}, by = "name"]
calibrants_pos <- calibrants_pos[abs(residual) <= 20] # omit outliers.

calibrants_pos[, N := .N, by = "name"]
calibrants_pos <- calibrants_pos[N >= 5] # only keep compounds with at
least five concentration points.
calibrants_pos <- calibrants_pos[RSQ >= 0.9] # ensure all the R2 for a
target is at least 0.9.

calibrants_pos <- calibrants_pos[!name %in% c("Fluxapyroxad",
"Thiacloprid", "Bezafibrate")] # removes unreliable calibrants.

# NEG CALIBRANTS ------------------------------------------------------
calibrants_neg <- getQuantCalibFromScreening(fGroups_calibr_neg,
concs_neg, areas = FALSE) # 946 obs of 5 variables

# Optimization - reiterative
calibrants_neg <- calibrants_neg[intensity > 0]

upperConcs_neg <- c(
  Bentazon = 12.800,
  "Bisphenol A" = 12.800,
  Hydrochlorothiazide = 12.800,
  Pyridafol = 8.000
)

lowerConcs_neg <- c(
  Pyridafol = 0.100
)

calibrants_neg <- calibrants_neg[
```

```
  is.na(upperConcs_neg[name]) | conc <= upperConcs_neg[name] &
    (is.na(lowerConcs_neg[name]) | conc >= lowerConcs_neg[name])
]

calibrants_neg[, c("RSQ", "residual") := {
  model <- summary(lm(intensity ~ conc, weights = 1/conc))
  slope <- model$coefficients[2]; intercept <- model$coefficients[1]
  list(
    model$r.squared,
    (intensity - (slope * conc + intercept)) / intensity * 100
  )
}, by = "name"]
calibrants_neg <- calibrants_neg[abs(residual) <= 20] # omit outliers.

calibrants_neg[, N := .N, by = "name"]
calibrants_neg <- calibrants_neg[N >= 5] # only keep compounds with at
least five concentration points.
calibrants_neg <- calibrants_neg[RSQ >= 0.88]

#---------------------
eluent <- data.frame(
  time = c(0, 360, 576, 600), # in seconds
  B = c(0, 100, 100, 0) # percentage of eluent B
)
plot(eluent, type = "l")

checkFeatures(fGroupsToPlot_bestID_clean,
"fGroupsToPlot_bestID_clean.yml")
fGroupsToPlot_bestID_clean <-
patRoon::filter(fGroupsToPlot_bestID_clean, checkFeaturesSession =
"fGroupsToPlot_bestID_clean.yml")
# I removed the fGroups with problems in SMILES due to hypervalence
(M302_R325_1648 and M309_R335_1703)

# Keeping only valid SMILES ---------------------

# Convert the feature group object to a data frame
# Extract screenInfo data frame
screen_info <- screenInfo(fGroupsToPlot_bestID_clean)

# Check SMILES column name
colnames(screen_info)

# Keep only those entries with non-null parse.smiles()
screen_info$valid_SMILES <- sapply(screen_info$SMILES, function(smi) {
  if (is.na(smi) || smi == "") return(FALSE)
```

```
  mol <- tryCatch(parse.smiles(smi)[[1]], error = function(e) NULL)
  !is.null(mol)
})

#------------------------------------------------------------------------
# MODEL
#------------------------------------------------------------------------

# Calculate concentrations for suspect hits.
fGroupsSuspConc <- predictRespFactors(
  fGroupsToPlot_bestID_clean, # filtered and cleaned fGroups from
experimental samples without hypervalence SMILES
  calibrants = list(calibrants_pos, calibrants_neg), eluent = eluent,
  organicModifier = "MeOH",
  pHAq = 3.41 # pH of the aqueous part of the mobile phase - ULC/MS
water with 0.05% acetic acid
)

# check with graphs if some compounds are negatively affecting the model
(bad R2 and residuals) and remove them, then rerun predictResFactors
with cleaned table
fGroupsSuspConc@setObjects[[1]]@MS2QuantMeta
fGroupsSuspConc@setObjects[[2]]@MS2QuantMeta

fGroupsSuspConc <- calculateConcs(fGroupsSuspConc, areas = FALSE)

Conc_results <-  as.data.table(fGroupsSuspConc, collapseSuspects = NULL)
# keeps multiple suspects assigned to same fGroups separated
write.csv(Conc_results, "ConcentrationPredictionsResults.csv", quote =
TRUE, row.names = FALSE)
```

Supplementary Excel 5

Supplementary Excel (SE) tables can be downloaded from:
https://doi.org/10.1016/j.jhazmat.2026.141775

Chapter 6

General discussion

6.1 Introduction

Climate change and population growth are major drivers for freshwater scarcity, intensifying pressure on natural water resources. Water reuse has therefore become essential for ensuring a sustainable and sufficient freshwater supply to a growing population with increasing living standards. Both the quantity and quality of available water determine its usability, and the subsurface environment offers solutions to address both aspects. It provides natural storage capacity for excess water during wet periods and serves as a natural treatment system that may improve water quality during infiltration and storage. However, reusable water sources often contain organic micropollutants (OMPs), which can enter the subsurface and potentially threaten water safety. OMPs in the subsurface may be transported to deeper aquifers or abstraction wells, or they might undergo (bio)degradation, resulting in the formation of transformation products (TPs). The fate of OMPs depends on both intrinsic properties (e.g., mobility, persistence, bioavailability) and environmental factors (e.g., redox conditions, soil composition, microbial community). Understanding the interplay among these factors is essential for optimizing safe and sustainable water reuse and for informing regulatory updates.

This thesis aimed at improving the understanding of OMP fate and TP formation processes in subsurface water systems. We adopted a comprehensive approach that combined field investigations and laboratory experiments. Field studies provided a realistic overview of OMP occurrence and transformation under natural conditions, while laboratory experiments enabled controlled investigation of the environmental parameters influencing biodegradation and TP formation. Two types of subsurface water reuse systems were investigated: a subsurface irrigation (SSI) system reusing wastewater treatment plant (WWTP) effluent for below-ground crop irrigation, and a managed aquifer recharge (MAR) system with infiltration ponds reusing surface water through infiltration for drinking water production. This integrated approach provided both empirical field and fundamental insights, contributing to improving our ability to predict OMP fate during water reuse in the subsurface.

Each chapter of this thesis contributed to the knowledge gaps presented in Chapter 1 (Figure 6.1). In particular, Chapters 2 and 3 expanded knowledge on the occurrence of OMPs, including TPs, in water reuse systems, with Chapter 3 also evaluating the treatment efficiency of the MAR system. The OMP fate, including transport and transformation, was investigated in the field (Chapters 2 and 3) and under controlled laboratory conditions (Chapters 4 and 5). Chapter 4 focused on the influence of microbial diversity on OMP biodegradation and TP formation under aerobic and nitrate-reducing conditions, while Chapter 5 explored the effects of a broader range of redox conditions (aerobic, nitrate-, iron-

and sulfate-reducing) and inoculum origin on these processes. Finally, here in Chapter 7, we integrate and discuss the overall outcomes of this work and provide perspectives for future research and application.

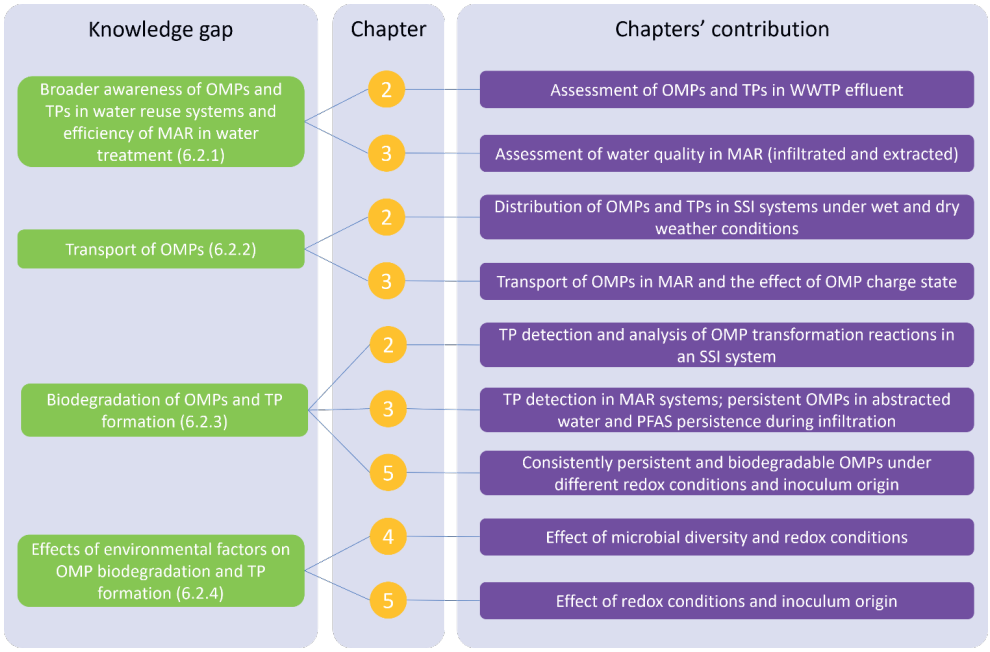

Figure 6.1. Overview of the contribution of each chapter to the knowledge gaps. The numbers in brackets refer to the section of the Research outcomes (Section 6.2) where the corresponding topic is discussed.

6.2 Research outcomes

6.2.1 Broader awareness of OMPs and TPs in water reuse systems and efficiency of MAR in water treatment

A deeper understanding of the chemical composition of reused water is essential for assessing its suitability and safety for reuse. In our research, two subsurface water reuse systems were investigated, and the reused water sources were comprehensively characterized through target and non-target analytical approaches.

While water authorities and drinking water companies monitor a wide range of OMPs through target analysis, our results show that many OMPs remain undetected with this approach. For instance, in Chapter 3, 371 OMPs were included in the target list, yet only 31 (excluding PFAS) were detected in the MAR system. In contrast, NTA and TP suspect screening (SS) revealed 50% more OMPs, including numerous (suspect) TPs that were not covered by the target list. This suggests that standard monitoring approaches underestimate the variety of OMPs in reused water.

In Chapter 2, we studied an SSI system in which municipal WWTP effluent was used for below-ground irrigation of a crop field. Previous research on this setup reported 57 compounds in the reused effluent through target analysis (Narain-Ford et al., 2022), while our SS approach detected, on average, 75 OMPs, of which the majority were TPs (59) (Figure 6.2). Although this effluent was reused for SSI in our case study, generally, effluents are discharged in ditches or into surface water bodies, which negatively affects surface water quality, particularly during dry seasons when WWTP effluents make up most of the water in the ditches.

The surface water reused in the MAR system studied in Chapter 3 was impacted by the release of effluents from five upstream WWTPs and by pesticide runoff from agricultural areas along the waterway. This was confirmed by target analysis, which highlighted high concentrations of pharmaceuticals, artificial sweeteners and pesticides, while NTA and SS further revealed the occurrence of many TPs in the infiltrating water (Figure 6.2). These results demonstrate that many OMPs currently present in reused water remain outside monitoring programs and are therefore inadvertently released in the environment.

Despite the chemical variety in infiltrating water, the MAR system proved to be an efficient treatment step to improve water quality, achieving an OMP removal efficiency of approximately 60% and reducing the overall number and concentration of OMPs in the abstracted water (excluding PFAS, Chapter 3). These results are in line with previous studies (Muschket et al., 2024; Specker et al., 2025). OMP removal in MAR was attributed to a combination of different processes in the subsurface, including dilution with naturally occurring groundwater, sorption, and (bio)degradation. However, persistent and mobile compounds, such as PFAS, were not efficiently removed in the MAR system. PFAS concentration remained largely stable along the infiltration path to the well capturing most of the infiltrated water, with short-chain PFAS (e.g., TFA – trifluoroacetic acid) reaching concentrations in the order of µg/L. Acceptable PFAS concentrations in the finished drinking water were likely achieved primarily through dilution with extracted water from other wells. Overall, the presence of residual OMPs in the abstracted water reflects the interplay between OMP-specific properties and site-specific environmental factors influencing their fate in the subsurface.

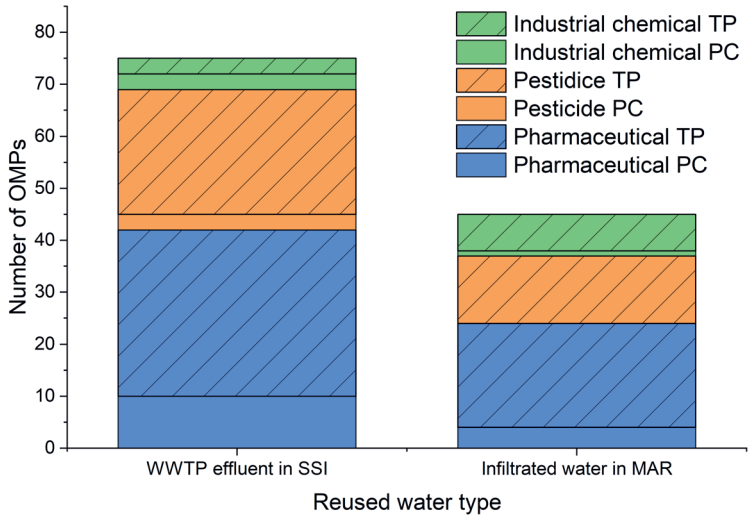

Figure 6.2. Chemical composition of reused water through suspect screening analysis.

6.2.2 Transport of OMPs

Transport of OMPs in subsurface water reuse systems is affected by both OMP-specific properties, like hydrophobicity and charge state, and site-specific environmental factors, including recharge dynamics, soil composition, and subsurface hydrology. Depending on molecular structure and electron distribution, OMPs can be polarized or exist in ionized forms (Reemtsma et al., 2016). In the subsurface, soil particles and mineral surfaces are typically negatively charged, thus electrostatic interactions with OMPs influence their sorption. Moreover, variations in soil composition, permeability, and organic matter content with soil depth can steer OMP movement in preferential flow directions (Mumberg et al., 2024).

Although not a perfect descriptor, the distribution coefficient (D_{ow}) is widely used as a proxy for OMP mobility in the environment (Sigmund et al., 2022). OMPs with high log D_{ow} values (>4) generally exhibit low water mobility and a stronger tendency for soil sorption, whereas those with lower log D_{ow} values are mobile (log D_{ow}<3) and very mobile (log D_{ow}<0). However, our study results confirmed that log D_{ow} alone is insufficient to describe OMP mobility in soil, consistent with previous studies suggesting the use of log K_{oc} or its optimized version for ionizable compounds (Sigmund et al., 2022). Yet, log K_{oc} values are difficult to measure experimentally, scarce in literature, and show high variability depending on the experimental conditions under which they are determined (Liu et al., 2025).

Our findings showed that including charge state provides a better description than log D_{ow} alone for OMP mobility in subsurface water systems (Chapter 3). In Figure 6.3, we combined data from both the SSI system (Chapter 2) and the MAR system (Chapter 3) to illustrate how

log D_{ow} and charge state together describe OMP transport in these two reuse systems. The figure reports OMPs detected via target and non-target analyses in the reused waters (WWTP effluent and infiltrated water) and the deepest points in the field, 2.3 m for both wells close to and between pipes of the SSI system, and 24-25 m depth in the MAR system (abstraction wells 1 and 2). The data show that the number of detected OMPs decreased gradually: more OMPs were detected in the infiltrating WWTP effluent or surface water, while fewer were found in the deepest points of the SSI system and MAR systems, indicating an overall removal of OMPs during infiltration and subsurface passage. Most OMPs detected in both systems had moderate mobility (log D_{ow}<4), suggesting that more hydrophobic OMPs were already removed during wastewater treatment, surface water transport, or the initial infiltration phase when water percolates through the loamy bottom of the infiltration pond (Honti et al., 2023; Monteiro and Boxall, 2010).

Although the overall log D_{ow} distribution was comparable across sampled points within each system, the median log D_{ow} decreased with depth, indicating that more mobile compounds travelled farther and reached deeper layers of the subsurface. Furthermore, negatively charged OMPs were more likely to reach the deepest points, where their proportion increased compared to the infiltrating water, while positively charged and neutral OMPs were gradually removed. This pattern was particularly visible in the MAR system (Figure 6.3 B), likely due to the greater depth and travel distance from the infiltration point. In the SSI system, the short vertical infiltration distance, prevalence of horizontal flow, and variable irrigation events limited travel times and thus OMP attenuation, whereas in the MAR system, longer residence times and deeper flow paths promoted more extensive electrostatic interactions and sorption along the flow path.

The mobility of OMPs in the subsurface, in fact, is not determined only by the OMP characteristics and sorption affinity. Environmental factors, including the heterogeneity of the subsurface conditions and hydrological dynamics, also play a crucial role in controlling OMP transport (Mumberg et al., 2024). The movement of water, and thus of dissolved OMPs, depends on recharge events (e.g., precipitation, irrigation, or infiltration), the presence of pumping wells that induce advective flow, natural groundwater flow, and capillary rise (particularly during dry seasons) (Tang et al., 2023a; Tang and van der Zee, 2021). For example, Figure 6.3 shows that approximately half of the OMPs detected in the WWTP effluent were detected in the deepest monitoring well close to the infiltration pipe, while only about a quarter were detected in the well located between pipes. The higher number of OMPs deep and close to the infiltration pipe, compared to in between pipes, may reflect localized vertical percolation below the pipes during irrigation events. Although the overall flow in the SSI field is predominantly horizontal towards the nearby ditch, such

vertical pulses may enhance downward transport through the unsaturated zone. In contrast, the zone in between pipes may experience longer residence times and greater interactions with soil particles, promoting OMP removal and leading to fewer detections.

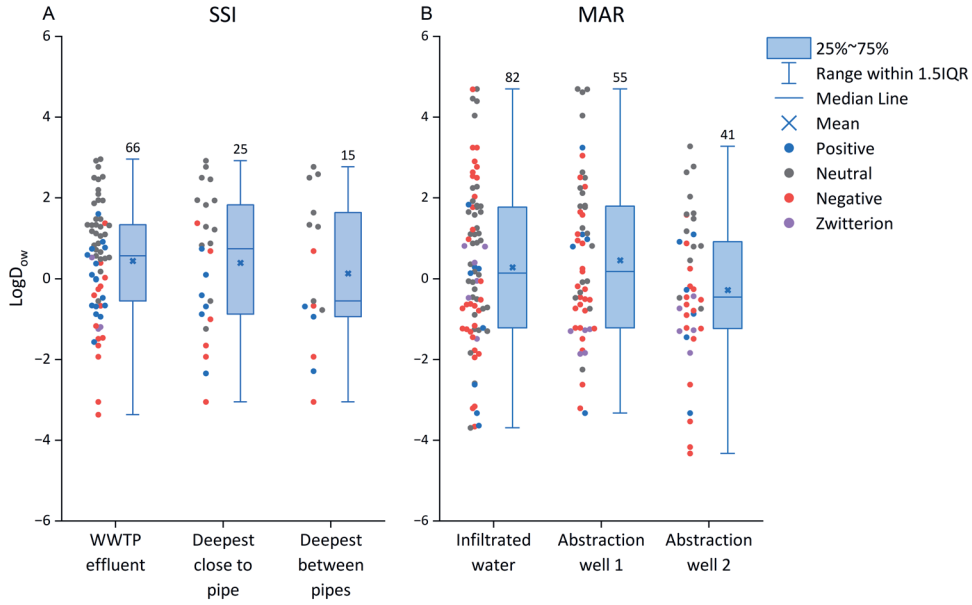

Figure 6.3. Distribution of log D_{ow} values for OMPs detected in the reused water and deepest sampling points in (A) the subsurface irrigation (SSI) and (B) managed aquifer recharge (MAR) systems. Data points are colored according to their charge state, and the numbers above the boxplots indicate the number of data points per location. WWTP = wastewater treatment plant; IQR = interquartile range. Outliers (n=3) have been removed.

Moreover, to be transported along the water flow over long distances, OMPs must be both mobile and persistent (Albergamo et al., 2019; Hillebrand et al., 2015; Mumberg et al., 2024). In Chapter 3, we observed that PFAS concentrations remained largely stable along the infiltration path in the MAR system, especially shorter-chain PFAS, confirming their persistent and mobile nature. Understanding which OMPs are capable of migrating to deeper zones is essential for evaluating the risk of groundwater contamination and for defining monitoring strategies in water reuse systems.

Beyond hydrological and physicochemical factors, biodegradation processes also influence the apparent transport of OMPs in the subsurface. As OMPs are transformed during infiltration, their concentrations decrease while new OMPs (i.e., TPs) with different mobility and persistence may be formed (Filter et al., 2021; Hillebrand et al., 2015). Thus, OMP transport is further complicated by biotransformation, which is discussed in the following section.

6.2.3 Biodegradation of OMPs and TP formation

Biodegradation has long been recognized as one of the main removal mechanisms of OMPs in the environment (Roberts et al., 1980). However, for many years, biodegradation was primarily interpreted as the disappearance of specific OMPs, often assuming mineralization, while transformation into TPs was largely overlooked (Celiz et al., 2009). More recently, the development of advanced analytical techniques has shifted attention toward TPs, revealing their widespread occurrence and raising concerns about the implications of their presence for environmental and human health (Escher and Fenner, 2011; Zahn et al., 2024). Many TPs are unknown and difficult to detect due to their low concentrations, diverse physicochemical properties, and the lack of reference standards. Non-targeted analytical approaches have been implemented to avoid dependency on reference standards for TP detection, yet challenges remain, especially for highly polar or unstable compounds (to be discussed further in Section 6.3.1) (Schymanski et al., 2014b; Zahn et al., 2024).

While it is generally assumed that TPs are more mobile than their PC, this is not always the case. Moreover, certain biotransformation pathways may lead to TPs that are more toxic and more persistent than their PC (Fenner et al., 2013; Zahn et al., 2024). The biotransformation pathways occurring in the subsurface strongly depend on *in situ* environmental parameters, including redox conditions, microbial community structure, and available nutrients (Filter et al., 2021). This complexity hampers the prediction of OMP fate and highlights the need to better understand how environmental factors influence the formation of TPs. A better understanding of the interplay between environmental conditions and TP formation is essential to predict OMP fate and assess the efficacy of nature-based treatments.

In our study, a variety of biotransformation reactions were observed in both field (Chapter 2) and laboratory investigations (Chapters 4 and 5), representing the diversity of biodegradation pathways and TPs that are likely to occur in the subsurface. In general, aerobic conditions and oxidative reactions were the most frequent and fastest pathways, producing the majority of TPs, both in the laboratory and in the field. Nonetheless, distinct biodegradation pathways were also observed under nitrate-, iron-, and sulfate-reducing conditions in our laboratory studies (Chapters 4 and 5), confirming that OMP biodegradation and resulting TP formation are highly dependent on environmental conditions. These findings underline the importance of considering site-specific conditions when modelling OMP degradation pathways and TP formation in the subsurface with prediction tools.

Our results showed that, overall, biodegradation tends to form TPs that are more mobile, more biodegradable, and less toxic than their PC, suggesting that biodegradation can support OMP treatment. In the SSI system (Chapter 2), mobility assessment revealed that TPs detected in the field were generally more mobile than the PCs, and that most OMPs

detected between infiltration pipes were highly mobile TPs capable of travelling longer distances. This observation highlights the importance of monitoring TPs in water reuse systems, as they might reach deeper groundwater layers and potentially affect the quality of the abstracted water.

In the laboratory experiments (Chapters 4 and 5), we further evaluated TP persistence and toxicity using prediction tools (Biowin3 and MS2Tox) (Peets et al., 2022; US EPA, 2025). The combined analysis (Figure 6.4) illustrates the relationship between biodegradability, mobility, and toxicity across all TPs formed under varying microbial diversity and redox conditions. The majority of TPs were more mobile, less toxic, and more biodegradable than their PC counterparts. This outcome suggests that, in most cases, biodegradation reduces the overall environmental toxicity of OMPs and that the TPs formed may be further degraded, potentially achieving mineralization. However, a few TPs in Figure 6.4 deviate from this trend. For example, a paracetamol-TP (blue dot in the bottom-left quadrant) showed lower biodegradability than its PC, while a 2,4-dichlorophenoxiacetic acid and a metoprolol TP (red dots in the bottom-right quadrant) were both less biodegradable and more toxic. Most of the more toxic TPs were also less biodegradable, implying potential persistence and accumulation in the environment. Such cases highlight that biodegradation does not always lead to detoxification.

Our findings demonstrate that biodegradation is generally a beneficial process for OMP attenuation, but its outcomes depend strongly on the specific compounds and environmental conditions. The integrated assessment of biodegradability, mobility, and toxicity provides a more complete picture of OMP fate, helping to improve risk assessment and predictive understanding of OMP fate in the environment.

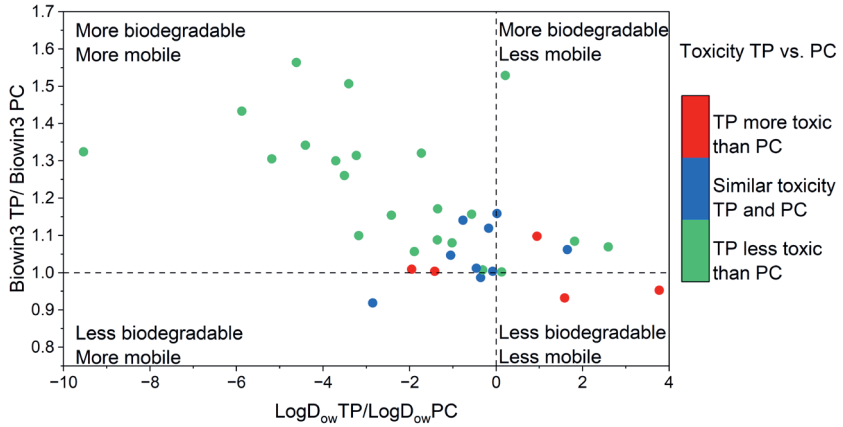

Figure 6.4. Comparison of TP and PC properties in terms of predicted hydrophobicity (LogD$_{ow}$, proxy for mobility), biodegradability (Biowin3 ratio), and toxicity (predicted LC$_{50}$s differences with MS2Tox). Color indicates the toxicity of TPs relative to PCs, with color classes representing two-fold differences. Dashed lines mark the threshold for equal mobility (x = 0) and biodegradability (y = 1).

6.2.4 Effects of environmental factors on OMP biodegradation and TP formation

While biodegradation was shown to generally yield more mobile, more biodegradable, and less toxic TPs, the extent and pathway of biodegradation processes strongly depended on environmental conditions and microbial community characteristics (Chapters 4 and 5). Previous studies have shown that OMP removal in subsurface systems depends on nutrient availability, retention time in the subsurface, hydrological and biogeochemical conditions, and microbial community characteristics (Filter et al., 2021; Greskowiak et al., 2017; Hellauer et al., 2019; Mumberg et al., 2024). Redox conditions, in particular, have been recognized as key controllers of OMP fate (Branco et al., 2023; He et al., 2018; Luo et al., 2019), but are often ambiguously reported in MAR studies (Filter et al., 2021; Ghattas et al., 2017). Remarkably, these parameters influence not only biodegradation efficiency, but also the type and properties of the TPs formed (Rutere et al., 2021; Stiegler et al., 2023). In our study, we specifically addressed the influence of redox conditions, microbial diversity, and inoculum origin on OMP biodegradation and TP formation.

Overall, redox conditions emerged as the factor with the most influence on biodegradation and TP formation in both field and laboratory investigations. Aerobic conditions generally promoted higher biodegradation performance, with higher removal efficiencies, shorter half-lives, and a greater diversity of TPs formed (Figure 6.5). Most TPs identified in Chapter 2 were produced through reactions likely to occur under aerobic conditions, such as oxidation and demethylation. However, most subsurface water reuse systems operate under anaerobic conditions (Mumberg et al., 2024). Therefore, in our laboratory experiments (Chapters 4 and 5), a range of redox conditions were tested (aerobic, nitrate-reducing, iron-reducing, and sulfate-reducing). Consistent with previous findings, aerobic systems showed greater biodegradation performance, likely due to the higher energy yields from aerobic respiration compared to anaerobic metabolic processes (Branco et al., 2023; Liu et al., 2013; Rauch-Williams et al., 2010). Nonetheless, redox-specific TPs were observed, highlighting that distinct redox conditions promote different biodegradation pathways.

Yet, aerobic transformations are not always superior in terms of producing more biodegradable TPs. Anaerobic pathways often support reductive reactions that can complement or compete with aerobic transformation. For example, as shown in Chapter 5, aerobic biodegradation of chloridazon led to the formation of chloridazon-desphenyl, a persistent and toxic TP (Zakhia et al., 2025), whereas nitrate-reducing conditions favoured a dechlorination pathway yielding a more biodegradable TP (as indicated by Biowin3 scores). Dehalogenation reactions are favoured under reducing environments, and may thus lead to less persistent TPs. However, biodegradation rates were overall slower under anaerobic

conditions; therefore, ensuring longer residence times is essential for effective OMP removal, particularly in laboratory assessments or subsurface water systems with short hydraulic retention times (Barbieri et al., 2011; Filter et al., 2021; Hillebrand et al., 2015). These findings suggest that alternating redox conditions and maintaining sufficient residence time under both oxidative and reductive environments may maximize OMP removal and promote more complete biotransformation.

Microbial diversity also showed a positive association with biodegradation extent and TP formation (Figure 6.5; Chapter 4). Communities with higher diversity achieved greater OMP removal, more extensive transformation, and higher TP formation, likely due to the higher variety of microbial species and associated enzymatic pool, which favoured the likelihood of greater presence of OMP degraders and complementary metabolic interactions among species (Coll et al., 2020; Hübner et al., 2022; Lindemann et al., 2016; Posselt et al., 2020; Stravs et al., 2019). However, this effect was more pronounced beyond a certain threshold in diversity; above it, communities were able to reach similar biodegradation performance, possibly due to functional redundancy (de Souza et al., 2017; Girvan et al., 2005). This pattern is reflected in Figure 6.5, where similar numbers of PC with half-life (DT_{50}) below 120 days (i.e., non-persistent) were observed across dilutions up to 10^{-3} (medium microbial diversity), whereas strongly diluted (less diverse) communities (10^{-6}) showed markedly reduced performance. These results show the interplay between microbial diversity and redox conditions on biodegradation performance, with redox conditions exerting a stronger influence: under aerobic conditions, even lower diversity supported moderate degradation, while under nitrate-reducing conditions, loss of diversity had stronger negative effects. Thus, maintaining sufficient microbial diversity is crucial for more extensive biodegradation, especially under less favorable redox conditions.

Inoculum origin and its pre-exposure history represented an additional, though secondary, factor shaping biodegradation performance and TP formation (Branco et al., 2023; de Wilt et al., 2018; Pett-Ridge and Firestone, 2005), which is particularly relevant for assessing OMP fate and persistence during standardized tests. In Chapter 5, two natural inocula with distinct redox and chemical pre-exposure were compared. The inocula showed differences in OMP biodegradation rates as well as distinct dynamics of TP formation and sets of TPs formed. These results likely reflected differences in microbial composition and metabolic adaptation to specific redox conditions and OMP structures previously encountered (Branco et al., 2023; Hoppe-Jones et al., 2012; Poursat et al., 2019). While the effect of inoculum origin was less pronounced than that of redox or diversity, it still highlights the importance of microbial community pre-exposure history when interpreting standardized biodegradation tests or designing field- and laboratory-scale biodegradation investigations.

In summary, our study demonstrated that OMP biodegradation and TP formation in the subsurface are primarily controlled by redox conditions, and further influenced by microbial diversity and inoculum pre-exposure history. Understanding these interdependent factors is essential for optimizing the design and operation of nature-based water reuse systems to maximize OMP removal and minimize the formation of persistent or toxic TPs.

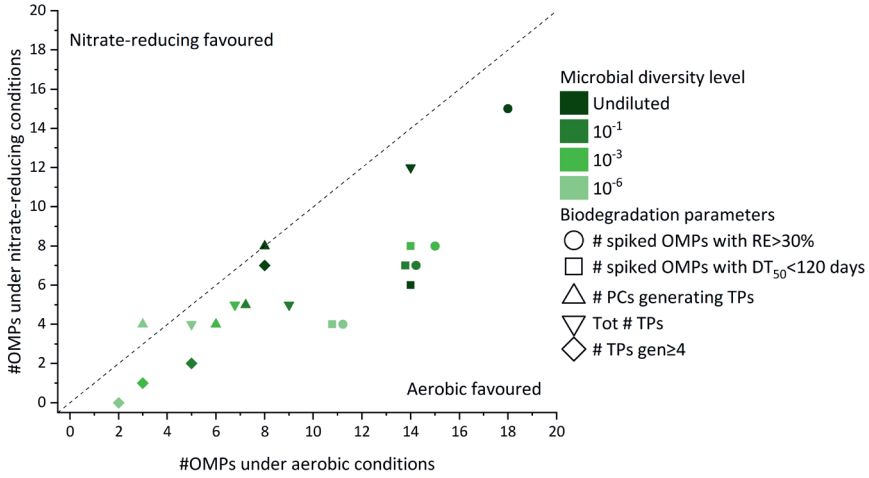

Figure 6.5. Soil biodegradation performance under varying redox (aerobic and nitrate-reducing conditions) and microbial diversity conditions. Color shades indicate the microbial diversity levels, from undiluted inocula to increasingly more diluted and less diverse communities (from 10^{-1} to 10^{-6}). The different shapes illustrate the numbers (#) of spiked OMPs, PCs, or TPs respecting the biodegradation parameters listed.

6.3 Practical implications and future perspectives

Building on the results presented in this thesis, the following section presents practical implications and highlights key directions for improving water reuse via subsurface water systems. Integrating analytical advances, a deeper understanding of environmental OMP fate and TP formation, optimized system design, and updated regulatory frameworks will contribute to safer and more sustainable water reuse (Figure 6.6).

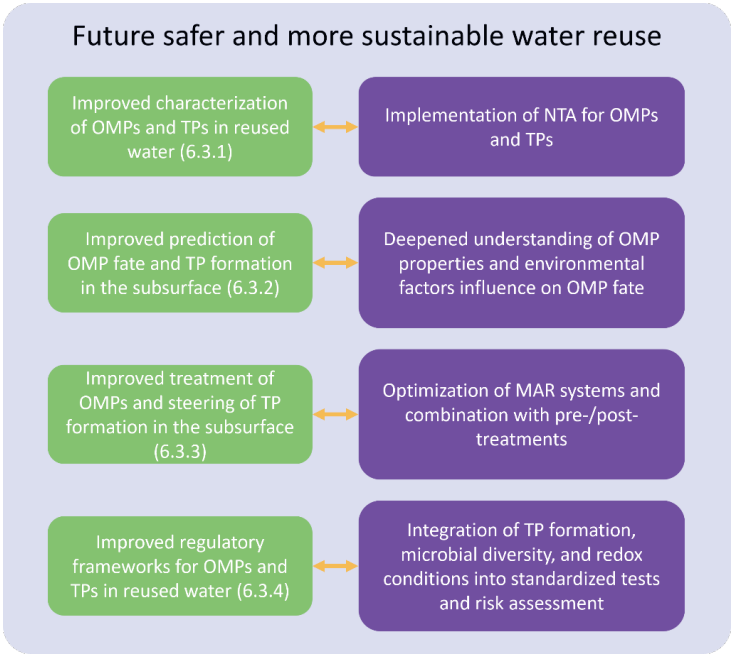

Figure 6.6. Overview of future directions and their expected contribution to improved water reuse through better understanding, treatment, and regulation for OMPs and TPs. The numbers in brackets refer to the section of the Practical implications and future perspectives (Section 6.3) where the corresponding topic is discussed.

6.3.1 Improved characterization of OMPs and TPs in reused water

Overall, our research demonstrated that a substantial portion of the OMPs present in reused water streams, such as WWTP effluents and surface water, is currently overlooked (Chapters 2 and 3). TPs represented the largest fraction of these overlooked chemicals, likely due to the multiple challenges related to their detection and identification (Brunner et al., 2019a). However, in our study, the complementary use of targeted and non-targeted analytical approaches proved useful for improving the characterization of a range of OMPs in reused waters. These findings suggest that current regulatory frameworks for water quality control and monitoring programs underestimate the actual load and diversity of OMPs in water streams. Consequently, WWTPs may unintentionally release OMPs with potential detrimental effects into the environment, which can enter water reuse systems, affecting groundwater and, subsequently, abstracted water quality (Specker et al., 2025).

A more thorough characterization of the chemical composition of reused water with targeted and non-targeted analytical approaches should be performed to evaluate the efficiency of wastewater treatment and the suitability of effluents or surface waters for reuse (Brack et al., 2019; Dulio et al., 2024; Hollender et al., 2023). NTA should be routinely implemented for this purpose, though not necessarily as frequently as targeted monitoring. Instead, the outcomes of NTA can inform and update target OMP lists to include OMPs and

TPs relevant for a given water stream. This approach would reduce analytical costs while ensuring a more comprehensive and realistic understanding of the compounds entering water reuse systems (Brack et al., 2019). Such improved knowledge would, in turn, support the refinement of regulatory frameworks by prioritizing OMPs that better represent the chemicals in reused waters (Dulio et al., 2024).

However, the effectiveness of NTA for comprehensive water quality assessment is still constrained by methodological challenges. Results can differ substantially depending on sample pre-treatment (e.g., filtration, extraction), chromatographic separation methods and eluents, as well as instrumental setup (Hale et al., 2022; Hollender et al., 2023). Additionally, data-processing workflows, including the selection of algorithms for peak integration, TP prediction, or toxicity estimation, can strongly influence which compounds are ultimately detected and reported. Since NTA generates large and complex datasets, prioritization strategies are necessary but introduce further variability across studies (Malm et al., 2024; Schulze et al., 2021). These methodological differences currently limit data comparability and reproducibility between laboratories. Therefore, harmonization of analytical methods, data interpretation workflows, and results reporting is needed to ensure that NTA results are robust, comparable, and suitable for regulatory or operational use (Hollender et al., 2023; Schymanski et al., 2015). Recent studies proposed methods to harmonize NTA application, but these are still in a development phase and will require some time before harmonization is achieved (Rich et al., 2025; Schymanski and Bolton, 2022).

Overall, the outcomes of our study underline the need for more inclusive monitoring strategies that go beyond fixed target lists and explicitly account for TPs and emerging OMPs. By coupling advanced analytical approaches (e.g., HRMS-based NTA and SS) with field-scale investigations, it becomes possible to gain a more realistic and comprehensive picture of chemical inputs into the subsurface. Future efforts should promote the harmonized application of such approaches for a more effective prioritization and regulation of OMPs based on their occurrence and predicted environmental fate.

6.3.2 Improved prediction of OMP fate and TP formation in the subsurface

In our study, we aimed to improve the understanding of the factors influencing OMP fate and TP formation in the subsurface. We demonstrated that combining intrinsic OMP properties, such as hydrophobicity (Log D_{ow}) and charge state, with site-specific hydrological and geochemical characteristics enhances the description of OMP transport (Chapters 2 and 3). However, we also highlighted the complexity of subsurface conditions, where multiple interacting factors influence OMP transport (Kodešová et al., 2015; Regnery et al., 2017; Tang et al., 2023a; Tang and van der Zee, 2021). Current transport models often oversimplify these factors (Kondor et al., 2024; Regnery et al., 2017), and should be improved to integrate

OMP-specific interactions (e.g., electrostatic sorption to soil particles) and field characteristics, such as geological composition, redox zonation, and dynamic flows.

Further progress in this direction will require improved detection, identification, and characterization of both OMPs and their TPs, as well as integrated studies that combine chemical properties with hydrological and biogeochemical parameters (Hale et al., 2022; Mumberg et al., 2024). In Chapters 2 and 3, we showed that mainly persistent and mobile compounds, including TPs, were able to reach deep subsurface layers and ultimately be abstracted with groundwater used for drinking water production. Developing more comprehensive models that couple chemical persistence, mobility, and field parameters could therefore improve the prediction of the fate of such OMPs in the subsurface, supporting early warning systems and prioritizing compounds requiring pre-removal or suitable treatment before reaching the subsurface.

For (partly) biodegradable OMPs, understanding their fate in the subsurface additionally requires considering biodegradation processes and the factors influencing them. Biotransformation depends strongly on the field conditions, like redox state, which shapes microbial community structure, diversity, and metabolic potential (Aldas-Vargas et al., 2022; Branco et al., 2023; Hübner et al., 2022; Pett-Ridge and Firestone, 2005). Our combined field and laboratory studies showed that aerobic conditions generally promote higher biodegradation performance; by analyzing TPs, we highlighted that later-generation TPs were reached within shorter timescales under aerobic than under a range of anaerobic conditions. However, aerobic biodegradation does not always yield “better” TPs; some aerobic pathways produced more persistent TPs, while under anaerobic conditions, alternative reactions led to more biodegradable and less toxic TPs from the same PC. These findings emphasize the need to expand the range of redox conditions considered in biodegradation research and predictive models, which currently focus predominantly on aerobic settings (Filter et al., 2021; Martínez-Quintela et al., 2023). The combination of field and laboratory data is essential to tailor controlled experiments based on realistic field conditions, where OMPs occur. As most subsurface water reuse systems operate under anaerobic conditions, thorough investigation of OMP biodegradation under such settings and transient redox states is crucial for realistic elucidation of their fate (Muntau et al., 2017; Pett-Ridge and Firestone, 2005). To advance this understanding, future research should more deeply explore microbial communities under different redox conditions using advanced molecular techniques, like metagenomics and metatranscriptomics (Hübner et al., 2022). Particular attention should be given to anaerobic consortia, whose metabolic potential remains largely unexplored (Ghattas et al., 2017; Martínez-Quintela et al., 2023). Moreover, bacteria are not the only players in biodegradation. Fungi, known for their ability

to degrade a wide range of OMPs (Chen et al., 2024; Olvera-Vargas et al., 2016; Sun et al., 2019), should be incorporated in future biodegradation studies, especially when investigating processes near the surface.

Our research also revealed that biodegradation and TP formation are influenced not only by redox conditions but also by microbial diversity and inoculum pre-exposure history (Chapters 4 and 5). Communities with higher diversity supported more extensive degradation performance, while pre-exposure to specific OMPs or redox environments shaped the metabolic potential of inocula. These factors are currently insufficiently contemplated in standardized persistence tests used for regulatory assessment (Coll et al., 2020; Davenport et al., 2022). Consequently, standardized tests are not so standard, as they might yield inconsistent results depending on the inoculum's characteristics and adaptation (Bertelkamp et al., 2016; Poursat et al., 2019). Future efforts should therefore aim to normalize or account for the inoculum properties, ensuring more reproducible and comparable persistence assessment.

Altogether, our findings and those from studies expanding upon them provide knowledge for improving prediction models for OMP fate and transformation. This integrated understanding can support the design of optimized nature-based water reuse systems that enhance OMP removal efficiency while minimizing the formation and persistence of undesirable TPs.

6.3.3 Improved OMP treatment and steering TP formation in the subsurface

Water reuse is increasingly necessary to cope with freshwater scarcity, population growth, and rising living standards. Subsurface water reuse systems are already often applied, and their use is expected to increase in the future to stabilize both water quality and quantity for drinking water production, among other purposes (Mumberg et al., 2024; Specker et al., 2025; Sprenger et al., 2017).

In this thesis, we assessed the transport and transformation of OMPs in reused water within two subsurface water reuse systems, an SSI and a MAR system. While previous studies evaluated the OMP removal efficiency of the SSI system and proved its efficacy for post-treatment and reuse of the WWTP effluent (Narain-Ford et al., 2022), we assessed the OMP removal efficiency of the MAR system reusing surface water for drinking water production. Consistent with previous studies, we found that soil passage achieved approximately 60% OMP removal efficiency through a combination of biodegradation, sorption, and dilution (Muschket et al., 2024; Specker et al., 2025). Moreover, our results demonstrated that biodegradation generally leads to the formation of TPs that are more biodegradable and less toxic, though often more mobile than their PCs (Figure 6.4). However, exceptions were observed: several persistent and mobile compounds, including TPs, were still detected in

the abstracted water or persisted throughout our experimental incubations. These results confirm that, while effective, MAR alone does not achieve complete OMP removal and thus further optimization and potential pre-treatment of the infiltrating water or post-treatment of the abstracted water are needed for safe water reuse.

Our findings on the processes behind OMP removal in the subsurface can inform the optimization of MAR and other subsurface water reuse systems: highly mobile and persistent OMPs may pass through the subsurface largely unchanged and thus require pre-removal or post-treatment (Chapters 2 and 3), whereas (moderately) biodegradable OMPs can be effectively biodegraded in MAR, as previously reported (Albergamo et al., 2019; Filter et al., 2021; Regnery et al., 2017), provided sufficient microbial diversity and activity are present (Chapter 4). Optimizing removal processes requires engineering subsurface conditions to support effective biodegradation and minimize the formation of undesired TPs. To achieve these purposes, our study emphasizes the importance of maintaining sufficient microbial diversity and managing redox condition dynamics (Chapters 4 and 5).

In our experiments, iron-reducing conditions in soil supported biodegradation performances comparable to those under aerobic conditions, in terms of both the number of TPs formed and the extent of biodegradation (Chapter 5). This indicates that communities in iron-reducing layers in the subsurface can contribute to OMP removal, but might require biostimulation or bioaugmentation to increase biomass levels and provide, for instance, more labile DOC. These approaches have previously been suggested for groundwater aquifers, known to have low microbial abundance and nutrient availability (Aldas-Vargas et al., 2021; Hübner et al., 2022). Bioaugmentation and/or biostimulation should be applied critically, tailoring them to the specific conditions of the site. Bioaugmentation with pre-adapted and diverse microbial communities is more effective than with specialized single-culture inocula, which may not survive under MAR conditions (Aldas-Vargas et al., 2024; Hübner et al., 2022; Lindemann et al., 2016). However, this approach requires a thorough characterization of the subsurface biogeochemical conditions. Moreover, an appropriate balance is needed to prevent an excessive microbial biomass growth and support OMP biodegradation rather than competing with it. In fact, some studies showed that OMP biodegradation is favoured in nutrient-limited systems, which support the growth of more diverse microbial communities (Alidina et al., 2014; Hoppe-Jones et al., 2012; Li et al., 2013).

We have demonstrated that redox conditions not only affect the rate of biodegradation but also influence which TPs are produced (Chapters 4 and 5). Sequential redox zones may enhance overall degradation, as the TPs formed and persistent under one condition may be further degraded under another. For example, in our analysis of chloridazon biodegradation, we observed different TPs under aerobic and nitrate-reducing conditions. Similar to previous

studies (Branco et al., 2023; Zakhia et al., 2025), the TP chloridazon-desphenyl persisted under aerobic conditions, but it may be further transformed under anaerobic ones, which support dechlorination. Thus, the continuation of the chloridazon pathway could proceed further towards mineralization under sequential redox conditions (Figure 6.7). Engineering sequential redox zones and optimizing retention time of OMPs within each zone may support more complete biodegradation and promote the formation of more biodegradable TPs (Mumberg et al., 2024; Regnery et al., 2013). Since natural subsurface systems have a layered redox structure, this can be used to improve OMP biodegradation. For instance, electron acceptors can be provided where lacking or conserved for OMP degradation rather than DOC consumption by reducing the DOC content of the infiltrated water (Hübner et al., 2022). An applied example of MAR optimization is the sequential managed aquifer recharge technology (SMART), which alternates anoxic and oxic infiltration phases under carbon-limited conditions, with an aeration step in between (Hübner et al., 2022; Regnery et al., 2016). This approach resulted in modifications to the microbial community and enhanced metabolic capacity, resulting in the transformation of more recalcitrant OMPs (Regnery et al., 2017). Future efforts should further study the possible optimization of MAR operating conditions as well as its combination with post-treatment processes, like activated carbon adsorption for the removal of PFAS from the abstracted water (Page et al., 2019; Piai et al., 2019; Sadia et al., 2024).

By understanding and managing key factors such as redox conditions, microbial community composition, and substrate availability, OMP and TP removal can be significantly enhanced in MAR. Future designs should therefore move toward a more integrated approach, where operational parameters and configurations are guided by insights into OMP biodegradation and transformation. Such knowledge-based optimization will be essential to ensure safe and sustainable water reuse under increasing environmental and regulatory pressures.

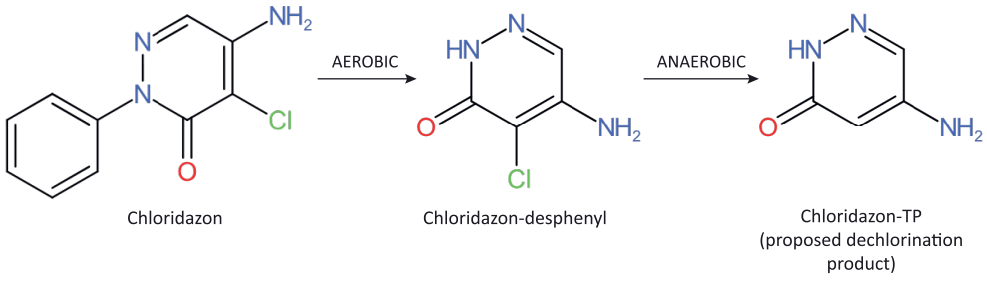

Figure 6.7. Proposed chloridazon degradation pathway under sequential redox conditions: aerobic (producing chloridazon-desphenyl) and anaerobic (producing a dechlorinated chloridazon-TP).

6.3.4 Improved regulatory frameworks for OMPs and TPs in reused water

Current quality and water reuse regulations inadequately address the wide variety of OMPs present in reused water and subsurface systems (Dingemans et al., 2020). While water reuse regulations include requirements for the removal of pathogenic microorganisms and general water quality indicators (e.g. turbidity, total suspended solids), no limits or monitoring requirements for specific chemical contaminants are included (European Commission, 2024; European Parliament and Council of the European Union, 2020b). However, the occurrence of OMPs and their TPs in WWTP effluent and other reuse water sources is documented (Chapters 2, 3 and Beretsou et al., 2022; Helmecke et al., 2020; Stadler et al., 2012; Yuan et al., 2017) and acknowledged in regulatory texts. For drinking water production through MAR, reuse regulations refer to the Directive 2006/118/EC (European Parliament and Council of the European Union, 2006b) to prevent groundwater pollution, yet without formally integrating reference thresholds. Consequently, the occurrence of OMPs in reused water sources remains insufficiently regulated, hindering the implementation of safe water reuse to meet growing freshwater demands.

It is crucial to understand the presence and fate of OMPs in reused waters to protect natural water resources and design fit-for-purpose reuse applications. A more comprehensive characterization of water intended for reuse can help determine its suitability for specific applications. For example, if an effluent still contains persistent OMPs and optimization of the WWTP is not feasible, an alternative reuse application may be considered instead of infiltration or environmental discharge. Such characterization requires the integration of NTA alongside routine target screening. Results from NTA, however, can also inform and update existing monitoring target lists in WWTPs and drinking water production plants, thereby improving both monitoring and regulatory prioritization.

At present, TPs are scarcely included in chemical risk assessment frameworks. Only pesticide registration requires the identification of TPs during product development, while pharmaceuticals and industrial chemicals have no such mandatory requirement (Zahn et al., 2024). Yet, some TPs may be more toxic than their PC or exhibit potential adverse health effects (Chapters 4 and 5). With the analytical and computational tools now available and considering future improvements, it is increasingly feasible to include TP formation and toxicity assessment into early-stage chemical design and risk assessment. For example, (miniaturized) ecotoxicity tests could be implemented to assess the toxicity of an OMP and its resulting TPs after a regulatory biodegradability test (Silva et al., 2025). Such an approach would help prevent the marketing of compounds likely to yield harmful TPs upon environmental release.

Moreover, existing standardized tests for environmental persistence require updates to reflect current chemical diversity and environmental complexity (Davenport et al., 2022). Most standardized tests were developed decades ago for a narrower set of chemicals and simplified environmental conditions, typically focusing on aerobic systems, resulting in a lack of data on anaerobic biodegradation. As awareness of the wide range of OMPs in the environment and the factors influencing their fate has grown, these tests no longer adequately reflect real water system conditions. Updated tests should therefore include TP formation, environmental, and microbial conditions to better capture realistic scenarios (as confirmed by the overall results of our study). Such improvements would increase the reliability of the tests, reduce interlaboratory variability, and promote harmonization across studies (Dingemans et al., 2020). The resulting data, generated by both regulatory testing and academic research, should be integrated into shared databases. For such developments, studies should harmoniously report test conditions in detail, including microbial community characterization and identified TPs with corresponding SMILES codes, similar to existing FAIR (findable, accessible, interoperable, and reusable) templates (Rich et al., 2025; Schymanski and Bolton, 2022). Biodegradation prediction tools like BioTransformer (Djoumbou-Feunang et al., 2019) can then benefit from the data and be refined to include reaction pathways representative of anaerobic environments, for instance. Improved data sharing and availability will thus support the refinement of prediction models, the development of high-throughput screening tools, and a faster chemical risk assessment process that can keep up with the continuous introduction of new OMPs.

A recent update to the OECD Test Guideline 308 for assessing the transformation of organic chemicals in aquatic sediment systems represents a significant step forward (OECD, 2025). The revision now includes the evaluation of anaerobic transformation in addition to the previously considered aerobic processes and requires TP monitoring via isotopic or radio-label tracing at multiple sampling times, using two different sediment types. The revised test, however, still has important limitations. In particular, the identification of TPs is restricted to those representing ≥10% of the applied radioactivity, which may overlook minor or highly polar products formed from unlabelled portions of the molecule. For example, small and persistent TPs such as TFA can be formed from fluorinated moieties but remain undetected if the radiolabel is placed elsewhere in the PC. This may lead to an incomplete assessment of the TPs and potential environmental risks. Pre-screening with in-silico tools (like patRoon) may help better design labelled molecules to confidently identify relevant TPs. Furthermore, while the updated guideline requires assessing microbial biomass (e.g., via respiration/methanogenesis rate, fumigation, or plate count), microbial diversity is still not evaluated. Our research demonstrated the importance of microbial

diversity for biodegradation performance (Chapter 4), which assessment could easily be implemented in the standardized test (e.g., by reporting amplicon sequence variants - ASVs). Similarly, there is no requirement to explicitly report the redox conditions, while different reducing environments might yield distinct biodegradation (Chapter 5). Both parameters are key to the reproducibility and interpretability of biodegradation and TP formation results.

Finally, results of standardized tests and guideline studies should be translated more rapidly into regulatory frameworks, which often take decades to be updated (Davenport et al., 2022). Accelerating this process requires collaboration of academia, industry, and regulatory authorities to ensure that new insights are efficiently integrated into policy and practice. The general population is also a key stakeholder that should be involved in the process (Dingemans et al., 2020), as social acceptance of water reuse strongly depends on transparent communication of water quality, treatment, and safety measures.

Altogether, integrating an improved understanding of OMP fate and transformation into regulatory and societal frameworks will be essential to achieve safer, more sustainable water reuse practices.

6.4 Conclusions

This thesis aimed to better understand OMP fate, biodegradation, and TP formation in the subsurface during water reuse. We combined field and laboratory investigations with target, non-target, and in-silico analytical approaches to assess OMP occurrence and evaluate how subsurface conditions influence their transformation. We highlighted the need to better account for TPs in water reuse regulations and showed that, while soil passage effectively removes many biodegradable OMPs, it is not sufficient: persistent and mobile OMPs can pass through largely unchanged, and potentially harmful TPs may form. Together with insights on the influence of redox conditions, microbial diversity, and inoculum pre-exposure on OMP transformation, these findings support improvement of monitoring programs, standardized testing, and the design of subsurface water reuse systems.

Freshwater scarcity is already a pressing global challenge, and increasing water demand will further intensify the pressure on available resources. Water reuse will therefore be essential to ensure a sustainable water supply. Now is the time to develop the tools, knowledge, and strategies to guarantee safe and efficient water reuse. Future studies should thus focus on advancing and implementing designs that allow the management of redox conditions and residence times to sustain OMP biodegradation while minimizing the formation of harmful TPs. In addition, in-silico prediction tools should be harmonized and refined to better represent subsurface conditions and redox-dependent reactions across subsurface layers. Such advances will help establish a virtuous cycle of improved prediction, realistic risk assessment, and system efficiency, leading to a safer and more sustainable water reuse.

References

Achermann, S., Mansfeldt, C.B., Müller, M., Johnson, D.R., Fenner, K., 2020. Relating Metatranscriptomic Profiles to the Micropollutant Biotransformation Potential of Complex Microbial Communities. Environ. Sci. Technol. 54, 235–244. https://doi.org/10.1021/acs.est.9b05421

Albergamo, V., Helmus, R., de Voogt, P., 2018. Direct injection analysis of polar micropollutants in natural drinking water sources with biphenyl liquid chromatography coupled to high-resolution time-of-flight mass spectrometry. J. Chromatogr. A 1569, 53–61. https://doi.org/10.1016/j.chroma.2018.07.036

Albergamo, V., Schollée, J.E., Schymanski, E.L., Helmus, R., Timmer, H., Hollender, J., De Voogt, P., 2019. Nontarget screening reveals time trends of polar micropollutants in a riverbank filtration system. Environ. Sci. Technol. 53, 7584–7594. https://doi.org/10.1021/acs.est.9b01750

Aldas-Vargas, A., Hauptfeld, E., Hermes, G.D.A., Atashgahi, S., Smidt, H., Rijnaarts, H.H.M., Sutton, N.B., 2022. Selective pressure on microbial communities in a drinking water aquifer – Geochemical parameters vs. micropollutants. Environ. Pollut. 299, 118807. https://doi.org/10.1016/j.envpol.2022.118807

Aldas-Vargas, A., Hauptfeld, E., Hermes, G.D.A., Atashgahi, S., Smidt, H., Rijnaarts, H.H.M., Sutton, N.B., 2019. Exploring groundwater microbial communities for natural attenuation potential of micropollutants (preprint). Microbiology. https://doi.org/10.1101/850750

Aldas-Vargas, A., Kers, J.G., Smidt, H., Rijnaarts, H.H.M., Sutton, N.B., 2024. Bioaugmentation has temporary effect on anaerobic pesticide biodegradation in simulated groundwater systems. Biodegradation 35, 281–297. https://doi.org/10.1007/s10532-023-10039-0

Aldas-Vargas, A., van der Vooren, T., Rijnaarts, H.H.M., Sutton, N.B., 2021. Biostimulation is a valuable tool to assess pesticide biodegradation capacity of groundwater microorganisms. Chemosphere 280, 130793. https://doi.org/10.1016/j.chemosphere.2021.130793

Alessandretti, I., Rigueto, C.V.T., Nazari, M.T., Rosseto, M., Dettmer, A., 2021. Removal of diclofenac from wastewater: A comprehensive review of detection, characteristics and tertiary treatment techniques. J. Environ. Chem. Eng. 9, 106743. https://doi.org/10.1016/j.jece.2021.106743

Alidina, M., Li, D., Ouf, M., Drewes, J.E., 2014. Role of primary substrate composition and concentration on attenuation of trace organic chemicals in managed aquifer recharge systems. J. Environ. Manage. 144, 58–66. https://doi.org/10.1016/j.jenvman.2014.04.032

Arcadis, Rijn en IJssel Water Board, Province of Gelderland, Vitens, 2008. AMIGO - Actueel Model Instrument Gelderland Oost.

Arp, H.P.H., Gredelj, A., Glüge, J., Scheringer, M., Cousins, I.T., 2024. The global threat from the irreversible accumulation of trifluoroacetic acid (TFA). Environ. Sci. Technol. 58, 19925–19935. https://doi.org/10.1021/acs.est.4c06189

Arp, H.P.H., Hale, S.E., 2022. Assessing the Persistence and Mobility of Organic Substances to Protect Freshwater Resources | ACS Environmental Au. ACS Environ. Au 2, 482–509. https://doi.org/10.1021/acsenvironau.2c00024

Bao, Y., Zhao, S., Wu, N., Yuan, Y., Ruan, L., He, J., 2024. Degradation of Atrazine by an Anaerobic Microbial Consortium Enriched from Soil of an Herbicide-

Manufacturing Plant. Curr. Microbiol. 81, 117. https://doi.org/10.1007/s00284-024-03624-w

Barbieri, M., Carrera, J., Sanchez-Vila, X., Ayora, C., Cama, J., Köck-Schulmeyer, M., López de Alda, M., Barceló, D., Tobella Brunet, J., Hernández García, M., 2011. Microcosm experiments to control anaerobic redox conditions when studying the fate of organic micropollutants in aquifer material. J. Contam. Hydrol. 126, 330–345. https://doi.org/10.1016/j.jconhyd.2011.09.003

Bartholomeus, R., Stofberg, S.F., Van den Eertwegh, G., Cirkel, G., 2017. BTO Rapport Hergebruik Restwater Voor Het Landelijk Gebied: Monitoring Sub-irrigatie met RWZI-effluent. (BTO report No. 2017.062). KWR Watercycle Research Institue, Nieuwegein.

Bartholomeus, R.P., Wiel, K. van der, Loon, A.F. van, Huijgevoort, M.H.J. van, Vliet, M.T.H. van, Mens, M., Geffen, S.M., Wanders, N., Pot, W., 2023. Managing water across the flood–drought spectrum: Experiences from and challenges for the Netherlands. Camb. Prisms Water 1, e2. https://doi.org/10.1017/wat.2023.4

Béen, F., Kruve, A., Vughs, D., Meekel, N., Reus, A., Zwartsen, A., Wessel, A., Fischer, A., ter Laak, T., Brunner, A.M., 2021. Risk-based prioritization of suspects detected in riverine water using complementary chromatographic techniques. Water Res. 204, 117612. https://doi.org/10.1016/j.watres.2021.117612

Beretsou, V.G., Nika, M.-C., Manoli, K., Michael, C., Sui, Q., Lundy, L., Revitt, D.M., Thomaidis, N.S., Fatta-Kassinos, D., 2022. Multiclass target analysis of contaminants of emerging concern including transformation products, soil bioavailability assessment and retrospective screening as tools to evaluate risks associated with reclaimed water reuse. Sci. Total Environ. 852, 158391. https://doi.org/10.1016/j.scitotenv.2022.158391

Bertelkamp, C., Verliefde, A.R.D., Schoutteten, K., Vanhaecke, L., Vanden Bussche, J., Singhal, N., van der Hoek, J.P., 2016. The effect of redox conditions and adaptation time on organic micropollutant removal during river bank filtration: A laboratory-scale column study. Sci. Total Environ. 544, 309–318. https://doi.org/10.1016/j.scitotenv.2015.11.035

Brack, W., Hollender, J., de Alda, M.L., Müller, C., Schulze, T., Schymanski, E., Slobodnik, J., Krauss, M., 2019. High-resolution mass spectrometry to complement monitoring and track emerging chemicals and pollution trends in European water resources. Environ. Sci. Eur. 31, 62. https://doi.org/10.1186/s12302-019-0230-0

Branco, R.H.R., Meulepas, R.J.W., Kadlecová, K., Cardoso, M.F.S., Rijnaarts, H.H.M., Sutton, N.B., 2024. Effect of dissolved organic carbon on micropollutant biodegradation by aquifer and soil microbial communities. Chemosphere 347, 140644. https://doi.org/10.1016/j.chemosphere.2023.140644

Branco, R.H.R., Meulepas, R.J.W., van Veelen, H.P.J., Rijnaarts, H.H.M., Sutton, N.B., 2023. Influence of redox condition and inoculum on micropollutant biodegradation by soil and activated sludge communities. Sci. Total Environ. 897, 165233. https://doi.org/10.1016/j.scitotenv.2023.165233

Brunner, A.M., Vughs, D., Siegers, W., Bertelkamp, C., Hofman-Caris, R., Kolkman, A., ter Laak, T., 2019a. Monitoring transformation product formation in the drinking water treatments rapid sand filtration and ozonation. Chemosphere 214, 801–811. https://doi.org/10.1016/j.chemosphere.2018.09.140

Brunner, A.M., Vughs, D., Siegers, W., Bertelkamp, C., Hofman-Caris, R., Kolkman, A., ter Laak, T., 2019b. Monitoring transformation product formation in the drinking water treatments rapid sand filtration and ozonation. Chemosphere 214, 801–811. https://doi.org/10.1016/j.chemosphere.2018.09.140

Burke, V., Greskowiak, J., Grünenbaum, N., Massmann, G., 2017. Redox and Temperature Dependent Attenuation of Twenty Organic Micropollutants - A Systematic Column Study. Water Environ. Res. 89, 155–167. https://doi.org/10.2175/106143016X14609975746000

Celiz, M.D., Tso, J., Aga, D.S., 2009. Pharmaceutical metabolites in the environment: Analytical challenges and ecological risks. Environ. Toxicol. Chem. 28, 2473–2484. https://doi.org/10.1897/09-173.1

ChemAxon, n.d. LogD Predictor - Chemicalize [WWW Document]. URL https://chemicalize.com (accessed 11.5.24).

Chen, S.-F., Chen, W.-J., Song, H., Liu, M., Mishra, S., Ghorab, M.A., Chen, S., Chang, C., 2024. Microorganism-Driven 2,4-D Biodegradation: Current Status and Emerging Opportunities. Molecules 29, 3869. https://doi.org/10.3390/molecules29163869

Cirkel, G., 2017. Kwantificeren korte reistijden door middel van traceronderzoek: tracerproef Olden Eibergen (BTO rapport No. BTO 2017.010), Managementsamenvatting. KWR Watercycle Research Institute, Nieuwegein.

Coll, C., Bier, R., Li, Z., Langenheder, S., Gorokhova, E., Sobek, A., 2020. Association between Aquatic Micropollutant Dissipation and River Sediment Bacterial Communities. Environ. Sci. Technol. 54, 14380–14392. https://doi.org/10.1021/acs.est.0c04393

Council of the European Communities, 1991. Urban Wastewater Treatment Directive 91/271/EEC.

Council of the European Union, 2025. Proposal for a Directive of the European Parliament and of the Council amending Directive 2000/60/EC establishing a framework for Community action in the field of water policy, Directive 2006/118/EC on the protection of groundwater against pollution and deterioration and Directive 2008/105/EC on environmental quality standards in the field of water policy - Analysis of the final compromise text with a view to agreement.

Crampon, M., Bodilis, J., Portet-Koltalo, F., 2018. Linking initial soil bacterial diversity and polycyclic aromatic hydrocarbons (PAHs) degradation potential. J. Hazard. Mater. 359, 500–509. https://doi.org/10.1016/j.jhazmat.2018.07.088

Cronin, M.T.D., Basiri, H., Chrysochoou, G., Enoch, S.J., Firman, J.W., Spînu, N., Madden, J.C., 2025. The predictivity of QSARs for toxicity: Recommendations for improving model performance. Comput. Toxicol. 33, 100338. https://doi.org/10.1016/j.comtox.2024.100338

Cruz-Hernández, M.A., Mendoza-Herrera, A., Bocanegra-García, V., Rivera, G., 2022. Azospirillum spp. from Plant Growth-Promoting Bacteria to Their Use in Bioremediation. Microorganisms 10, 1057. https://doi.org/10.3390/microorganisms10051057

Davenport, R., Curtis-Jackson, P., Dalkmann, P., Davies, J., Fenner, K., Hand, L., McDonough, K., Ott, A., Ortega-Calvo, J.J., Parsons, J.R., Schäffer, A., Sweetlove, C., Trapp, S., Wang, N., Redman, A., 2022. Scientific concepts and methods for moving

persistence assessments into the 21st century. Integr. Environ. Assess. Manag. 18, 1454–1487. https://doi.org/10.1002/ieam.4575

de Souza, A.J., de Andrade, P.A.M., de Araújo Pereira, A.P., Andreote, F.D., Tornisielo, V.L., Regitano, J.B., 2017. The depleted mineralization of the fungicide chlorothalonil derived from loss in soil microbial diversity. Sci. Rep. 7, 14646. https://doi.org/10.1038/s41598-017-14803-0

de Wilt, A., He, Y., Sutton, N., Langenhoff, A., Rijnaarts, H., 2018. Sorption and biodegradation of six pharmaceutically active compounds under four different redox conditions. Chemosphere 193, 811–819. https://doi.org/10.1016/j.chemosphere.2017.11.084

de Wit, J., Ritsema, C.J., van Dam, J.C., van den Eertwegh, G.A.P.H., Bartholomeus, R.P., 2022. Development of subsurface drainage systems: Discharge – retention – recharge. Agric. Water Manag. 269, 107677. https://doi.org/10.1016/j.agwat.2022.107677

de Wit, J., van Huijgevoort, M., van den Eertwegh, G., van Deijl, D., Stofberg, S., Bartholomeus, R., 2023. Data underlying the publication: Hydrological consequences of controlled drainage with subirrigation. https://doi.org/10.4121/6E5F65F6-530F-438D-8E43-3593E259AABA.V3

de Wit, J.A., van Huijgevoort, M.H.J., van Dam, J.C., van den Eertwegh, G.A.P.H., van Deijl, D., Ritsema, C.J., Bartholomeus, R.P., 2024. Hydrological consequences of controlled drainage with subirrigation. J. Hydrol. 628, 130432. https://doi.org/10.1016/j.jhydrol.2023.130432

Dillon, P., Pavelic, P., Declan, P., Beringen, H., Ward, J., 2009. Managed aquifer recharge: An introduction (No. 13), Waterline Report Series. National Water Commission, Canberra.

Dillon, P., Stuyfzand, P., Grischek, T., Lluria, M., Pyne, R.D.G., Jain, R.C., Bear, J., Schwarz, J., Wang, W., Fernandez, E., Stefan, C., Pettenati, M., van der Gun, J., Sprenger, C., Massmann, G., Scanlon, B.R., Xanke, J., Jokela, P., Zheng, Y., Rossetto, R., Shamrukh, M., Pavelic, P., Murray, E., Ross, A., Bonilla Valverde, J.P., Palma Nava, A., Ansems, N., Posavec, K., Ha, K., Martin, R., Sapiano, M., 2019. Sixty years of global progress in managed aquifer recharge. Hydrogeol. J. 27, 1–30. https://doi.org/10.1007/s10040-018-1841-z

Dingemans, M.M.L., Smeets, P.W.M.H., Medema, G., Frijns, J., Raat, K.J., van Wezel, A.P., Bartholomeus, R.P., 2020. Responsible Water Reuse Needs an Interdisciplinary Approach to Balance Risks and Benefits. Water 12, 1264. https://doi.org/10.3390/w12051264

Directorate-General for Environment, 2022a. Annexes to the "Proposal for a Directive of the European parliament and of the Council amending Directive 2000/60/EC establishing a framework for Community action in the field of water policy, Directive 2006/118/EC on the protection of groundwater against pollution and deterioration and Directive 2008/105/EC on environmental quality standards in the field of water policy."

Directorate-General for Environment, 2022b. Proposal for a Directive amending the Water Framework Directive, the Groundwater Directive and the Environmental Quality Standards Directive.

Djoumbou-Feunang, Y., Fiamoncini, J., Gil-de-la-Fuente, A., Greiner, R., Manach, C., Wishart, D.S., 2019. BioTransformer: a comprehensive computational tool for small molecule metabolism prediction and metabolite identification. J. Cheminformatics 11, 2. https://doi.org/10.1186/s13321-018-0324-5

Drewes, J.E., 2009. Ground water replenishment with recycled water - Water quality improvements during managed aquifer recharge. Ground Water 47, 502–505. https://doi.org/10.1111/j.1745-6584.2009.00587_5.x

Drewes, J.E., Heberer, T., Rauch, T., Reddersen, K., 2003. Fate of Pharmaceuticals During Ground Water Recharge. Groundw. Monit. Remediat. 23, 64–72. https://doi.org/10.1111/j.1745-6592.2003.tb00684.x

Dulio, V., Alygizakis, N., Ng, K., Schymanski, E.L., Andres, S., Vorkamp, K., Hollender, J., Finckh, S., Aalizadeh, R., Ahrens, L., Bouhoulle, E., Čirka, Ľ., Derksen, A., Deviller, G., Duffek, A., Esperanza, M., Fischer, S., Fu, Q., Gago-Ferrero, P., Haglund, P., Junghans, M., Kools, S.A.E., Koschorreck, J., Lopez, B., Lopez de Alda, M., Mascolo, G., Miège, C., Osté, L., O'Toole, S., Rostkowski, P., Schulze, T., Sims, K., Six, L., Slobodnik, J., Staub, P.-F., Stroomberg, G., Thomaidis, N.S., Togola, A., Tomasi, G., von der Ohe, P.C., 2024. Beyond target chemicals: updating the NORMAN prioritisation scheme to support the EU chemicals strategy with semi-quantitative suspect/non-target screening data. Environ. Sci. Eur. 36, 113. https://doi.org/10.1186/s12302-024-00936-3

Edgar, R.C., 2010. Search and clustering orders of magnitude faster than BLAST. Bioinformatics 26, 2460–2461. https://doi.org/10.1093/bioinformatics/btq461

Escher, B.I., Fenner, K., 2011. Recent advances in environmental risk assessment of transformation products. Environ. Sci. Technol. 45, 3835–3847. https://doi.org/10.1021/es1030799

Escher, B.I., Stapleton, H.M., Schymanski, E.L., 2020. Tracking complex mixtures of chemicals in our changing environment. Science 367, 388–392. https://doi.org/10.1126/science.aay6636

European Commission, 2024. Commission Delegated Regulation (EU) 2024/1765 of 11 March 2024 supplementing Regulation (EU) 2020/741 of the European Parliament and of the Council with regard to technical specifications of the key elements of risk management.

European Commission, n.d. EU Pesticides Database - Active Substances.

European Environmental Agency, 2024. Water Framework Directive [WWW Document]. Wise Freshw. Freshw. Inf. Syst. Eur. URL https://water.europa.eu/freshwater/europe-freshwater/water-framework-directive (accessed 10.9.25).

European Parliament, 2023. Report (A9-0276/2023) on the proposal for a directive of the European Parliament and of the Council concerning urban wastewater treatment (recast) - COM(2022)541 – C9-6363/2022 – 2022/0345(COD).

European Parliament, Council of the European Union, 2024. Regulation (EU) 2024/2865 of the European Parliament and of the Council of 23 October 2024 amending Regulation (EC) No 1272/2008 on classification, labelling and packaging of substances and mixtures (Text with EEA relevance), 2024/2865.

European Parliament, Council of the European Union, 2020a. Directive (EU) 2020/2184 of the European Parliament and of the Council on the quality of water intended for human consumption, L435/1.

European Parliament, Council of the European Union, 2020b. REGULATION (EU) 2020/741 OF THE EUROPEAN PARLIAMENT AND OF THE COUNCIL of 25 May 2020 on minimum requirements for water reuse. Official Journal of the European Union. https://doi.org/10.5040/9781782258674

European Parliament, Council of the European Union, 2008. Directive 2008/105/EC on Environmental Quality Standards (EQS) in the field of water policy.

European Parliament, Council of the European Union, 2006a. REGULATION (EC) No 1907/2006 concerning the Registration, Evaluation, Authorisation and Restriction of Chemicals (REACH), establishing a European Chemicals Agency, amending Directive 1999/45/EC and repealing Council Regulation (EEC) No 793/93 and Commission Regulation (EC) No 1488/94 as well as Council Directive 76/769/EEC and Commission Directives 91/155/EEC, 93/67/EEC, 93/105/EC and 2000/21/EC.

European Parliament, Council of the European Union, 2006b. Directive 2006/118/EC on the protection of groundwater against pollution and deterioration, Official Journal of the European Union.

European Parliament, Council of the European Union, 2000. Directive 2000/60/EC establishing a framework for Community action in the field of water policy, Official Journal of the European Union.

European Parliament, European Commission, Torvalds, N., 2024. European Green Deal | Revision of the Urban Wastewater Treatment Directive.

Falås, P., Wick, A., Castronovo, S., Habermacher, J., Ternes, T.A., Joss, A., 2016. Tracing the limits of organic micropollutant removal in biological wastewater treatment. Water Res. 95, 240–249. https://doi.org/10.1016/j.watres.2016.03.009

Fenner, K., Canonica, S., Wackett, L.P., Elsner, M., 2013. Evaluating Pesticide Degradation in the Environment: Blind Spots and Emerging Opportunities. Science 341, 752–758. https://doi.org/10.1126/science.1236281

Fenner, K., Elsner, M., Lueders, T., McLachlan, M.S., Wackett, L.P., Zimmermann, M., Drewes, J.E., 2021. Methodological Advances to Study Contaminant Biotransformation: New Prospects for Understanding and Reducing Environmental Persistence? ACS EST Water 1, 1541–1554. https://doi.org/10.1021/acsestwater.1c00025

Fent, K., Escher, C., Caminada, D., 2006. Estrogenic activity of pharmaceuticals and pharmaceutical mixtures in a yeast reporter gene system. Reprod. Toxicol., 34th Annual Conference of the European Teratology Society 22, 175–185. https://doi.org/10.1016/j.reprotox.2006.04.010

Filter, J., Zhiteneva, V., Vick, C., Ruhl, A.S., Jekel, M., Hübner, U., Drewes, J.E., 2021. Varying attenuation of trace organic chemicals in natural treatment systems – A review of key influential factors. Chemosphere 274, 129774. https://doi.org/10.1016/j.chemosphere.2021.129774

Fischer, A., van Wezel, A.P., Hollender, J., Cornelissen, E., Hofman, R., van der Hoek, J.P., 2019. Development and application of relevance and reliability criteria for water treatment removal efficiencies of chemicals of emerging concern. Water Res. 161, 274–287. https://doi.org/10.1016/j.watres.2019.05.088

Fox, J., Weisberg, S., 2019. An {R} Companion to Applied Regression, Third. ed. Sage, Thousand Oaks (CA).

Freeling, F., Behringer, D., Heydel, F., Scheurer, M., Ternes, T.A., Nödler, K., 2020. Trifluoroacetate in precipitation: Deriving a benchmark data set. Environ. Sci. Technol. 54, 11210–11219. https://doi.org/10.1021/acs.est.0c02910

Fu, K., Wang, L., Wei, C., Li, J., Zhang, J., Zhou, Z., Liang, Y., 2020. Sucralose and acesulfame as an indicator of domestic wastewater contamination in Wuhan surface water. Ecotoxicol. Environ. Saf. 189, 109980. https://doi.org/10.1016/j.ecoenv.2019.109980

Gao, J., Ellis, L.B.M., Wackett, L.P., 2010. The University of Minnesota Biocatalysis/Biodegradation Database: improving public access. Nucleic Acids Res. 38, D488–D491. https://doi.org/10.1093/nar/gkp771

Ghattas, A.-K., Fischer, F., Wick, A., Ternes, T.A., 2017. Anaerobic biodegradation of (emerging) organic contaminants in the aquatic environment. Water Res. 116, 268–295. https://doi.org/10.1016/j.watres.2017.02.001

Girvan, M.S., Campbell, C.D., Killham, K., Prosser, J.I., Glover, L.A., 2005. Bacterial diversity promotes community stability and functional resilience after perturbation. Environ. Microbiol. 7, 301–313. https://doi.org/10.1111/j.1462-2920.2005.00695.x

Golovko, O., Örn, S., Sörengård, M., Frieberg, K., Nassazzi, W., Lai, F.Y., Ahrens, L., 2021. Occurrence and removal of chemicals of emerging concern in wastewater treatment plants and their impact on receiving water systems. Sci. Total Environ. 754, 142122. https://doi.org/10.1016/j.scitotenv.2020.142122

González-Gaya, B., Lopez-Herguedas, N., Bilbao, D., Mijangos, L., Iker, A.M., Etxebarria, N., Irazola, M., Prieto, A., Olivares, M., Zuloaga, O., 2021. Suspect and non-target screening: the last frontier in environmental analysis. Anal. Methods 13, 1876–1904. https://doi.org/10.1039/D1AY00111F

Greskowiak, J., Hamann, E., Burke, V., Massmann, G., 2017. The uncertainty of biodegradation rate constants of emerging organic compounds in soil and groundwater – A compilation of literature values for 82 substances. Water Res. 126, 122–133. https://doi.org/10.1016/j.watres.2017.09.017

Guerra, C.A., Bardgett, R.D., Caon, L., Crowther, T.W., Delgado-Baquerizo, M., Montanarella, L., Navarro, L.M., Orgiazzi, A., Singh, B.K., Tedersoo, L., Vargas-Rojas, R., Briones, M.J.I., Buscot, F., Cameron, E.K., Cesarz, S., Chatzinotas, A., Cowan, D.A., Djukic, I., van den Hoogen, J., Lehmann, A., Maestre, F.T., Marín, C., Reitz, T., Rillig, M.C., Smith, L.C., de Vries, F.T., Weigelt, A., Wall, D.H., Eisenhauer, N., 2021. Tracking, targeting, and conserving soil biodiversity. Science 371, 239–241. https://doi.org/10.1126/science.abd7926

Gutiérrez-Noya, V.M., Gómez-Oliván, L.M., Ramírez-Montero, M. del C., Islas-Flores, H., Galar-Martínez, M., García-Medina, S., 2021. Survival and malformations rates, oxidative status in early life stages of *Cyprinus carpio* due to exposure to environmentally realistic concentrations of paracetamol. Sci. Total Environ. 768, 144585. https://doi.org/10.1016/j.scitotenv.2020.144585

Hale, S.E., Neumann, M., Schliebner, I., Schulze, J., Averbeck, F.S., Castell-Exner, C., Collard, M., Drmač, D., Hartmann, J., Hofman-Caris, R., Hollender, J., de Jonge, M., Kullick, T., Lennquist, A., Letzel, T., Nödler, K., Pawlowski, S., Reineke, N., Rorije, E.,

Scheurer, M., Sigmund, G., Timmer, H., Trier, X., Verbruggen, E., Arp, H.P.H., 2022. Getting in control of persistent, mobile and toxic (PMT) and very persistent and very mobile (vPvM) substances to protect water resources: strategies from diverse perspectives. Environ. Sci. Eur. 34, 22. https://doi.org/10.1186/s12302-022-00604-4

Hamann, E., Stuyfzand, P.J., Greskowiak, J., Timmer, H., Massmann, G., 2016. The fate of organic micropollutants during long-term/long-distance river bank filtration. Sci. Total Environ. 545–546, 629–640. https://doi.org/10.1016/j.scitotenv.2015.12.057

He, Y., Sutton, N.B., Rijnaarts, H.H.M., Langenhoff, A.A.M., 2018. Pharmaceutical biodegradation under three anaerobic redox conditions evaluated by chemical and toxicological analyses. Sci. Total Environ. 618, 658–664. https://doi.org/10.1016/j.scitotenv.2017.07.219

Hellauer, K., Martínez Mayerlen, S., Drewes, J.E., Hübner, U., 2019. Biotransformation of trace organic chemicals in the presence of highly refractory dissolved organic carbon. Chemosphere 215, 33–39. https://doi.org/10.1016/j.chemosphere.2018.09.166

Helmecke, M., Fries, E., Schulte, C., 2020. Regulating water reuse for agricultural irrigation: risks related to organic micro-contaminants. Environ. Sci. Eur. 32, 4. https://doi.org/10.1186/s12302-019-0283-0

Helmus, R., 2025. patRoon Handbook.

Helmus, R., 2024. patRoon (2.3.3) GitHub repository - Workflows for mass-spectrometry based non-target analysis [WWW Document]. patRoon. URL https://rickhelmus.github.io/patRoon/index.html (accessed 3.21.24).

Helmus, R., Bagdonaite, I., de Voogt, P., van Bommel, M.R., Schymanski, E.L., van Wezel, A.P., ter Laak, T.L., 2025. Comprehensive mass spectrometry workflows to systematically elucidate transformation processes of organic micropollutants: A case study on the photodegradation of four pharmaceuticals. Environ. Sci. Technol. 59, 3723–3736. https://doi.org/10.1021/acs.est.4c09121

Helmus, R., ter Laak, T.L., van Wezel, A.P., de Voogt, P., Schymanski, E.L., 2021. patRoon: open source software platform for environmental mass spectrometry based non-target screening. J. Cheminformatics 13, 1. https://doi.org/10.1186/s13321-020-00477-w

Helmus, R., Velde, B. van de, Brunner, A.M., Laak, T.L. ter, van Wezel, A.P., Schymanski, E.L., 2022. patRoon 2.0: Improved Non-Target Analysis workflows including automated transformation product screening. J. Open Source Softw. 9. https://doi.org/10.5281/zenodo.6337883

Hermes, N., Jewell, K.S., Schulz, M., Müller, J., Hübner, U., Wick, A., Drewes, J.E., Ternes, T.A., 2019. Elucidation of removal processes in sequential biofiltration (SBF) and soil aquifer treatment (SAT) by analysis of a broad range of trace organic chemicals (TOrCs) and their transformation products (TPs). Water Res. 163, 114857. https://doi.org/10.1016/j.watres.2019.114857

Hillebrand, O., Nödler, K., Sauter, M., Licha, T., 2015. Multitracer experiment to evaluate the attenuation of selected organic micropollutants in a karst aquifer. Sci. Total Environ. 506–507, 338–343. https://doi.org/10.1016/j.scitotenv.2014.10.102

Hollender, J., Schymanski, E.L., Ahrens, L., Alygizakis, N., Béen, F., Bijlsma, L., Brunner, A.M., Celma, A., Fildier, A., Fu, Q., Gago-Ferrero, P., Gil-Solsona, R., Haglund, P., Hansen,

M., Kaserzon, S., Kruve, A., Lamoree, M., Margoum, C., Meijer, J., Merel, S., Rauert, C., Rostkowski, P., Samanipour, S., Schulze, B., Schulze, T., Singh, R.R., Slobodnik, J., Steininger-Mairinger, T., Thomaidis, N.S., Togola, A., Vorkamp, K., Vulliet, E., Zhu, L., Krauss, M., 2023. NORMAN guidance on suspect and non-target screening in environmental monitoring. Environ. Sci. Eur. 35, 75. https://doi.org/10.1186/s12302-023-00779-4

Holzmann, H., Simeoni, A., Schäffer, A., 2021. Influence of chemical charge on the fate of organic chemicals in sediment particle size fractions. Chemosphere 265, 129105. https://doi.org/10.1016/j.chemosphere.2020.129105

Honti, M., Zsugyel, M., Seller, C., Fenner, K., 2023. Benchmarking the persistence of active pharmaceutical ingredients in river systems. Environ. Sci. Technol. 57, 14684–14693. https://doi.org/10.1021/acs.est.3c01627

Hoppe-Jones, C., Dickenson, E.R.V., Drewes, J.E., 2012. The role of microbial adaptation and biodegradable dissolved organic carbon on the attenuation of trace organic chemicals during groundwater recharge. Sci. Total Environ. 437, 137–144. https://doi.org/10.1016/j.scitotenv.2012.08.009

Horai, H., Arita, M., Kanaya, S., Nihei, Y., Ikeda, T., Suwa, K., Ojima, Y., Tanaka, Kenichi, Tanaka, S., Aoshima, K., Oda, Y., Kakazu, Y., Kusano, M., Tohge, T., Matsuda, F., Sawada, Y., Hirai, M.Y., Nakanishi, H., Ikeda, K., Akimoto, N., Maoka, T., Takahashi, H., Ara, T., Sakurai, N., Suzuki, H., Shibata, D., Neumann, S., Iida, T., Tanaka, Ken, Funatsu, K., Matsuura, F., Soga, T., Taguchi, R., Saito, K., Nishioka, T., 2010. MassBank: a public repository for sharing mass spectral data for life sciences. J. Mass Spectrom. JMS 45, 703–714. https://doi.org/10.1002/jms.1777

Hothorn, T., Bretz, F., Westfall, P., 2008. Simultaneous inference in general parametric models. Biom. J. Biom. Z. 50, 346–363. https://doi.org/10.1002/bimj.200810425

Hübner, U., Wurzbacher, C., Helbling, D.E., Drewes, J.E., 2022. Engineering of managed aquifer recharge systems to optimize biotransformation of trace organic chemicals. Curr. Opin. Environ. Sci. Health 27, 100343. https://doi.org/10.1016/j.coesh.2022.100343

Isidori, M., Bellotta, M., Cangiano, M., Parrella, A., 2009. Estrogenic activity of pharmaceuticals in the aquatic environment. Environ. Int., Pharmaceutical products in the environment: trends toward lowering presence and impact 35, 826–829. https://doi.org/10.1016/j.envint.2008.11.006

Jayaramaiah, R.H., Egidi, E., Macdonald, C.A., Wang, J.-T., Jeffries, T.C., Megharaj, M., Singh, B.K., 2022. Soil initial bacterial diversity and nutrient availability determine the rate of xenobiotic biodegradation. Microb. Biotechnol. 15, 318–336. https://doi.org/10.1111/1751-7915.13946

Joerss, H., Freeling, F., van Leeuwen, S., Hollender, J., Liu, X., Nödler, K., Wang, Z., Yu, B., Zahn, D., Sigmund, G., 2024. Pesticides can be a substantial source of trifluoroacetate (TFA) to water resources. Environ. Int. 193, 109061. https://doi.org/10.1016/j.envint.2024.109061

Johnson, D.R., Helbling, D.E., Men, Y., Fenner, K., 2015. Can meta-omics help to establish causality between contaminant biotransformations and genes or gene products? Environ. Sci. Water Res. Technol. 1, 272–278. https://doi.org/10.1039/C5EW00016E

Jou-Claus, S., Rodríguez-Escales, P., Martínez-Landa, L., Diaz-Cruz, M.S., Carrera, J., Sunyer-Caldú, A., Quintana, G., Valhondo, C., 2024. Assessing the fate of benzophenone-type UV filters and transformation products during soil aquifer treatment: The biofilm compartment as bioaccumulator and biodegrader in porous media. Environ. Sci. Technol. 58, 5472–5482. https://doi.org/10.1021/acs.est.3c08465

Jugder, B.-E., Ertan, H., Bohl, S., Lee, M., Marquis, C.P., Manefield, M., 2016. Organohalide Respiring Bacteria and Reductive Dehalogenases: Key Tools in Organohalide Bioremediation. Front. Microbiol. 7. https://doi.org/10.3389/fmicb.2016.00249

Kennes-Veiga, D.M., Gónzalez-Gil, L., Carballa, M., Lema, J.M., 2022. Enzymatic cometabolic biotransformation of organic micropollutants in wastewater treatment plants: A review. Bioresour. Technol. 344, 126291. https://doi.org/10.1016/j.biortech.2021.126291

Kern, S., Singer, H., Hollender, J., Schwarzenbach, R.P., Fenner, K., 2011. Assessing Exposure to Transformation Products of Soil-Applied Organic Contaminants in Surface Water: Comparison of Model Predictions and Field Data. Environ. Sci. Technol. 45, 2833–2841. https://doi.org/10.1021/es102537b

Kessner, D., Chambers, M., Burke, R., Agus, D., Mallick, P., 2008. ProteoWizard: open source software for rapid proteomics tools development. Bioinformatics 24, 2534–2536. https://doi.org/10.1093/bioinformatics/btn323

Khaledian, Y., Brevik, E.C., Pereira, P., Cerdà, A., Fattah, M.A., Tazikeh, H., 2017. Modeling soil cation exchange capacity in multiple countries. CATENA 158, 194–200. https://doi.org/10.1016/j.catena.2017.07.002

Khemka, R., Eberhard, R., 2025. Scaling Water Reuse: A Tipping Point for Municipal and Industrial Use.

Khemka, R., Lopez, P., Jensen, O., 2023. Scaling up Finance for Water: A WBG Strategic Framework and Roadmap for Action.

Kim, S., Chen, J., Cheng, T., Gindulyte, A., He, J., He, S., Li, Q., Shoemaker, B.A., Thiessen, P.A., Yu, B., Zaslavsky, L., Zhang, J., Bolton, E.E., 2025. PubChem 2025 update. Nucleic Acids Res. 53, D1516–D1525. https://doi.org/10.1093/nar/gkae1059

Kim, S., Chen, J., Cheng, T., Gindulyte, A., He, J., He, S., Li, Q., Shoemaker, B.A., Thiessen, P.A., Yu, B., Zaslavsky, L., Zhang, J., Bolton, E.E., 2023. PubChem 2023 update. Nucleic Acids Res. 51, D1373–D1380. https://doi.org/10.1093/nar/gkac956

Knight, C.G., Nicolitch, O., Griffiths, R.I., Goodall, T., Jones, B., Weser, C., Langridge, H., Davison, J., Dellavalle, A., Eisenhauer, N., Gongalsky, K.B., Hector, A., Jardine, E., Kardol, P., Maestre, F.T., Schädler, M., Semchenko, M., Stevens, C., Tsiafouli, M.A., Vilhelmsson, O., Wanek, W., de Vries, F.T., 2024. Soil microbiomes show consistent and predictable responses to extreme events. Nature 636, 690–696. https://doi.org/10.1038/s41586-024-08185-3

KNMI, R.D.W.I., n.d. Daily weather data in the Netherlands [WWW Document]. URL https://www.knmi.nl/nederland-nu/klimatologie/daggegevens (accessed 3.22.24).

Kodešová, R., Grabic, R., Kočárek, M., Klement, A., Golovko, O., Fér, M., Nikodem, A., Jakšík, O., 2015. Pharmaceuticals' sorptions relative to properties of thirteen different soils. Sci. Total Environ. 511, 435–443. https://doi.org/10.1016/j.scitotenv.2014.12.088

Kondor, A.C., Vancsik, A.V., Bauer, L., Szabó, L., Szalai, Z., Jakab, G., Maász, G., Pedrosa, M., Sampaio, M.J., Lado Ribeiro, A.R., 2024. Efficiency of the bank filtration for removing organic priority substances and contaminants of emerging concern: A critical review. Environ. Pollut. 340, 122795. https://doi.org/10.1016/j.envpol.2023.122795

Krauss, M., Singer, H., Hollender, J., 2010. LC–high resolution MS in environmental analysis: from target screening to the identification of unknowns. Anal. Bioanal. Chem. 397, 943–951. https://doi.org/10.1007/s00216-010-3608-9

Krutz, L.J., Senseman, S.A., McInnes, K.J., Hoffman, D.W., Tierney, D.P., 2004. Adsorption and desorption of metolachlor and metolachlor metabolites in vegetated filter strip and cultivated soil. J. Environ. Qual. 33, 939. https://doi.org/10.2134/jeq2004.0939

Kümmerer, K., 2009. Antibiotics in the aquatic environment – A review – Part I. Chemosphere 75, 417–434. https://doi.org/10.1016/j.chemosphere.2008.11.086

Lange, F.T., Scheurer, M., Brauch, H.-J., 2012. Artificial sweeteners—a recently recognized class of emerging environmental contaminants: a review. Anal. Bioanal. Chem. 403, 2503–2518. https://doi.org/10.1007/s00216-012-5892-z

Lapworth, D.J., Baran, N., Stuart, M.E., Manamsa, K., Talbot, J., 2015. Persistent and emerging micro-organic contaminants in Chalk groundwater of England and France. Environ. Pollut. 203, 214–225. https://doi.org/10.1016/j.envpol.2015.02.030

Lapworth, D.J., Baran, N., Stuart, M.E., Ward, R.S., 2012. Emerging organic contaminants in groundwater: A review of sources, fate and occurrence. Environ. Pollut. 163, 287–303. https://doi.org/10.1016/j.envpol.2011.12.034

Law, V., Knox, C., Djoumbou, Y., Jewison, T., Guo, A.C., Liu, Y., Maciejewski, A., Arndt, D., Wilson, M., Neveu, V., Tang, A., Gabriel, G., Ly, C., Adamjee, S., Dame, Z.T., Han, B., Zhou, Y., Wishart, D.S., 2014. DrugBank 4.0: shedding new light on drug metabolism. Nucleic Acids Res. 42, D1091-1097. https://doi.org/10.1093/nar/gkt1068

Lei, H.-J., Yang, B., Ye, P., Yang, Y.-Y., Zhao, J.-L., Liu, Y.-S., Xie, L., Ying, G.-G., 2021. Occurrence, fate and mass loading of benzodiazepines and their transformation products in eleven wastewater treatment plants in Guangdong province, China. Sci. Total Environ. 755, 142648. https://doi.org/10.1016/j.scitotenv.2020.142648

Letzel, T., Bayer, A., Schulz, W., Heermann, A., Lucke, T., Greco, G., Grosse, S., Schüssler, W., Sengl, M., Letzel, M., 2015. LC–MS screening techniques for wastewater analysis and analytical data handling strategies: Sartans and their transformation products as an example. Chemosphere 137, 198–206. https://doi.org/10.1016/j.chemosphere.2015.06.083

Lewis, K.A., Tzilivakis, J., Warner, D.J., Green, A., 2016. An international database for pesticide risk assessments and management. Hum. Ecol. Risk Assess. Int. J. 22, 1050–1064. https://doi.org/10.1080/10807039.2015.1133242

Li, D., Alidina, M., Ouf, M., Sharp, J.O., Saikaly, P., Drewes, J.E., 2013. Microbial community evolution during simulated managed aquifer recharge in response to different biodegradable dissolved organic carbon (BDOC) concentrations. Water Res. 47, 2421–2430. https://doi.org/10.1016/j.watres.2013.02.012

Li, X.-F., Mitch, W.A., 2018. Drinking Water Disinfection Byproducts (DBPs) and Human Health Effects: Multidisciplinary Challenges and Opportunities. Environ. Sci. Technol. 52, 1681–1689. https://doi.org/10.1021/acs.est.7b05440

Li, Y., Zhu, G., Ng, W.J., Tan, S.K., 2014. A review on removing pharmaceutical contaminants from wastewater by constructed wetlands: Design, performance and mechanism. Sci. Total Environ. 468–469, 908–932. https://doi.org/http://dx.doi.org/10.1016/j.scitotenv.2013.09.018

Lim, S.J., Seo, J., Seid, M.G., Lee, J., Ejerssa, W.W., Lee, D.-H., Jeong, E., Chae, S.H., Lee, Y., Son, M., Hong, S.W., 2023. Clustering micropollutants and estimating rate constants of sorption and biodegradation using machine learning approaches. Npj Clean Water 6, 1–10. https://doi.org/10.1038/s41545-023-00282-6

Lindeboom, R.E.F., 2014. Autogenerative high pressure digestion : biogass production and upgrading in a single step. (PhD Thesis). Wageningen University.

Lindemann, S.R., Bernstein, H.C., Song, H.-S., Fredrickson, J.K., Fields, M.W., Shou, W., Johnson, D.R., Beliaev, A.S., 2016. Engineering microbial consortia for controllable outputs. ISME J. 10, 2077–2084. https://doi.org/10.1038/ismej.2016.26

Liu, F., Fan, F., Yu, Q., Ren, H., Geng, J., 2025. Variable KOC and Poor-Quality Data Sources Cause High Discrepancy in Current Mobility Assessment of Organic Substances. ACS EST Water. https://doi.org/10.1021/acsestwater.4c00731

Liu, S., Ding, R., Nie, X., 2019. Assessment of oxidative stress of paracetamol to *Daphnia magna* via determination of *Nrf1* and genes related to antioxidant system. Aquat. Toxicol. 211, 73–80. https://doi.org/10.1016/j.aquatox.2019.03.014

Liu, S., Zhang, Y., Feng, X., Pyo, S.-H., 2024. Current problems and countermeasures of constructed wetland for wastewater treatment: A review. J. Water Process Eng. 57, 104569. https://doi.org/10.1016/j.jwpe.2023.104569

Liu, Y.-S., Ying, G.-G., Shareef, A., Kookana, R.S., 2013. Biodegradation of three selected benzotriazoles in aquifer materials under aerobic and anaerobic conditions. J. Contam. Hydrol. 151, 131–139. https://doi.org/10.1016/j.jconhyd.2013.05.006

Löffler, D., Römbke, J., Meller, M., Ternes, T.A., 2005. Environmental Fate of Pharmaceuticals in Water/Sediment Systems. Environ. Sci. Technol. 39, 5209–5218. https://doi.org/10.1021/es0484146

Loos, R., Locoro, G., Comero, S., Contini, S., Schwesig, D., Werres, F., Balsaa, P., Gans, O., Weiss, S., Blaha, L., Bolchi, M., Gawlik, B.M., 2010. Pan-European survey on the occurrence of selected polar organic persistent pollutants in ground water. Water Res. 44, 4115–4126. https://doi.org/10.1016/j.watres.2010.05.032

Loos, R., Raquel, C., Diana C., A., Blaha, L., Jarosova, B., Voorspoels, S., Schwesig, D., Haglund, P., Fick, J., Gans, O., Comero, S., Ghiani, M., Lettieri, T., Locoro, G., Paracchini, B., Tavazzi, S., Gawlik, B.M., 2012. EU wide monitoring survey on waste water treatment plant effluents. Publications Office of the European Union, Luxemburg.

Luo, Y., Atashgahi, S., Rijnaarts, H.H.M., Comans, R.N.J., Sutton, N.B., 2019. Influence of different redox conditions and dissolved organic matter on pesticide biodegradation in simulated groundwater systems. Sci. Total Environ. 677, 692–699. https://doi.org/10.1016/j.scitotenv.2019.04.128

Luo, Y.-L., Pan, Y.-R., Wang, X., Wang, Z.-Y., Daigger, G., Ma, J.-X., Tang, L.-H., Liu, J., Ren, N.-Q., Butler, D., 2025. Leveraging the water-environment-health nexus to

characterize sustainable water purification solutions. Nat. Commun. 16, 1269. https://doi.org/10.1038/s41467-025-56656-6

Luu, G.T., Freitas, M.A., Lizama-Chamu, I., McCaughey, C.S., Sanchez, L.M., Wang, M., 2022. TIMSCONVERT: a workflow to convert trapped ion mobility data to open data formats. Bioinformatics 38, 4046–4047. https://doi.org/10.1093/bioinformatics/btac419

Maeng, S.K., Sharma, S.K., Lekkerkerker-Teunissen, K., Amy, G.L., 2011. Occurrence and fate of bulk organic matter and pharmaceutically active compounds in managed aquifer recharge: A review. Water Res. 45, 3015–3033. https://doi.org/10.1016/j.watres.2011.02.017

Malm, L., Liigand, J., Aalizadeh, R., Alygizakis, N., Ng, K., Frøkjær, E.E., Nanusha, M.Y., Hansen, M., Plassmann, M., Bieber, S., Letzel, T., Balest, L., Abis, P.P., Mazzetti, M., Kasprzyk-Hordern, B., Ceolotto, N., Kumari, S., Hann, S., Kochmann, S., Steininger-Mairinger, T., Soulier, C., Mascolo, G., Murgolo, S., Garcia-Vara, M., López de Alda, M., Hollender, J., Arturi, K., Coppola, G., Peruzzo, M., Joerss, H., van der Neut-Marchand, C., Pieke, E.N., Gago-Ferrero, P., Gil-Solsona, R., Licul-Kucera, V., Roscioli, C., Valsecchi, S., Luckute, A., Christensen, J.H., Tisler, S., Vughs, D., Meekel, N., Talavera Andújar, B., Aurich, D., Schymanski, E.L., Frigerio, G., Macherius, A., Kunkel, U., Bader, T., Rostkowski, P., Gundersen, H., Valdecanas, B., Davis, W.C., Schulze, B., Kaserzon, S., Pijnappels, M., Esperanza, M., Fildier, A., Vulliet, E., Wiest, L., Covaci, A., Macan Schönleben, A., Belova, L., Celma, A., Bijlsma, L., Caupos, E., Mebold, E., Le Roux, J., Troia, E., de Rijke, E., Helmus, R., Leroy, G., Haelewyck, N., Chrastina, D., Verwoert, M., Thomaidis, N.S., Kruve, A., 2024. Quantification Approaches in Non-Target LC/ESI/HRMS Analysis: An Interlaboratory Comparison. Anal. Chem. https://doi.org/10.1021/acs.analchem.4c02902

Mansouri, K., Abdelaziz, A., Rybacka, A., Roncaglioni, A., Tropsha, A., Varnek, A., Zakharov, A., Worth, A., Richard, A.M., Grulke, C.M., Trisciuzzi, D., Fourches, D., Horvath, D., Benfenati, E., Muratov, E., Wedebye, E.B., Grisoni, F., Mangiatordi, G.F., Incisivo, G.M., Hong, H., Ng, H.W., Tetko, I.V., Balabin, I., Kancherla, J., Shen, J., Burton, J., Nicklaus, M., Cassotti, M., Nikolov, N.G., Nicolotti, O., Andersson, P.L., Zang, Q., Politi, R., Beger, R.D., Todeschini, R., Huang, R., Farag, S., Rosenberg, S.A., Slavov, S., Hu, X., Judson, R.S., 2016. CERAPP: Collaborative Estrogen Receptor Activity Prediction Project. Environ. Health Perspect. 124, 1023–1033. https://doi.org/10.1289/ehp.1510267

Mansouri, K., Grulke, C.M., Judson, R.S., Williams, A.J., 2018. OPERA models for predicting physicochemical properties and environmental fate endpoints. J. Cheminformatics 10. https://doi.org/https://doi.org/10.1186/s13321-018-0263-1

Mansouri, K., Kleinstreuer, N., Abdelaziz, A.M., Alberga, D., Alves, V.M., Andersson, P.L., Andrade, C.H., Bai, F., Balabin, I., Ballabio, D., Benfenati, E., Bhhatarai, B., Boyer, S., Chen, J., Consonni, V., Farag, S., Fourches, D., García-Sosa, A.T., Gramatica, P., Grisoni, F., Grulke, C.M., Hong, H., Horvath, D., Hu, X., Huang, R., Jeliazkova, N., Li, J., Li, X., Liu, H., Manganelli, S., Mangiatordi, G.F., Maran, U., Marcou, G., Martin, T., Muratov, E., Nguyen, D.-T., Nicolotti, O., Nikolov, N.G., Norinder, U., Papa, E., Petitjean, M., Piir, G., Pogodin, P., Poroikov, V., Qiao, X., Richard, A.M., Roncaglioni, A., Ruiz, P., Rupakheti, C., Sakkiah, S., Sangion, A., Schramm, K.-W., Selvaraj, C.,

Shah, I., Sild, S., Sun, L., Taboureau, O., Tang, Y., Tetko, I.V., Todeschini, R., Tong, W., Trisciuzzi, D., Tropsha, A., Van Den Driessche, G., Varnek, A., Wang, Z., Wedebye, E.B., Williams, A.J., Xie, H., Zakharov, A.V., Zheng, Z., Judson, R.S., 2020. CoMPARA: Collaborative Modeling Project for Androgen Receptor Activity. Environ. Health Perspect. 128, 027002. https://doi.org/10.1289/EHP5580

Martens, L., Chambers, M., Sturm, M., Kessner, D., Levander, F., Shofstahl, J., Tang, W.H., Römpp, A., Neumann, S., Pizarro, A.D., Montecchi-Palazzi, L., Tasman, N., Coleman, M., Reisinger, F., Souda, P., Hermjakob, H., Binz, P.-A., Deutsch, E.W., 2011. mzML--a community standard for mass spectrometry data. Mol. Cell. Proteomics MCP 10, R110.000133. https://doi.org/10.1074/mcp.R110.000133

Martínez-Quintela, M., Balboa, S., Coves, J.R., Omil, F., Suárez, S., 2023. Influence of metabolism and microbiology on organic micropollutants biotransformation in anoxic heterotrophic reactors. J. Hazard. Mater. 442, 129983. https://doi.org/10.1016/j.jhazmat.2022.129983

Martins, T.A.E., Muñoz Sierra, J.D., Nieuwlands, J.A., Lousada-Ferreira, M., Amaral, L., 2024. Micropollutant biotransformation under different redox conditions in *PhoRedox* conventional activated sludge systems. Environ. Technol. Innov. 35, 103639. https://doi.org/10.1016/j.eti.2024.103639

McLachlan, M.S., Zou, H., Gouin, T., 2017. Using Benchmarking To Strengthen the Assessment of Persistence. Environ. Sci. Technol. 51, 4–11. https://doi.org/10.1021/acs.est.6b03786

Meckenstock, R.U., Elsner, M., Griebler, C., Lueders, T., Stumpp, C., Aamand, J., Agathos, S.N., Albrechtsen, H.-J., Bastiaens, L., Bjerg, P.L., Boon, N., Dejonghe, W., Huang, W.E., Schmidt, S.I., Smolders, E., Sørensen, S.R., Springael, D., van Breukelen, B.M., 2015. Biodegradation: Updating the Concepts of Control for Microbial Cleanup in Contaminated Aquifers. Environ. Sci. Technol. 49, 7073–7081. https://doi.org/10.1021/acs.est.5b00715

Meng, P., Pei, H., Hu, W., Shao, Y., Li, Z., 2014. How to increase microbial degradation in constructed wetlands: Influencing factors and improvement measures. Bioresour. Technol. 157, 316–326. https://doi.org/10.1016/j.biortech.2014.01.095

Meringer, M., Reinker, S., Zhang, J., Muller, A., 2011. MS/MS data improves automated determination of molecular formulas by mass spectrometry. MATCH – Commun. Math. Comput. Chem. 65, 259–290.

Mohr, M., Dockhorn, T., Drewes, J.E., Karwat, S., Lackner, S., Lotz, B., Nahrstedt, A., Nocker, A., Schramm, E., Zimmermann, M., 2020. Assuring water quality along multi-barrier treatment systems for agricultural water reuse. J. Water Reuse Desalination 10, 332–346. https://doi.org/10.2166/wrd.2020.039

Monteiro, S.C., Boxall, A.B.A., 2010. Occurrence and fate of human pharmaceuticals in the environment, in: Whitacre, D.M. (Ed.), Reviews of Environmental Contamination and Toxicology. Springer, New York, NY, pp. 53–154. https://doi.org/10.1007/978-1-4419-1157-5_2

Morris, B.E.L., Henneberger, R., Huber, H., Moissl-Eichinger, C., 2013. Microbial syntrophy: interaction for the common good. FEMS Microbiol. Rev. 37, 384–406. https://doi.org/10.1111/1574-6976.12019

Mumberg, T., Ahrens, L., Wanner, P., 2024. Managed aquifer recharge as a potential pathway of contaminants of emerging concern into groundwater systems – A

systematic review. Chemosphere 364, 143030. https://doi.org/10.1016/j.chemosphere.2024.143030

Muntau, M., Schulz, M., Jewell, K.S., Hermes, N., Hübner, U., Ternes, T., Drewes, J.E., 2017. Evaluation of the short-term fate and transport of chemicals of emerging concern during soil-aquifer treatment using select transformation products as intrinsic redox-sensitive tracers. Sci. Total Environ. 583, 10–18. https://doi.org/10.1016/j.scitotenv.2016.12.165

Muschket, M., Neuwald, I.J., Zahn, D., Seelig, A.H., Kuckelkorn, J., Knepper, T.P., Reemtsma, T., 2024. Fate of persistent and mobile chemicals in the water cycle: From municipal wastewater discharges to river bank filtrate. Water Res. 266, 122436. https://doi.org/10.1016/j.watres.2024.122436

Narain-Ford, D.M., Bartholomeus, R.P., Raterman, B.W., van Zaanen, I., ter Laak, T.L., van Wezel, A.P., Dekker, S.C., 2021. Shifting the imbalance: Intentional reuse of Dutch sewage effluent in sub-surface irrigation. Sci. Total Environ. 752, 142214. https://doi.org/10.1016/j.scitotenv.2020.142214

Narain-Ford, D.M., Bartholomeus, R.P., van Wezel, A.P., 2020. Natural purification through soils: Risks and opportunities of sewage effluent reuse in sub-surface irrigation. Reviews of Environmental Contamination and Toxicology 250, 85–117. https://doi.org/https://doi.org/10.1007/398_2020_49

Narain-Ford, D.M., van Wezel, A.P., Helmus, R., Dekker, S.C., Bartholomeus, R.P., 2022. Soil self-cleaning capacity: Removal of organic compounds during sub-surface irrigation with sewage effluent. Water Res. 226, 119303. https://doi.org/10.1016/j.watres.2022.119303

National Cancer Institute, 2024. NCI/CADD Chemical Identifier Resolver [WWW Document]. Chem. Identifier Resolv. URL https://cactus.nci.nih.gov/chemical/structure (accessed 11.5.24).

National Research Council, 1993. In Situ Bioremediation: When Does it Work? National Academies Press, Washington, D.C. https://doi.org/10.17226/2131

Neef, J., Leverenz, D., Launay, M.A., 2022. Performance of Micropollutant Removal during Wet-Weather Conditions in Advanced Treatment Stages on a Full-Scale WWTP. Water 14, 3281. https://doi.org/10.3390/w14203281

Nunes, B., Antunes, S.C., Santos, J., Martins, L., Castro, B.B., 2014. Toxic potential of paracetamol to freshwater organisms: A headache to environmental regulators? Ecotoxicol. Environ. Saf. 107, 178–185. https://doi.org/10.1016/j.ecoenv.2014.05.027

Oberleitner, D., Schmid, R., Schulz, W., Bergmann, A., Achten, C., 2021. Feature-based molecular networking for identification of organic micropollutants including metabolites by non-target analysis applied to riverbank filtration. Anal. Bioanal. Chem. 413, 5291–5300. https://doi.org/10.1007/s00216-021-03500-7

OECD, 2025. Test No. 308: Aerobic and Anaerobic Transformation in Aquatic Sediment Systems. OECD Publ., OECD Guidelines for the Testing of Chemicals, Section 3. https://doi.org/10.1787/9789264070523-en

OECD, 2024. (Q)SAR Assessment Framework: Guidance for the regulatory assessment of (Quantitative) Structure Activity Relationship models and predictions, Second Edition, OECD Series on Testing and Assessment. Organisation for Economic Co-

operation and Development Publishing, Paris. https://doi.org/10.1787/bbdac345-en

OECD, 2004. Test No. 309: Aerobic Mineralisation in Surface Water – Simulation Biodegradation Test. OECD Publ., OECD Guidelines for the Testing of Chemicals, Section 3.

Olvera-Vargas, H., Leroy, S., Rivard, M., Oturan, N., Oturan, M., Buisson, D., 2016. Microbial biotransformation of furosemide for environmental risk assessment: identification of metabolites and toxicological evaluation. Environ. Sci. Pollut. Res. 23, 22691–22700. https://doi.org/10.1007/s11356-016-7398-2

Ore, A., Helmus, R., Narain-Ford, D.M., Bartholomeus, R., Sutton, N.B., Van Wezel, A., 2025a. Presence of micropollutants and transformation products during subsurface irrigation with treated wastewater assessed by non-target screening analysis. ACS EST Water 2025. https://doi.org/https://doi.org/10.1021/acsestwater.4c00930

Ore, A., Palm, E.H., van Wezel, A.P., Sutton, N.B., 2025b. Higher microbial diversity enhances the extent and rate of organic micropollutant biodegradation under aerobic and nitrate-reducing conditions. Water Res. 289, 124921. https://doi.org/10.1016/j.watres.2025.124921

Ore, A., Sigmund, G., Specker, J., Helmus, R., Aguilar-Alarcón, P., Schriks, M., van Wezel, A.P., Sutton, N.B., 2025c. Removal, transport, and transformation of organic micropollutants in managed aquifer recharge: Insights from target and non-target analyses. Water Res. 287, 124409. https://doi.org/10.1016/j.watres.2025.124409

Page, D., Vanderzalm, J., Kumar, A., Cheng, K.Y., Kaksonen, A.H., Simpson, S., 2019. Risks of Perfluoroalkyl and Polyfluoroalkyl Substances (PFAS) for Sustainable Water Recycling via Aquifers. Water 11, 1737. https://doi.org/10.3390/w11081737

Patsch, D., Vliet, S., Marcantini, L.G., Johnson, D.R., 2018. Generality of associations between biological richness and the rates of metabolic processes across microbial communities. Environ. Microbiol. 20, 4356–4368. https://doi.org/10.1111/1462-2920.14352

Peets, P., Wang, W.-C., MacLeod, M., Breitholtz, M., Martin, J.W., Kruve, A., 2022. MS2Tox Machine Learning Tool for Predicting the Ecotoxicity of Unidentified Chemicals in Water by Nontarget LC-HRMS. Environ. Sci. Technol. 56, 15508–15517. https://doi.org/10.1021/acs.est.2c02536

Peng, F.-J., Feng, X.-J., Li, S., Yu, X.-L., Chen, J., Liu, S.-S., Ying, G.-G., Liu, Y.-S., 2025. Removal of emerging organic contaminants in a subsurface wastewater infiltration system: A preliminary study of microbial mechanism. Water Res. 284, 123960. https://doi.org/10.1016/j.watres.2025.123960

Petrie, B., Barden, R., Kasprzyk-Hordern, B., 2015. A review on emerging contaminants in wastewaters and the environment: Current knowledge, understudied areas and recommendations for future monitoring. Water Res., Occurrence, fate, removal and assessment of emerging contaminants in water in the water cycle (from wastewater to drinking water) 72, 3–27. https://doi.org/10.1016/j.watres.2014.08.053

Pett-Ridge, J., Firestone, M.K., 2005. Redox Fluctuation Structures Microbial Communities in a Wet Tropical Soil. Appl. Environ. Microbiol. 71, 6998–7007. https://doi.org/10.1128/AEM.71.11.6998-7007.2005

Philippot, L., Spor, A., Hénault, C., Bru, D., Bizouard, F., Jones, C.M., Sarr, A., Maron, P.-A., 2013. Loss in microbial diversity affects nitrogen cycling in soil. ISME J. 7, 1609–1619. https://doi.org/10.1038/ismej.2013.34

Piai, L., Dykstra, J.E., Adishakti, M.G., Blokland, M., Langenhoff, A.A.M., van der Wal, A., 2019. Diffusion of hydrophilic organic micropollutants in granular activated carbon with different pore sizes. Water Res. 162, 518–527. https://doi.org/10.1016/j.watres.2019.06.012

Pistocchi, A., Alygizakis, N.A., Brack, W., Boxall, A., Cousins, I.T., Drewes, J.E., Finckh, S., Gallé, T., Launay, M.A., McLachlan, M.S., Petrovic, M., Schulze, T., Slobodnik, J., Ternes, T., Van Wezel, A., Verlicchi, P., Whalley, C., 2022. European scale assessment of the potential of ozonation and activated carbon treatment to reduce micropollutant emissions with wastewater. Sci. Total Environ. 848, 157124. https://doi.org/10.1016/j.scitotenv.2022.157124

Posselt, M., Mechelke, J., Rutere, C., Coll, C., Jaeger, A., Raza, M., Meinikmann, K., Krause, S., Sobek, A., Lewandowski, J., Horn, M.A., Hollender, J., Benskin, J.P., 2020. Bacterial Diversity Controls Transformation of Wastewater-Derived Organic Contaminants in River-Simulating Flumes. Environ. Sci. Technol. 54, 5467–5479. https://doi.org/10.1021/acs.est.9b06928

Poursat, B.A.J., van Spanning, R.J.M., de Voogt, P., Parsons, J.R., 2019. Implications of microbial adaptation for the assessment of environmental persistence of chemicals. Crit. Rev. Environ. Sci. Technol. 49, 2220–2255. https://doi.org/10.1080/10643389.2019.1607687

Pronk, G.J., Stofberg, S.F., Van Dooren, T.C.G.W., Dingemans, M.M.L., Frijns, J., Koeman-Stein, N.E., Smeets, P.W.M.H., Bartholomeus, R.P., 2021. Increasing Water System Robustness in the Netherlands: Potential of Cross-Sectoral Water Reuse. Water Resour. Manag. 35, 3721–3735. https://doi.org/10.1007/s11269-021-02912-5

Pujar, N.K., Premakshi, H.G., Ganeshkar, M.P., Kamanavalli, C.M., 2022. Biodegradation of Pesticides Used in Agriculture by Soil Microorganisms, in: Mulla, S.I., Bharagava, R.N. (Eds.), Enzymes for Pollutant Degradation, Microorganisms for Sustainability. Springer Nature, Singapore, pp. 213–235. https://doi.org/10.1007/978-981-16-4574-7_11

R Core Team, 2024. R: A Language and Environment for Statistical Computing.

Rauch-Williams, T., Hoppe-Jones, C., Drewes, J.E., 2010. The role of organic matter in the removal of emerging trace organic chemicals during managed aquifer recharge. Water Res. 44, 449–460. https://doi.org/10.1016/j.watres.2009.08.027

Redeker, M., Wick, A., Meermann, B., Ternes, T.A., 2018. Anaerobic Transformation of the Iodinated X-ray Contrast Medium Iopromide, Its Aerobic Transformation Products, and Transfer to Further Iodinated X-ray Contrast Media. Environ. Sci. Technol. 52, 8309–8320. https://doi.org/10.1021/acs.est.8b01140

Reemtsma, T., Berger, U., Arp, H.P.H., Gallard, H., Knepper, T.P., Neumann, M., Quintana, J.B., Voogt, P. de, 2016. Mind the gap: Persistent and mobile organic compounds—Water contaminants that slip through. Environ. Sci. Technol. 50, 10308–10315. https://doi.org/10.1021/acs.est.6b03338

Regnery, J., Gerba, C.P., Dickenson, E.R.V., Drewes, J.E., 2017. The importance of key attenuation factors for microbial and chemical contaminants during managed

aquifer recharge: A review. Crit. Rev. Environ. Sci. Technol. 47, 1409–1452. https://doi.org/10.1080/10643389.2017.1369234

Regnery, J., Lee, J., Kitanidis, P., Illangasekare, T., Sharp, J.O., Drewes, J.E., 2013. Integration of Artificial Recharge and Recovery Systems for Impaired Water Sources in Urban Settings: Overcoming Current Limitations and Engineering Challenges. Environ. Eng. Sci. 30, 409–420. https://doi.org/10.1089/ees.2012.0186

Regnery, J., Wing, A.D., Kautz, J., Drewes, J.E., 2016. Introducing sequential managed aquifer recharge technology (SMART) – From laboratory to full-scale application. Chemosphere 154, 8–16. https://doi.org/10.1016/j.chemosphere.2016.03.097

Revitt, D.M., Lundy, L., Fatta-Kassinos, D., 2021. Development of a qualitative approach to assessing risks associated with the use of treated wastewater in agricultural irrigation. J. Hazard. Mater. 406, 124286. https://doi.org/10.1016/j.jhazmat.2020.124286

Rich, S.L., Hafner, J., Salz, M., Qanbarzadeh, M., Geng, F., Yan, L., Liu, J., Helbling, D.E., Higgins, C.P., Fenner, K., 2025. FAIR and Effective Communication of Data on Chemical Contaminant Biotransformation in the Environment. Environ. Sci. Technol. Lett. https://doi.org/10.1021/acs.estlett.5c00753

Rios-Miguel, A.B., Smith, G.J., Cremers, G., van Alen, T., Jetten, M.S.M., Op den Camp, H.J.M., Welte, C.U., 2022. Microbial paracetamol degradation involves a high diversity of novel amidase enzyme candidates. Water Res. X 16, 100152. https://doi.org/10.1016/j.wroa.2022.100152

Rios-Miguel, A.B., van Bergen, T.J.H.M., Zillien, C., Ragas, A.M.J., van Zelm, R., Jetten, M.S.M., Hendriks, A.J., Welte, C.U., 2023. Predicting and improving the microbial removal of organic micropollutants during wastewater treatment: A review. Chemosphere 333, 138908. https://doi.org/10.1016/j.chemosphere.2023.138908

Rivett, M.O., Buss, S.R., Morgan, P., Smith, J.W.N., Bemment, C.D., 2008. Nitrate attenuation in groundwater: A review of biogeochemical controlling processes. Water Res. 42, 4215–4232. https://doi.org/10.1016/j.watres.2008.07.020

Roberts, P.V., McCarty, P.L., Reinhard, M., Schreiner, J., 1980. Organic Contaminant Behavior during Groundwater Recharge. J. Water Pollut. Control Fed. 52, 161–172.

Röst, H.L., Sachsenberg, T., Aiche, S., Bielow, C., Weisser, H., Aicheler, F., Andreotti, S., Ehrlich, H.-C., Gutenbrunner, P., Kenar, E., Liang, X., Nahnsen, S., Nilse, L., Pfeuffer, J., Rosenberger, G., Rurik, M., Schmitt, U., Veit, J., Walzer, M., Wojnar, D., Wolski, W.E., Schilling, O., Choudhary, J.S., Malmström, L., Aebersold, R., Reinert, K., Kohlbacher, O., 2016. OpenMS: a flexible open-source software platform for mass spectrometry data analysis. Nat. Methods 13, 741–748. https://doi.org/10.1038/nmeth.3959

Rutere, C., 2020. Microbial degradation of organic micropollutants in hyporheic zone sediments (Doctoral thesis).

Rutere, C., Posselt, M., Ho, A., Horn, M.A., 2021. Biodegradation of metoprolol in oxic and anoxic hyporheic zone sediments: unexpected effects on microbial communities. Appl. Microbiol. Biotechnol. 105, 6103–6115. https://doi.org/10.1007/s00253-021-11466-w

Ruttkies, C., Schymanski, E.L., Wolf, S., Hollender, J., Neumann, S., 2016. MetFrag relaunched: incorporating strategies beyond in silico fragmentation. J. Cheminformatics 8, 3. https://doi.org/10.1186/s13321-016-0115-9

Sadia, M., Beut, L.B., Pranić, M., Wezel, A.P. van, Laak, T.L. ter, 2024. Sorption of per- and poly-fluoroalkyl substances and their precursors on activated carbon under realistic drinking water conditions: Insights into sorbent variability and PFAS structural effects. Heliyon 10. https://doi.org/10.1016/j.heliyon.2024.e25130

Schaffer, M., Börnick, H., Nödler, K., Licha, T., Worch, E., 2012. Role of cation exchange processes on the sorption influenced transport of cationic β-blockers in aquifer sediments. Water Res. 46, 5472–5482. https://doi.org/10.1016/j.watres.2012.07.013

Schaper, J.L., Posselt, M., Bouchez, C., Jaeger, A., Nuetzmann, G., Putschew, A., Singer, G., Lewandowski, J., 2019. Fate of Trace Organic Compounds in the Hyporheic Zone: Influence of Retardation, the Benthic Biolayer, and Organic Carbon. Environ. Sci. Technol. 53, 4224–4234. https://doi.org/10.1021/acs.est.8b06231

Schepens, M., te Biesebeek, J., Hartmann, J., van der Aa, N., Zijlstra, R., Boon, P., 2023. Risk assessment of exposure to PFAS through food and drinking water in the Netherlands. Rijksinstituut voor Volksgezondheid en Milieu RIVM. https://doi.org/10.21945/RIVM-2023-0011

Schmid, R., Heuckeroth, S., Korf, A., Smirnov, A., Myers, O., Dyrlund, T.S., Bushuiev, R., Murray, K.J., Hoffmann, N., Lu, M., Sarvepalli, A., Zhang, Z., Fleischauer, M., Dührkop, K., Wesner, M., Hoogstra, S.J., Rudt, E., Mokshyna, O., Brungs, C., Ponomarov, K., Mutabdžija, L., Damiani, T., Pudney, C.J., Earll, M., Helmer, P.O., Fallon, T.R., Schulze, T., Rivas-Ubach, A., Bilbao, A., Richter, H., Nothias, L.-F., Wang, M., Orešič, M., Weng, J.-K., Böcker, S., Jeibmann, A., Hayen, H., Karst, U., Dorrestein, P.C., Petras, D., Du, X., Pluskal, T., 2023. Integrative analysis of multimodal mass spectrometry data in MZmine 3. Nat. Biotechnol. 41, 447–449. https://doi.org/10.1038/s41587-023-01690-2

Schulz, M., Löffler, D., Wagner, M., Ternes, T.A., 2008. Transformation of the X-ray Contrast Medium Iopromide In Soil and Biological Wastewater Treatment. Environ. Sci. Technol. 42, 7207–7217. https://doi.org/doi/10.1021/es800789r

Schulze, B., van Herwerden, D., Allan, I., Bijlsma, L., Etxebarria, N., Hansen, M., Merel, S., Vrana, B., Aalizadeh, R., Bajema, B., Dubocq, F., Coppola, G., Fildier, A., Fialová, P., Frøkjær, E., Grabic, R., Gago-Ferrero, P., Gravert, T., Hollender, J., Huynh, N., Jacobs, G., Jonkers, T., Kaserzon, S., Lamoree, M., Le Roux, J., Mairinger, T., Margoum, C., Mascolo, G., Mebold, E., Menger, F., Miège, C., Meijer, J., Moilleron, R., Murgolo, S., Peruzzo, M., Pijnappels, M., Reid, M., Roscioli, C., Soulier, C., Valsecchi, S., Thomaidis, N., Vulliet, E., Young, R., Samanipour, S., 2021. Inter-laboratory mass spectrometry dataset based on passive sampling of drinking water for non-target analysis. Sci. Data 8, 223. https://doi.org/10.1038/s41597-021-01002-w

Schymanski, E., Bolton, E., Cheng, T., Thiessen, P., Zhang, J. (Jeff), Helmus, R., Blanke, G., 2024. Transformations in PubChem - Full Dataset. https://doi.org/10.5281/zenodo.10998412

Schymanski, E.L., Bolton, E.E., 2022. FAIRifying the exposome journal: Templates for chemical structures and transformations. Exposome 2, osab006. https://doi.org/10.1093/exposome/osab006

Schymanski, E.L., Jeon, J., Gulde, R., Fenner, K., Ruff, M., Singer, H.P., Hollender, J., 2014a. Identifying Small Molecules via High Resolution Mass Spectrometry: Communicating Confidence. Environ. Sci. Technol. 48, 2097–2098. https://doi.org/10.1021/es5002105

Schymanski, E.L., Singer, H.P., Longrée, P., Loos, M., Ruff, M., Stravs, M.A., Ripollés Vidal, C., Hollender, J., 2014b. Strategies to Characterize Polar Organic Contamination in Wastewater: Exploring the Capability of High Resolution Mass Spectrometry. Environ. Sci. Technol. 48, 1811–1818. https://doi.org/10.1021/es4044374

Schymanski, E.L., Singer, H.P., Slobodnik, J., Ipolyi, I.M., Oswald, P., Krauss, M., Schulze, T., Haglund, P., Letzel, T., Grosse, S., Thomaidis, N.S., Bletsou, A., Zwiener, C., Ibáñez, M., Portolés, T., de Boer, R., Reid, M.J., Onghena, M., Kunkel, U., Schulz, W., Guillon, A., Noyon, N., Leroy, G., Bados, P., Bogialli, S., Stipaničev, D., Rostkowski, P., Hollender, J., 2015. Non-target screening with high-resolution mass spectrometry: critical review using a collaborative trial on water analysis. Anal. Bioanal. Chem. 407, 6237–6255. https://doi.org/10.1007/s00216-015-8681-7

Sepman, H., Malm, L., Peets, P., MacLeod, M., Martin, J., Breitholtz, M., Kruve, A., 2023. Bypassing the Identification: MS2Quant for Concentration Estimations of Chemicals Detected with Nontarget LC-HRMS from MS2 Data. Anal. Chem. 95, 12329–12338. https://doi.org/10.1021/acs.analchem.3c01744

Seth, N., Vats, S., Lakhanpaul, S., Arafat, Y., Mazumdar-Leighton, S., Bansal, M., Babu, C.R., 2024. Microbial community diversity of an integrated constructed wetland used for treatment of sewage. Front. Microbiol. 15. https://doi.org/10.3389/fmicb.2024.1355718

Shamshad, J., Rehman, R.U., 2025. Innovative approaches to sustainable wastewater treatment: a comprehensive exploration of conventional and emerging technologies. Environ. Sci. Adv. 4, 189–222. https://doi.org/10.1039/D4VA00136B

Sidhu, J.P.S., Ahmed, W., Gernjak, W., Aryal, R., McCarthy, D., Palmer, A., Kolotelo, P., Toze, S., 2013. Sewage pollution in urban stormwater runoff as evident from the widespread presence of multiple microbial and chemical source tracking markers. Sci. Total Environ. 463–464, 488–496. https://doi.org/10.1016/j.scitotenv.2013.06.020

Sigmund, G., Arp, H.P.H., Aumeier, B.M., Bucheli, T.D., Chefetz, B., Chen, W., Droge, S.T.J., Endo, S., Escher, B.I., Hale, S.E., Hofmann, T., Pignatello, J., Reemtsma, T., Schmidt, T.C., Schönsee, C.D., Scheringer, M., 2022. Sorption and mobility of charged organic compounds: How to confront and overcome limitations in their assessment. Environ. Sci. Technol. 56, 4702–4710. https://doi.org/10.1021/acs.est.2c00570

Silva, J.G.M., Oliveira, G.R. de, Oliveira, Á.C. de, Albuquerque, A.F. de, Vacchi, F.I., Suares-Rocha, P., Umbuzeiro, G. de A., 2025. Acute immobilization assay with *Daphnia similis*: A miniaturized protocol. NAM J. 1, 100010. https://doi.org/10.1016/j.namjnl.2025.100010

Sinclair, C.J., Boxall, A.B.A., 2003. Assessing the Ecotoxicity of Pesticide Transformation Products. Environ. Sci. Technol. 37, 4617–4625. https://doi.org/10.1021/es030038m

Singh, B.K., Quince, C., Macdonald, C.A., Khachane, A., Thomas, N., Al-Soud, W.A., Sørensen, S.J., He, Z., White, D., Sinclair, A., Crooks, B., Zhou, J., Campbell, C.D., 2014. Loss of microbial diversity in soils is coincident with reductions in some specialized functions. Environ. Microbiol. 16, 2408–2420. https://doi.org/10.1111/1462-2920.12353

Sithamparanathan, E., Kujawa-Roeleveld, K., Soedarso, J.A.R., Sutton, N.B., Grolle, K., Bruning, H., Rijnaarts, H.H.M., 2021. Sorption of micropollutants to hydroponic substrata: Effects of physico-chemical properties. Environ. Adv. 4, 100049. https://doi.org/10.1016/j.envadv.2021.100049

Specker, J.C., Praetorius, A., de Baat, M.L., Sutton, N.B., van Wezel, A.P., 2025. Risk characterisation of chemicals of emerging concern in real-life water reuse applications. Environ. Int. 195, 109226. https://doi.org/10.1016/j.envint.2024.109226

Sprenger, C., Hartog, N., Hernández, M., Vilanova, E., Grützmacher, G., Scheibler, F., Hannappel, S., 2017. Inventory of managed aquifer recharge sites in Europe: historical development, current situation and perspectives. Hydrogeol. J. 25, 1909–1922. https://doi.org/10.1007/s10040-017-1554-8

Stadler, L.B., Delgado Vela, J., Jain, S., Dick, G.J., Love, N.G., 2018. Elucidating the impact of microbial community biodiversity on pharmaceutical biotransformation during wastewater treatment. Microb. Biotechnol. 11, 995–1007. https://doi.org/10.1111/1751-7915.12870

Stadler, L.B., Ernstoff, A.S., Aga, D.S., Love, N.G., 2012. Micropollutant Fate in Wastewater Treatment: Redefining "Removal." Environ. Sci. Technol. 46, 10485–10486. https://doi.org/10.1021/es303478w

Stamper, D.M., Tuovinen, O.H., 1998. Biodegradation of the acetanilide herbicides alachlor, metolachlor, and propachlor. Crit. Rev. Microbiol. 24, 1–22. https://doi.org/10.1080/10408419891294163

Stiegler, A.N., Cecchetti, A.R., Scholes, R.C., Sedlak, D.L., 2023. Persistent Trace Organic Contaminants Are Transformed Rapidly under Sulfate- and Fe(III)-Reducing Conditions in a Nature-Based Subsurface Water Treatment System. Environ. Sci. Technol. 57, 16616–16627. https://doi.org/10.1021/acs.est.3c03719

Stravs, M.A., Pomati, F., Hollender, J., 2019. Biodiversity Drives Micropollutant Biotransformation in Freshwater Phytoplankton Assemblages. Environ. Sci. Technol. 53, 4265–4273. https://doi.org/10.1021/acs.est.8b07018

Sturm, S., Freeling, F., Bauer, F., Vollmer, T., aus der Beek, T., Karges, U., 2022. Trifluoroacetate (TFA): Laying the foundations for effective mitigation - Spatial analysis of the input pathways into the water cycle (No. (UBA-FB) FB001274/ENG), TEXTE 167/2023. German Environmental Agency, Dessau-Roßlau.

Stuyfzand, P.J., Segers, W., van Rooijen, N., 2007. Behavior of pharmaceuticals and other emerging pollutants in various artificial recharge systems in the Netherlands, in: ISMAR6. Presented at the Management of aquifer recharge for sustainability, pp. 231–245.

Summers, R.M., Mohanty, S.K., Gopishetty, S., Subramanian, M., 2015. Genetic characterization of caffeine degradation by bacteria and its potential applications. Microb. Biotechnol. 8, 369–378. https://doi.org/10.1111/1751-7915.12262

Sun, Y., Zhao, L., Li, X., Hao, Y., Xu, H., Weng, L., Li, Y., 2019. Stimulation of earthworms (*Eisenia fetida*) on soil microbial communities to promote metolachlor degradation. Environ. Pollut. 248, 219–228. https://doi.org/10.1016/j.envpol.2019.01.058

Tang, D.W.S., Bartholomeus, R.P., Ritsema, C.J., 2024a. Wastewater irrigation beneath the water table: analytical model of crop contamination risks. Agric. Water Manag. 298, 108848. https://doi.org/10.1016/j.agwat.2024.108848

Tang, D.W.S., van der Zee, S.E.A.T.M., 2021. Dispersion and recovery of solutes and heat under cyclic radial advection. J. Hydrol. 602, 126713. https://doi.org/10.1016/j.jhydrol.2021.126713

Tang, D.W.S., Van der Zee, S.E.A.T.M., Bartholomeus, R.P., 2024b. Phreatic zone wastewater irrigation: Sensitivity analysis of contaminant fate. J. Hydrol. 645, 132263. https://doi.org/10.1016/j.jhydrol.2024.132263

Tang, D.W.S., Van der Zee, S.E.A.T.M., Narain-Ford, D.M., van den Eertwegh, G.A.P.H., Bartholomeus, R.P., 2023a. Managed phreatic zone recharge for irrigation and wastewater treatment. J. Hydrol. 626, 130208. https://doi.org/10.1016/j.jhydrol.2023.130208

Tang, D.W.S., Van der Zee, S.E.A.T.M., Narain-Ford, D.M., van den Eertwegh, G.A.P.H., Bartholomeus, R.P., 2023b. Managed phreatic zone recharge for irrigation and wastewater treatment. J. Hydrol. 626, 130208. https://doi.org/10.1016/j.jhydrol.2023.130208

Tardy, V., Mathieu, O., Lévêque, J., Terrat, S., Chabbi, A., Lemanceau, P., Ranjard, L., Maron, P.-A., 2014. Stability of soil microbial structure and activity depends on microbial diversity. Environ. Microbiol. Rep. 6, 173–183. https://doi.org/10.1111/1758-2229.12126

Teodosiu, C., Gilca, A.-F., Barjoveanu, G., Fiore, S., 2018. Emerging pollutants removal through advanced drinking water treatment: A review on processes and environmental performances assessment. J. Clean. Prod. 197, 1210–1221. https://doi.org/10.1016/j.jclepro.2018.06.247

Tian, S., Feunang, Y.D., Oler, E., Wang, F., Greiner, R., Palm, E.H., Schymanski, E.L., Wishart, D.S., 2025. BioTransformer4.0 a comprehensive computational tool for small molecule metabolism prediction. https://doi.org/10.1101/2025.07.28.667289

Tran, N.H., Urase, T., Ngo, H.H., Hu, J., Ong, S.L., 2013. Insight into metabolic and cometabolic activities of autotrophic and heterotrophic microorganisms in the biodegradation of emerging trace organic contaminants. Bioresour. Technol. 146, 721–731. https://doi.org/10.1016/j.biortech.2013.07.083

Tröger, R., Köhler, S.J., Franke, V., Bergstedt, O., Wiberg, K., 2020. A case study of organic micropollutants in a major Swedish water source – Removal efficiency in seven drinking water treatment plants and influence of operational age of granulated active carbon filters. Sci. Total Environ. 706, 135680. https://doi.org/10.1016/j.scitotenv.2019.135680

UBA, 2020. Trifluoressigsäure (No. ENTWURF_TFA_UQN_Datenblatt). German Environmental Agency.

Ulrich, N., Endo, S., Brown, T.N., Watanabe, N., Bronner, G., Abraham, M.H., Goss, K.-U., 2017. UFZ - LSER Database.

UN World Water Assessment Programme, 2015. The United Nations World Water Development Report 2015: Water for a Sustainable World., UN World Water Development Report. UNESCO, Paris.

Underwood, J.C., Harvey, R.W., Metge, D.W., Repert, D.A., Baumgartner, L.K., Smith, R.L., Roane, T.M., Barber, L.B., 2011. Effects of the Antimicrobial Sulfamethoxazole on Groundwater Bacterial Enrichment. Environ. Sci. Technol. 45, 3096–3101. https://doi.org/10.1021/es103605e

United Nations, 2024a. World Population Prospects 2024: Summary of Results | DESA Publications (No. UN DESA/POP/2024/TR/NO. 9). United Nations, New York, NY.

United Nations, 2024b. The United Nations World Water Development Report 2024: water for prosperity and peace. UNESCO, Paris.

United Nations Department of Economic and Social Affairs, 2025. The Sustainable Development Goals Report 2025. New York, NY.

UN-Water, 2018. The United Nations World Water Development Report 2018 - Nature Based Solutions for Water. UNESCO, Paris.

US EPA, 2025. Estimation Programs Interface Suite™ for Microsoft® Windows.

Wang, J., de Ridder, D., Sutton, N.B., Poursat, B.A.J., Saha, P., van der Wal, A., 2023. The abiotic removal of organic micropollutants with iron and manganese oxides in rapid sand filters for groundwater treatment. Water Res. 241, 120146. https://doi.org/10.1016/j.watres.2023.120146

Wang, J., Poursat, B.A.J., Feng, J., de Ridder, D., Zhang, C., van der Wal, A., Sutton, N.B., 2022. Exploring organic micropollutant biodegradation under dynamic substrate loading in rapid sand filters. Water Res. 221, 118832. https://doi.org/10.1016/j.watres.2022.118832

Wang, Y., Tian, Y.-S., Gao, J.-J., Xu, J., Li, Z.-J., Fu, X.-Y., Han, H.-J., Wang, L.-J., Zhang, W.-H., Deng, Y.-D., Qian, C., Zuo, Z.-H., Wang, B., Peng, R.-H., Yao, Q.-H., 2023. Complete biodegradation of the oldest organic herbicide 2,4-Dichlorophenoxyacetic acid by engineering *Escherichia coli*. J. Hazard. Mater. 451, 131099. https://doi.org/10.1016/j.jhazmat.2023.131099

White, D., Lapworth, D.J., Civil, W., Williams, P., 2019. Tracking changes in the occurrence and source of pharmaceuticals within the River Thames, UK; from source to sea. Environ. Pollut. 249, 257–266. https://doi.org/10.1016/j.envpol.2019.03.015

Wicker, J., Lorsbach, T., Gütlein, M., Schmid, E., Latino, D., Kramer, S., Fenner, K., 2016. enviPath – The environmental contaminant biotransformation pathway resource. Nucleic Acids Res. 44, D502–D508. https://doi.org/10.1093/nar/gkv1229

Winkler, M.-K.H., Kleerebezem, R., de Bruin, L.M.M., Verheijen, P.J.T., Abbas, B., Habermacher, J., van Loosdrecht, M.C.M., 2013. Microbial diversity differences within aerobic granular sludge and activated sludge flocs. Appl. Microbiol. Biotechnol. 97, 7447–7458. https://doi.org/10.1007/s00253-012-4472-7

Wishart, D.S., Tian, S., Allen, D., Oler, E., Peters, H., Lui, V.W., Gautam, V., Djoumbou-Feunang, Y., Greiner, R., Metz, T.O., 2022. BioTransformer 3.0—a web server for accurately predicting metabolic transformation products. Nucleic Acids Res. 50, W115–W123. https://doi.org/10.1093/nar/gkac313

Yan, X., Liu, D., de Smit, S.M., Komin, V., Buisman, C.J.N., ter Heijne, A., 2024. Oxygen-to-ammonium-nitrogen ratio as an indicator for oxygen supply management in microoxic bioanodic ammonium oxidation. Water Res. 261, 121993. https://doi.org/10.1016/j.watres.2024.121993

Yu, C.L., Kale, Y., Gopishetty, S., Louie, T.M., Subramanian, M., 2008. A Novel Caffeine Dehydrogenase in Pseudomonas sp. Strain CBB1 Oxidizes Caffeine to Trimethyluric Acid. J. Bacteriol. 190, 772–776. https://doi.org/10.1128/jb.01390-07

Yuan, J., Van Dyke, M.I., Huck, P.M., 2017. Identification of critical contaminants in wastewater effluent for managed aquifer recharge. Chemosphere 172, 294–301. https://doi.org/10.1016/j.chemosphere.2016.12.120

Yuh, H., Schartman, E., Tritz, K., 2020. Vapor Adsorption Distillation for Renewable, High-Efficiency, Low-Cost, Zero Discharge Desalination (No. 231). Bureau of Reclamation, Denver, Colorado.

Zahn, D., Arp, H.P.H., Fenner, K., Georgi, A., Hafner, J., Hale, S.E., Hollender, J., Letzel, T., Schymanski, E.L., Sigmund, G., Reemtsma, T., 2024. Should transformation products change the way we manage chemicals? Environ. Sci. Technol. 58, 7710–7718. https://doi.org/10.1021/acs.est.4c00125

Zakhia, A., Balestra, L.B., Dhainaut, J., Merlier, F., Boussetta, N., 2025. Review on the removal and degradation methods of chloridazon and its metabolites. Sep. Purif. Technol. 376, 133998. https://doi.org/10.1016/j.seppur.2025.133998

Zhang, L., Hu, J., Zhu, R., Zhou, Q., Chen, J., 2013. Degradation of paracetamol by pure bacterial cultures and their microbial consortium. Appl. Microbiol. Biotechnol. 97, 3687–3698. https://doi.org/10.1007/s00253-012-4170-5

Zhao, M.-L., Fu, J., Ji, X., Zhang, J., He, Z., Yang, G.-P., 2024. Comprehensive analysis of benzothiazoles (BTHs), benzotriazoles (BTRs), and benzotriazole ultraviolet absorbers (BUVs) in the western South China Sea: Spatial distributions, migration tendencies and ecotoxicological relevance. Water Res. 266, 122372. https://doi.org/10.1016/j.watres.2024.122372

Zhou, T., Brunetti, G., Ruud, N., Šimůnek, J., Cui, W., Liao, A., Nasta, P., Gao, J., Levintal, E., García, C.P., Dahlke, H.E., 2025. Simulation of pesticide transport in 70-m-thick soil profiles in response to large water applications. J. Hazard. Mater. 489, 137517. https://doi.org/10.1016/j.jhazmat.2025.137517

Summary

Summary

Freshwater scarcity increasingly challenges the stability and reliability of water supply systems. Currently, half the global population experiences water scarcity at least part of the year, while one quarter lives in water-scarce regions year-round. This situation is expected to worsen due to climate change and population growth, which will further reduce water availability and increase demand. Water reuse is therefore essential to reduce the gap between demand and supply, but improved water management strategies are necessary.

The subsurface has great potential for water reuse. It provides natural storage for surplus water during wet seasons, which can be reused during water-scarce periods, and it can improve water quality through soil passage. Managed aquifer recharge (MAR) technologies have been used for decades to ensure a more stable quantity and a higher quality of water for drinking water production compared to direct use of surface water. Different water sources can be infiltrated in MAR, such as treated wastewater and surface water. However, these sources often contain organic micropollutants (OMPs) that may compromise the groundwater quality. OMPs are a wide range of chemicals, including pharmaceuticals, pesticides, industrial chemicals, and their transformation products (TPs), which can be detected in the environment at concentrations ranging from ng/L to µg/L. Although some are included in monitoring programs for the quality of treated effluents, surface water, and groundwater, regulatory frameworks target only a limited subset of OMPs, overlooking numerous potentially hazardous compounds, particularly TPs. A more complete characterization of reused water sources is needed to establish safe and sustainable water reuse.

Moreover, the fate of OMPs entering the subsurface remains uncertain. A combination of factors plays a role in determining whether OMPs are transported unchanged with the water flow, retained in soil and aquifers, or (further) transformed into TPs. These factors include molecular properties (e.g., charge state) and environmental conditions (e.g., subsurface redox conditions). The extent of their influence on OMP fate and transformation needs further investigation, especially under anaerobic conditions typical of the subsurface. Previous MAR studies focused mainly on the removal of OMPs to evaluate water quality improvements, while transformation into TPs, potentially more persistent and toxic, needs further investigation.

This thesis aimed to provide new insights into the occurrence and fate of OMPs and their TPs in reused water and in the subsurface. To achieve this, we combined field investigations (Chapters 2 and 3) and laboratory experiments (Chapters 4 and 5) to better understand the range of OMPs present in reused water, their transport and transformation processes in the subsurface, and the environmental factors influencing OMP transformation. This integrated

approach relied on advanced methods, including target and non-target analytical techniques and in-silico prediction methods.

Chapter 1 introduces the global challenge of water scarcity and the potential of the subsurface to support water reuse for a growing population. It outlines the different factors, both intrinsic molecular characteristics of OMPs and environmental conditions, influencing the fate of OMPs in the subsurface, and identifies the main research gaps that still need to be addressed to achieve a more sustainable and safe water reuse.

In Chapter 2, we investigated a subsurface irrigation system in which treated effluent from a municipal wastewater treatment plant (WWTP) was infiltrated below the surface to irrigate an agricultural field. The study included two years: one with normal precipitation (2017) and one dry year (2019), allowing for the assessment of climate change effects on water quality. Non-target analysis of the WWTP effluent revealed that TPs were prevalent, accounting for up to 80% of all detected OMPs. This finding highlights the need to include TPs in water quality monitoring for a more accurate risk assessment of water reuse. We also studied OMP transport and transformation by analyzing samples collected at different depths close and between infiltration pipes. The results indicated that some OMPs were persistent and reached deeper layers in the field, while the detection of TPs not present in the effluent is a potential indicator of OMP biodegradation. The movement of OMPs in the irrigated field was influenced by several factors, including hydrological conditions: in the dry year, capillary rise and TP formation were enhanced in the vadose zone, whereas under normal precipitation, vertical percolation and movement along the groundwater fluxes were predominant. The main transformation reactions inferred were demethylation and oxidation, both supported by aerobic OMP transformation.

Chapter 3 focuses on a MAR system where surface water (receiving effluents from five WWTP upstream) was infiltrated into the subsurface through infiltration ponds. MAR removal efficiency was evaluated by comparing the quality of infiltrated and abstracted water. Target OMP analysis based on drinking water monitoring programs showed an overall OMP removal of approximately 60%. Non-target analysis, however, revealed the presence of numerous TPs in both the infiltrated and abstracted water, as well as in the finished drinking water. As TPs are overlooked in most water quality monitoring programs, their inclusion is crucial for a more accurate risk assessment of water reuse. Transport and (bio)degradation of OMPs along the flow path towards the main abstraction well was also examined. The combination of charge state and hydrophobicity (log D_{ow}) proved useful for describing and predicting the OMP transport. Persistent, mobile, and negatively charged compounds passed through the system unchanged. For example, PFAS concentrations remained largely stable during soil passage and were detected in the abstracted water. The

detection of TPs not present in the infiltrated water indicated OMP transformation in MAR. However, some of the TPs were more persistent than the parent compounds and were detected in the abstracted water. Overall, while MAR can improve water quality, pre- or post-treatment may still be needed to remove persistent OMPs or those generating persistent TPs.

Chapter 4 presents a laboratory study investigating the effects of microbial diversity on OMP biodegradation and TP formation. Solid-phase dilution-to-extinction was applied to an active inoculum from the subsurface irrigation field (Chapter 2) to create microbial communities with sequentially reduced diversity. Batch experiments with communities at three diversity levels were incubated under aerobic and nitrate-reducing conditions for an initial regrowth period, after which they were spiked with a mixture of 20 OMPs, including pharmaceuticals, pesticides, and industrial chemicals. Over the > 100-day incubation, OMP biodegradation was followed with target LC-MS analysis, while TP formation was tracked through non-target LC-HRMS analysis. High- and medium-diversity communities showed faster rates and more extensive biodegradation, producing more later-generation TPs. In contrast, low diversity communities showed slower and less complete OMP biodegradation. Degradation under nitrate-reducing conditions was slower and less efficient than under aerobic conditions, yet the positive association between biodegradation, TP formation, and diversity remained valid. In-silico predictions with BioTransformer and OPERA models indicated that none of the detected TPs were dead-end, though two showed potential endocrine-disruptive effects. Microbial diversity, therefore, highly influenced OMP biodegradation and TP formation processes, but it is still largely overlooked in standardized persistence tests such as OECD guidelines. Incorporating diversity measures, such as alpha diversity metrics, could improve their environmental relevance.

Chapter 5 further studies the role of redox conditions using batch experiments under aerobic, nitrate-, iron-, and sulfate-reducing conditions using two natural inocula: soil (as in Chapters 2 and 4) and WWTP effluent-impacted ditch. Aerobic conditions supported the highest biodegradation performance, with more OMPs being degraded, higher rates, and more TPs produced, including later-generation TPs. In contrast, sulfate-reducing conditions were the least effective. Biodegradation patterns of most OMPs were redox-dependent also in terms of biodegradation pathway. Redox-specific TPs were detected, indicating different removal pathways likely reflecting distinct microbial community composition under each redox condition. Predictions of TP biodegradability (with Biowin3) and toxicity (with MS2Tox) indicated that TPs were more biodegradable and less toxic compared to their PCs, though a few exceptions with increased toxicity and lower biodegradability potential were observed. Notably, some TPs obtained under anaerobic conditions were less toxic than

those formed under aerobic conditions from the same parent compound. These findings underline the need to account for redox conditions, too, in regulatory assessment of OMP persistence and support the optimization of redox zones in MAR systems.

Finally, Chapter 6 provides a summary and a general discussion of the outcomes of this research, outlining practical implications and future perspectives. Throughout our study, TPs emerged as widespread yet overlooked in water reuse systems. Although our assessment showed that generally TPs produced are less toxic, more biodegradable, and more mobile than the respective parent compounds, some exceptions were observed, highlighting the need for a better representation of TPs in monitoring programs, regulatory frameworks, and standardized persistence assessment. Likewise, in situ environmental conditions should be better considered in the standardized tests. This thesis demonstrated how microbial community characteristics and redox conditions influence the fate of OMPs in the subsurface, dictating their persistence or biodegradation potential. As the subsurface is mainly an anaerobic environment, with redox-shifting layers and consequently different microbial communities, it is important to further unravel OMP biodegradation and TP formation dynamics in such environments. These insights will provide a more realistic understanding of OMP fate in water (re)cycle, supporting a safer and more sustainable water reuse to meet the increasing freshwater demands.

Sommario

Sommario

La scarsità di acqua dolce mette sempre più a dura prova la stabilità e l'affidabilità dei sistemi di approvvigionamento idrico. Attualmente, metà della popolazione mondiale soffre di scarsità d'acqua per almeno una parte dell'anno, mentre un quarto vive in regioni con scarsità d'acqua tutto l'anno. È previsto che questa situazione peggiorerà a causa dei cambiamenti climatici e della crescita demografica, che ridurranno ulteriormente la disponibilità d'acqua e aumenteranno la domanda. Il riutilizzo dell'acqua è quindi essenziale per ridurre il divario tra domanda e offerta, ma sono necessarie migliori strategie di gestione idrica.

Il sottosuolo ha un grande potenziale per tale scopo. Durante le stagioni umide, fornisce spazio per l'immagazzinamento dell'acqua in eccesso, la quale potrà essere riutilizzata nei periodi di siccità, e può inoltre migliorare la sua qualità durante il passaggio attraverso il terreno. Le tecnologie di ricarica gestita delle falde acquifere (in inglese: *Managed Aquifer Recharge* – MAR) sono utilizzate da decenni per garantire una quantità più stabile e una migliore qualità dell'acqua per la produzione di acqua potabile rispetto all'uso diretto delle acque di superficie, quali laghi e fiumi. Diverse risorse idriche possono essere infiltrate tramite MAR, ad esempio le acque reflue trattate e le acque di superficie. Tuttavia, queste fonti spesso contengono microinquinanti organici (in inglese: *Organic MicroPollutants* – OMP) che possono compromettere la qualità delle acque sotterranee. Gli OMP sono un'ampia gamma di sostanze chimiche, tra cui farmaci, pesticidi, prodotti chimici industriali e i loro prodotti di trasformazione (in inglese: *Transformation Products* – TP), che possono essere rilevati nell'ambiente in concentrazioni da ng/L a µg/L. Sebbene alcuni siano inclusi nei programmi di monitoraggio qualità delle acque reflue trattate, delle acque superficiali e delle acque sotterranee, i quadri normativi considerano solo un sottoinsieme limitato di OMP, trascurando numerosi composti potenzialmente pericolosi, in particolare i TP. È dunque necessaria una caratterizzazione più completa delle acque riutilizzate per garantire un riutilizzo sicuro e sostenibile.

Inoltre, il destino degli OMP che entrano nel sottosuolo rimane incerto, in quanto dato da una combinazione di fattori che determina se gli OMP vengano trasportati inalterati con il flusso d'acqua, trattenuti nel suolo o nelle falde acquifere, o (ulteriormente) trasformati in TP. Questi fattori includono proprietà molecolari degli OMP (ad esempio la loro carica elettrica) e condizioni ambientali (come le condizioni di ossidoriduzione - *redox* - del sottosuolo). L'entità della loro influenza sul destino e sulla trasformazione degli OMP necessita ulteriori indagini, soprattutto in condizioni anaerobiche, tipiche del sottosuolo. Studi precedenti riguardanti MAR hanno tenuto conto principalmente della rimozione degli

OMP per valutare i miglioramenti della qualità dell'acqua, tralasciando la trasformazione in TP, che però potrebbero essere più persistenti e tossici.

Questa Tesi si pone come obiettivo quello di fornire nuove conoscenze sulla presenza e sul destino degli OMP e i loro TP nelle acque riutilizzate e nel sottosuolo. Per farlo, abbiamo combinato indagini sul campo (discusse nei Capitoli 2 e 3) ed esperimenti di laboratorio (Capitoli 4 e 5), al fine di comprendere meglio la varietà di OMPs attualmente presenti nelle acque riutilizzate, i loro processi di trasporto e trasformazione nel sottosuolo e i fattori ambientali che influenzano la trasformazione degli OMP. Questo approccio integrato si è basato su metodi avanzati, tra cui tecniche per l'analisi dei microinquinanti target e non-target e metodi di previsione computerizzati.

Il Capitolo 1 introduce il problema della scarsità idrica globale e il potenziale del sottosuolo nel supportare il riutilizzo delle acque in un contesto di crescita demografica. Descrive inoltre i diversi fattori che influenzano il destino degli OMPs nel sottosuolo, includendo sia le caratteristiche molecolari intrinseche degli OMPs che le condizioni ambientali, e individua le principali lacune di ricerca che devono essere colmate per raggiungere un riutilizzo delle acque più sostenibile e sicuro.

Nel Capitolo 2 abbiamo studiato un sistema di subirrigazione in cui l'effluente trattato di un impianto di depurazione municipale veniva infiltrato nel sottosuolo per irrigare un campo agricolo. Lo studio ha considerato due anni: uno con precipitazioni normali (2017) e uno secco (2019), consentendo di valutare l'influenza delle condizioni climatiche sulla qualità dell'acqua. L'analisi non-target dell'effluente ha mostrato che i TP erano prevalenti, rappresentando fino all'80% di tutti gli OMP rilevati. Questo risultato evidenzia la necessità di includere i TP nel monitoraggio della qualità dell'acqua per una più accurata valutazione del rischio di riutilizzo idrico. Sono stati inoltre studiati i processi di trasporto e trasformazione degli OMP tramite l'analisi di campioni prelevati a diverse profondità in prossimità dei tubi di infiltrazione e tra essi. I risultati indicano che alcuni OMP sono persistenti e in grado di raggiungere gli strati più profondi del sottosuolo. Il movimento degli OMPs nel campo irrigato è risultato influenzato da diversi fattori, tra cui le condizioni idrologiche: nell'anno secco, la risalita capillare e la formazione di TP sono stati più accentuati nella zona vicina alla superficie, mentre in condizioni di precipitazioni normali la percolazione verticale e il trasporto lungo i flussi di falda hanno predominato. Il rilevamento nel terreno di TP non presenti nell'effluente è un potenziale indicatore di biodegradazione. Le principali reazioni di trasformazione individuate sono state la demetilazione e l'ossidazione, entrambe favorite da processi aerobici di biodegradazione degli OMPs.

Il Capitolo 3 è focalizzato su un sistema MAR in cui acqua di superficie (da un fiume che riceve gli scarichi di 5 impianti di depurazione) viene attualmente infiltrata nel terreno

tramite dei bacini di infiltrazione. L'efficienza di rimozione degli OMP del sistema è stata valutata confrontando la qualità dell'acqua infiltrata con quella estratta. L'analisi target degli OMP, basata sui programmi di monitoraggio correntemente utilizzati per l'analisi delle acque destinate al consumo umano, ha mostrato una rimozione complessiva di circa il 60%. Tuttavia, l'analisi non-target ha rivelato la presenza di numerosi TP, sia nell'acqua infiltrata che in quella estratta e nell'acqua potabile prodotta. Dato che i TP sono generalmente trascurati nella maggior parte dei programmi di monitoraggio qualità dell'acqua, anche questi risultati sottolineano quanto la loro inclusione sia fondamentale per una accurata valutazione del rischio di riutilizzo idrico. Sono stati inoltre esaminati il trasporto e la (bio)degradazione degli OMP lungo il percorso verso il pozzo di estrazione principale. La combinazione tra carica elettrica e idrofobicità (espressa tramite log D_{ow}) si è dimostrata utile per descrivere e prevedere il trasporto degli OMP nel sottosuolo. Microinquinanti persistenti, mobili e con carica negativa hanno attraversato il sistema pressoché intatti. Ad esempio, le concentrazioni di PFAS (sostanze perfluoroalchiliche di sintesi) sono rimaste praticamente costanti durante il passaggio nel sottosuolo, venendo rilevati persino nell'acqua estratta. Inoltre, il rilevamento di TP nel sottosuolo che non erano presenti nell'acqua infiltrata ha indicato che processi di trasformazione degli OMP avvengono all'interno del sistema MAR. Tuttavia, alcuni TP sono risultati più persistenti dei microinquinanti di partenza e sono stati anch'essi misurati nell'acqua estratta. Nel complesso, sebbene il sistema MAR possa migliorare la qualità dell'acqua, spesso sono necessari trattamenti pre- o post-infiltrazione per rimuovere gli OMP persistenti o quelli che generano TP a loro volta persistenti.

Il Capitolo 4 presenta uno studio di laboratorio sugli effetti della diversità delle popolazioni microbiche sulla biodegradazione degli OMP e sulla formazione di TP. La tecnica di diluizione per estinzione in fase solida è sata applicata a un inoculo attivo proveniente dal campo di subirrigazione descritto nel Capitolo 2, al fine di creare comunità con diversità di speci microbiche progressivamente ridotta. Esperimenti in batch con comunità a tre livelli di diversità sono stati incubati in condizioni aerobiche e nitrato-riducenti per un periodo iniziale di ricrescita, dopo il quale sono stati addizionati con una miscela di 20 OMP, comprendente farmaci, pesticidi e composti industriali. Durante l'incubazione (durata oltre 100 giorni), la biodegradazione degli OMP è stata monitorata mediante analisi target LC-MS, mentre la formazione dei TP tramite analisi non-target LC-HRMS. Le comunità ad alta e media diversità hanno mostrato velocità di biodegradazione più elevate e una degradazione più estesa, producendo un numero maggiore di TP di generazioni successive. Al contrario, le comunità a bassa diversità hanno mostrato una biodegradazione più lenta e meno completa degli OMP. La degradazione in condizioni nitrato-riducenti è risultata più lenta e

meno efficiente rispetto a quella in condizioni aerobiche, ma la correlazione tra biodegradazione, formazione di TP e diversità microbica è rimasta valida in entrambi i casi. Le previsioni computerizzate ottenute con i modelli BioTransformer e OPERA hanno indicato che nessuno dei TP rilevati rappresentava un punto terminale di degradazione, sebbene due di essi mostrassero un potenziale effetto di interferenza endocrina. In conclusione, la diversità microbica ha un'influenza significativa sui processi di biodegradazione degli OMP e di formazione di TP, ma è ancora ampiamente trascurata nei test di persistenza standardizzati, come quelli descritti nelle linee guida OECD applicate a livello globale. L'inclusione della diversità microbica, ad esempio tramite l'analisi dell'indice di *alpha-diversity*, potrebbe migliorare la rilevanza ambientale di tali test.

Il Capitolo 5 approfondisce ulteriormente il ruolo delle condizioni redox tramite esperimenti in batch condotti in condizioni aerobiche, nitrato-riducenti, ferro-riducenti e solfato-riducenti, utilizzando due inoculi naturali: suolo (lo stesso utilizzato nei Capitoli 2 e 4) e sedimenti da un canale che riceve effluente da un impianto di depurazione. Le condizioni aerobiche hanno mostrato le migliori prestazioni in termini di biodegradazione, con un numero maggiore di OMP degradati, tassi di biodegradazione più elevati e una maggiore produzione di TP, inclusi TP di generazioni successive. Al contrario, le condizioni solfato-riducenti si sono rivelate le meno efficaci. Gli andamenti di biodegradazione della maggior parte degli OMP sono risultati dipendenti dalle condizioni redox, anche per quanto riguarda i processi metabolici di degradazione. Infatti, sono stati rilevati TP specifici per ciascuna condizione redox, suggerendo la presenza di vie di rimozione differenti, probabilmente legate alla diversa composizione delle comunità microbiche in ciascuna condizione redox. I calcoli di biodegradabilità (mediante Biowin3) e tossicità (mediante MS2Tox) hanno indicato che, in generale, i TP prodotti tramite biodegradazione sono più biodegradabili e meno tossici rispetto alle rispettive sostanze di partenza, sebbene siano state osservate alcune eccezioni con tossicità e persistenza aumentata. In particolare, alcuni TP formati in condizioni anaerobiche sono risultati meno tossici rispetto a quelli generati in condizioni aerobiche a partire dalla stessa molecola. Questi risultati sottolineano la necessità di includere anche le condizioni redox nelle norme per la valutazione della persistenza degli OMP nell'ambiente e supportano l'ottimizzazione dei sistemi MAR caratterizzati da dinamiche redox.

Infine, il Capitolo 6 fornisce un riepilogo e una discussione generale dei risultati di questa ricerca, evidenziandone le implicazioni pratiche e le prospettive future. Nel corso di questo studio, i TP sono emersi come componenti diffusi ma ampiamente trascurati nei sistemi di riutilizzo delle acque. Sebbene la nostra valutazione abbia mostrato che, in generale, i TP prodotti risultino meno tossici, più biodegradabili e più mobili rispetto alle rispettive

molecole di partenza, alcune eccezioni evidenziano la necessità di una migliore inclusione dei TP nei programmi di monitoraggio, nei quadri normativi e nei test di persistenza standardizzati. Allo stesso modo, è importante che tali test standardizzati tengano in considerazione le condizioni ambientali in cui avviene la (bio)degradazione. Questa Tesi ha infatti dimostrato come le caratteristiche delle comunità microbiche e le condizioni redox influenzino il destino degli OMP nel sottosuolo, determinandone la loro persistenza o biodegradabilità. Poiché il sottosuolo è prevalentemente un ambiente anaerobico, caratterizzato da strati con condizioni redox variabili e, di conseguenza, con comunità microbiche differenti, è importante approfondire ulteriormente le dinamiche di biodegradazione degli OMP e di formazione dei TP in tali ambienti. Queste conoscenze saranno utili per una comprensione più realistica del destino degli OMP nel ciclo idrico, contribuendo a un riutilizzo dell'acqua più sicuro e sostenibile, in modo da soddisfare la crescente domanda di risorse idriche.

Acknowledgments

Acknowledgements

Since the beginning of my PhD, I have grown quite a lot; I feel I am wiser and more assertive, and (unfortunately) have gained a few grey hairs in the process. The journey has not always been easy, but it has taught me resilience, patience, and perseverance. Along the way, and thanks to the people I met, I made choices that will stay with me for the rest of my life. I would therefore like to express my gratitude to those who accompanied me on this journey and helped shape the person I am today.

I would not be here today without the support, guidance, and encouragement of my supervisors. **Nora**, I admire your zen and balanced approach to anything in life, which has been especially grounding for someone like me, who tends to overthink and overcomplicate things. You taught me how to be more assertive, how to take ownership of my project, and how to grow into an independent researcher. Thank you for pulling me out of the "data jungle" whenever I was getting lost, for your critical questions that sharpened my thinking, and for your honest feedback that greatly improved the quality of my work. And thank you, also, for your positive comments, which I truly value.
Annemarie, even though we did not meet in person very often, your contribution to my research was invaluable. Your feedback, ideas, and encouraging words meant a lot to me. I often received your kind and supportive messages at moments when I was struggling or feeling like I was falling behind, and they truly lifted my spirits. You consistently brought fresh perspectives to our meetings and facilitated collaborations that became an important part of this work. I am deeply grateful for your support.

A big thank you to my paranymphs, Zhaolu and Marko. We shared this journey from the very beginning, and I could not have wished for better companions. **Zhaolu**, my dear, there must be something special about people born on December 8th, because, just like my mum, you have been a point of reference for me. Over the years, we built a special bond, sharing trips, meals, thoughts, research, and dreams. You are always the person I turn to, whether I have good or bad news, doubts, or simply the need to chat. I truly hope that, wherever life takes us, we will always stay close. **Marko**, I feel so lucky to have had you as a true friend throughout this journey. Looking back at our pictures, I can see how much we have grown over the years, and it makes me proud. Thank you for your advice, your patience, and for always being there to listen. I hope our friendship will last a lifetime.

I would also like to thank **all members of the OMP group**, both past and present: Nora, Gabriel, Thomas, Zhaolu, Anne, Jill, Marko, Reiner, Selina, Merel, Silvana, Han, Nena, Marija, Shuhao, Claudia, Chenxiao, as well as Sha, Koen, Laura, Rita, Andrea, and Jinsong. Beyond

the scientific discussions and shared challenges during group meetings, we created wonderful memories together, especially during conferences. Travelling, hiking, and exploring places such as Portugal, Spain, Taipei, Vienna, and Prague brought some of us closer and made the journey truly special.

Gabriel, I admire your dedication to research and your genuine passion for making an impact in science. I truly appreciate your kindness, both professionally and personally. Thank you for your contribution to my PhD and for trusting me and my brain enough to offer me a postdoctoral position. I value the energy and ideas you bring to our meetings; I will do my best for MOST WaNTS. **Thomas**, thank you for fostering a sense of unity within the OMP group and the AquaConnect consortium, and for organizing such enjoyable activities for us. **Jill**, thank you for being the first person to welcome me into the ETE environment, for your support during difficult moments, and for always checking in on me. I also cherish our dinners and the sourdough baking lessons! **Merel**, thank you for your kindness and for the thoughtful messages you shared after deeper conversations. I often feel we are similar in some ways, and I am sure that the kindness you bring into the world will come back to you. **Silvana**, I will always cherish the nice moments we shared and the cute activities you organized. I hope we can have more fancy brunches, painting sessions, and flower trips. **Reiner**, thank you for the stimulating conversations about your research, as well as for all the ironic and funny PhD-life videos we shared, I love them! **Sha**, I will always carry the memories of you, Yu, and Qiqi with me. Thank you for the yoga sessions, the delicious food, and for trusting me with the care of Qiqi.

This research would not have been possible without the support of the **ETE lab team** – Livio, Betty, Lucian, Pieter, Katja, Thomas Slinkert, Nick, Michiel, and Julian – to whom I am very grateful. **Livio**, thank you not only for your help in the lab but also for our conversations about veganism, which ultimately gave me the final push to make a choice I had long been considering and of which I am so very proud. **Betty**, thank you for your reassurance in the lab, for your thoughtful gifts, and for sharing both professional and personal moments with me—your note “Have a nice day! 😊” still brightens my mornings. I would also like to thank the **ETE secretary team –** Liesbeth, Wies, Petra, and Adriana – for your help in this journey.

I am grateful to my **students** – Guangyu, Winda, Wouke, and Silvia – for their contribution to this research and my personal growth.

To **all the colleagues at ETE and fellow researchers, both current and past**, thank you for making this a pleasant and inspiring place to work and for making me proud to be part of such a nice group. **Halimat**, my dear officemate, thank you for your presence and all our chats. We supported each other through both good and difficult moments. I am truly

grateful for our time together, including our baking experiments. **Yme**, the more we talk, the more I appreciate your kindness. Thank you for all the chair shakes and the delicious dinners we shared. **Xiaofang**, you are one of the funniest people I know, and I love your energy! I admire your confidence in entertaining a big group of people; I always feel cozy (or I should say "gezellig") around you. **Jorn**, thank you for your humor, kindness, and genuine interest when you ask me how I am doing. **Anran**, your energy and poetic soul always made our conversations special. Thank you also for the gossip!

I would also like to thank my **colleagues from UvA**. **Jan**, thank you for our collaboration and for your help with HRMS in Amsterdam. Fieldwork in Haaksbergen and Eibergen is something I will never forget: from early mornings and long drives to storms, sunshine, and lunches in the field… or the IBED van. And if we ever decide to change careers, I am still fully on board with opening a café bakery together. **Rick**, thank you for your support and patience in guiding me through patRoon; I feel very fortunate to have learned directly from its developer. I suspect I will keep reaching out during my postdoc years. **Patri**, thank you for your help during my measurement days at UvA and remotely. I am happy I got to know you more during the NTA conference in Germany. Also, thank you for saving me from awkward conversations and for your career advice!

Although physically distant for most of the time, my family and friends from Sardinia have always been close to my heart. **Chiara, Federica M., Giulia, Sonia, Veronica**, **and Federica A.,** no matter how difficult it is to find time to meet, every moment we spend together brings me back to our university years. I am deeply grateful for our friendship. To **Manuel and Denise, my aunts, uncles, and cousins**, distance has not weakened our bond, but rather made our time together even more meaningful. I want to thank my whole family in Sardinia for the special bond and all the love you give me, and especially my parents.
Uno pensa che, crescendo, si diventi indipendenti dai propri genitori, ma penso che, per certi aspetti, ciò non sarà mai possibile per me. **Mamma**, sei il mio porto sicuro ogni giorno e il mio faro nei momenti difficili. Crescendo mi rendo conto di quanto stia diventando simile a te nei modi di fare. Sei la prima persona con cui voglio condividere le notizie belle e quella a cui mi rivolgo nei momenti difficili. Grazie per tutto quello che mi hai insegnato, per esserci sempre e per il tuo supporto emotivo, che per me è fondamentale.
Papà, tutti mi dicono che sono l'unica persona che ascolti, ma non so se sia così. Sicuramente abbiamo tratti del carattere in comune e, magari, anche per questo ho imparato a conoscerti nel profondo. Sono felice di quanto tu sia fiero di me; lo vedo nei tuoi occhi e nei tuoi messaggi in stampatello. Se sono arrivata fin qui, è anche grazie a te, al tuo impegno e ai

sacrifici che hai fatto. Grazie per avermi sempre ricordato di credere in me stessa e per avermi trasmesso l'orgoglio sardo.

Last but not least, thank you to my partner, **Alessandro**. Ormai ti conosco come le mie tasche, e so che preferisci tenere le dichiarazioni romantiche private. Per questo voglio semplicemente dirti grazie per essermi stato accanto in tutti questi anni, per aver assecondato e sostenuto le mie scelte, anche se queste ci hanno fatto stare lontani. Grazie per farmi stare bene.

About the author

About the author

Alessia Ore was born on August 23rd, 1996, in Oristano (Sardinia, Italy). She grew up in the small village of Bonarcado, just a few hundred meters from her school, yet somehow always managed to arrive late. From an early age, she developed a strong sense of environmental responsibility, often returning home with pockets full of snack wrappers that her friends would have otherwise left behind, and picking up litter on the beach whenever she could.

Driven by a wide-ranging curiosity, her childhood ambitions shifted frequently, from archaeologist to fashion designer, before settling on a career in science during high school. In 2015, she began her Bachelor's studies in Biotechnology, attracted particularly by environmental and bioremediation-related topics and their practical relevance. During her Bachelor's Erasmus experience at the Université Libre de Bruxelles, she worked on a project combining bioremediation and biofuels, consolidating her interest and confirming her desire to pursue a career in this field.

Encouraged by her BSc thesis supervisors, she continued her studies at Wageningen University to further explore environmental sciences and technology. Eager to experience life abroad, she moved from Sardinia to the Netherlands in 2019 to begin her Master's in Biobased Sciences. Although leaving her loved ones (and the sun) was not easy, she never doubted that it was the right choice to follow her interests. During her MSc thesis at Wetsus, she realized that bioremediation motivated her more than biorefinery, and how much she enjoyed research. When her biodegradation experiments did not perform as expected, she took it as a challenge and decided to pursue a PhD at the Environmental Technology (ETE) group at Wageningen University.

Her doctoral research focused on the formation of transformation products during the biodegradation of organic micropollutants in the subsurface. Through this work, she aimed to understand the environmental fate of micropollutants better and to contribute to safer and more sustainable water reuse strategies. After completing her PhD, Alessia continues her journey as a postdoctoral researcher at ETE, where she investigates transformation product formation in wastewater treatment processes to help identify technologies that minimize the release of harmful pollutants into the environment.

List of publications

Ore, A., Helmus, R., Narain-Ford, D.M., Bartholomeus, R., Sutton, N.B., Van Wezel, A., **2025**. Presence of micropollutants and transformation products during subsurface irrigation with treated wastewater assessed by non-target screening analysis. ACS EST Water 2025. https://doi.org/https://doi.org/10.1021/acsestwater.4c00930

Ore, A., Palm, E.H., van Wezel, A.P., Sutton, N.B., **2025**. Higher microbial diversity enhances the extent and rate of organic micropollutant biodegradation under aerobic and nitrate-reducing conditions. Water Res. 289, 124921. https://doi.org/10.1016/j.watres.2025.124921

Ore, A., Sigmund, G., Specker, J., Helmus, R., Aguilar-Alarcón, P., Schriks, M., van Wezel, A.P., Sutton, N.B., **2025**. Removal, transport, and transformation of organic micropollutants in managed aquifer recharge: Insights from target and non-target analyses. Water Res. 287, 124409. https://doi.org/10.1016/j.watres.2025.124409

Ore, A., Helmus, R., van Wezel, A.P., Sutton, N.B., **2026**. Uncovering redox-specific biotransformation of organic micropollutants. J. Hazard. Mater. 507, 141775. https://doi.org/10.1016/j.jhazmat.2026.141775

SENSE

Netherlands Research School for the
Socio-Economic and Natural Sciences of the Environment

D I P L O M A

for specialised PhD training

The Netherlands research school for the
Socio-Economic and Natural Sciences of the Environment
(SENSE) declares that

Alessia Ore

born on 23rd August 1996 in Oristano, Italy

has successfully fulfilled all requirements of the
educational PhD programme of SENSE.

Wageningen, 26 June 2026

SENSE coordinator PhD education

Dr Ir Peter Vermeulen

The SENSE Director

Dr Jampel Dell'Angelo

The SENSE Research School declares that **Alessia Ore** has successfully fulfilled all requirements of the educational PhD programme of SENSE with a workload of 49.3 EC, including the following activities:

SENSE PhD Courses

- A1: Environmental Research in Context (2021)
- A2 Research in context activity: Organization of 'PhD trip to Scandinavia' (2023)

Other PhD and Advanced MSc Courses

- Micropollutants in the water cycle, WIMEK (2022)
- Introduction to R, VLAG (2022)
- Bioinformatics with Linux and Python, WIMEK (2023)
- Tidy data transformation and visualization with R, PE&RC (2023)
- Adobe Illustrator: Scientific Artwork & Infographics, WUR Library (2024)
- EU Water Policy and Legislation, European Water Association (2025)
- Scientific writing, Wageningen in'to Languages (2023-2024)
- Project and time management, Wageningen Graduate Schools (2022)
- Communication styles, Wageningen Graduate Schools (2021)
- PhD competence assessment, Wageningen Graduate Schools (2022)
- Basic Dutch 2, Wageningen in'to Languages (2022)
- Critical Thinking and Argumentation, Wageningen Graduate Schools (2022)
- Career perspectives, Wageningen Graduate Schools (2025)

Management and Organisational activities

- PhD trip committee (2022-2023)

External training at a foreign research institute

- patRoon course, University of Amsterdam, The Netherlands (2022)

Teaching and supervision

- Supervision of three MSc students with thesis and one Erasmus+ post-lauream student (2024)
- Lab assistant in the BSc course 'Introduction to Environmental Technology' (2022 – 2024)

Oral Presentations

- *Micropollutant transformation products formation during subsurface irrigation.* AquaConSoil 11-15 September 2023, Prague, Czech Republic
- *Circular water management for regional drought resilience*. AquaConSoil, 11-15 September 2023, Prague, Czech Republic
- *Microbial community diversity determines micropollutant transformation products formation*. Micropol and Ecohazard Conference, 16-20 June 2024, Taipei, Taiwan
- *Removal, transport and transformation of organic micropollutants in managed aquifer recharge*. SETAC 2025, 11-15 May 2025, Wien, Austria

This research was performed within the framework of the research program AquaConnect, funded by the Dutch Research Council (NWO, grant-ID P19-45) and public and private partners of the AquaConnect consortium and coordinated by Wageningen University.

Financial support from Wageningen University for printing this thesis is gratefully acknowledged.

Cover design by Alessia Ore
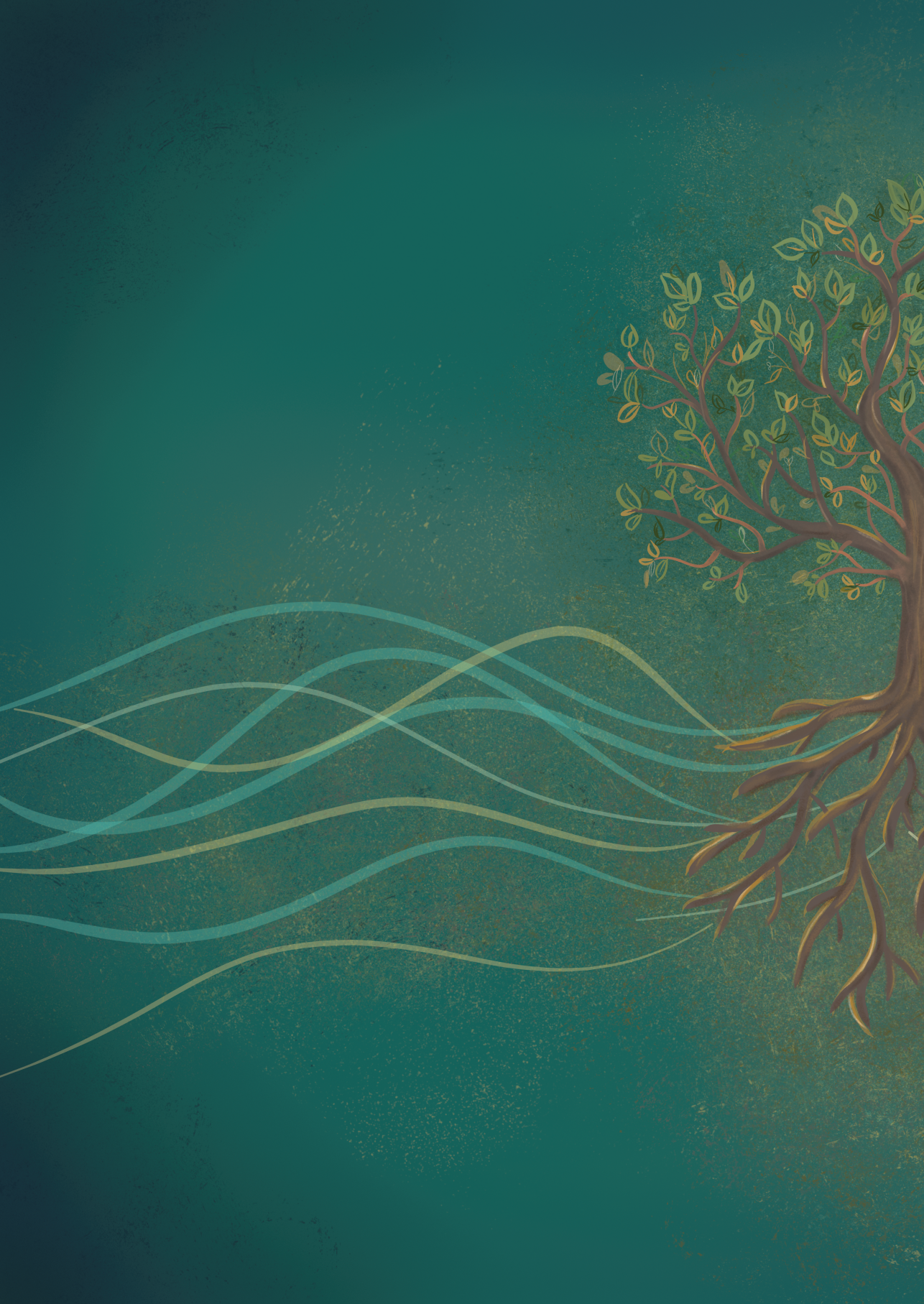
Printed by ProefschriftMaken